Peel Russeting in 'Apple' Mango (*Mangifera indica* L.): Characterization, Mechanisms and Management

Von der Naturwissenschaftlichen Fakultät der

Gottfried Wilhelm Leibniz Universität Hannover

zur Erlangung des Grades

Doktor der Gartenbauwissenschaften (Dr. rer. hort.)

genehmigte Dissertation

von

Thomas Ochieng Athoo, Master of Science in International Horticulture

2023

Referent: Prof. Dr. agr. Moritz Knoche

Korreferent: Prof. Dr. sc. agr. Hartmut Stützel

Korreferent: Assoc. Prof. Dr. Willis Owino

Tag der Promotion: 20.09.2023

Abstract

The aesthetic value and marketability of table fruits are greatly reduced by russeting, a disorder that severely affects the 'Apple' mango (*Mangifera indica* L.) cultivar in Kenya. Despite its prevalence, the underlying mechanisms and prevention strategies for russeting in mangoes are unknown. To address this gap in knowledge, this project aimed to: (1) review existing literature on russeting, (2) characterize the disorder in 'Apple' mango, (3) identify its mechanistic basis in comparison to a non-russet susceptible cultivar, (4) investigate the role of moisture and (5) lenticels on russeting, and (6) develop strategies to prevent the disorder.

To achieve these objectives, russeting was quantified in 'Apple' mango within fruit and in different geographic locations in Kenya. Fruit skins and cuticles from russet susceptible 'Apple' and russet tolerant 'Tommy Atkins' mangoes were examined during fruit development, and cuticular strain was partitioned into its reversible and irreversible components. Mechanical properties of isolated cuticles from both cultivars were tested. The role of moisture in microcrack development and russeting was studied by partially wetting the fruit surface. Lenticels were characterized microscopically across cultivars and locations. Field studies were also conducted to establish the effect of pre-harvest bagging on russeting and postharvest performance.

The results showed that russeting in 'Apple' mango increased with fruit development particularly in the stem end region. Russeting was triggered by rainfall and low temperature. The skin's permeance to water vapor was larger in russeted than in non-russeted skin. The cuticle of 'Apple' mango was thinner than that of 'Tommy Atkins'. Strains released on excision and isolation and wax extraction were higher in 'Apple' than in 'Tommy Atkins'. Stiffness, fracture force, and strain at fracture were consistently lower in 'Apple' than in 'Tommy Atkins'. Surface wetness induced microcracking and increased the skin's water vapor permeance, and moisture-treated fruit skins later developed russet symptoms in 'Apple' mango. Russeting began at lenticels and then spread across the surface, ultimately forming a network of rough, brown patches over the skin. Cross-sections of russeted areas revealed stacks of phellem cells. Pre-harvest bagging of mangoes effectively prevented russeting and lowered the rates of transpiration postharvest.

Keywords: *Mangifera indica*, fruit, periderm, cuticle, lenticels, microcracks, permeance, bagging

Zusammenfassung

Die äußere Fruchtqualität und die Vermarktbarkeit von Mango (*Mangifera indica* L.) der wichtigen kenianischen Sorte ‚Apple' wird durch Berostungen der Schale stark beeinträchtigt. Obwohl Berostung weit verbreitet ist, sind die zugrunde liegenden Mechanismen und Präventionsstrategien zur Vermeidung weitgehend unbekannt. Ziel der Untersuchungen war es, (1) vorhandene Literatur zu Berostung zu sichten, (2) Berostung von 'Apple' Mango präzise zu beschreiben, (3) die Ursache von Berostung bei ‚Apple' Mango zu identifizieren, (4) die Rolle von Feuchtigkeit und (5) Lentizellen bei der Entstehung von Berostung aufzuklären und (6) eine Präventionsstrategie zur Vermeidung von Berostung zu entwickeln.

Um diese Ziele zu erreichen, wurde die Berostung bei 'Apple' Mango in verschiedenen geografischen Lagen in Kenia quantifiziert. Fruchtoberflächen und Kutikulas von berostungsanfälligen 'Apple' und berostungsresistenten 'Tommy Atkins' Mangos wurden während der Fruchtentwicklung untersucht und die Dehnungsrelaxation der Kutikula nach Isolation und Wachsextraktion quantifiziert. Mechanische Eigenschaften der Kutikulas beider Sorten wurden in Zugtests geprüft. Die Rolle von Feuchtigkeit bei der Mikrorissbildung und Lentizellen bei der Entstehung von Berostung wurde untersucht. Feldexperimente wurden durchgeführt, um den Einfluss des Eintütens von Früchten während der Fruchtentwicklung auf die Berostung und die Fruchtqualität nach der Ernte zu bestimmen.

Die Ergebnisse zeigten, dass die Berostung bei 'Apple' Mango mit der Fruchtreife vor allem am Stielende der Frucht zunahm. Berostung wurde durch Regen und niedrige Temperaturen ausgelöst. Berostung erhöhte die Permeanz der Fruchthaut für Wasserdampf. Die Kutikula von 'Apple' Mango war dünner als die von 'Tommy Atkins'. Die Dehnungsrelaxation nach Ausschneiden und Isolation und Entwachsen war bei 'Apple' höher als bei 'Tommy Atkins'. Steifheit, Bruchkraft und Bruchdehnung waren bei Kutikulas von 'Apple' niedriger als bei 'Tommy Atkins'. Oberflächenfeuchtigkeit führte zu Mikrorissbildung, erhöhte die Wasserdampfpermeanz und führte zu Berostung. Berostung begann an Lentizellen und breitete sich dann über die Oberfläche aus. Querschnitte berosteter Bereiche zeigten Stapel von Phellem Zellen. Das Eintüten der Früchte verhinderte Berostung wirkungsvoll und reduzierte die Wasserdampfverlust nach der Ernte.

Schlagwörter: *Mangifera indica*, Frucht, Periderm, Cuticula, Lentizellen, Mikrorisse, Permeanz, Fruchtschutzbeutel

Table of Contents

Abbreviations

C_0 Water-vapor concentration in the surrounding atmosphere

C_i Water-vapor concentration inside of the fruit

F_{max} Membrane fracture force

l_0 Clamping distance

ε_{max} Membrane strain at fracture

µm micrometer

A Fruit surface area

ANOVA Analysis of variance

B Boron

BA Benzyladenine

C_2H_4 Ethylene

Ca Calcium

CA Chlorogenic acid

$CHCl_3$/MeOH Chloroform: methanol solution

cm Centimeter

CM Cuticular membrane

CO_2 Carbon dioxide

CPPU N-(2-Chloro-4-pyridyl)-N′-phenyl urea

cv. Cultivar

d day

DAFB Days after full bloom

Daminozide 4-(2,2-Dimethylhydrazin-1-yl)-4-oxobutanoic acid

DAPF Days after petal fall

DAT Days after termination

DCM Dewaxed CM

Dithane: Ethylene-bis dithy-ocarbamate manganese

ECW Epicuticular wax

ES epidermal segment

F Rate of transpiration

FB Full bloom

FS Fruit set

GA Gibberellic acid

h hour

ICW Intracuticular wax

J Flux density

Kocide Copper oxychloride

m.a.s.l Meters above sea level

Mn Manganese

NaCl Sodium chloride

NaN_3 sodium azide

NaOH sodium hydroxide

O_2 oxygen

p (statistics) probability level

P Permeance of the fruit skin

Paclobutrazol (2RS, 3RS)-1-(4-chlorophenyl)-4,4-dimethyl-2-(lH1,2,4-triazol-1-yl) pentan-3-ol

PE Polythene

PEG Polyethylene glycol

PF Petal fall

pH Potential hydrogen

r Radius of the fruit

R^2/r^2 (statistics) Coefficient of determination

RH Relative humidity

S stiffness

SE standard error

SQRT square root

T Absolute temperature

t Time

UV ultra violet

v/v volume by volume

w/v weight in volume

Zn Zinc

ΔC Difference in water-vapor concentration between C_i and C_0

ἐ Apparent strain

ε Cumulative strain

1. General Introduction

Fruit appearance influences consumers' quality perception. Skin defects like russeting compromise fruit appearance, and thus are a concern for many growers. A russeted skin surface is brown, rough and dull (Winkler et al., 2022). Russeted fruit of cultivars that usually have a smooth skin are of lower economic value, and therefore excluded from high end markets. Postharvest performance is impaired because of accelerated water loss through russeted fruit skin (Athoo et al., 2020; Khanal et al., 2019) resulting in economic losses (Winkler et al., 2022).

In botanical terms, russet refers to a fruit skin covered by a periderm. A periderm comprises phellem, phellogen and phelloderm. Russeting affects many fruit crops species like *Malus* Apples (*Malus x domestica* Borkh) (Legay et al., 2016; Skene, 1982; Tukey, 1969), pears (Macnee et al., 2020; Scharwies et al., 2014; Shi et al., 2019), citrus (Johnson et al., 1957; McCoy, 1996), mango (Athoo et al., 2020), prune (Michailides, 1991), pomegranate (Drogoudi et al., 2021) and tomato (Bakker, 1988; Huang and Snapp, 2004). Rind netting in melons (Cohen et al., 2019; Combrink et al., 2001) and the brown skin of many kiwi fruit cultivars are also symptoms of russeting (Macnee et al., 2020; Wei et al., 2018).

Mango is the second most cultivated fruit crop in Kenya (AFA Horticultural Crops, 2020). In 2020, it accounted for about 17% of total fruit value in Kenya (AFA Horticultural Crops, 2020). Important export cultivars in Kenya include 'Apple', 'Keitt', 'Tommy Atkins' and 'Van dyke' (AFA Horticultural Crops, 2018). 'Apple' is the most widely cultivated mango cultivar in Kenya (Griesbach, 2003). Its fruits are round in shape, excellent in taste and nearly fiber-free (Griesbach, 2003). Unfortunately, it's highly susceptible to russeting. This limits its export potential. Despite its prevalence, the mechanisms of russeting and prevention strategies for russeting in mangoes are unknown. This research project was therefore conducted to (1) identify the mechanistic basis of the russet disorder in 'Apple' mango and (2) develop strategies to manage it.

2. Background information

This introduction sets a brief overview of the russeting problem in fruits. It provides the background information to assist the reader in better understanding the russet disorder of fruits. A

comprehensive review of the literature can be found in chapter 3.1 of this thesis and in recently published review papers (Macnee et al., 2020; Wang et al., 2016).

2.1   Anatomy of mango fruit

Mango is a fleshy indehiscent drupe. The ovarian wall evolves into a pericarp (Cerri and Reale, 2020). The pericarp is composed of a thin exocarp (skin), fleshy mesocarp and stony endocarp (Fig.1). The mesocarp is resinous and highly variable in size, color, fiber content and flavor (Mukherjee and Litz, 2009). It is the most consumed part of the fruit (Tharanathan et al., 2006). The endocarp is hard and fibrous (Mukherjee and Litz, 2009) and encloses a single seed (Figure 1). The seed is coated with a thin leathery testa. It contains the endosperm and one or more embryos (Griesbach, 2003). 'Apple' mango seed is mono-embryonic (Griesbach, 2003).
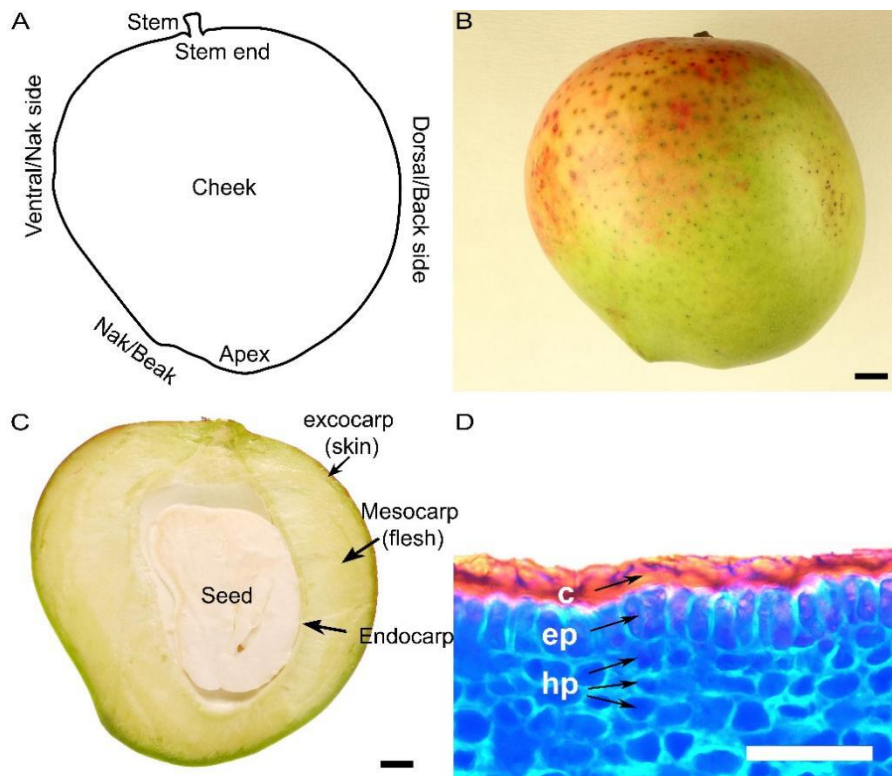

Fig. 1. (A) Schematic drawing of whole fruit illustrating the nomenclature used to address different regions of the fruit surface. (B) Image of mature mango cv 'Apple'. C) Longitudinal cut through the fruit showing a developing seed embedded in the mesocarp. D) Microscopic view of mango fruit skin stained with calcofluor white at 55 days after full

bloom (DAFB). The skin is comprised of a cuticle (c), epidermis (ep) and hypodermal (hp) cell layers. Scale bar is 1 cm (B, C) and 50 µm (D).

2.1.1 The primary fruit skin

Mango fruit skin is primary in nature. It is composed of a cuticle, epidermis, and hypodermis (Figure 1). The cuticle lies above the epidermis (Martin and Juniper, 1970). Its inner layer is interlinked to the cell walls of the epidermis (Jeffree, 1996). It is actually synthesized by, and therefore considered an extension of, the epidermal cell walls (Curry and Arey, 2010; Yeats and Rose, 2013). The principle function of the cuticle is to prevent dehydration of the fruit (Lara et al., 2014; Martin and Juniper, 1970; Riederer and Schreiber, 2001). It also acts as a mechanical barrier against pathogen intrusion (Lara et al., 2014; Martin and Juniper, 1970). Other roles include regulating the movement of solutes and attenuation of harmful light radiation (Riederer, 2018).

The cuticle is polymeric and lipophilic in nature (Bargel et al., 2004). It is composed of cutin, cutan, waxes and cell-wall polysaccharides (Jeffree, 1996). Wax accumulates on the outer surface (epicuticular wax) and within the cuticular membrane (intracuticular wax). Crystalline epicuticular wax (ECW) appears as a white bloom or as a glossy coating above the fruit surface (Trivedi et al., 2019). ECW may be amorphous or crystalline in structure (Kunst and Samuels, 2003). ECW is responsible for light attenuation. Intracuticular wax (ICW) is mostly amorphous in structure (Kunst and Samuels, 2003). Wax is responsible for water-proofing the skin. Major components of cuticular waxes include very long-chain fatty acids, alkanes, aldehydes, primary and secondary alcohols, ketones, esters, and secondary metabolites (Kunst and Samuels, 2003; Yeats and Rose, 2013). However, the composition and structure of cuticular waxes differ among genotypes.

The epidermis is single layered (Figure 1). It is interrupted by protuberances such as stomates, lenticels and trichomes (Bezuidenhout et al., 2005; Gazzola et al., 2004; Ponce de León et al., 2000; Wagner et al., 2004). The substomatal cavity maybe lined with an internal cuticle (Du Plooy et al., 2004). The hypodermis is multilayered. Hypodermal cells are smaller than the parenchyma cells beneath it (Figure 1). Both epidermal and hypodermal cell layers represent the structural backbone of the exocarp (Khanal and Knoche, 2014).

2.1.2 The secondary fruit skin

Secondary fruit skin, botanically termed 'periderm', replaces damaged primary skin. It is formed to restore the skin's barrier functions (Faust and Shear, 1972). The periderm consists of phellem (cork cells), phellogen (cork cambium) and phelloderm (Evert, 2006; Macnee et al., 2020). The phellogen is a meristem. It divides to form phellem on the outside and a phelloderm on the inside (Evert, 2006). Phellem cells are compactly arranged and often prismatic in shape. Their cell walls are suberized and lignified (Evert, 2006). Phelloderm cells appear in the same radial file as the phellem (Evert, 2006). However, their cell walls remain non-suberized (Evert, 2006).

Fruit lenticels are secondary in nature. They develop underneath stomates that rapture during growth (Bezuidenhout et al., 2005). Their phellogen have a more open and loose arrangement with large intercellular spaces (Evert, 2006).

2.2   *Fruit growth and development*

Mango fruit, seed and embryo development follow a single sigmoidal pattern (Carella et al., 2021; Kennard, 1955; Mukherjee and Litz, 2009). This pattern consists of three phases. Phase I is characterized by a slower fruit growth. Epidermal cells are more elongated radially (Figure 1). Fruit expansion is mainly by cell division (Carella et al., 2021). Epidermal and hypodermal cells divide anticlinally (Ponce de León et al., 2000), forming cells that are isodiametric in the tangential plane of the fruit (Athoo et al., 2021). At this stage stomata are still functional (Gazzola et al., 2004). A thick layer of amorphous epicuticular wax scales covers the skin (Bally, 1999).

The fruit is most susceptible to skin damages during phase II (Gazzola et al., 2004). This phase is characterized by rapid fruit growth in mango (Davenport, 2009). During this phase, cell expansion exceeds cell division (Carella et al., 2021). Epidermal cells change their orientation from 'portrait' to 'square' (Athoo et al., 2021), i.e., the anticlinal cell diameter decreases with concomitant increase of the periclinal diameter. Cellular arrangement becomes irregular and chaotic (Tamjinda et al., 1992). The cuticle forms a wave-like pattern with crests and valleys (Ponce de León et al., 2000). The valleys occasionally transverse the epidermis (Ponce de León et al., 2000). Stomata at this stage are closed and non-functional (Gazzola et al., 2004). Stomata swell and lenticels appear (Athoo et al., 2023). The ECW structure changes from amorphous to crystalline (Gazzola et al., 2004). During this phase, microcracks appear in the cuticle (Gazzola et al., 2004) especially around lenticels (Athoo et al., 2023).

The fruit mature during Phase III. Internal changes like accumulation of sugars and hardening of seed coat prevail over fruit growth (Carella et al., 2021). Lenticels become fully developed (Bally, 1999). Loose cells fill the holes beneath the lenticels (Tamjinda et al., 1992). A periderm forms beneath the lenticel cavity in 'Apple' mango (Athoo et al., 2020). Fruit maturity is completed between 90-180 DAFB depending on cultivar, climate and cultural practices (Lobo and Sidhu, 2017).

Cuticular thickness and composition changes during fruit ontogeny (Bally, 1999; Trivedi et al., 2019). This is necessary if the cuticle is to maintain its barrier role (Trivedi et al., 2019). In mango, cuticle deposition is continuous (Ponce de León et al., 2000). Cuticle mass per unit area increases continuously as the fruit mature or ripen (Tafolla-Arellano et al., 2017). But, cuticle thickness, wax architecture and deposition differs among genotypes (Barbosa-Martínez et al., 2009; Camacho-Vázquez et al., 2019; Dietz et al., 1989). At maturity, 'Kent' exhibited the thickest cuticle while 'Criollo' fruit had the thinnest cuticle among tested mango cultivars (Camacho-Vázquez et al., 2019). Also, the ECW was crystalline in 'Kent' and 'Manililla' but amorphous in 'Tommy Atkins', 'Ataulfo', 'Manila', and 'Criollo' (Camacho-Vázquez et al., 2019). Cuticle deposition is also affected by the fruit position on the tree (Léchaudel et al., 2013). Sun exposed fruits developed thicker cuticles than those that were shaded (Léchaudel et al., 2013). More cutin and waxes were also observed on sun exposed leaves than on shaded leaves in citrus (Skoss, 1955). The pattern of cuticle deposition in 'Apple' mango is unknown.

2.3   Russet formation

To our knowledge, there is little information on russeting in mango. What is known about russeting has been studied in *Malus* apple. Literature on russeting has been recently reviewed (Faust and Shear, 1972; Macnee et al., 2020). Briefly, russeting is generally viewed as periderm formation in response to damage of the primary skin. Important triggers include wounding, surface wetness and infections with pests and pathogens. For detailed information, the reader is referred to the above reviews and to chapter 3.1 of this thesis.

2.4   Study objectives

To our knowledge, russeting has not been studied in mango. The triggers, mechanistic basis and counter measures against russeting have not been investigated in 'Apple' mango. Some research

has been conducted on cuticle deposition in mango (Bally, 1999; Gazzola et al., 2004), however, this work excluded russet susceptible cultivars like 'Apple'. The role of surface moisture and lenticels in russet formation has not been studied in mango. Also, there is no information on countermeasures against russeting in 'Apple' mango.

This PhD project was therefore conducted to identify the mechanistic basis of russeting in 'Apple' mango and to develop strategies to manage it.

The specific objectives of this PhD project were to:

   i.   Review the literature on russeting, particularly its triggers, mechanism, and management strategies (Chapter 3.1)

  ii.   Identify factors, mechanisms, and consequences of russeting in 'Apple' mango (Chapter 3.2)

 iii.   Identify the mechanistic basis for the high susceptibility of 'Apple' mango, with special focus on fruit growth, cuticle and wax deposition, strain release in comparison to the non-susceptible 'Tommy Atkin' cultivar (Chapter 3.3)

 iv.   Study the effect of exposing the fruit skin surface to moisture on microcracking and on water vapor permeance (Chapter 3.4)

  v.   Establish whether lenticels predispose cv. 'Apple' mango to russeting (Chapter 3.5)

 vi.   Establish the effect of pre-harvest bagging on russeting in susceptible mango cv. 'Apple' (Chapter 3.6)

3. Publications and Manuscripts

3.1 Russeting of Fruits: Etiology and Management

Authors:

Andreas Winkler (**AW**), Thomas O. Athoo (**TOA**) and Moritz Knoche (**MK**)

Author affiliation:

Institute of Horticultural Production Systems, Fruit Science Section, Leibniz University Hannover, Herrenhäuser Straße 2, 30419 Hannover, Germany

Author Contributions:

A.W. and T.O.A. compiled the tables; A.W., T.O.A. and M.K. wrote the manuscript.

Review

Russeting of Fruits: Etiology and Management

Andreas Winkler [D], Thomas Athoo [D] and Moritz Knoche *[D]

Institute of Horticultural Production Systems, Leibniz University Hannover, Herrenhäuser Straße 2,
30419 Hannover, Germany; andreas.winkler@obst.uni-hannover.de (A.W.); t.athoo@obst.uni-hannover.de (T.A.)
* Correspondence: moritz.knoche@obst.uni-hannover.de; Tel.: +49-511-762-9020

Abstract: The skin of a fruit protects the vulnerable, nutrient-rich flesh and seed(s) within from the hostile environment. It is also responsible for the fruit's appearance. In many fruitcrop species, russeting compromises fruit appearance and thus commercial value. Here, we review the literature on fruit russeting, focusing on the factors and mechanisms that induce it and on the management and breeding strategies that may reduce it. Compared with a primary fruit skin, which is usually distinctively colored and shiny, a secondary fruit skin is reddish-brown, dull and slightly rough to the touch (i.e., russeted). This secondary skin (periderm) comprises phellem cells with suberized cell walls, a phellogen and a phelloderm. Russeted (secondary) fruit skins have similar mechanical properties to non-russeted (primary) ones but are more plastic. However, russeted fruit skins are more permeable to water vapor, so russeted fruits suffer higher postharvest water loss, reduced shine, increased shrivel and reduced packed weight (most fruit is sold per kg). Orchard factors that induce russeting include expansion-growth-induced strain, surface wetness, mechanical damage, freezing temperatures, some pests and diseases and some agrochemicals. All these probably act via an increased incidence of cuticular microcracking as a result of local concentrations of mechanical stress. Microcracking impairs the cuticle's barrier properties. Potential triggers of russeting (the development of a periderm), consequent on cuticular microcracking, include locally high concentrations of O_2, lower concentrations of CO_2 and more negative water potentials. Horticulturists sometimes spray gibberellins, cytokinins or boron to reduce russeting. Bagging fruit (to exclude surface moisture) is also reportedly effective. From a breeding perspective, genotypes having small and more uniform-sized epidermal cells are judged less likely to be susceptible to russeting.

Keywords: disorder; periderm; repair mechanism

1. Introduction

The skin of a fruit lies at the interface between the vulnerable, nutrient-rich fleshy tissues and seed(s) inside and the surrounding 'hostile' environment outside. The fruit skin is exposed to a broad range of abiotic and biotic challenges, thus serving as a critical barrier protecting the fruit tissues against (a) uncontrolled water loss/uptake [1], (b) uncontrolled exchanges of respiratory gasses (O_2, CO_2) and the hormone ethylene (C_2H_4) [2], (c) UV-radiation [2,3] and (d) invasion by pathogens [4,5]. In modern horticulture, some of these functions require opposing properties, such as protection against cell content leakage, while at the same time permitting penetration of foliar-applied nutrients, growth regulators or other agrochemicals [6]. To fulfill these functions, the fruit skin must remain intact throughout the period of fruit growth and development. This review deals with the development of a secondary surface (a periderm) on the skins of commercial fruit types that usually retain their shiny, distinctively-colored, primary surfaces through to harvest and consumption.

A plant organ's primary surface comprises a complex of materials. On the outside, there is a polymeric cuticle that overlies a cellular structure usually consisting of a single epidermal cell layer, which itself overlies one to several layers of hypodermal cells. In most fruit crops, the epidermis and hypodermis are responsible for the skin's mechanical

properties, while the cuticle is responsible for the skin's barrier properties [7,8]. It is also the primary fruit skin that determines the appearance and attractiveness of the fruit to end consumers, as well as to seed-dispersing animals. After all, the wild types of most commercial fruitcrop species evolved to attract animals as their agents of seed dispersal. Thus, the epicuticular waxes on the cuticle are responsible for the skin's gloss, and the pigments in the cuticle and subtending cell layers for the skin's distinctive color [9,10].

However, the skins of a significant number of commercial fruit types are partially or wholly covered by areas of a secondary surface. Horticulturists refer to this as russeting [11,12]. The proportion of the surface of a mature fruit that is primary vs. secondary is genetically determined. Thus, in apple, some cultivars rarely exhibit areas of russeting (Royal Gala); in some, russeting is a cultivar characteristic (Cox's Orange Pippin); while in others, the whole fruit surface is usually russeted (Egremont Russet). Russeting is seen as a market defect (market value is reduced) only in the first case or in the second if the russeted area is excessive.

A secondary surface forms when the primary surface fails. Failure may occur for various reasons. Potential reasons include the normal internal processes of ontogeny (e.g., growth strain) or external factors such as mechanical or chemical damage or harsh environmental conditions such as freezing [7]. A periderm forms to (partially) restore the impaired barrier properties of the damaged primary fruit skin. The proportion of the fruit-skin affected by russeting ranges from small patches in particular regions of the fruit surface to a uniform layer that covers the entire fruit.

From a horticultural point of view, the dull, reddish-brown appearance of russeting is usually unattractive to the consumer. Russeting is therefore considered to be a fruit surface disorder in many fruitcrop species and in all 'smooth-skinned' cultivars. In many russet-susceptible cultivars, russeting is readily accepted as being 'normal'. Thus, the entire fruit skin is russeted in most kiwifruit cultivars/species. Similarly, russeting is considered normal and acceptable in the 'Reinette' apple cultivars and in pear cultivars, such as Bosc, Conference and Gold La France, the latter being a russeted sport of the non-russeted cultivar La France [13]. Similarly, in Asian pear, smooth-skinned cultivars, as well as entirely russeted cultivars, are known. Melons form a notable exception. Here, the 'netting' pattern of russeting of the fruit skin is seen as a positive indicator of fruit quality and, so, is considered highly desirable [14].

Russeting is not a new phenomenon. The first research publications date back nearly two centuries [12,15–22]. Most of the literature on russeting relates to pome fruit, and especially to apple. Fewer studies relate to pear, kiwifruit, mango, tomato, bell pepper and others (Table 1). Occasionally, russeting has been reported for plums and grapes. Sweet and sour cherries, peaches, apricots and most 'berryfruit' crops, including currants, blueberries, raspberries, blackberries and strawberries, are essentially free of russet. The published information on russeting is scattered and often not conclusive. The objective of this paper is to review the literature on the practical aspects of russeting, including its occurrence, triggers, mechanical bases and management strategies adopted to reduce russeting under orchard conditions by cultivation and breeding. For a comprehensive review of the biochemistry and molecular biology of russet formation, the reader is referred to the excellent recent reviews by Macnee et al. [23] and Wang et al. [24].

2. Occurrence and Symptoms of Russet

Russeting occurs in a large number of fruitcrop species (Table 1). Often, russet-susceptible and non-susceptible cultivars are known within a species. In apple, some highly russet-susceptible cultivars are identified by the cultivar name. Examples include Red Russet, Golden Russet, Roxbury Russet [22] or Egremont Russet [25], as well as the Reinette-type cultivars [26].

Table 1. Occurrence, symptoms, causes and management of russeting. Results are compiled from literature sources.

Cultivar	Symptoms	Causes	Management
Apple	Russet as rough and brown skin [17,28], often in stem [29] and calyx cavities [30], some cultivars with entire surface russeted [31], high susceptibility during early fruit development [12,29,32–34]	Moisture [35–38] or high humidity [17,35], damage by pesticides, growth regulators, surfactants and other substances [19,39–61], frost [27,34], fungi [62–66], viruses [67–69], insects [70,71]	Spray application of growth regulators [30,32,33,56,58,72–81], CaCl₂ [82], prohexadione-calcium [72], organic-/mineral bio-stimulators [83], chlorogenic acid [84], coatings [82], insecticides to prevent insect damage [71], shading nets [85], rain shelters [48], bagging [17,48,82,86]
Pear	Russet as dull-brownish skin patches, more in calyx and cheek than in neck [87], some cultivars completely russeted [23], high susceptibility during early development [87]	Surface moisture [88–90], high humidity [90], growth stress [87], fungicides, thinners and growth regulators [89–93], insects [94–96], bacteria [97], fungi [98,99]	Bagging [100–104], spray application of GA₄₊₇ [105], mancozeb + sulfur [105] or kaolin ± mancozeb [106]
Citrus	Russet as rough texture, brownish-black, greyish discoloration [107].	(Rust) mites, thrips and other sucking insects [107–109], mechanical damage by wind, hail, contact with branches [110,111]	Zineb against citrus mites [108,109,112]
Prune	On immature fruit: longitudinal stripes at stylar end [113], mature: rough, brown, dried surface [113]	Copper spray [113], mechanical damage by wind, abrasion by leaves, shoots, adjacent fruits [113,114], exposure to surface wetness or free water, high humidity [113,114], scab [115]	Captafol, ziram for scab control [113]
Loquat	Deep brown stripes, approx. 1 mm wide [116,117]	Growth stress [116,117], microclimate (high temperature) [116], very high light intensities [116]	Shading using nets to decrease growth rate during cell division phase [116,118]
Tomato	Russet as rough corky discolored surface [119], also referred to as 'shoulder check' [119] or 'cuticle cracking' [120]	Rust mites [71,121], growth stress [120,122,123], surface moisture [119]	Non-susceptible cultivars [123], moderate thinning [123], spray application of Ca+B [119,124]
Melon	Rind netting common in some cultivars [14], russet as dry, white to brownish ridges [14]	Growth stress [125,126], surface moisture [125], wounding [14]	Rind netting desirable, countermeasures not needed
Grape berry	Brown patches of russet [127]	Surfactants [128], fungicides [129], insects [71,130], surface moisture [131]	Spray applications of GA₃, GA₃ + CPPU [132], insecticides [71], Ca [133]
Mango	Rough brownish irregular patches of russet [134], beginning at lenticels [134]	Surface moisture, cold nights [134]	Bagging [135]
Pomegranate	Corky surface [136]	High humidity [136,137], heat waves [138], temperature fluctuation during maturation [136], pomegranate mite [139]	Spray applications of GA₃, CPPU [137,140], acetylsalicylic acid [136], sulfur dust against pomegranate mites [139]

The symptoms of russet are similar between different fruitcrop species. A rough, reddish-brown and corky appearance is characteristic of a russeted surface (Table 1 and Figure 1). The region of the fruit surface affected by russet can differ. In apples, the spatial distribution of russeting differs depending on the cause. Russet induced by growth strain or by exposure to high humidity or dew occurs in large, uniform patches and may cover the entire fruit surface. Russeting limited to the stem cavity is more likely the result of long wetness durations and high growth strains. Russeting in response to mechanical wounding (e.g., scratching or abrasion from contact with a neighboring fruit or leaf or stem) is typically well defined spatially, being strictly limited to the region of direct physical contact. Russeting caused by spray chemicals occurs in regions of the fruit surface where spray droplets collect and later concentrate excessively during drying. Small fruitlets that come into contact with spray solutions during the particularly russet-susceptible early stages of fruit development may be entirely russeted [27]. A net-like pattern of russeting on apple is characteristic of infection with powdery mildew. Russeting caused by the feeding of pests (thrips, stink bugs, mites, etc.) is limited to the site of the puncture wound and the immediately surrounding cells. Forms of russeting caused by frost are typically in rings. These are induced by freezing temperatures when only part of the flower or fruitlet is damaged (Table 1).
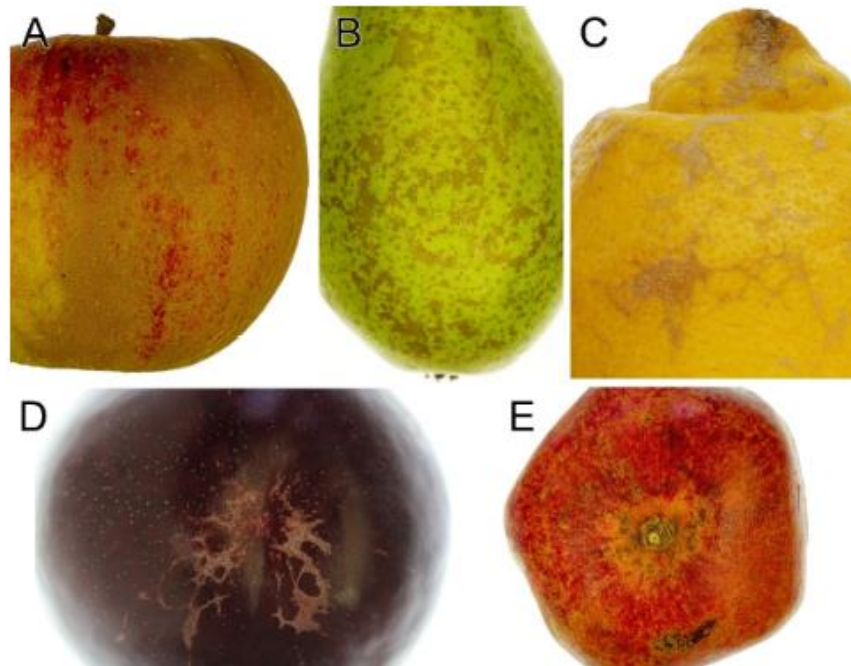

Figure 1. Russeting in different fruit crops. (**A**) Apple; (**B**) pear; (**C**) citrus; (**D**) plum; (**E**) pomegranate. Images: (**A,C**) Andreas Winkler, (**B,D,E**) Martin Brüggenwirth.

3. Some Fruit Skin Disorders Not Related to Periderm Formation

There are some fruit skin disorders that can be confused with russeting. These include skin spots and scarf skin in apple and maturity bronzing (sometimes also called maturity stain) in banana (Table 2). These disorders can bear a visual similarity to russeting. However, they differ from russeting in that a periderm does not develop.

In skin spots, cuticular microcracks are causal. These form due to moisture exposure during late-stage fruit development [36]. In this stage, the apple fruit skin is no longer able to form a periderm [36,38]. Here, the impaired barrier properties of the skin

11

are restored to some extent by the deposition of lignin in the cell walls immediately underlying a microcrack. This process hydraulically isolates the portion of the fruit skin underlying a microcrack. The characteristic spot-like appearance is caused by the resulting cell death [141].

Apples with scarf skin symptoms look as if they have a thin and very 'soft' periderm. However, periderm formation is not involved in scarf skin. Instead, scarf skin is thought to result from the formation of subepidermal air spaces [142]. The cause of this is not yet known. Surface moisture may be involved since bagging during early fruit development (when russet susceptibility is particularly high) reduces scarf skin [143].

Maturity bronzing in banana is also connected to fractures in the cuticle, which propagate into the epidermis [144]. Maturity bronzing occurs primarily in the tropical wet season when temperatures and humidities are especially high, and the sky is overcast [145]. These conditions result in high rates of growth strain, which may be causal in maturity bronzing [144].

Table 2. Fruit surface disorders that bear some similarity with russet, but where no periderm is involved. Data are compiled from literature sources.

Disorder	Crop Affected	Symptoms	Causes	Management
Skin spots	Apple	Irregular patches of small, round and brown spots, develops in CA-storage, promoted by 1-MCP [141]	Moisture-induced microcracks late in the season [36,141]	Reducing surface wetness duration, for susceptible batches, no storage or cool-storage only [36,141]
Scarf skin	Apple	Whitish lines or stripes [146], whitish or opalescent sheen [147], due to formation of subepidermal air spaces [142]	Unknown	-
Maturity bronzing or maturity stain	Banana	Pre-harvest necrosis of the skin, bronze coloration [144]	Growth stress [148], water stress [144]	Bagging [149], reducing the number of leaves [150]

4. Anatomy of Russeted Fruit Skin

In botanical terms, a russeted fruit skin represents a periderm consisting of phellem, phellogen and phelloderm [7,23]. The phellem is the outermost layer of this composite, the phelloderm the innermost. The phellogen is the interfacing sheet-like meristematic layer. The phellogen is formed in the hypodermal cell layer by dedifferentiation of hypodermal cells [16,151]. Periclinal cell division in the phellogen generates stacks of phellem cells where each cell of a stack originates from the division of a single underlying mother cell of the phellogen [7].

Phellem cells have suberized cell walls. When the stacks of phellem cells reach the surface, they come into contact with the atmosphere. Here, the suberized cell walls turn brown. It is the suberin that is responsible for the dull and reddish/brown color of a russeted fruit surface [152]. Due to the lipophilic character of suberin, suberized cell walls present a significant barrier to water loss [153].

From the above, it is evident that during the early stages of periderm formation, the periderm may still be covered by a cuticle, epidermal cells and some hypodermal cells. The periderm reaches the surface as growth proceeds and as the residues of the primary fruit skin (now hydraulically isolated and desiccated) tear and are sloughed off.

5. Physiology of Russeted Fruit Skin

The physiological properties of the fruit skin change with russeting. For the fruit of a particular apple cultivar, the water vapor permeance of a russeted area of skin is higher than that of a non-russeted area [11,134]. Furthermore, a non-russeted area of the primary surface of a russet-susceptible apple cultivar has a higher water vapor permeance than a

12

non-russeted area of a non-russet-susceptible cultivar [38]. This latter finding is likely due to a higher incidence of microcracking of the cuticles of the russet-susceptible cultivars. Compared to non-russet-susceptible cultivars, the higher water vapor permeance results in greater water loss during storage, and thus, a higher mass loss and (possibly) more shrivel. In this way, russeted fruit have reduced cool-storage potential and shorter supermarket shelf-lives compared to non-russeted fruit. We are unaware of studies that measure the fruit skin permeances to O_2, CO_2 or ethylene of russeted fruit.

The mechanical properties of fruit skins differ slightly between russeted and non-russeted fruit surfaces. The maximum stress and maximum strain that the fruit skin can withstand without failure are of similar magnitude for non-russeted and russeted skins [18]. Enzymatically isolated periderms of apple and pear are more plastic than isolated cuticles as indexed by a higher strain at maximum stress and a lower modulus of elasticity [18]. The higher plasticity renders the periderm a very suitable 'repair patch' for an overly-strained fruit surface. It allows the periderm to cope with ongoing area expansion during growth without excessive increases in stress build up [18,154].

6. Factors in Russet Formation

Russeting has been related to a number of factors. Growth strains are considered causal in russet formation in apple [18], pear [87], loquat [116,117], tomato [120,122,123] and melon [125,126]. During growth, the skin of developing fruit is subject to considerable tangential strain [7], arising from the increase in fruit volume and hence in fruit surface (area strain). Support for the idea that excessive growth strain lies behind the formation of russet comes from the following observations. First, susceptibility to russet is highest during early fruit development [12,29,32–34,155]. During early development, the relative surface area growth rate is at a maximum, resulting in maximum rates of strain [156]. The relative surface area growth rate equals the increase in surface area per unit time ($cm^2\ d^{-1}$) divided by the surface area (cm^2) at that time. Relative surface area growth rate, thus, has the units d^{-1}. Second, the calyx and cheek regions of pear are more russeted than the neck [87]. Both these regions have higher relative surface area growth rates than the neck [87]. Third, the stem cavity of apple fruit is often russeted. Here, stress concentration is at maximum due to the small radius of curvature of the fruit surface [154].

Extended periods of exposure of fruit surfaces to moisture, either as liquid water or as high water-vapor concentration (high relative humidity), has been identified as causal in russeting. Typical examples include russet in apple, pear, prune, tomato, melon, grape and mango (Table 1). Surface moisture is particularly critical during the early stages of fruit development when susceptibility to russeting is high [38]. The following observations support a role for moisture in russeting: First, the development of fruit under cool, rainy and high-humidity conditions stimulates russet formation in apple [156,157] and pear [88–90]. Second, experimental exposure of fruit surfaces to water, by immersion [73], by mounting a test tube filled with water on the fruit surface [38] or by overhead sprinkling [36], results in enhanced russeting. Indeed, these techniques are often used experimentally to induce russeting [37,158].

Mechanical damage of the fruit surface is also a trigger for russeting. Mechanical damage may be caused by a combination of wind and contact of fruit with a neighboring branch, shoot, leaf or fruit. Hail also damages fruit skin and causes russeting [110,111,113,114].

Pests and diseases may cause russeting in several fruitcrops. Examples of such pests include the citrus rust mite [107–109] and the tomato rust mite [71,121]. Similarly, fungi, such as powdery mildew in apple or epiphytic yeast species in apple and pear, have been reported to be causal in russeting (Table 1).

Exposure of fruit to freezing temperatures may result in formation of russet. Characteristic shapes of russet due to frost in apple are "periderm tongues" that run from the stem cavity downwards to the equatorial plane along one side of the fruit or rings of russeting that completely surround the fruit [27,34]. Why these characteristic shapes arise is unknown.

13

Application of agrochemicals may increase, not affect or decrease russeting. Compounds known to induce russeting include lime sulfur, copper hydroxide and thinners such as ammonium thiosulfate or ethephon (Table 3). Surfactants such as Tween 20 or Citowett that are often used in agrochemical formulations are reported to induce russeting in some fruitcrops (Table 3). An important factor would seem to be the developmental stage at the time of agrochemical application. Applications made during periods of high susceptibility to russet (e.g., during early fruit development) are more likely to induce russet. Meanwhile, the same chemical compounds may have no effect on russet formation when applied at a later stage when susceptibility is lower. In addition, environmental conditions, such as high temperatures, that favor the rapid uptake of agrochemicals are more likely to induce russeting. Rapid uptake may result in overloading of the contacted cells and thus a phytotoxic reaction. This occurs particularly in regions of the fruit surface where spray droplets collect; the droplets coalesce, and highly-concentrated chemical deposits form as the droplets dry. Then, when the critical concentration is exceeded, the cells collapse.

Reduced incidence of russeting has been found following the application of fungicides, such as mancozeb. This effect is accounted for by a reduction in the population of fungal species that induce russet.

Table 3. Effect of fungicides, surfactants and foliar fertilizers on russet. Results are compiled from literature sources.

Chemical	Category	Crop	Cultivar	Time of Application	Effect on Russet	Reference
Di-l-p-methene (2.5%)	Antitranspirant	Apple	Golden Delicious	4, 13, 21 and 27 DAFB	Increased	[48]
B (300 mg L^{-1})	Foliar fertilizer	Tomato	Mountain Spring	Weekly	Decreased	[119]
B (300 mg L^{-1}) + Ca (2 g L^{-1})						
Dithane (4 kg ha^{-1})	Foliar fertilizer	Apple	Golden Delicious Spur	Flowering, PF and FS	Increased	[39]
Packhard (0.5% Ca)						
Zn (100 g ha^{-1})	Foliar fertilizer	Apple	Elstar	Green and pink stage and at bloom beginning	Increased	[40]
Captafol (1.8 g a.i. L^{-1})	Fungicide	Plum	French	60–90% FB	Decreased	[113]
Chlorothalonil (3.37 kg ha^{-1})	Fungicide	Grape berry	Concord	10 DAFB	Increased	[129]
Kocide (Copper hydroxide) (0.32 g L^{-1})	Fungicide	Apple	Braeburn	Weekly starting at pink tip stage	Increased	[41]
Kocide (Copper hydroxide) (1.5 g L^{-1})	Fungicide	Apple	Golden Delicious	3 to 9 weeks after FB	Increased	[42]
Kocide (Copper hydroxide) (16 or 63 g L^{-1})	Fungicide	Apple	Granny Smith	Pink bud, FB and PF	Increased	[43]
Copper hydroxide (50%) (2.5 kg ha^{-1}) + amino acids (10%) (2 L ha^{-1})	Fungicide	Pear	Conference	PF and 1 week after PF	Increased	[89]
Copper hydroxide (0.3 g L^{-1})	Fungicide	Pear	Beurré Bosc	PF, 7, 14 and 21 DAPF	Increased	[91]
Copper hydroxide	Fungicide	Pear	Bosc	PF	Increased	[90]
Copper hydroxide	Fungicide	Apple	Idared	FB	Increased	[44]
Copper oxychloride						
Copper oxychloride (4 g L^{-1})	Fungicide	Apple	Red Fuji	Green tip stage	Increased	[19]
Lime sulfur (6 g L^{-1})	Fungicide	Apple	Fuji More	90% FB	Increased	[45]
Lime sulfur (2%)	Fungicide	Apple	Honeycrisp	Fruitlet stage	Increased	[46]
Lime sulfur (2%) + winter oil						
Fish emulsion (3%) + 2% fish oil	Fungicide	Apple	Gala	20% and 80% FB	Increased	[47]
Fish emulsion (3%) + Tween 20 (0.125%)						
Mancozeb (2 g L^{-1}) + Sulfur (2 g L^{-1})	Fungicide	Pear	Packham's Triumph	80% FB	Decreased	[105]
Wettable sulfur (17 kg ha^{-1})	Fungicide	Apple	Golden Delicious Spur	FB, PF and FS	Decreased	[39]
Ziram (2.4 g a.i. L^{-1})	Fungicide	Plum	French	60–90% FB	Decreased	[113]
Diazinon (0.08%)	Insecticide	Apple	Golden Delicious	18 DAFB	Increased	[48]
Rape oil (10 or 30 g L^{-1}), Sunflower oil (30 g L^{-1}), Soya oil (30 g L^{-1})	Oil	Apple	Golden Delicious	FB	Increased	[49]
Superior oil (0.5%)	Oil	Apple	Golden Delicious	18 DAFB	Increased	[48]
Citowett (>1%)	Surfactant	Apple	Golden Delicious	FB, PF and 10 weeks after FB	Increased	[50]
Tween 20 (≥1%)						
Ortho X-77 (1.0%)	Surfactant	Apple	Suntan	3 weeks after FB	Increased	[51]

Table 3. *Cont.*

Chemical	Category	Crop	Cultivar	Time of Application	Effect on Russet	Reference
Polysorbate 20 (0.5%), Polysorbate 60 (0.5%), Polysorbate 80 (0.5%), Lecithin (0.5%)	Surfactant	Apple	Golden Delicious	At 12.5 + 18 or 18 + 20 mm diameter	Increased	[52]
Polysorbate 20 (0.5%), Polysorbate 60 (0.5%)	Surfactant	Apple	Fuji	At 12.5 + 18 mm diameter	Increased	[52]
Potassium soap (500 mg L^{-1})	Surfactant	Apple	Golden Delicious Smoothee	FB and 2 DAFB	Increased	[53]
Ammonium thiosulphate (4%)	Thinner	Apple	Golden Delicious	20% FB	Increased	[55]
Ammonium thiosulphate (1.2%)	Thinner	Pear	Conference	20% or 50% FB	Increased	[92]
Endothal (0.8–1.2 mL L^{-1}) + CyLex (150 mg L^{-1})	Thinner	Apple	Oregon Spur Red Delicious	80% FB	Increased	[54]
Apasil (silicon dioxide) (2.5%)	Other	Apple	Golden Delicious	1 to 4 applications between 4–25 DAFB	Decreased	[48]
PEG 20000 (2.5%)	Other	Apple	Golden Delicious	4, 13, 21 and 27 DAFB	Increased	[48]

PEG = polyethylene glycol; FB: full bloom; PF: petal fall; FS: fruit set; DAFB: days after full bloom; DAPF: days after petal fall; Dithane: ethylene-bis dithy-ocarbamate manganese 62%, Mn 16%, Zn 2%; Packard: 8% Ca, 6% carboxylic acids, 0.5% B, pH < 3.0.

7. The Mechanism of Russeting—A Central Role for Cuticular Microcracks

Microscopic cracks in the cuticle, so-called microcracks, play a key role in russet formation [12,159]. Microcracks are invisible, or barely visible, to the naked eye. They are limited to the thickness of the cuticle and do not propagate deeper into the underlying cell layers [160]. Importantly, the formation of microcracks provides a unifying explanation for a diverse list of factors found to trigger russeting.

7.1. Temporal and Spatial Heterogeneity

High growth strains represent the critical factor for microcracking of the cuticle. The skin of a developing fruit is subject to ongoing tangential strain as the fruit volume and, hence, the fruit surface area increases during growth [7]. In the epidermal and hypodermal cell layers, the increase in skin surface area is accommodated by a combination of cell division (more cells) and cell extension (larger cells). Furthermore, some epidermal cells change their shape from 'portrait' to 'landscape' (in anticlinal view) as they increase in periclinal area and decrease in anticlinal height, but without significant change in (anticlinal) perimeter [16,151,161,162]. The change in cell shape implies that areas of previously anticlinal cell walls de-bond and change their orientation to form part of the expanding periclinal cell wall [162]. Such a re-orientation of cell wall material will focus the associated cuticular strain on the narrow region immediately above the anticlinal cell walls. Because the cuticle is a non-living polymer, it cannot divide but instead is dragged along (stretched) as the underlying surface expands. The strain concentration above the anticlinal cell wall (see just above) makes the cuticle particularly vulnerable to microcracking in this region. This explains the characteristic pattern of microcracks above the anticlinal cell walls as seen in a number of fruit crops, including in apple [162,163]. It also explains why fruits of many species are particularly susceptible to microcracking and russet formation during early-stage development [73]. In early-stage fruit development, the relative surface area growth rate is maximal.

Whether the microcracks propagate more deeply to traverse the entire cuticle or instead remain shallow and limited to the outer (older) volume of the cuticle depends on the relativity between the rate of deposition of new cuticular material (on the inside, adjacent to the cell wall) and the rate of fruit area growth. As mimicked in a uniaxial tensile test of a portion of fruit skin, a high surface area growth rate, in the absence of an appropriately high cuticle deposition, causes the cuticle to thin and thus fail. This occurs before the cellular components fail [164]. Correspondingly, a high rate of cuticle deposition in the absence of an appropriate surface area occurs and results in an increase in cuticle thickness. In apple fruit skin, the rate of cutin and wax deposition usually exceeds that required to match the increase in fruit surface area. Hence, cuticle thickness increases during development [165].

As previously noted, the deposition of cutin occurs on the inner surface of the cuticle (i.e., adjacent to the cell wall) [166]. Thus, the outer cuticle layers are older and, thus, have a longer history of being stretched and are more strained than the younger, inner layers [167]. This results in a radial gradient in strain across the cuticle. The gradient also accounts for the occurrence of shallow microcracks in the outer layers of the apple fruit cuticle that do not extend through to the inner layers [12,168,169]. Because cuticular microcracks differ in depth, the extent of impairment of the cuticle's barrier properties differ. These factors explain why shallow microcracks occur on fruit surfaces without triggering periderm formation, whereas deep ones do trigger it.

Temporal and spatial heterogeneity in fruit expansion during growth is another factor in strain concentration and thus microcracking of the cuticle. The heterogeneity may be due to irregular and variable cell sizes in the epidermis [151,161,170]. Moreover, structures in the epidermis may vary cuticle stiffness—structures such as stomata [171], lenticels [172] and trichomes. Thus, cuticular microcracks may be associated with trichomes and lenticels [173]. Furthermore, cellular heterogeneity may also arise from damage caused by browsing pests,

17

diseases, agrochemical phytotoxicity or freezing injury. Again, periods of high rates of surface area growth result in high susceptibility to microcracking.

Moisture induces microcracking and subsequent russeting—occurring either as liquid-phase water on the fruit surface or as high concentrations of vapor-phase water close by (high humidity). While these trigger effects are well documented for a number of fruitcrop species, including apple, grape and sweet cherry [27,37,62,158], the mechanistic bases for these effects are not known. A possible explanation for moisture-induced microcracking is a higher state of hydration of the cuticle. Cuticular hydration decreases its modulus of elasticity, stiffness and fracture force, whereas its fracture strain increases [8,73]. All these changes increase the likelihood of cuticular microcracking. Other possible explanations include a weakening of cell-to-cell adhesion due to the swelling of cell walls [174].

7.2. Trigger and Signal Transmission

The question remains, how does cuticular microcracking trigger periderm formation? Microcracking occurs in the cuticle, but periderm formation occurs in the hypodermis, several cell layers below. This implies that some signals are transmitted across several cell layers that connect the two processes.

We know that microcracks impair the barrier properties of the cuticle and that this seems to trigger periderm formation. We hypothesize that these two are related, with the reduction in barrier properties somehow triggering the initiation of the periderm. What support is there for this hypothesis? First, when periderm formation is induced experimentally in apple fruit by exposing the fruit surface to moisture, the periderm begins to form only after the surface moisture is removed [37,158]. Apparently, although surface moisture has induced the cuticular microcracking, the periderm formation has been induced by the re-exposure of the (now) microcracked cuticle to the atmosphere. This conclusion is based on histological evidence [37] and gene expression analysis [158]. Second, in another experiment with apple, the formation of a wound periderm was markedly delayed when the periderm-inducing wound was sealed by silicone rubber (Chen, unpublished data). Both these experimental results indicate that the trigger is related to the impaired barrier function. Potential candidate triggers are (1) a decrease in the tissue water potential (more negative) as a result of an increase in transpiration through the microcrack and/or (2) an increase in internal O_2 concentration and/or a decrease in internal CO_2 concentration [37,158]. Based on the literature, an increase in the internal O_2 concentration is the more likely trigger. Thus, in kiwifruit, O_2 is essential for wound-induced suberization [175]; in grape, the O_2 concentrations just below the cuticle is lower than in the ambient atmosphere and decreases with increasing distance from the surface [176]; in apple, similar results have been reported [177] and, in potato, periderm and suberin formation are inhibited by a low O_2 concentration and a high CO_2 concentration [178,179].

8. Management

Various approaches have been investigated to reduce or eliminate russeting: (1) Spray applications of gibberellins and other plant growth regulators (PGRs), (2) applications of foliar fertilizers and other compounds, (3) the exclusion of moisture using bagging and (4) selective breeding.

8.1. Application of PGRs

The gibberellins A_3 (GA_3) and A_{4+7} (GA_{4+7}) are used to improve peel finish and reduce russet in russet-susceptible cultivars of apple, pear, grape and pomegranate (Table 1). Typically, four sprays of 10 mg L^{-1} gibberellic acid (GA) at 10 d intervals starting from petal fall are applied. Russet is reduced significantly (Table 4). The modes of action of GA in decreasing russet formation are several-fold. First, GA results in more uniform and smaller epidermal cells [30]. Skins comprising smaller epidermal cells are likely to be mechanically stiffer. Furthermore, the structural support of the cuticle provided by smaller cells is more uniform. This decreases stress concentrations, a critical factor in microcracking. Second,

18

GA decreases moisture-induced microcracking in russet-susceptible 'Golden Delicious' apple [73]. Applications of GA have no effect on cuticle mass, wax content or mechanical strength of the isolated apple fruit cuticle [73].

Often, GA is combined with the cytokinin benzyladenine (BA). In this combination, BA is thought to offset certain adverse effects that GA may have on flowering [58,80]. Further, GA_{4+7} plus BA (known commercially as 'Promalin') increases fruit size and alters fruit shape. The length to width ratio of the fruit increases, particularly in the calyx region, with the result that fruit have more extended calyx lobes [80,180]. If BA is applied alone, it increases russeting [58,93]. The reason for this negative effect is unknown. The combination GA_{4+7} plus BA decreases russet only to the same extent as GA_{4+7} (Table 4).

In grapes, GA_3 plus the cytokinin N-(2-chloro-4-pyridyl)-N'-phenylurea (CPPU) reduces russeting, but GA_3 alone has little effect on russeting [181]. It is thought that CPPU stimulates cell division with the result that fruit have larger numbers of smaller cells [182,183]. Whether these effects also apply for the epidermis and whether microcracking of the cuticle is decreased, as observed in apple, is unknown. We suggest that such an effect would not be unlikely, and it would also account for reduced russeting following CPPU application.

8.2. Foliar Sprays of Fertilizers and Other Compounds

Insufficient supplies of boron (B) cause a number of fruit disorders, including russeting [184]. In mango, sprays of B plus Ca result in thicker cell walls and smaller intercellular spaces. As a consequence, cells are more densely packed, thereby providing greater mechanical stiffness and thus better support for the cuticle [185]. The potential roles of B in russeting also include effects on cell wall synthesis, lignification and cell wall structure, for example, by cross-linking cell wall constituents, such as pectins [186]. It is thought that B also helps maintain cell wall extensibility. In B-deficient plants, cell walls become less elastic and more rigid [184]. This causes cell walls to crack more easily and/or cells to separate from one another under tension along their middle lamellae. A separation of epidermal and/or hypodermal cells weakens the cellular support substrate for the cuticle and is therefore likely to increase cuticular microcracking. There were no effects on russeting following applications of B in pomegranate [137]. However, B applied alone or in combination with Ca did reduce russeting in tomato [119,124]. Several studies have reported decreased microcracking of fruit following applications of B, with or without Ca [187–190]. Since the initial steps in fruit cracking (macrocracking) and russeting would seem to be the same, in that both processes first require cuticular microcracking [191], it would not seem unlikely that applications of B will also decrease microcracking and russeting.

A small number of studies have reported on the effects of 'exotic' compounds on russeting. Thus, chlorogenic acid applied during early development reduced russet formation in 'Golden Delicious' apples. The authors suggest inhibition of lignin synthesis is the underlying mechanism [84]. In other studies, calmodulin and various fruit coatings have been applied, and these are reported to reduce russeting [82]. While the mode of action of calmodulin in inhibiting russeting is unknown, fruit coatings are likely to cover and thus help seal cuticular microcracks and thereby may help restore the impaired barrier functions of a microcracked cuticle. Unfortunately, direct evidence for the effect is lacking. For such an effect, the permeance of the 'exotic' coating to O_2, CO_2 and ethylene should be similar to that of an intact cuticle. Ideally, the coating should be waterproof if it is to be rain-fast. Lastly, the stomatal conductance of the leaves must not be compromised by these exotic coatings, or photosynthesis will be adversely affected—note that it is commercially impracticable to apply these coatings to the fruit without also applying them to the leaves.

19

Table 4. Effect of the plant growth regulators (PGR) benzyladenine (BA), 4-(2,2-Dimethylhydrazin-1-yl)-4-oxobutanoic acid (daminozide), ethephon, gibberellin A_{4+7} (GA_{4+7}), gibberellic acid (GA_3) acid (GA), N-(2-chloro-4-pyridyl)-N'-phenylurea (CPPU), (2RS, 3RS)-1-(4-chlorophenyl)-4,4-dimethyl-2-(1H-1,2,4-triazol-1-yl) pentan-3-ol (Paclobutrazol) on russeting. Results are compiled from literature sources.

PGR	Crop	Cultivar	Concentration ($mg\ L^{-1}$)	Time and Frequency of Application	Effect on Russet	Reference
BA	Apple	Golden Delicious, Jonathan	50 or 150	80% PF and once after 7–10 d	Increased	[56]
BA	Apple	Elstar	200 or 300	At 10–12 mm fruit diameter	Increased	[57]
BA	Apple	Golden Delicious	50	0, 4, 12, 26, 42, 57 DAFB	Increased	[58]
BA	Pear	Bartlett	150	PF and 10 mm stage	Increased	[93]
Daminozide	Apple	Golden Delicious	2000	3 DAFB	Increased	[48]
Ethephon	Apple	Fuji	400	FB	Increased	[59]
GA_4, GA_7 and GA_{4+7}	Apple	Golden Delicious, Karmijn de Sonnaville	10	4 applications in 10 d intervals beginning at PF	Decreased	[32]
GA_{4+7}	Apple	Golden Delicious	200	4 applications in 7 d intervals beginning at PF	Decreased	[75]
GA_{4+7}	Apple	Golden Delicious	62.5, 125 or 250	8–15 DAFB	Decreased	[76]
GA_{4+7}	Apple	Golden Delicious	25	0, 4, 12, 26, 42, 57 DAFB	Decreased	[58]
GA_{4+7}	Apple	Golden Delicious	10	4 applications in 10 d intervals beginning at PF	Decreased	[73]
GA_{4+7}	Apple	Golden Delicious	10	4 applications in 10 d intervals beginning at PF	Decreased	[77]
GA_{4+7}	Apple	Golden Delicious	10	PF	Decreased	[33]
GA_{4+7}	Apple	Golden Delicious	15 or 30	5 applications in 7 to 10 d intervals beginning at PF	Decreased	[30]
GA_{4+7}	Apple	Golden Delicious	10	5 applications in 7 d intervals beginning at FB	Decreased	[78]
GA_{4+7}	Apple	Golden Delicious	20	3 applications in 10 d intervals beginning at PF	Decreased	[72]
GA_{4+7}	Apple	Golden Delicious, Jonathan	25–200	80% PF and once after 7–10 d	Decreased	[56]
GA_{4+7}	Apple	Golden Delicious	5, 10	4 applications in 7 d intervals beginning at PF	Decreased	[79]
GA_{4+7}	Pear	Packham's Triumph	5, 10, 20	80% PF and 0 to 3 additional sprays at 10 or 15 d intervals	Decreased	[105]
GA_{4+7} + BA	Apple	Golden Delicious	6, 12, 24, 50	Beginning of bloom and 3 additional sprays at 7 d intervals	Decreased	[80]
GA_{4+7} + BA	Apple	Scarlet Spur II	1, 2.5 or 5	3 to 4 applications in 10 d intervals beginning at PF	Decreased	[81]
GA_3	Apple	Karmijn de Sonnaville	10	4 applications in 10 d intervals beginning at PF	Decreased	[32]
GA_3	Apple	Golden Delicious	100 or 200	PF	Decreased	[33]
GA_3	Apple	Golden Delicious	100	PF	Increased	[60]
GA_3	Pomegranate	G-137	50	Mid May–Mid June	Decreased	[137]
CPPU	Apple	Scarlet Spur II	2, 5 or 10	3 to 4 applications in 10 d intervals beginning at PF	Decreased	[81]
CPPU	Apple	Golden Delicious	20	PF	Increased	[60]
CPPU	Pomegranate	Kandhari	5 or 10	Mid May	Decreased	[140]
CPPU	Pomegranate	G-137	5	Mid May–Mid June	Decreased	[137]

Table 4. *Cont.*

PGR	Crop	Cultivar	Concentration (mg L^{-1})	Time and Frequency of Application	Effect on Russet	Reference
CPPU+GA$_3$	Grapes	Shine Muscat	10 CPPU + 25 GA$_3$	FB	Decreased	[132]
CPPU+GA$_3$, CPPU+GA$_4$	Apple	Golden Delicious	20 CPPU + 100 GA$_3$/GA$_4$	PF	Increased	[60]
Paclobutrazol	Apple	Suntan	120 or 240	3 weeks after FB	Increased	[51]
Paclobutrazol	Apple	Smoothee Golden Delicious	250	Between early bloom and PF	Increased	[61]

FB: full bloom; PF: petal fall; DAFB: days after full bloom.

21

Where russeting is induced primarily by insect pests or fungi, spray applications of suitable agrochemicals will likely be successful in decreasing russeting. Examples reported include applications of zineb for citrus mites [108,109,112] or captafol or ziram for scab in prune [113]. However, the right dose and timing must be chosen, or the product may itself cause russeting.

8.3. Bagging

Fruit bagging is reported to be a successful countermeasure to inhibit russeting in several fruitcrop species (Table 5). Bagging prevents russeting by keeping the fruit surface dry. However, selecting a suitable material for the bag is critical as the bag material must prevent contact of the fruit surface with liquid water and, at the same time, avoid an elevated humidity in the microclimate of the enclosed fruit. A high-humidity environment inside the bag severely increases russeting [17], probably by increasing cuticular microcracking [73].

Furthermore, the bagged fruit must not overheat [192]. The spectral properties of the bagging material affect the amount and wavelengths of light reaching the fruit surface [193]. In those fruitcrop species and cultivars with colored skins, and where light absorption by the bag impairs pre-harvest fruit coloring, the bag is removed shortly before harvest to induce coloring. With this, there is an increased risk of sunburn, so removal of the bag must be done cautiously, possibly stepwise—for example, by using multi-layer bags [192]. Other benefits of pre-harvest bagging include a decreased incidence of sunburn [194,195], pest infestation and hail damage [196]. However, bagging fruit is laborious, so it requires a high-value product, a high-end market and/or a low labor cost for it to be economic.

Table 5. Effect of bagging fruit on russet and color. Data are compiled from literature sources.

Type of Bag	Crop	Cultivar	Time of Bagging	Effect on Russet	Effect on Color	Reference
Polythene bag (Kordite freeze bags)	Apple	Golden Delicious, Rome Beauty	18 mm diameter	Increased	Greener groundcolor	[17]
Polythene bag with aluminum paper	Pear	Packham's Triumph	Fruit set	Increased	Not determined	[105]
Microperforated polypropylene bags	Pear	Doyenne du Comice	30 DAFB	Decreased	Not determined	[100]
Nylon (polyamide)	Apple	Golden Delicious, Rome Beauty	18 mm diameter	Increased	Decreased red color	[17]
Kraft paper bags	Apple	Golden Delicious, Rome Beauty	18 mm diameter	Decreased	Decreased red color	[17]
Kraft paper bags	Mango	Apple	70 DAFB	Reduced	Decreased red color	[135]
Kraft paper bags	Apple	Golden Delicious	5 DAFB	Reduced	Not determined	[48]
White, yellow and discoloration bags	Apple	Gamhong	20, 30 and 40 DAFB	Reduced	No change	[82]
Light impermeable double layer paper bags	Apple	Golden Delicious	20 DAFB	No russet	Not determined	[86]
Paper bags (single layer)	Pear	Cuiguan	35 DAFB	Decreased	More yellow	[101]
Paper bags (white, single layer)	Pear	Cuiguan	20 DAFB	No russet	No change	[102]
Paper bags (yellow-white, double layer)	Pear	Cuiguan	40 DAFB	No russet	No change	[102]
Papers bags (single layer + double layers)	Pear	Cuiguan	28 DAFB	Decreased	Lighter color	[103]
Paper bags (double layer)	Pear	Cuiguan	20 + 45 DAFB	No russet	Greener groundcolor	[101]
Paper bag (double layered with attached filter)	Pear	Niitaka	30–40 DAFB	Decreased	Lighter color	[104]
Paper bag (triple layer)	Pear	Concorde	After June drop	Increased	Lighter color	[197]

DAFB = days after full bloom.

23

8.4. Breeding

In the long term, a breeding approach to control russet will likely be the most successful since russet susceptibility is a genetically controlled trait [198–201]. For a review on the molecular biology of russet formation, the reader is referred to the recent reviews by Macnee et al. [23] and Wang et al. [24].

In apple, the anatomies of the skins of russet-susceptible and russet-non-susceptible cultivars have been compared. The cellular layers of the skin differ [151,161]. The russet-susceptible cultivars have larger cells and more variable cell sizes in both the epidermis and hypodermis [161,170]. These result in higher stiffness and lower strain at fracture during early fruit development when russet susceptibility is highest [161]. When subjected to a tangential growth strain, skin cells of irregular size and shape result in greater stress concentrations and increased likelihood of failure. Comparisons of russet-susceptible and russet-non-susceptible cultivars reveal no consistent differences in cuticular properties—such as mass per unit area of the cuticular membrane, the dewaxed cuticular membrane or wax content [31]. Furthermore, there were no significant differences relating to russet susceptibility in cuticular strain or cuticular mechanical properties, as determined in uniaxial tensile tests (i.e., maximum force, strain at maximum force or stiffness of the cuticular membrane) [18]. Genotypes meeting the following criteria are likely to exhibit low susceptibility to russeting: (1) A long period of skin cell division, so the increase in fruit surface area is substantially accounted for by increases in the numbers of cells, rather than by increased cell expansion (which is often associated with changes in epidermal cell aspect ratio). (2) Smaller epidermal and hypodermal cells are also of more uniform size. These are better able to sustain high tensile forces and offer less stress concentration and lower chances of failure. (3) Lack of stress concentration at stomata, lenticels and trichomes. Susceptibility to failure at these sites may be checked by monitoring formation of microcracks following moisture exposure of the fruit surface. Incubating fruit in the fluorescent tracer acridine orange permits localized penetration through microcracks. When viewed using a fluorescence microscope, microcracks are easily identified by the fluorescing 'halo' surrounding sites of preferential uptake.

9. Conclusions

The locally impaired barrier properties of the cuticle due to a microcrack and, probably, increased O_2 diffusion seem to be the primary trigger for periderm formation. Microcracking is likely the integrator of a range of factors that induce russeting. These factors include growth stress, surface moisture and high humidity, but also pests and diseases, mechanical wounds and freezing temperatures. Significant progress has been made in our understanding of molecular biology and of the physiology of russeting.

The classical concepts of reducing russeting by spray applications of gibberellins, with or without cytokinins, or of B and/or of Ca have a sound mechanistic basis and are reported to be effective in a range of fruitcrop species. The identification of impaired barrier properties of the cuticle as the trigger causing periderm formation now provides promising options for russet management that merit further research. These include applications of 'exotic' coatings during critical phases of fruit development, especially when relative surface area growth rates are high. In addition, the prevention of radial extension (i.e., deepening) of microcracks by stimulating the rate of cuticle deposition is not an unrealistic strategy.

Recently, evidence has been presented that feeding oleic acid to the apple fruit surface results in significant incorporation of oleic acid into the cutin fraction [202]. If this treatment could be upscaled in the field to generate gravimetrically detectable increases in cuticle thickness following spray application of a suitable precursor, the increased cutin deposition could hinder cuticle microcracks from propagating so as to fully traverse the cuticle. When applied during phases of high rates of relative surface area growth, the formation of traversing microcracks and, hence, of russet may be prevented or reduced. Several of these aspects merit further study.

References

1. Becker, M.; Kerstiens, G.; Schönherr, J. Water permeability of plant cuticles: Permeance, diffusion and partition coefficients. *Trees* **1986**, *1*, 54–60. [CrossRef]
2. Yeats, T.H.; Rose, J.K. The formation and function of plant cuticles. *Plant Physiol.* **2013**, *163*, 5–20. [CrossRef] [PubMed]
3. Krauss, P.; Markstadter, C.; Riederer, M. Attenuation of UV radiation by plant cuticles from woody species. *Plant Cell Environ.* **1997**, *20*, 1079–1085. [CrossRef]
4. Serrano, M.; Coluccia, F.; Torres, M.; L'Haridon, F.; Metraux, J.P. The cuticle and plant defense to pathogens. *Front. Plant Sci.* **2014**, *5*, 274. [CrossRef]
5. Reina-Pinto, J.J.; Yephremov, A. Surface lipids and plant defenses. *Plant Physiol. Biochem.* **2009**, *47*, 540–549. [CrossRef] [PubMed]
6. Bukovac, M.J.; Petracek, P.D. Characterizing pesticide and surfactant penetration with isolated plant cuticles. *Pestic. Sci.* **1993**, *37*, 179–194. [CrossRef]
7. Knoche, M.; Lang, A. Ongoing growth challenges fruit skin integrity. *Crit. Rev. Plant Sci.* **2017**, *36*, 190–215. [CrossRef]
8. Khanal, B.P.; Knoche, M. Mechanical properties of cuticles and their primary determinants. *J. Exp. Bot.* **2017**, *68*, 5351–5367. [CrossRef]
9. Piringer, A.A.; Heinze, P.H. Effect of light on the formation of a pigment in the tomato fruit cuticle. *Plant Physiol.* **1954**, *29*, 467–472. [CrossRef]
10. Lancaster, J.E. Regulation of skin color in apples. *Crit. Rev. Plant Sci.* **1992**, *10*, 487–502. [CrossRef]
11. Khanal, B.P.; Ikigu, G.M.; Knoche, M. Russeting partially restores apple skin permeability to water vapour. *Planta* **2019**, *249*, 849–860. [CrossRef] [PubMed]
12. Faust, M.; Shear, C.B. Russeting of apples, an interpretive review. *HortScience* **1972**, *7*, 233–235.
13. Charoenchongsuk, N.; Matsumoto, D.; Itai, A.; Murayama, H. Ripening characteristics and pigment changes in russeted pear fruit in response to ethylene and 1-MCP. *Horticulturae* **2018**, *4*, 22. [CrossRef]
14. Gerchikov, N.; Keren-Keiserman, A.; Perl-Treves, R.; Ginzberg, I. Wounding of melon fruits as a model system to study rind netting. *Sci. Hortic.* **2008**, *117*, 115–122. [CrossRef]
15. Sorauer, P.; Lindau, G.; Reh, L. *Manual of Plant Diseases*, 3rd ed.; The Record Press: Wilkes-Barré, PA, USA, 1922.
16. Bell, H.P. The origin of russeting in the Golden Russet apple. *Can. J. Res.* **1937**, *15*, 560–566. [CrossRef]
17. Tukey, L.D. Observations on the russeting of apples growing in plastic bags. *Proc. Am. Soc. Hortic. Sci.* **1959**, *74*, 30–39.
18. Khanal, B.P.; Grimm, E.; Knoche, M. Russeting in apple and pear: A plastic periderm replaces a stiff cuticle. *AoB Plants* **2013**, *5*, pls048. [CrossRef]
19. Jones, K.M.; Bound, S.A.; Oakford, M.J.; Wilson, D. A strategy for reducing russet in Red Fuji apples while maintaining control of black spot (*Venturia inaequalis*). *Aust. J. Exp. Agric.* **1994**, *34*, 127–130. [CrossRef]
20. Gossard, H.A. Commercial apple orcharding in Ohio. *Ohio Agric. Exp. Stn.* **1911**, *12*, 3–15.
21. Hall, F.H.; Stewart, F.C.; Blodgett, F.H. Fruit diseases found along the Hudson. *N. Y. Agric. Exp. Stn. Bull.* **1899**, *167*, 1–6.
22. Cole, S.W. *The American Fruit Book; Containing Directions for Raising, Propagating, and Managing Fruit Trees, Shrubs, and Plants; with a Description of the Best Varieties of Fruit, Including New and Valuable Kinds*; A.O. Moore Agricultural Book Publisher: New York, NY, USA, 1858.
23. Macnee, N.C.; Rebstock, R.; Hallett, I.C.; Schaffer, R.J.; Bulley, S.M. A review of current knowledge about the formation of native periderm exocarp in fruit. *Funct. Plant. Biol.* **2020**, *47*, 1019–1031. [CrossRef] [PubMed]
24. Wang, Y.; Dai, M.; Cai, D.; Zhang, S.J.; Shi, Z. A review for the molecular research of russet/semi-russet of sand pear exocarp and their genetic characters. *Sci. Hortic.* **2016**, *210*, 138–142. [CrossRef]
25. Duggan, J.B. The training of apple trees. *Sci. Hortic.* **1957**, *13*, 62–73.
26. Biedenfeld, F. *Handbuch Aller Bekannten Obstsorten, Band 2*; Frommann: Jena, Germany, 1854.
27. Thalheimer, M. About the russetting of apples in 2018. *Laimburg J.* **2019**, *1*, 1–4.
28. Legay, S.; Guerriero, G.; Andre, C.; Guignard, C.; Cocco, E.; Charton, S.; Boutry, M.; Rowland, O.; Hausman, J.F. MdMyb93 is a regulator of suberin deposition in russeted apple fruit skins. *New Phytol.* **2016**, *212*, 977–991. [CrossRef]
29. Skene, D.S. The development of russet, rough russet and cracks on the fruit of the apple Coxs Orange Pippin during the course of the season. *J. Hortic. Sci.* **1982**, *57*, 165–174. [CrossRef]

25

30. Curry, E. Increase in epidermal planar cell density accompanies decreased russeting of 'Golden Delicious' apples treated with Gibberellin A$_{4+7}$. *HortScience* **2012**, *47*, 232–237. [CrossRef]
31. Khanal, B.P.; Shrestha, R.; Hückstädt, L.; Knoche, M. Russeting in apple seems unrelated to the mechanical properties of the cuticle at maturity. *HortScience* **2013**, *48*, 1135–1138. [CrossRef]
32. Wertheim, S.J. Fruit russeting in apple as affected by various gibberellins. *J. Hortic. Sci.* **1982**, *57*, 283–288. [CrossRef]
33. Taylor, B.K. Effects of gibberellin sprays on fruit russet and tree performance of Golden Delicious apple. *J. Hortic. Sci.* **1978**, *53*, 167–169. [CrossRef]
34. Simons, R.K.; Chu, M.C. Periderm morphology of mature Golden Delicious apple with special reference to russeting. *Sci. Hortic.* **1978**, *8*, 333–340. [CrossRef]
35. Knoche, M.; Grimm, E. Surface moisture induces microcracks in the cuticle of 'Golden Delicious' apple. *HortScience* **2008**, *43*, 1929–1931. [CrossRef]
36. Winkler, A.; Grimm, E.; Knoche, M.; Lindstaedt, J.; Köpcke, D. Late-season surface water induces skin spot in apple. *HortScience* **2014**, *49*, 1324–1327. [CrossRef]
37. Chen, Y.H.; Straube, J.; Khanal, B.P.; Knoche, M.; Debener, T. Russeting in apple is initiated after exposure to moisture ends-I. Histological evidence. *Plants* **2020**, *9*, 1293. [CrossRef]
38. Khanal, B.P.; Imoro, Y.; Chen, Y.H.; Straube, J.; Knoche, M. Surface moisture increases microcracking and water vapour permeance of apple fruit skin. *Plant. Biol.* **2021**, *23*, 74–82. [CrossRef]
39. Sánchez, E.; Soto, J.M.; Uvalle, J.X.; Hernández, A.P.; Ruiz, J.M.; Romero, L. Chemical treatments in "Golden Delicious Spur" fruits in relation to russeting and nutritional status. *J. Plant. Nutr.* **2001**, *24*, 191–202. [CrossRef]
40. Wójcik, P.; Filipczak, J.; Wójcik, M. Effects of prebloom sprays of tryptophan and zinc on calcium nutrition, yielding and fruit quality of 'Elstar' apple trees. *Sci. Hortic.* **2019**, *246*, 212–216. [CrossRef]
41. Palmer, J.W.; Davies, S.B.; Shaw, P.W.; Wünsche, J.N. Growth and fruit quality of 'Braeburn' apple (*Malus domestica*) trees as influenced by fungicide programmes suitable for organic production. *N. Z. J. Crop Hortic. Sci.* **2003**, *31*, 169–177. [CrossRef]
42. Brown, G.S.; Kitchener, A.E.; Barnes, S. Calcium hydroxide sprays for the control of black spot on apples—Treatment effects on fruit quality. *Acta Hortic.* **1998**, *513*, 47–52. [CrossRef]
43. Teviotdale, B.L.; Viveros, M. Fruit russetting and tree toxicity symptoms associated with copper treatments of Granny Smith apple trees (*Malus sylvestris* Mill.). *Acta Hortic.* **1999**, *489*, 565–571. [CrossRef]
44. Momol, M.T.; Norelli, J.L.; Aldwinckle, H.S. Evaluation of biological control agents, systemic acquired resistance inducers and bactericides for the control of fire blight on apple blossom. *Acta Hortic.* **1999**, *489*, 553–557. [CrossRef]
45. Marchioretto, L.D.; De Rossi, A.; do Amaral, L.O.; Ribeiro, A.M.A.D. Efficacy and mode of action of blossom thinners on 'Fuji More' apple trees. *Sci. Hortic.* **2019**, *246*, 634–642. [CrossRef]
46. Peck, G.M.; DeLong, C.N.; Combs, L.D.; Yoder, K.S. Managing apple crop load and diseases with bloom thinning applications in an organically managed 'Honeycrisp'/'MM.111' orchard. *HortScience* **2017**, *52*, 377–381. [CrossRef]
47. Bound, S.A. Alternate thinning chemicals for apples. *Acta Hortic.* **2010**, *884*, 229–236. [CrossRef]
48. Creasy, L.L.; Swartz, H.J. Agents influencing russet on Golden Delicious apple fruits. *J. Am. Soc. Hortic. Sci.* **1981**, *106*, 203–206.
49. Stopar, M. Vegetable oil emulsions, NaCl, CH$_3$COOH and CaS$_x$ as organically acceptable apple blossom thinning compounds. *Eur. J. Hortic. Sci.* **2008**, *73*, 55–61.
50. Noga, G.J.; Bukovac, M.J. Impact of surfactants on fruit quality of 'Schattenmorelle' sour cherries and 'Golden Delicious' apples. *Acta Hortic.* **1986**, *179*, 771–778. [CrossRef]
51. Richardson, P.J.; Webster, A.D.; Quinlan, J.D. The effect of paclobutrazol sprays with or without the addition of surfactants on the shoot growth, yield and fruit quality of the apple cultivars Cox and Suntan. *J. Hortic. Sci.* **1986**, *61*, 439–446. [CrossRef]
52. Stopar, M.; Hladnik, J. Polysorbates 20, 60 and 80 are apple thinning agents. *Acta Hortic.* **2020**, *1295*, 57–62. [CrossRef]
53. Alegre, S.; Alins, G. The flower thinning effect of different compounds on organic 'Golden Smoothee (R)' apple trees. *Acta Hortic.* **2007**, *737*, 67–69. [CrossRef]
54. Bound, S.A. The influence of endothal and 6-benzyladenine on crop load and fruit quality of red 'Delicious' apple. *J. Hortic. Sci. Biotechnol.* **2001**, *76*, 691–699. [CrossRef]
55. Bound, S.A.; Jones, K.M. Ammonium thiosulphate as a blossom thinner of 'Delicious' apple, 'Winter Cole' pear and 'Hunter' apricot. *Aust. J. Exp. Agric.* **2004**, *44*, 931–937. [CrossRef]
56. Taylor, B.K. Reduction of apple skin russeting by gibberellin A$_{4+7}$. *J. Hortic. Sci.* **1975**, *50*, 169–172. [CrossRef]
57. Maas, F. Thinning 'Elstar' apple with benzyladenine. *Acta Hortic.* **2006**, *727*, 415–421. [CrossRef]
58. McLaughlin, J.M.; Greene, D.W. Effects of BA, GA$_{4+7}$, and daminozide on fruit set, fruit quality, vegetative growth, flower initiation, and flower quality of 'Golden Delicious' apple. *J. Am. Soc. Hortic. Sci.* **1984**, *109*, 34–39.
59. Jones, K.M.; Koen, T.B.; Bound, S.A.; Oakford, M.J. Some reservations in thinning 'Fuji' apples with naphthalene acetic acid (NAA) and ethephon. *N. Z. J. Crop Hortic. Sci.* **1991**, *19*, 225–228. [CrossRef]
60. Bangerth, F.; Schröder, M. Strong synergistic effects of gibberellins with the synthetic cytokinin N-(2-Chloro-4-Pyridyl)-N-Phenylurea on parthenoscarpic fruit set and some other fruit characteristics of apple. *Plant. Growth Regul.* **1994**, *15*, 293–302. [CrossRef]
61. El-Khoreiby, A.M.; Unrath, C.R.; Lehman, L.J. Paclobutrazol spray timing influences apple tree growth. *HortScience* **1990**, *25*, 310–312. [CrossRef]

62. Daines, R.; Weber, D.J.; Bunderson, E.D.; Roper, T. Effect of early sprays on control of powdery mildew fruit russet on apples. *Plant. Dis.* **1984**, *68*, 326–328. [CrossRef]
63. Heidenreich, M.C.M.; Corral-Garcia, M.R.; Momol, E.A.; Burr, T.J. Russet of apple fruit caused by *Aureobasidium pullulans* and *Rhodotorula glutinis*. *Plant Dis.* **1997**, *81*, 337–342. [CrossRef]
64. Gildemacher, P.; Heijne, B.; Silvestri, M.; Houbraken, J.; Hoekstra, E.; Theelen, B.; Boekhout, T. Interactions between yeasts, fungicides and apple fruit russeting. *FEMS Yeast Res.* **2006**, *6*, 1149–1156. [CrossRef] [PubMed]
65. Goffinet, M.C.; Burr, T.J.; Heidenreich, M.C.; Welsel, M.J. Developmental anatomy of russet of 'McIntosh' apple fruit induced by the fungus *Aureobasidium pullulans*. *HortScience* **2006**, *41*, 983. [CrossRef]
66. Gildemacher, R.; Heijne, B.; Houbraken, J.; Vromans, T.; Hoekstra, S.; Boekhout, T. Can phyllosphere yeasts explain the effect of scab fungicides on russeting of Elstar apples? *Eur. J. Plant. Pathol.* **2004**, *110*, 929–937. [CrossRef]
67. Li, C.J.; Yaegashi, H.; Kishigami, R.; Kawakubo, A.; Yamagishi, N.; Ito, T.; Yoshikawa, N. Apple russet ring and apple green crinkle diseases: Fulfillment of Koch's postulates by virome analysis, amplification of full-length cDNA of viral genomes, in vitro transcription of infectious viral RNAs, and reproduction of symptoms on fruits of apple trees inoculated with viral RNAs. *Front. Microbiol.* **2020**, *11*, 1627. [CrossRef] [PubMed]
68. Wood, G.A. Russet ring and some associated virus disorders of apple (*Malus sylvestris* (L.) Mill) in New England. *N. Z. J. Argric. Res.* **1972**, *15*, 405–412. [CrossRef]
69. Welsh, M.F.; May, J. Virus etiology of foliar vein-flecking or ring pattern and fruit russeting or blotch on apple. *Can. J. Plant. Sci.* **1967**, *47*, 703–708. [CrossRef]
70. Easterbrook, M.A.; Fuller, M.M. Russeting of apples caused by apple rust mite *Aculus schlechtendali* (Acarina, Eriophyidae). *Ann. Appl. Biol.* **1986**, *109*, 1–9. [CrossRef]
71. Duso, C.; Castagnoli, M.; Simoni, S.; Angeli, G. The impact of eriophyids on crops: Recent issues on Aculus schlechtendali, Calepitrimerus vitis and *Aculops lycopersici*. *Exp. Appl. Acarol.* **2010**, *51*, 151–168. [CrossRef]
72. McArtney, S.; Obermiller, J.D.; Green, A. Prohexadione-Ca reduces russet and does not negate the efficacy of GA$_{4+7}$ sprays for russet control on 'Golden Delicious' apples. *HortScience* **2007**, *42*, 550–554. [CrossRef]
73. Knoche, M.; Khanal, B.P.; Stopar, M. Russeting and microcracking of 'Golden Delicious' apple fruit concomitantly decline due to gibberellin A$_{4+7}$ application. *J. Am. Soc. Hortic. Sci.* **2011**, *136*, 159–164. [CrossRef]
74. Fogelman, E.; Redel, G.; Doron, I.; Naor, A.; Ben-Yashar, E.; Ginzberg, I. Control of apple russeting in a warm and dry climate. *J. Hortic. Sci. Biotechnol.* **2009**, *84*, 279–284. [CrossRef]
75. Eccher, T. Russeting of Golden Deliciois apples as related to endogenous and exogenous gibberellins. *Acta Hortic.* **1978**, *80*, 381–386. [CrossRef]
76. Eccher, T.; Boffelli, G. Effects of dose and time of application of GA$_{4+7}$ on russeting, fruit set and shape of 'Golden Delicious' apples. *Sci. Hortic.* **1981**, *14*, 307–314. [CrossRef]
77. Wertheim, S.J. Chemical thinning of Golden Delicious apple with NAAm and/or carbaryl in combination with a spreader and the anti-russeting agent GA$_{4+7}$. *Acta Hortic.* **1986**, *179*, 659–666. [CrossRef]
78. Steenkamp, J.; Vanzyl, H.J.; Westraad, I. A preliminary evaluation of various chemical substances for the control of calyx-end russeting in Golden Delicious apples. *J. Hortic. Sci.* **1984**, *59*, 501–505. [CrossRef]
79. Bubán, T.; Rátz, M.; Oláh, L. Improved fruit shape and less russeting of apples by using gibberellins. *Acta Hortic.* **1993**, *329*, 137–139. [CrossRef]
80. Eccher, T. Control of russeting of Golden Delicious apples by growth regulator treatments. *Acta Hortic.* **1983**, *137*, 375–382. [CrossRef]
81. Sharma, S.; Sharma, N.; Sharma, D.P.; Chauhan, N. Effects of GA$_{4+7}$ + BA and CPPU on russeting and fruit quality in apple (*Malus × domestica*). *Indian J. Agric. Sci.* **2020**, *90*, 74–77.
82. Moon, Y.J.; Nam, K.W.; Kang, I.K.; Moon, B.W. Effects of tree-spray of calcium agent, coating agent, GA$_{4+7}$ + BA and paper bagging on russet prevention and quality of 'Gamhong' apple fruits. *Korean J. Hortic. Sci. Technol.* **2016**, *34*, 528–536. [CrossRef]
83. Basak, A.; Bielicki, P. Effect of novel organic/mineral biostimulators on fruit quality parameters in apple. *Acta Hortic.* **2010**, *873*, 295–302. [CrossRef]
84. Wang, L.; Li, J.; Gao, J.; Feng, X.; Shi, Z.; Gao, F.; Xu, X.; Yang, L. Inhibitory effect of chlorogenic acid on fruit russeting in 'Golden Delicious' apple. *Sci. Hortic.* **2014**, *178*, 14–22. [CrossRef]
85. Dayioglu, A.; Hepaksoy, S. Effects of shading nets on sunburn and quality of 'Granny Smith' apple fruits. *Acta Hortic.* **2016**, *1139*, 523–528. [CrossRef]
86. Yuan, G.; Bian, S.; Han, X.; He, S.; Liu, K.; Zhang, C.; Cong, P. An integrated transcriptome and proteome analysis reveals new insights into russeting of bagging and non-bagging "Golden Delicious" apple. *Int. J. Mol. Sci.* **2019**, *20*, 4462. [CrossRef] [PubMed]
87. Scharwies, J.D.; Grimm, E.; Knoche, M. Russeting and relative growth rate are positively related in 'Conference' and 'Condo' pear. *HortScience* **2014**, *49*, 746–749. [CrossRef]
88. Shi, C.H.; Qi, B.X.; Wang, X.Q.; Shen, L.Y.; Luo, J.; Zhang, Y.X. Proteomic analysis of the key mechanism of exocarp russet pigmentation of semi-russet pear under rainwater condition. *Sci. Hortic.* **2019**, *254*, 178–186. [CrossRef]
89. Asin, L.; Torres, E.; Vilardell, P. Orchard cooling with overtree microsprinkler irrigation to increase fruit russet on 'Conference' pear. *Acta Hortic.* **2011**, *909*, 557–564. [CrossRef]

27

90. Sugar, D.; Villardel, P.; Asin, L. Relationship of weather factors to russet incidence in 'Comice' and 'Bosc' pear fruit. *Acta Hortic.* **2015**, *1094*, 533–538. [CrossRef]
91. Sugar, D.; Basile, S.R. Russet induction in 'Beurre Bosc' and 'Taylor's Gold' pears. *Acta Hortic.* **2008**, *800*, 257–261. [CrossRef]
92. Maas, F.M.; Kanne, H.J.; van der Steeg, P.A.H. Chemical thinning of 'Conference' pears. *Acta Hortic.* **2010**, *884*, 293–304. [CrossRef]
93. Greene, D.W. Influence of abscisic acid and benzyladenine on fruit set and fruit quality of 'Bartlett' pears. *HortScience* **2012**, *47*, 1607–1611. [CrossRef]
94. Civolani, S. The past and present of pear protection against the pear psylla, *Cacopsylla pyri* L. In *Insecticides—Pest Engineering*; Perveen, F., Ed.; IntechOpen: London, UK, 2012.
95. Sanchez, J.A.; Carrasco-Ortiz, A.; López-Gallego, E.; Ramírez-Soria, M.J.; La Spina, M. Ants reduce fruit damage caused by psyllids in Mediterranean pear orchards. *Pest. Manag. Sci.* **2020**, *77*, 1886–1892. [CrossRef]
96. Westigard, P.H. Pest status of insects and mites on pear in Southern Oregon. *J. Econ. Entomol.* **1973**, *66*, 227–232. [CrossRef]
97. Lindow, S.E.; Desurmont, C.; Elkins, R.; McGourty, G.; Clark, E.; Brandl, M.T. Occurrence of indole-3-acetic acid-producing bacteria on pear trees and their association with fruit russet. *Phytopathology* **1998**, *88*, 1149–1157. [CrossRef]
98. Serdani, M.; Spotts, R.A.; Calabro, J.M.; Postman, J.D. Powdery mildew resistance in *Pyrus* germplasm. *Acta Hortic.* **2005**, *671*, 609–613. [CrossRef]
99. Spotts, R.A.; Cervantes, L.A. Involvement of *Aureobasidium pullulans* and *Rhodotorula glutinis* in russet of d'Anjou pear fruit. *Plant. Dis.* **2002**, *86*, 625–628. [CrossRef] [PubMed]
100. Amarante, C.; Banks, N.H.; Max, S. Preharvest bagging improves packout and fruit quality of pears (*Pyrus communis*). *N. Z. J. Crop Hortic. Sci.* **2002**, *30*, 93–98. [CrossRef]
101. Lin, J.; Wang, Z.H.; Li, X.G.; Chang, Y.H. Effects of bagging twice and room temperature storage on quality of 'Cuiguan' pear fruit. *Acta Hortic.* **2012**, *934*, 837–840. [CrossRef]
102. Zhang, J.; Zhang, Y.F.; Zhang, P.F.; Bian, Y.H.; Liu, Z.Y.; Zhang, C.; Liu, X.; Wang, C.L. An integrated metabolic and transcriptomic analysis reveals the mechanism through which fruit bagging alleviates exocarp semi-russeting in pear fruit. *Tree Physiol.* **2021**, *41*, 1306–1318. [CrossRef]
103. Lin, J.; Chang, Y.H.; Yan, Z.M.; Li, X.G. Effects of bagging on the quality of pear fruit and pesticide residues. *Acta Hortic.* **2008**, *772*, 315–318. [CrossRef]
104. Seo, H.H.; Lee, J.Y.; Jung, H.W. Fruit appearance improvement by using filter-attached paper bags in 'Niitaka' Pears. *Hortic. Environ. Biotechnol.* **2010**, *51*, 73–77.
105. Yuri, J.A.; Castelli, R. Pear russet control with gibberellins and other products, in cv. Packham's Triumph. *Acta Hortic.* **1998**, *475*, 303–310. [CrossRef]
106. Sugar, D.; Powers, K.A.; Basile, S.R. Mancozeb and kaolin applications can reduce russet of 'Comice' pear. *HortTechnology* **2005**, *15*, 272–275. [CrossRef]
107. McCoy, C.W. Damage and control of eriophyoid mites in crops: Stylar feeding injury and control of eriophyoid mites in citrus. In *Eriophyoid Mites: Their Biology, Natural Enemies and Control*; Lindquist, E.E., Sabelis, M.W., Bruin, J., Eds.; Elsevier: Amsterdam, The Netherlands, 1996; Volume 6, pp. 481–490.
108. Fisher, F.E. Control of citrus fruit russet in Florida with zineb. *Phytopathology* **1957**, *47*, 433–437.
109. Johnson, R.B.; King, J.R.; McBride, J.J. Zineb controls citrus rust mite. *Proc. Fla. State Hortic. Soc.* **1957**, *70*, 38–48.
110. Smoot, J.J.; Houck, L.G.; Johnson, H.B. *Market. Diseases of Citrus and Other Subtropical Fruits*; U.S. Department of Agriculture, Agricultural Research Service: Washington, DC, USA, 1971.
111. Winston, J.R. *Tear-Stain of Citrus Fruits*; U.S. Department of Agriculture: Washington, DC, USA, 1921; Volume 924.
112. Johnson, R.B. The effect of copper compounds on control of citrus rust mite with zineb. *J. Econ. Entomol.* **1960**, *53*, 395–397. [CrossRef]
113. Michailides, T.J. Russeting and russet scab of prune, an environmentally induced fruit disorder: Symptomatology, induction, and control. *Plant Dis.* **1991**, *75*, 1114–1123. [CrossRef]
114. Michailides, T.J.; Ogawa, J.M. Control and induction of russet scab and wind bruise damage ("wind scab") of French prunes. In *Prune Research Reports*; Calinfornia Prune Board: San Francisco, CA, USA, 1988.
115. Corbin, J.B.; Lider, J.V.; Roberts, K.O. Controlling prune russet scab. *Calif. Agric.* **1968**, *22*, 6–7.
116. Avidan, B.; Klein, I. Physiological disorders in loquat (*Eriobotrya japonica* Lindl.). I. Russeting. *Adv. Hortic. Sci.* **1998**, *12*, 190–195.
117. Wang, L.; Wang, H.C.; Hu, Y.L.; Huang, X.M. Loquat fruit physiological disorders: Creasing and russeting. *Acta Hortic.* **2007**, *750*, 269–273. [CrossRef]
118. Barone, F.; Farina, V.; Lo Bianco, R. Growth, yield and fruit quality of 'Peluche' loquat under windbreak nets. *Acta Hortic.* **2011**, *887*, 155–159. [CrossRef]
119. Huang, J.S.; Snapp, S.S. The effect of boron, calcium, and surface moisture on shoulder check, a quality defect in fresh-market tomato. *J. Am. Soc. Hortic. Sci.* **2004**, *129*, 599–607. [CrossRef]
120. Bakker, J.C. Russeting (cuticle cracking) in glasshouse tomatoes in relation to fruit growth. *J. Hortic. Sci.* **1988**, *63*, 459–463.
121. Kamau, A.W.; Mueke, J.M.; Khaemba, B.M. Resistance of tomato varieties to the tomato russet mite, *Aculops lycopersici* (Massee) (Acarina, Eriophyidae). *Insect Sci. Appl.* **1992**, *13*, 351–356. [CrossRef]
122. Ehret, D.L.; Hill, B.D.; Raworth, D.A.; Estergaard, B. Artificial neural network modelling to predict cuticle cracking in greenhouse peppers and tomatoes. *Comput. Electron. Agric.* **2008**, *61*, 108–116. [CrossRef]

28

123. Demers, D.A.; Dorais, M.; Papadopoulos, A.P. Yield and russeting of greenhouse tomato as influenced by leaf-to-fruit ratio and relative humidity. *HortScience* **2007**, *42*, 503–507. [CrossRef]

124. Jobin-Lawler, F.; Simard, K.; Gosselin, A.; Papadopoulos, A.P.; Dorais, M. The influence of solar radiation and boron-calcium fruit application on cuticle cracking of a winter tomato crop grown under supplemental lighting. *Acta Hortic.* **2002**, *580*, 235–239. [CrossRef]

125. Meissner, F. Die Korkbildung der Früchte von *Aesculus*- und *Cucumis*-Arten. *Osterr. Bot. Z.* **1952**, *99*, 606–624. [CrossRef]

126. Keren-Keiserman, A.; Tanami, Z.; Shoseyov, O.; Ginzberg, I. Differing rind characteristics of developing fruits of smooth and netted melons (*Cucumis melo*). *J. Hortic. Sci. Biotechnol.* **2015**, *79*, 107–113. [CrossRef]

127. Rose, D.H.; Bratley, C.O.; Pentzer, W.T. *Market. Diseases of Fruits and Vegetables: Grapes and Other Small Fruits*; U.S. Department of Agriculture: Washington, DC, USA, 1939.

128. Sholberg, P.L.; Boule, J. Palmolive (R) detergent controls apple, cherry, and grape powdery mildew. *Can. J. Plant. Sci.* **2009**, *89*, 1139–1147. [CrossRef]

129. Goffinet, M.C.; Pearson, R.C. Anatomy of russeting induced in concord grape berries by the fungicide chlorothalonil. *Am. J. Enol. Vitic.* **1991**, *42*, 281–289.

130. Araya, J.E.; Merino, C.; Santibanez, F.; Sazo, L. Ring spots by feeding of *Frankliniella occidentalis* (Thysanoptera: Thripidae) on white table grapes. *Rev. Colom. Entomol.* **2014**, *40*, 1–6.

131. De Villiers, F.J. Physiological studies of the grape. *Union S. Afr. Dep. Agric. Sci.* **1926**, *45*, 38–48.

132. Xu, Y.S.; Hou, X.D.; Feng, J.; Khalil-Ur-Rehman, M.; Tao, J.M. Transcriptome sequencing analyses reveals mechanisms of eliminated russet by applying GA$_3$ and CPPU on 'Shine Muscat' grape. *Sci. Hortic.* **2019**, *250*, 94–103. [CrossRef]

133. Huang, Y.; Wang, P.; Wang, X.; Wang, J.; Liu, F. Effects of calcium on the formation of berry russet and phenolic compounds in 'Shine Muscat' grape. *IOP Conf. Ser. Earth Environ. Sci.* **2021**, *792*, 012038. [CrossRef]

134. Athoo, T.O.; Winkler, A.; Knoche, M. Russeting in 'Apple' mango: Triggers and mechanisms. *Plants* **2020**, *9*, 898. [CrossRef]

135. Mathooko, F.M.; Kahangi, E.M.; Runkuab, J.M.; Onyangob, C.A.; Owinob, W.O. Preharvest mango (*Mangifera indica* L. 'Apple') fruit bagging controls lenticel discolouration and improves postharvest quality. *Acta Hortic.* **2011**, *906*, 55–62. [CrossRef]

136. Drogoudi, P.; Pantelidis, G.E.; Vekiari, S.A. Physiological disorders and fruit quality attributes in pomegranate: Effects of meteorological parameters, canopy position and acetylsalicylic acid foliar sprays. *Front. Plant Sci.* **2021**, *12*, 645547. [CrossRef]

137. Sharma, N.; Belsare, C. Effect of plant bio-regulators and nutrients on fruit cracking and quality in pomegranate (*Punica granatum* L.) 'G-137' in Himachal Pradesh. *Acta Hortic.* **2011**, *890*, 347–352. [CrossRef]

138. Joshi, M.; Schmilovitch, Z.; Ginzberg, I. Pomegranate fruit growth and skin characteristics in hot and dry climate. *Front. Plant. Sci.* **2021**, *12*, 725479. [CrossRef]

139. Ebeling, W.; Pence, R.J. New pomegranate mite: Russeting and cracking of peel characterize injury responsible for much culling. *Calif. Agric.* **1949**, *3*, 11–14.

140. Sahu, P.; Sharma, N. Fruit cracking and quality of pomegranate (*Punica granatum* L.) cv. Kandhari as influenced by CPPU and boron. *J. Pharmacogn. Phytochem.* **2019**, *8*, 2644–2648. [CrossRef]

141. Grimm, E.; Khanal, B.P.; Winkler, A.; Knoche, M.; Köpcke, D. Structural and physiological changes associated with the skin spot disorder in apple. *Postharvest Biol. Technol.* **2012**, *64*, 111–118. [CrossRef]

142. Byers, M.A. A scarf skin-like disorder of apples. *HortScience* **1977**, *12*, 226–227. [CrossRef]

143. Ferree, D.C.; Ellis, M.A.; Bishop, B.L. Scarf skin on 'Rome Beauty': Time of origin and influence of fungicides and GA$_{4+7}$. *J. Am. Soc. Hortic. Sci.* **1984**, *109*, 422–427.

144. Williams, M.H.; Vesk, M.; Mullins, M.G. Development of the banana fruit and occurrence of the maturity bronzing disorder. *Ann. Bot.* **1990**, *65*, 9–19. [CrossRef]

145. Campbell, S.J.; Williams, W.T. Factors associated with maturity bronzing of banana fruit. *Aust. J. Exp. Agric.* **1976**, *16*, 428–432. [CrossRef]

146. Beach, S.A.; Booth, N.O.; Taylor, O.M. *The Apples of New York*; J.B. Lyon: Albany, GA, USA, 1905; Volume 1.

147. Weber, R.W.S.; Zabel, D. White haze and scarf skin, two little-known cosmetic defects of apples in northern Germany. *Eur. J. Hortic. Sci.* **2011**, *76*, 45–50.

148. Williams, M.H.; Vesk, M.; Mullins, M.G. Characteristics of the surface of banana peel in cultivars susceptible and resistant to maturity bronzing. *Can. J. Bot.* **1989**, *67*, 2154–2160. [CrossRef]

149. Daniells, J.W.; Lisle, A.T.; Ofarrell, P.J. Effect of bunch-covering methods on maturity bronzing, yield, and fruit quality of bananas in North Queensland. *Aust. J. Exp. Agric.* **1992**, *32*, 121–125. [CrossRef]

150. Daniells, J.W.; Lisle, A.T.; Bryde, N.J. Effect of bunch trimming and leaf removal at flowering on maturity bronzing, yield, and other aspects of fruit quality of bananas in North Queensland. *Aust. J. Exp. Agric.* **1994**, *34*, 259–265. [CrossRef]

151. Meyer, A. A study of the skin structure of Golden Delicious apples. *Proc. Am. Soc. Hortic. Sci.* **1944**, *45*, 105–110.

152. Schreiber, L.; Franke, R.; Hartmann, K. Wax and suberin development of native and wound periderm of potato (*Solanum tuberosum* L.) and its relation to peridermal transpiration. *Planta* **2005**, *220*, 520–530. [CrossRef] [PubMed]

153. Franke, R.; Schreiber, L. Suberin—A biopolyester forming apoplastic plant interfaces. *Curr. Opin. Plant. Biol.* **2007**, *10*, 252–259. [CrossRef] [PubMed]

154. Considine, J.; Brown, K. Physical aspects of fruit growth: Theoretical analysis of distribution of surface growth forces in fruit in relation to cracking and splitting. *Plant Physiol.* **1981**, *68*, 371–376. [CrossRef] [PubMed]

155. Eccher, T.; Hajnajari, H. Fluctuations of endogenous gibberellin A$_4$ and A$_7$ content in apple fruits with different sensitivity to russet. *Acta Hortic.* **2006**, *727*, 537–543. [CrossRef]
156. Creasy, L.L. The correlation of weather parameters with russet of Golden Delicious apples under orchard conditions. *J. Am. Soc. Hortic. Sci.* **1980**, *105*, 735–738.
157. Barcelo-Vidal, C.; Bonany, J.; Martin-Fernandez, J.A.; Carbo, J. Modelling of weather parameters to predict russet on 'Golden Delicious' apple. *J. Hortic. Sci. Biotechnol.* **2013**, *88*, 624–630. [CrossRef]
158. Straube, J.; Chen, Y.H.; Khanal, B.P.; Shumbusho, A.; Zeisler-Diehl, V.; Suresh, K.; Schreiber, L.; Knoche, M.; Debener, T. Russeting in apple is initiated after exposure to moisture ends: Molecular and biochemical evidence. *Plants* **2021**, *10*, 65. [CrossRef]
159. Faust, M.; Shear, C.B. Fine structure of the fruit surface of three apple cultivars. *J. Am. Soc. Hortic. Sci.* **1972**, *97*, 351–355.
160. Peschel, S.; Knoche, M. Characterization of microcracks in the cuticle of developing sweet cherry fruit. *J. Am. Soc. Hortic. Sci.* **2005**, *130*, 487–495. [CrossRef]
161. Khanal, B.P.; Le, T.L.; Si, Y.; Knoche, M. Russet susceptibility in apple is associated with skin cells that are larger, more variable in size, and of reduced fracture strain. *Plants* **2020**, *9*, 1118. [CrossRef] [PubMed]
162. Maguire, K.M. *Factors Affecting Mass Loss of Apples*; Massey University: Palmerston North, New Zealand, 1998.
163. Knoche, M.; Khanal, B.P.; Brüggenwirth, M. Patterns of microcracking in apple fruit skin reflect those of the cuticular ridges and of the epidermal cell walls. *Planta* **2018**, *248*, 293–306. [CrossRef] [PubMed]
164. Khanal, B.P.; Knoche, M. Mechanical properties of apple skin are determined by epidermis and hypodermis. *J. Am. Soc. Hortic. Sci.* **2014**, *139*, 139–147. [CrossRef]
165. Lai, X.; Khanal, B.P.; Knoche, M. Mismatch between cuticle deposition and area expansion in fruit skins allows potentially catastrophic buildup of elastic strain. *Planta* **2016**, *244*, 1145–1156. [CrossRef] [PubMed]
166. Si, Y.; Khanal, B.P.; Schlüter, O.K.; Knoche, M. Direct evidence for a radial gradient in age of the apple fruit cuticle. *Front. Plant Sci.* **2021**, *12*, 730837. [CrossRef] [PubMed]
167. Khanal, B.P.; Knoche, M.; Bußler, S.; Schlüter, O. Evidence for a radial strain gradient in apple fruit cuticles. *Planta* **2014**, *240*, 891–897. [CrossRef]
168. Konarska, A. The structure of the fruit peel in two varieties of *Malus domestica* Borkh. (Rosaceae) before and after storage. *Protoplasma* **2013**, *250*, 701–714. [CrossRef]
169. Roy, S.; Conway, W.S.; Watada, A.E.; Sams, C.E.; Erbe, E.F.; Wergin, W.P. Heat treatment affects epicuticular wax structure and postharvest calcium uptake in 'Golden Delicious' apples. *HortScience* **1994**, *29*, 1056–1058. [CrossRef]
170. Eccher, T. Influenza di alcuni fitormoni sulla rugginosità della "Golden Delicious". *Riv. Ortoflorofruttic. Ital.* **1975**, *59*, 246–261.
171. Knoche, M.; Peschel, S. Deposition and strain of the cuticle of developing European plum fruit. *J. Am. Soc. Hortic. Sci.* **2007**, *132*, 597–602. [CrossRef]
172. Athoo, T.O.; Khanal, B.P.; Knoche, M. Low cuticle deposition rate in 'Apple' mango increases elastic strain, weakens the cuticle and increases russet. *PLoS ONE* **2021**, *16*, e0258521. [CrossRef] [PubMed]
173. Konarska, A. Morphological, histological and ultrastructural changes in fruit epidermis of apple *Malus domestica* cv. Ligol (*Rosaceae*) at fruit set, maturity and storage. *Acta Biol. Crac. Ser. Bot.* **2014**, *56*, 35–48. [CrossRef]
174. Brüggenwirth, M.; Knoche, M. Cell wall swelling, fracture mode, and the mechanical properties of cherry fruit skins are closely related. *Planta* **2017**, *245*, 765–777. [CrossRef] [PubMed]
175. Wei, X.; Mao, L.; Han, X.; Lu, W.; Xie, D.; Ren, X.; Zhao, Y. High oxygen facilitates wound induction of suberin polyphenolics in kiwifruit. *J. Sci. Food Agric.* **2018**, *98*, 2223–2230. [CrossRef]
176. Xiao, Z.; Rogiers, S.Y.; Sadras, V.O.; Tyerman, S.D. Hypoxia in grape berries: The role of seed respiration and lenticels on the berry pedicel and the possible link to cell death. *J. Exp. Bot.* **2018**, *69*, 2071–2083. [CrossRef]
177. Ho, Q.T.; Verboven, P.; Verlinden, B.E.; Schenk, A.; Delele, M.A.; Rolletschek, H.; Vercammen, J.; Nicolai, B.M. Genotype effects on internal gas gradients in apple fruit. *J. Exp. Bot.* **2010**, *61*, 2745–2755. [CrossRef]
178. Wigginton, M.J. Effects of temperature, oxygen tension and relative humidity on the wound-healing process in the potato tuber. *Potato Res.* **1974**, *17*, 200–214. [CrossRef]
179. Lipton, W.J. Some effects of low-oxygen atmospheres on potato tubers. *Am. Potato J.* **1967**, *44*, 292–298. [CrossRef]
180. Jindal, K.K.; Pal, S.; Chauhan, P.S.; Mankotia, M.S. Effect of promalin and mixtatol on fruit growth, yield efficiency and quality of 'Starking Delicious' apple. *Acta Hortic.* **2004**, *636*, 533–536. [CrossRef]
181. Hou, X.; Wei, L.; Xu, Y.; Khalil-Ur-Rehman, M.; Feng, J.; Zeng, J.; Tao, J. Study on russet-related enzymatic activity and gene expression in 'Shine Muscat' grape treated with GA3 and CPPU. *J. Plant. Interact.* **2018**, *13*, 195–202. [CrossRef]
182. Flaishman, M.A.; Shargal, A.; Shlizerman, L.; Stern, R.A.; Lev-Yadun, S.; Grafi, G. The synthetic cytokinins CPPU and TDZ prolong the phase of cell division in developing pear (*Pyrus communis* L.) fruit. *Acta Hortic.* **2005**, *671*, 151–157. [CrossRef]
183. Kano, Y. Effects of CPPU treatment on fruit and rind development of watermelons (*Citrullus lanatus* Matsum. et Nakai). *J. Hortic. Sci. Biotechnol.* **2015**, *75*, 651–654. [CrossRef]
184. Ganie, M.A.; Akhter, F.; Bhat, M.A.; Malik, A.R.; Junaid, J.M.; Shah, M.A.; Bhat, A.H.; Bhat, T.A. Boron—A critical nutrient element for plant growth and productivity with reference to temperate fruits. *Curr. Sci.* **2013**, *104*, 76–85.
185. Muengkaew, R.; Whangchai, K.; Chaiprasart, P. Application of calcium—boron improve fruit quality, cell characteristics, and effective softening enzyme activity after harvest in mango fruit (*Mangifera indica* L.). *Hortic. Environ. Biotechnol.* **2018**, *59*, 537–546. [CrossRef]

186. Broadley, M.; Brown, P.; Cakmak, I.; Rengel, Z.; Zhao, F. Function of Nutrients: Micronutrients. In *Marschner's Mineral Nutrition of Higher Plants*, 3rd ed.; Marschner, P., Ed.; Academic Press: San Diego, CA, USA, 2012; pp. 191–248.
187. Ferri, V.C.; Rombaldi, C.V.; Silva, J.A.; Pegoraro, C.; Nora, L.; Antunes, P.L.; Girardi, C.L.; Tibola, C.S. Boron and calcium sprayed on 'Fuyu' persimmon tree prevent skin cracks, groove and browning of fruit during cold storage. *Cienc. Rural.* **2008**, *38*, 2146–2150. [CrossRef]
188. Ghanbarpour, E.; Rezaei, M.; Lawson, S. Reduction of cracking in pomegranate fruit after foliar application of humic acid, calcium-boron and kaolin during water stress. *Erwerbs Obstbau* **2019**, *61*, 29–37. [CrossRef]
189. Singh, A.; Shukla, A.K.; Meghwal, P.R. Fruit cracking in pomegranate: Extent, cause, and management—A review. *Int. J. Fruit Sci.* **2020**, *20*, S1234–S1253. [CrossRef]
190. Kavvadias, V.; Daggas, T.; Paschalidis, C.; Vavoulidou, E.; Theocharopoulos, S. Effect of boron application on yield, quality, and nutritional status of peach cultivar Andross. *Commun. Soil Sci. Plant. Anal.* **2012**, *43*, 134–148. [CrossRef]
191. Schumann, C.; Winkler, A.; Brüggenwirth, M.; Köpcke, K.; Knoche, M. Crack initiation and propagation in sweet cherry skin: A simple chain reaction causes the crack to 'run'. *PLoS ONE* **2019**, *14*, e0219794. [CrossRef]
192. Racsko, J.; Schrader, L.E. Sunburn of apple fruit: Historical background, recent advances and future perspectives. *Crit. Rev. Plant Sci.* **2012**, *31*, 455–504. [CrossRef]
193. Chonhenchob, V.; Kamhangwong, D.; Kruenate, J.; Khongrat, K.; Tangchantra, N.; Wichai, U.; Singh, S.P. Preharvest bagging with wavelength-selective materials enhances development and quality of mango (*Mangifera indica* L.) cv. Nam Dok Mai #4. *J. Sci. Food Agric.* **2011**, *91*, 664–671. [CrossRef] [PubMed]
194. Abdel Gawad-Nehad, M.A.; EL-Gioushy, S.F.; Baiea, M.H.M. Impact of different bagging types on preventing sunburn injury and quality improvement of Keitt mango fruits. *Middle East J. Agric. Res.* **2017**, *6*, 484–494.
195. Sarkomi, F.H.; Moradinezhad, F.; Khayat, M. Pre-harvest bagging influences sunburn, cracking and quality of pomegranate fruits. *J. Hortic. Postharvest Res.* **2019**, *2*, 131–142. [CrossRef]
196. Buthelezi, N.M.D.; Mafeo, T.P.; Mathaba, N. Preharvest bagging as an alternative technique for enhancing fruit quality: A review. *HortTechnology* **2021**, *31*, 4–13. [CrossRef]
197. Hudina, M.; Stampar, F. Bagging of 'Concorde' pears (*Pyrus communis* L.) influences fruit quality. *Acta Hortic.* **2011**, *909*, 625–630. [CrossRef]
198. Macnee, N.; Hilario, E.; Tahir, J.; Currie, A.; Warren, B.; Rebstock, R.; Hallett, I.C.; Chagne, D.; Schaffer, R.J.; Bulley, S.M. Peridermal fruit skin formation in *Actinidia* sp. (kiwifruit) is associated with genetic *loci* controlling russeting and cuticle formation. *BMC Plant Biol.* **2021**, *21*, 334. [CrossRef]
199. Petit, J.; Bres, C.; Mauxion, J.P.; Bakan, B.; Rothan, C. Breeding for cuticle-associated traits in crop species: Traits, targets, and strategies. *J. Exp. Bot* **2017**, *68*, 5369–5387. [CrossRef]
200. Falginella, L.; Cipriani, G.; Monte, C.; Gregori, R.; Testolin, R.; Velasco, R.; Troggio, M.; Tartarini, S. A major QTL controlling apple skin russeting maps on the linkage group 12 of 'Renetta Grigia di Torriana'. *BMC Plant Biol.* **2015**, *15*, 150. [CrossRef]
201. Legay, S.; Guerriero, G.; Deleruelle, A.; Lateur, M.; Evers, D.; André, C.M.; Hausman, J.F. Apple russeting as seen through the RNA-seq lens: Strong alterations in the exocarp cell wall. *Plant Mol. Biol.* **2015**, *88*, 21–40. [CrossRef]
202. Si, Y.; Khanal, B.P.; Sauheitl, L.; Knoche, M. Cutin synthesis in developing, field-grown apple fruit examined by external feeding of labelled precursors. *Plants* **2021**, *10*, 497. [CrossRef]

31

3.2 Russeting in 'Apple' Mango: Triggers and Mechanisms

Authors:

Thomas O. Athoo (**TOA**), Andreas Winkler (**AW**), and Moritz Knoche (**MK**)

Author affiliation:

Institute of Horticultural Production Systems, Fruit Science Section, Leibniz University Hannover, Herrenhäuser Straße 2, 30419 Hannover, Germany

Author Contributions:

Conceptualization, T.O.A. and M.K.; Funding acquisition, M.K.; Investigation, T.O.A., A.W. and M.K.; Methodology, T.O.A., A.W. and M.K.; Supervision, M.K.; Visualization, T.O.A. and A.W.; Writing-original draft, T.O.A., A.W., and M.K.; Writing-review & editing, T.O.A., A.W. and M.K.

Russeting in 'Apple' Mango:
Triggers and Mechanisms

Thomas O. Athoo, Andreas Winkler and Moritz Knoche *

Institute of Horticultural Production Systems, Leibniz University Hannover, Herrenhäuser Straße 2,
30419 Hannover, Germany; thomasathoo@gmail.com (T.O.A.); andreas.winkler@obst.uni-hannover.de (A.W.)
* Correspondence: moritz.knoche@obst.uni-hannover.de; Tel.: +49-511-762-9020

Abstract: Russeting is an important surface disorder of many fruitcrop species. The mango cultivar 'Apple' is especially susceptible to russeting. Russeting compromises both fruit appearance and postharvest performance. The objective was to identify factors, mechanisms, and consequences of russeting in 'Apple' mango. Russeting was quantified on excised peels using image analysis and a categorical rating scheme. Water vapour loss was determined gravimetrically. The percentage of the skin area exhibiting russet increased during development. Russet began at lenticels then spread across the surface, ultimately forming a network of rough, brown patches over the skin. Cross-sections revealed stacks of phellem cells, typical of a periderm. Russet was more severe on the dorsal surface of the fruit than on the ventral and more for fruit in the upper part of the canopy than in the lower. Russet differed markedly across orchards sites of different climates. Russet was positively correlated with altitude, the number of rainy days, and the number of cold nights but negatively correlated with minimum, maximum, and mean daily temperatures, dew point temperature, and heat sum. Russeted fruit had higher transpiration rates than non-russeted fruits and higher skin permeance to water vapour. Russet in 'Apple' mango is due to periderm formation that is initiated at lenticels. Growing conditions conducive for surface wetness exacerbate russeting.

Keywords: *Mangifera indica*; skin; periderm; cuticle; epidermis; lenticel

1. Introduction

Russeting is a surface disorder of many fruitcrop species worldwide. In botanical terms, russet represents the formation of a periderm [1] comprising three layers: a phellogen (meristematic) that gives rise to a phelloderm (to the inside) and a phellem (to the outside). The phellem comprises stacks of cork cells. It is their suberised cell walls that are responsible for the rough, brown appearance of a russeted fruit skin. This appearance is generally unattractive to the consumer [2]. Russet therefore compromises the visual quality of a fruit and thus excludes it from the high-value export markets. Russet is also associated with increased postharvest water loss, which further compromises postharvest performance [3]. This requires fruit cartons to be "overpacked" if they are to reach the end consumer at the pre-specified weight. For both these reasons, russeting has serious economic consequences for the grower.

Malus apple is a prominent example of a susceptible fruit crop. Most information on the ontogeny of russet is available for this species. In apple, russet is preceded by the formation of microcracks in the cuticle [4,5]. Surface wetness [6,7], agrichemicals [8,9], and pests and diseases such as mites [10], epiphytic fungi [11], and bacteria [12] are all factors aggravating russeting. A periderm forms, presumably in the hypodermal cell layers [13,14]. The cuticle and the epidermis dry

out and slough off as the phellem develops. The brownish cork cells are then revealed on the fruit surface.

The 'Apple' mango is a valuable mango cultivar in the Kenyan market. It has excellent texture and flavour. Unfortunately, 'Apple' mango is also highly susceptible to a skin disorder that bears similarity to the well-known russet of many apple and pear cultivars. To our knowledge, there is no information available on this disorder in mango.

The objective of this study was (1) to identify whether the "russet" of 'Apple' mango is caused by a periderm formation and (2) to identify the agronomic and the environmental factors affecting the incidence and severity of "russeting" in this cultivar.

2. Results

Russet severity in 'Apple' mango was non-uniform within a tree and across an orchard. The severity of russet in the same orchard ranged from non-russeted (Figure 1a, score 0) to moderate (Figure 1c, score 2) to extreme (Figure 1b, score 4). The russet scores of the rating scheme used to quantify russet were closely correlated to the actual russeted surface area measured by image analysis (Figure 1d).
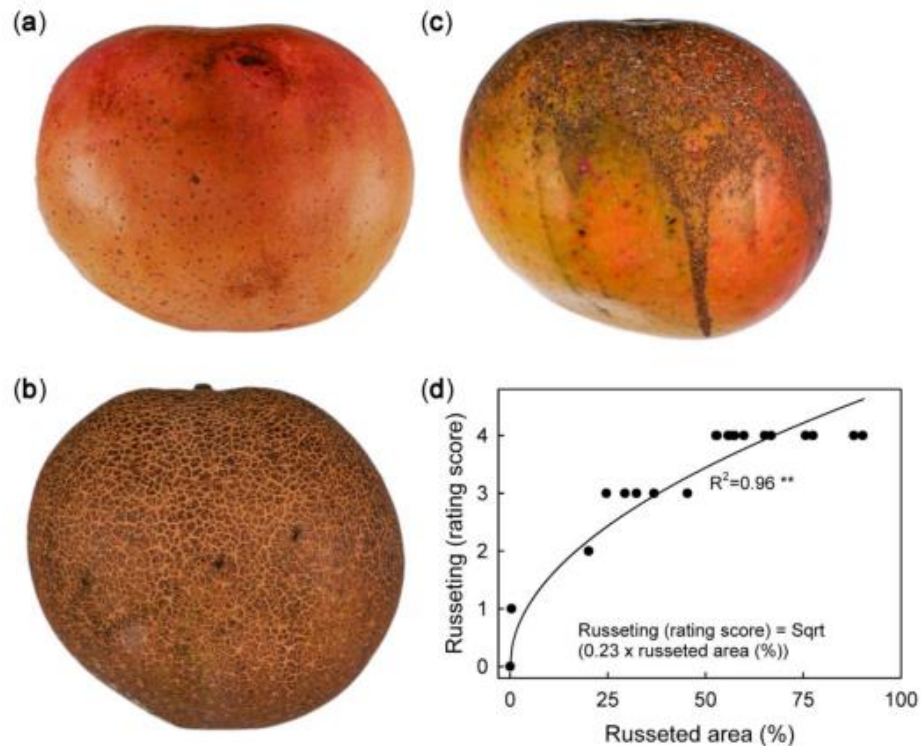
Figure 1. Macroscope view of mature 'Apple' mango without (**a, score 0**), moderate (**b, score 2**), and extreme (**c, score 4**) russet symptoms. (**d**): Plot of russeting (rating score) against percentage area affected by russet (image analysis). Each fruit was rated visually prior to image analysis. The number of observations was 18.

Fruit surface area increased with time (Figure 2a). The growth rate in surface area was at a maximum of 2.3 cm^2 day^{-1} at about 114 days after full bloom (DAFB) and decreased continuously thereafter (Figure 2a inset). The percentage of the surface area of the skin exhibiting russet increased with time throughout development (Figure 2b,c).

34
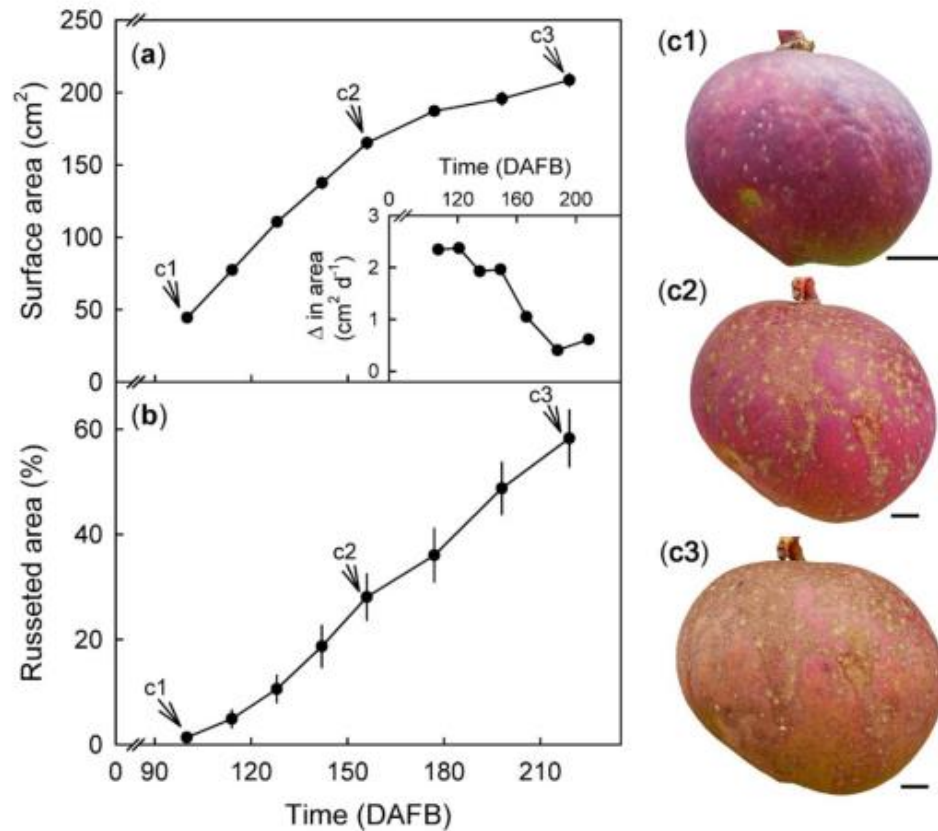
Figure 2. Change in fruit surface area (cm²) and rate of surface expansion (**a** and **a inset**) with time (days after full bloom, DAFB). Percent of skin with russet in developing fruit (**b**) calculated from a defined area of the fruit cheek. The same fruit was photographed at 100, 156, and 216 DAFB (see arrows). Pictorial representation of russet progression in a developing 'Apple' mango fruit (**c1–c3**). Scale bar is 10 mm. Data represent means ± SE of 19 replicates.

Microscopic inspection of the fruit surface following labelling with acridine orange revealed that initial cracking always began at a lenticel (Figure 3a–d). Lenticels ruptured and developed into (usually) three- or four-pointed star- or triangular-shaped short cracks. These were filled with periderm (Figure 3e–h). These stellate cracks enlarged and merged as cracks propagated and development progressed. They eventually formed islands of crack networks. These islands later expanded and merged. The end result was an extensive network of rough, brown patches. Occasionally, these patches extended over the entire fruit surface (Figure 3i–n). Only during the initial stages of cracking was there significant infiltration of acridine orange at the lenticels (Figure 3b,d). There was essentially no infiltration after the periderm had developed (Figure 3h,j,l,n).
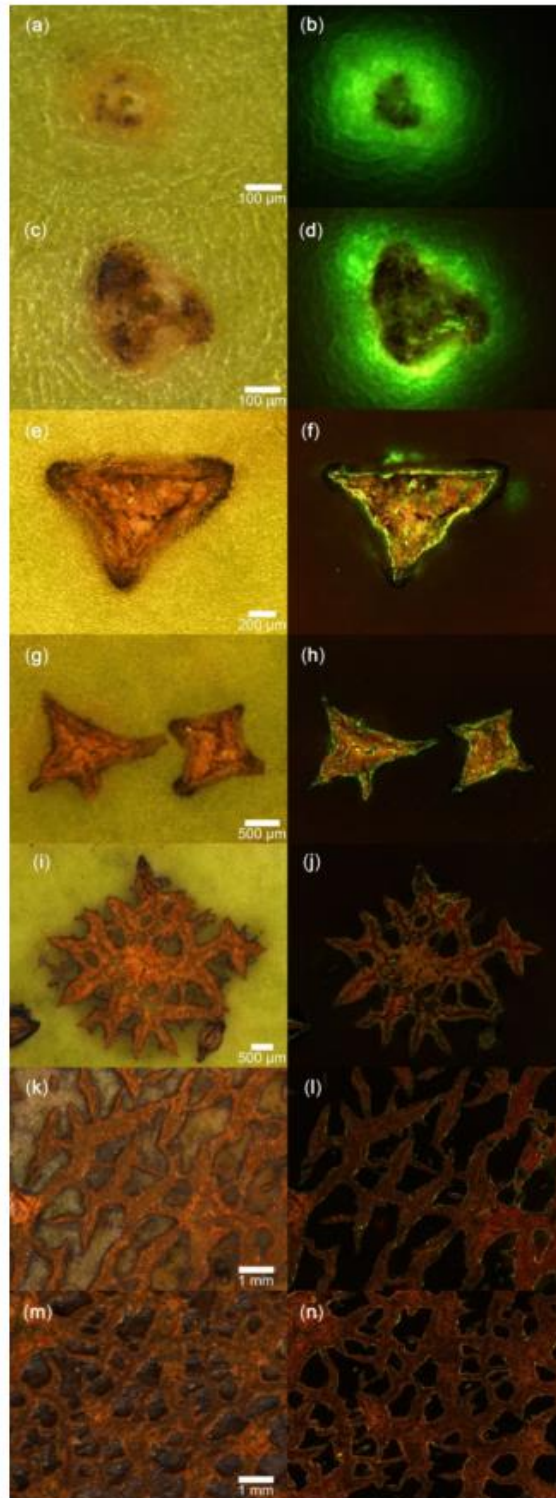
Figure 3. Microscopic view of 'Apple' mango skin infiltrated with acridine orange dye when viewed with a binocular microscope under natural (**a,c,e,g,i,k,m**) or fluorescent light (**b,d,f,h,j,l,n**). The scale bars refer to the corresponding pairs of images.

36

The non-russeted fruit skin had an intact cuticle, epidermis, and hypodermis (Figure 4a,b). There was no cuticle or epidermis on the lenticels (Figure 4c–j). The pore of the lenticel was filled with stacks of thick-walled cells varying from three layers (initial stage of russeting) to more than five (extreme russeting) (Figure 4c–j). The walls of these cells fluoresced following staining with fluorol yellow. This identified them as the suberised (corky) walls of a typical periderm (Figure 4d,f,h,j).
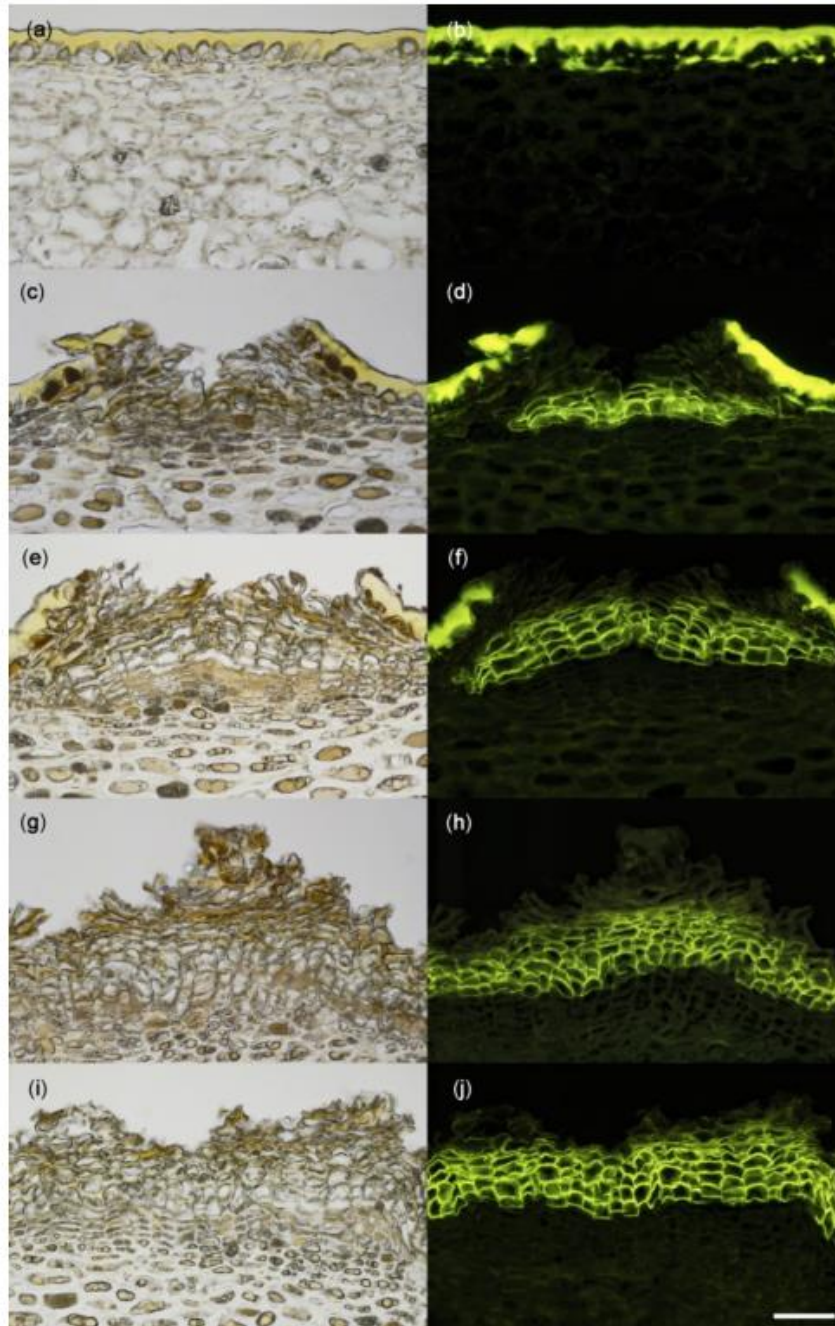
Figure 4. Cross-sectional microscope images of a non-russeted (**a,b**) and russeted (**c–j**) skin of 'Apple' mango viewed under incident white (**a,c,e,g,i**) or fluorescent light (**b,d,f,h,j**) following staining with fluorol yellow dye. Scale bar is 50 μm.

For any particular fruit, russet severity decreased along the stem/apex axis. Russet was most severe at the stem end and least severe at the apex (Table 1). There were no significant differences in the severity of russeting between the blushed and the non-blushed sides of a fruit (Table 1).

Table 1. Percent distribution of russet on 'Apple' mango fruit along the stem/apex axis on either the blushed or the non-blushed sides of the fruit. Percentage of russet was quantified using image analysis following photography. For the different regions of the fruit, see Figure 7.

Fruit Region	Russeted Area (%)		
	Blushed Side	Non-Blushed Side	Mean Side
Stem end	85.8 ± 6.9	87.2 ± 5.7	86.5 ± 4.4 a[z]
Basal cheek	47.7 ± 5.7	43.8 ± 5.5	45.8 ± 4.0 b
Apical cheek	19.2 ± 5.8	18.4 ± 5.3	18.8 ± 3.9 c
Apex	15.4 ± 6.1	17.2 ± 6.3	16.3 ± 4.3 c
Mean Fruit region	42.0 ± 4.5 a	41.7 ± 4.4 a	

[z] Main effect but not interaction significant by analysis of variance. Main effect for fruit regions differs according to the Tukey studentised range test, $p \leq 0.05$. The number of replicates was 18.

Russeting was significantly less severe in the ventral region than in the dorsal region of a fruit (Table 2). This effect was consistent across the three orchard sites, which differed significantly in overall russeting severity. Russeting was consistently most severe in Kaiti, followed by Mumbuni, and was least severe in Yeemulwa (Table 2).

Table 2. Russeting in ventral and dorsal regions of 'Apple' mango from three different sites. The sites were selected because they differed in elevation. Russeting was quantified using a five-score rating scheme. Score 0: 0% of the fruit surface area russeted; score 1: 1–10% russeted area; score 2: 11–25% russeted area; score 3: 26–50% russeted area; and score 4: 51–100% russeted area. For ventral and dorsal regions of the fruit, see Figure 7.

Site	Extent of Russet (Rating Score)		
	Ventral	Dorsal	Mean Region
Kaiti	2.9 ± 0.1	3.5 ± 0.1	3.2 ± 0.1 a[z]
Mumbuni	2.0 ± 0.1	2.8 ± 0.1	2.4 ± 0.1 b
Yeemulwa	1.6 ± 0.1	2.3 ± 0.1	1.9 ± 0.1 c
Mean Site	2.2 ± 0.1 b	2.8 ± 0.0 a	

[z] Main effects "site" and "region" of the fruit were significant at $p \leq 0.05$. Interaction between site and region of the fruit was not significant in a two factorial ANOVA. Mean separation by Tukey studentised range test, $p \leq 0.05$. The number of replicates was 200.

Within the canopy, there were no significant differences in russeting between peripheral (exposed) or central (shaded) fruits on a tree. Again, fruit from the Kaiti site had the highest incidence of russeting followed by Mumbuni and Yeemulwa (Table 3).

38

Table 3. Russeting of peripheral (exposed) or central (shaded) 'Apple' mango fruit in the canopy at three different sites. The sites were selected because they differ in elevation. Russeting was quantified using a five-score rating scheme. Score 0: 0% of the fruit surface area russeted; score 1: 1–10% russeted area; score 2: 11–25% russeted area; score 3: 26–50% russeted area; and score 4: 51–100% russeted area.

Site	Russeting (Rating Score)		
	Exposed Fruits	**Shaded Fruits**	**Mean** Fruit Position
Kaiti	3.7 ± 0.0	3.7 ± 0.0	3.7 ± 0.0 a[z]
Mumbuni	2.3 ± 0.1	2.5 ± 0.1	2.4 ± 0.1 b
Yeemulwa	2.0 ± 0.1	1.8 ± 0.1	1.9 ± 0.1 c
Mean Site	2.7 ± 0.1 a	2.7 ± 0.1 a	

[z] Main effect of site was significant but neither fruit position nor interaction was significant by analysis of variance at $p \leq 0.05$. Mean separation according to the Tukey studentised range test, $p \leq 0.05$. The number of replicates was 200.

There was significant interaction between the orchard site and the position of the fruit within the tree. Across all sites, fruits located in the top of the canopy were more russeted than those in the middle or the bottom parts of the canopy (Table 4).

Table 4. Effect of fruit position within the tree canopy on russeting of 'Apple' mango in different sites. Fruit positions were: top (>2 m above the ground), middle (1–2 m), and bottom (0.5–1 m). Russeting was quantified using a five-score rating scheme. Score 0: 0% of the fruit surface area russeted; score 1: 1–10% russeted area; score 2: 11–25% russeted area; score 3: 26–50% russeted area; and score 4: 51–100% russeted area.

Site	Russeting (Rating Score)			
	Top	**Middle**	**Bottom**	**Mean** Fruit position
Kaiti	3.9 ± 0.0 a[z]	3.7 ± 0.0 b	3.5 ± 0.1 c	3.7 ± 0.0
Mumbuni	3.1 ± 0.1 a	2.3 ± 0.1 b	1.9 ± 0.1 c	2.4 ± 0.0
Yeemulwa	2.5 ± 0.1 a	1.7 ± 0.1 b	1.0 ± 0.1 c	1.7 ± 0.0
Mean Site	3.0 ± 0.0	2.4 ± 0.0	1.9 ± 0.0	

[z] Significant interaction between site and fruit position in the canopy in a two factorial ANOVA. Therefore, ANOVA was run by site. Means within the rows followed by the same letter are not significantly different. Mean separation by Tukey studentised range test, $p \leq 0.05$. The number of replicates was 352.

There was no significant effect of the geographical orientation of the fruit (aspect) in the canopy on russeting. Fruits exposed to north, south, east, and west all showed similar russeting across the three sites (Table 5).

Table 5. Effect of geographical orientation (aspect) of 'Apple' mango on russeting. Fruits were sampled from north-, south-, east-, and west-facing sides of the canopy. The tree rows were aligned perpendicularly to the slope and N, S, E, and W positions. Russeting was quantified using a five-score rating scheme. Score 0: 0% of the fruit surface area russeted; score 1: 1–10% russeted area; score 2: 11–25% russeted area; score 3: 26–50% russeted area; and score 4: 51–100% russeted area.

Site	Russeting (Rating Score)				
	North	**South**	**East**	**West**	**Mean** Aspect
Kaiti	3.6 ± 0.0	3.6 ± 0.0	3.8 ± 0.0	3.5 ± 0.1	3.6 ± 0.0 a[z]
Mumbuni	2.4 ± 0.1	2.5 ± 0.1	2.2 ± 0.1	2.6 ± 0.1	2.4 ± 0.0 b
Yeemulwa	1.8 ± 0.1	1.7 ± 0.1	1.6 ± 0.1	1.8 ± 0.1	1.7 ± 0.0 c
Mean Site	2.5 ± 0.1 a	2.6 ± 0.1 a	2.5 ± 0.1 a	2.6 ± 0.1 a	

[z] Main effect of site was significant but neither aspect of fruit nor interaction were significant by analysis of variance significant at $p \leq 0.05$. Mean separation according to the Tukey studentised range test, $p \leq 0.05$. The number of replicates was 264.

Russeting differed markedly between the ten sites across Kenya. Russeting was highest in Thika, Kaiti, Machakos, and Kasafari and lowest in Garissa and Malindi (Table 6). These sites differed markedly in climate. Analysis of potential relationships between climatic parameters and russet severity revealed the following relationships; highly significant, linear, positive relationships were obtained between altitude and russeting, i.e., there was more russeting at higher altitudes. Furthermore, russeting was significantly correlated with the number of rainy days but not with either the amount of rainfall (mm) or the relative humidity (%). Russeting was negatively correlated with minimum, maximum, and mean daily temperatures, and dew point temperatures. Positive relationships were observed for the number of cold nights, a negative sigmoidal one for the heat sum (Figure 5).

Table 6. Russeting of 'Apple' Mango at ten different sites across Kenya. Russeting was quantified using a five-score rating scheme: score 0: 0% of the fruit surface area russeted; score 1: 1–10% russeted area; score 2: 11–25% russeted area; score 3: 26–50% russeted area; and score 4: 51–100% russeted area.

Site	Maturity (Days after Full Bloom)	Rating (Score)
Thika	196	3.6 ± 0.1 a[z]
Kaiti	189	3.5 ± 0.1 a
Machakos	226	3.4 ± 0.1 ab
Kasafari	166	3.4 ± 0.1 ab
Chepsigot	146	3.2 ± 0.1 b
Kambirwa	136	3.1 ± 0.1 b
Mumbuni	175	2.3 ± 0.1 c
Yeemulwa	180	1.9 ± 0.1 d
Malindi	113	0.2 ± 0.0 e
Garissa	111	0.1 ± 0.0 e

[z] Mean separation according to the Tukey studentised range test, $p \leq 0.05$. Means followed by the same letter are not significantly different. The number of replicates was 210.
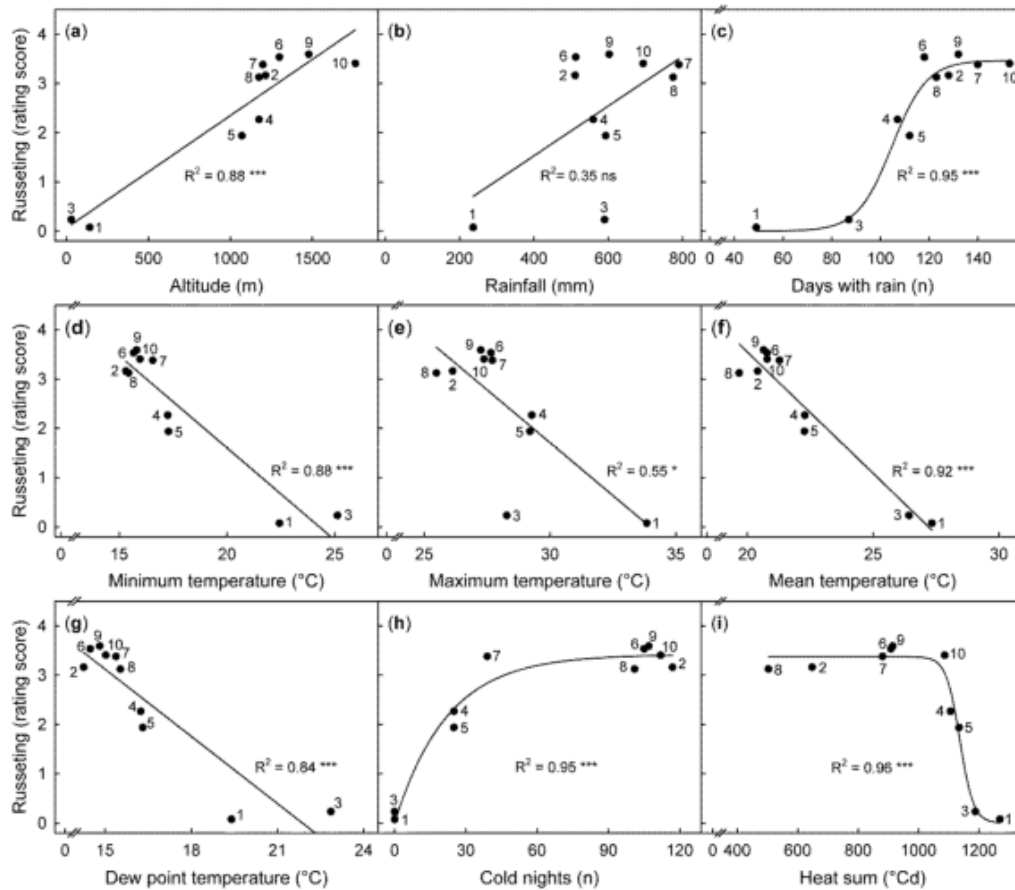
Figure 5. Relationship between climatic variables and average russeting (rating score) determined for the cumulative period of fruit maturity at ten locations in Kenya. The ten locations were: Garissa (1), Chepsigot (2), Malindi (3), Mumbuni (4), Yeemulwa (5), Kaiti (6), Kasafari (7), Kambirwa (8), Thika (9), and Machakos (10) situated at different altitudes. (**a**) The climatic variables include: rainfall amount (**b**), days with rainfall (**c**), relative humidity (**d**), minimum, maximum, and mean daily temperatures (**e, f,** and **g**, respectively). Cold nights (**h**) correspond to the number of days when the minimum temperature fell below the base temperature of 16 °C. Heat sum (**i**) was calculated based on a base temperature of 16 °C. Russeting was quantified using a five-score rating scheme: score 0: 0% of the fruit surface area russeted; score 1: 1–10% russeted area; score 2: 11–25% russeted area; score 3: 26–50% russeted area; and score 4: 51–100% russeted area. Data points represent means of 210 fruit per site.

There was little difference in the correlation coefficients between russet and the various weather variables during the first, the middle, and the later parts of the growing season. The only remarkable exception was the relationship of russet to the number of cold nights. Here, cold nights during early fruit development were particularly associated with increased russeting (Table 7).

Table 7. Pearson correlation between climatic variables and russeting for 'Apple' mango fruits grown at ten sites throughout Kenya. Climatic variables include rainfall amount, number (n) of rainy days, relative humidity, maximum, minimum, and mean daily temperatures, and heat sum. Heat sum is the sum of mean temperatures above the base temperature of 16 °C. Number of cold nights is the sum of the number of days when the minimum temperature was less than 16 °C. The growth season was divided into three periods of equal duration at each site (early, middle, and late phases). "Cumulative" refers to the entire growth period. Climatic data were obtained from the NASA Langley Research Centre (LaRC) POWER Project.

Weather Parameter	Pearson Coefficients of Correlation (r)			
	Time Period			
	Early	Middle	Late	Cumulative
Rainfall (mm)	0.39 ns²	0.44 ns	0.26 ns	0.60 ns
Rainy days (n)	0.66 *	0.67 *	0.79 **	0.90 ***
Relative humidity (%)	−0.27 ns	0.11 ns	0.08 ns	−0.05 ns
Maximum temperature (°C)	−0.56 ns	−0.71 *	−0.85 **	−0.74 *
Minimum temperature (°C)	−0.94 ***	−0.93 ***	−0.94 ***	−0.94 ***
Mean temperature (°C)	−0.96 ***	−0.95 ***	−0.96 ***	−0.96 ***
Heat sum (°Cd)	−0.57 ns	−0.67 *	−0.72 *	−0.67 *
Dew point temperature (°C)	−0.88 ***	−0.85 **	−0.91 ***	−0.92 ***
Cold nights (n)	0.88 ***	0.73 *	0.63 ns	0.84 **

² Correlation coefficients followed by *, **, and *** were significant at $p \leq 0.05$, $p \leq 0.01$, and $p \leq 0.001$, respectively. Correlation coefficients followed by ns were not significant ($p > 0.05$). The number of fruits inspected at anyone site was 210.

Transpiration increased linearly with time. Russeted fruit had significantly higher rates of transpiration compared to non-russeted fruits (Figure 6a). The epidermal sections (ES) from russeted skin also exhibited higher transpiration compared to non-russeted ES (Figure 6b). Permeance to water loss was constant with time but higher in russeted ES compared to control (Figure 6b inset).
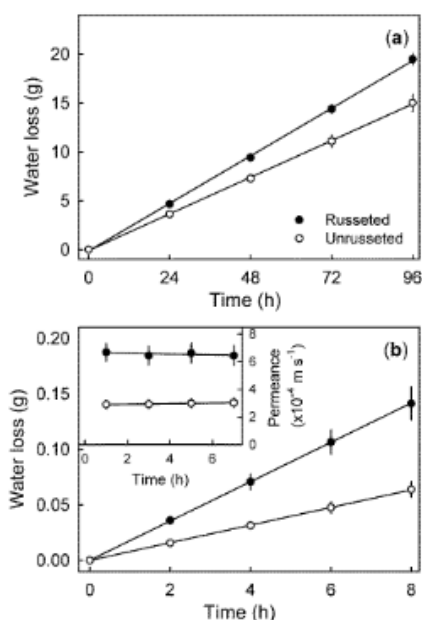
Figure 6. Time course of transpiration by whole fruits with extreme (>50%) (russeted) and with minimal (<25%) russet (not russeted) (**a**) and through epidermal sections (ES) excised from the cheek of mature 'Apple' mango fruit with and without russeting (**b**). Permeance of water vapour diffusion

through the ES (**b inset**) was calculated under conditions of steady state water loss. Data represent means ± SE of a minimum of 10 replicates.

3. Discussion

The most important findings in our study were:

(1) Russet in 'Apple' mango involves the formation of a periderm.
(2) Russet begins at the lenticels and from there spreads over the fruit surface.
(3) Rainy days and low night temperatures are especially conducive to russeting.

3.1. Russet in 'Apple' Mango Involves Formation of a Periderm

Russet in 'Apple' mango is similar to russet phenomena in other fruitcrop species, such as *Malus* apple [15,16], pear [17], citrus [18], grape [8], and melon [19]. This conclusion is based on the following arguments: (1) the appearance of the disorder in 'Apple' mango with rough brownish irregular patches surrounded by interconnected light brownish cracks is identical to that previously described for *Malus* apple [7]. (2) Cross-sections of the skin of 'Apple' mango identified stacks of suberised cells typical for a phellem produced by a phellogen as found in potatoes [20], *Malus* apple [3,13], reticulated melon [19], and grape [8]. The periderm of 'Apple' mango was stained with fluorol yellow, such as that of *Malus* apple [3]. (3) Russeting in 'Apple' mango increased during development. Russet symptoms began during early fruit development and became progressively more severe. The number of phellem layers in these stacks increased continuously. Similar observations were made in *Malus* apple, pear, and melons [15,19,21]. However, the maximum rate of increase in russet was reached later in developing 'Apple' mango compared with *Malus* apple or pear [15,21], where early fruit development is considered the most susceptible phase [22]. (4) As discussed below, surface wetness aggravates russeting in 'Apple' mango as it does in *Malus* apple [23,24]. (5) The formation of russet in 'Apple' mango is consistent with a repair process for cracks in the skin [16,25]. While some infiltration of lenticels was observed before the onset of russeting, there was practically no infiltration of the periderm during the later stages of russet development. Thus, formation of the periderm in 'Apple' mango would seem to perform the same function as that in *Malus* apple. It restores the barrier function of an impaired cuticle, thereby restoring, in part, the low water vapour permeance of the skin [3]. These arguments show that russeting in 'Apple' mango is similar to russeting in other fruitcrop species. It involves the formation of a classical periderm.

3.2. Russeting Begins at Lenticels and Then Spreads over the Surface

Lenticels are the sites where russeting is initiated in 'Apple' mango. The ontogeny of russet formation reveals an initial, usually stellate, crack in the centre of a lenticel. The crack then propagates across the fruit surface, merges, and thus comes to form a network of periderm that continue to spread over the enlarging fruit surface. In mango, lenticels develop under ruptured stomata [26,27]. This observation holds also for *Malus* apple [28,29]. In *Malus* apple, lenticels are often the source of multiple microcracks [30]. Microcracks in the cuticle are the first visible symptoms of russeting [4,5]. Whether this applies also to 'Apple' mango is not currently known. Growth strain is the driver for skin failure. Supporting evidence for a role of growth strain in russeting of 'Apple' mango comes from the observation that the ventral region was less russeted than the dorsal region. Compared to the ventral region, the dorsal region has a larger curvature and a larger strain rate, as indexed by a lower density of lenticels (Athoo, personal observation). Similar relationships have been reported for pear. In the latter, the cheek has a higher growth rate and, hence, a more rapid strain rate and thus is more prone to russeting than the neck [21].

Several hypotheses may account for lenticels being the sites of russet initiation in 'Apple' mango: (1) lenticels serve as stress concentrators, as demonstrated for the grape skin [31]. According to [31], lenticels of grapes represent a rigid structure embedded in an extensible skin. When strained, the lack of extensibility of the lenticel must be compensated for by a larger extension of the skin surrounding the lenticel. This causes stress concentrations and microcracking in the cuticle

43

surrounding lenticels. (2) Alternatively, lenticels of 'Apple' mango may be structurally weaker and less rigid than the surrounding skin. When strained, the lenticel must make up for the lower extension of the surrounding skin. A lower rigidity may result from a loose, irregular arrangement of cells with large intercellular spaces in mango [27]. This may imply a lower tensile force to tear them. Here, one would expect microcracks to be associated with lenticels, as was observed in 'Apple' mango. Interestingly, microcracks that formed in plum were almost all associated with stomata, the usual precursors of lenticels [32]. (3) Lastly, lenticels were infiltrated by aqueous acridine orange during early development, indicating high permeability, even for liquid water. This could expose underlying cells to moisture, causing bursting of some cells or cell wall swelling, which in turn may decrease cell–cell adhesion. This sequence of events lead to cracking in sweet cherry fruit skin [33]. It is worth noting that the infiltration with dye solution was limited to the early development of a lenticel. In subsequent stages, lenticels were sufficiently suberised (lipophilic), thus they presented a formidable barrier to water vapour diffusion from the fruit and also for viscous water flow into the fruit. At present, it is not known which of the above two (opposing) hypotheses accounts for the periderm formation in 'Apple' mango.

3.3. Rainy Days and Low Night Temperatures Are Conducive to Russeting

Our study reveals surprisingly close relationships between a range of environmental variables and the extent of russet in 'Apple' mango in different agroecological regions across Kenya. Apparently, conditions conducive to surface wetness aggravate russeting. Higher elevations, more rainy days, decreasing night temperature, low dew point temperatures, and increasing numbers of cold nights all aggravate russeting. Our observations are consistent with the finding that exposure to moisture causes russeting in *Malus* apple [23]. The moisture-induced russeting probably resulted from moisture-induced microcracking. That surface wetness induces microcracks in the cuticle has been demonstrated for *Malus* apple [6,7,23], sweet cherry [34], and grapes [35]. Thus, we expected microcracks also to form when the skin of 'Apple' mango was exposed to moisture.

We do not have an explanation for the lack of a significant relationship between rainfall amount or relative humidity and russet. This may have been an artefact resulting from the confounding effects of temperature and humidity. The hot coastal region of Kenya (Malindi) also has high rainfall. Yet, fruit in this region was only marginally russeted. High temperatures and higher wind speeds in coastal areas make long periods of wetness duration less likely.

The mechanistic basis for moisture induced russeting is not clear. Knoche and Peschel [34] suggested changes in the mechanical properties of the cuticle due to hydration. A hydrated cuticle generally has a lower modulus of elasticity and a lower fracture force [34,36,37]. Additionally, hydration causes cell wall swelling, and this may decrease cell–cell adhesion, as demonstrated for the sweet cherry fruit skin [33,38]. Both findings increase the likelihood of fracture of a hydrated, strained cuticle. The microcracks formed then trigger periderm formation.

3.4. Conclusion

Our results provide evidence that the surface disorder of russet in 'Apple' mango is due to periderm formation initiated at lenticels. Growth strains then cause the periderm to spread over the fruit surface. Close relationships between the incidence of russet of 'Apple' mango grown at ten different sites in Kenya and the climatic conditions at the different sites indicate that conditions conducive for surface wetness clearly stimulate russeting. This is consistent with moisture-induced microcracking in the cuticle reported for many fruitcrop species. The resulting periderm partially restores the barrier function of the skin of 'Apple' mango. However, the permeance remains at a significantly elevated level, and this increases postharvest moisture loss of russeted 'Apple' mango. Whether or not developing 'Apple' mango is also more susceptible to fungal infections merits further investigation.

44

4. Materials and Methods

4.1. Plant Materials

Mature and immature 'Apple' mango (*Mangifera indica* L.) fruit grafted on local seedling rootstocks were harvested or observed in situ in several commercial orchards across Kenya. The sites selected and their geographical coordinates are: Chepsigot (0°31′N, 35°34′E), Garissa (0°26′S, 39°37′E), Kaiti (1°45′S, 37°28′E), Kambirwa (0°44′S, 37°12′E), Kasafari (0°28′S, 37°40′E), Machakos (1°26′S, 37°13′E), Malindi (3°14′S, 40°05′E), Mumbuni (1°50′S, 37°36′E), Thika (1°01′S, 37°06′E), and Yeemulwa (1°53′S, 37°47′E). Fruits were grown conventionally using recommended integrated crop management programmes. Unless otherwise specified, fruits were harvested at commercial maturity and processed within two days.

4.2. Quantifying Russeting

To quantify russeting, fruits were peeled, and the peels were flattened on a glass plate. Russeted areas were painted with blue acrylic paint using a soft hair brush to enhance contrast. The flattened peels were photographed under standardised conditions with a digital camera (Lumix DMC-G80; Panasonic Corporation, Osaka, Japan) fitted with a macro lens (Olympus M. Zuiko Digital 60 mm; Olympus Corporation, Tokyo, Japan). A ruler was included in each image for scaling. Total fruit surface area and the areas with and without russet were quantified using image processing software (ImageJ 1.52P; National Health Institute, Bethesda, MD, USA). This method provided a precise and objective assessment of the severity of russet. For routine analyses, a five-score rating scheme was developed. Scores were 0 for 0% of the fruit surface area russeted, 1 for 1–10% of russeted area, 2 for 11–25% of russeted area, 3 for 26–50% of russeted area, and 4 for 51–100% of russeted area.

Russeted fruit surfaces were also examined by light microscopy. Microscopic cracks ("microcracks") on the fruit surface were identified following immersion of whole fruits in 0.1% (*w/w*) aqueous acridine orange (Carl Roth, Karlsruhe, Germany) for 10 min. Fruits were then rinsed with deionised water (30 s) and blotted dry using soft tissue paper. The fruit surface was then inspected under incident white and UV light using a fluorescence binocular microscope (Leica MZ10F with filter GFP plus 480–440 nm excitation, ≥510 nm emission; Leica Microsystems GmbH, Wetzlar, Germany). Calibrated digital photographs were taken (Olympus DP71; Olympus Europa Holding GmbH, Hamburg, Germany) and then analysed using image processing software (cellSens version 1.7.1.; Olympus).

4.3. Histology

Tissue blocks (5 × 2 mm) of the skin of mature fruit were excised using a razor blade and fixed in Karnovsky solution [39] until use. The fruit were selected to express a range of severities of russet. Prior to sectioning, the blocks were rinsed with deionised water and placed in 70% ethanol in plastic cassettes overnight (PrintMate biopsy Cassetes; Thermo Fisher Scientific, Kalamazoo, MI, USA). Samples were embedded and dehydrated as described before [40]. Briefly, tissue blocks were dehydrated in an ascending series of alcohol (70, 80, 90, and 96% *v/v* ethanol and 100% isopropanol). Thereafter, the blocks were dipped in xylol and then in a 1:1 *v/v* paraffin-xylol mixture before embedding in hot paraffin wax. The embedded tissue blocks were then cooled on ice and stored at 4 °C until use. Sections (10 μm thick) were cut with a microtome (Zeiss Hyrax M55; Carl Zeiss MicroImaging, Jena, Germany). The sections were relaxed on the surface of a warm water bath (40 °C), mounted on glass slides, and dried overnight at 40 °C. To remove the paraffin, the sections were washed in xylol, then rehydrated in aqueous ethanol solutions of decreasing concentration (96–60% *v/v*) and finally in deionised water. Staining was done for 60 min using 0.005% (*w/v*) fluorol yellow 088 (Santa Cruz Biotechnology, Dallas, TX, USA) dissolved in 50% *w/v* PEG 4000 (SERVA Electrophoresis, Heidelberg, Germany) and 45% *v/v* glycerol. The sections were rinsed with deionised water and viewed under incident bright and incident fluorescent light (filter module

45

U-MWU 330–385 nm excitation wavelength, ≥420 nm emission wavelength; Olympus) using a fluorescence microscope (BX-60; Olympus). Calibrated images were taken (DP 73; Olympus).

4.4. Experiments

4.4.1. Developmental Time Course

The developmental time courses of fruit growth and russeting were established. Five fruitlets per tree from a total of five trees were selected and tagged in a commercial orchard in Machakos County. Fruit were photographed (Lumix DMC-G80; Panasonic) every 14 to 21 days between 100 to 219 days after full bloom (DAFB). A ruler was included in each photograph for calibration. Fruit length and two orthogonal equatorial diameters were measured by image analysis (ImageJ 1.52P; National Health Institute). Fruit surface area was calculated from mean diameter assuming the fruit shape of a sphere as a first approximation ($A = 4\pi r^2$). The rate of increase in surface area (cm^2 d^{-1}) was calculated as the increase in surface area in a time interval divided by the duration of the interval. The russeted area was estimated from the percentage of russeted area on virtual circular epidermal sections of about 2.5 to 3.0 cm diameter of the cheek. This region exhibited minimum curvature, and the skin section was approximately planar. The russeted area was quantified by image analysis (ImageJ 1.52P; National Health Institute). The mass of 15 fruits picked at random on each sampling date was determined.

4.4.2. Effect of Region of the Fruit Surface

To quantify the distribution of russet along the stem/apex axis of the fruit, fresh fruit were selected with russet incidence ranging from a score of 1 to 4. The fruits were sliced into four regions perpendicular to the stem/apex axis representing the stem end, the basal cheek, the apical cheek, and the apex (Figure 7). These regions were further partitioned into the ventral and the dorsal sides or the blushed and the non-blushed sides of the fruit. The ventral side refers to the cheek on the side of the stylar scar, the dorsal side to the opposite side. The blushed side refers to the side that was exposed to sunlight and developed a red/orange colouration. The non-blushed side refers to the side opposite the blushed side. Russeting was quantified in the different regions on a total of 18 fruit using image analysis (ImageJ 1.52P; National Health Institute).
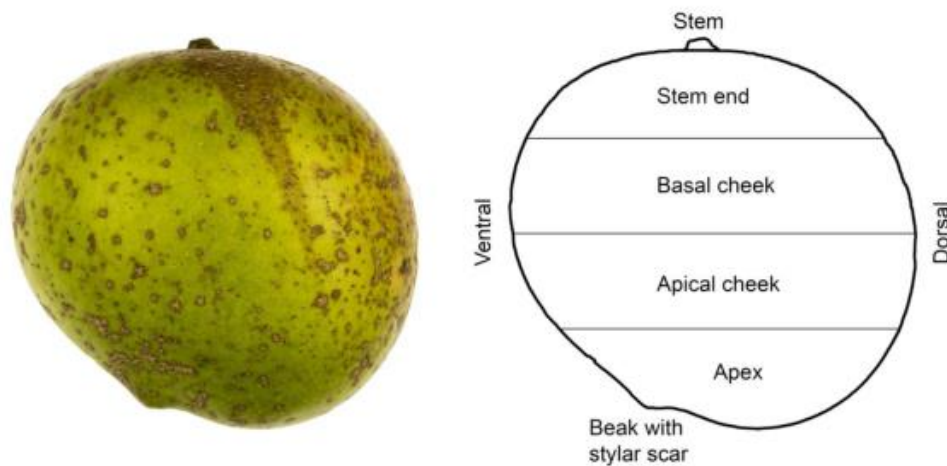
Figure 7. Photograph of 'Apple' mango and sketch illustrating the nomenclature used to describe regions of the fruit surface [41].

Potential differences in the severity of russeting between the ventral and the dorsal sides of the same fruit were investigated. A minimum of 200 fruits per site were rated for russeting using the

46

rating scheme described above. The analysis was carried out at Kaiti (1468 m), Mumbuni (1240 m) and Yeemulwa (1013 m). These sites were selected because they differ significantly in elevation.

4.4.3. Distribution of Russeted Fruit within the Canopy

The distribution of russeted fruit within the canopy was determined on a minimum of 200 fruits per site using the rating scheme described above. The three sites were Kaiti, Mumbuni, and Yeemulwa. Mature fruits located either in the periphery of the canopy (exposed) or in the centre of the canopy (shaded) were inspected and rated. In a second experiment, the role of the height of the fruit in the canopy was investigated. Here, fruits from the top (over 2 m above the ground), the middle (1–2 m), and the bottom (0.5–1 m) layers of the canopy were rated. Fruits below 0.5 m from the ground were excluded.

To test the effect of tree orientation, fruits exposed from north, south, east, and west quadrants of the canopy were selected, inspected, and rated for russeting, as described above.

4.4.4. Effect of Orchard Site on Russeting

To establish potential relationships between russeting and climatic conditions, mature fruits were selected from ten different sites. Fruit were inspected and rated for russeting using the scheme described above. The sites were: Thika, Machakos, Yeemulwa, Mumbuni, Kaiti, Malindi, Garissa, Kasafari, Kambirwa, and Chepsigot. The altitude of these sites was determined using Google Earth (Version 9.3.109.1, Google LLC, Mountain View, CA, USA). Daily rainfall, relative humidity, and daily minimum, mean, and maximum temperatures during the growing season were obtained from the website of the NASA Langley Research Center (LaRC) POWER Project funded through the NASA Earth Science/Applied Science Program (NASA Langley Research Center, Hampton, VA, USA). Potential relationships between russet scores and climatic variables were investigated using correlation and regression analyses. Heat sums were calculated using a base temperature of 16 °C [42].

4.4.5. Transpiration

The effect of russet on postharvest water vapour loss was investigated on intact mature fruits with and without russet. Since it was impossible to identify a sufficient number of fruits with 0% russet (score 0), fruits with less than 10% russet (score 1) were included in the category of non-russeted fruit. The russeted category had a russet score of 3–4. Fruit heights and diameters were measured using digital callipers (CD-30PK; Mitutoyo, Kawasaki/Kanagawa, Japan). The stem end was sealed with silicone rubber (Dow Corning SE 9186; Dow Corning Corp, Midland, MI, USA). Fruits were incubated in a polyethylene (PE) box containing a saturated slurry of NaCl generating a relative humidity of about 75% (equivalent to 14.6 g m^{-3} at 22 °C; [43]). Fruit were weighed (Sartorius Pro 32/34F micro scales, Sartorious AG, Göttingen, Germany) every 24 h for 96 h. The rate of water loss (F, g h^{-1}) was calculated from the slope of a linear regression line fitted through a plot of water loss (g) against time (h) on an individual fruit basis.

Epidermal skin segments (ES) were excised from russeted and non-russeted regions of the fruit surface using a biopsy punch (10 mm diameter) (Kai Europe, Solingen, Germany). The cut surface of the ES was blotted dry. The ES were mounted in custom made stainless steel diffusion cells using high-vacuum grease (Korasilon-Paste; Kurt Obermeier GmbH & Co. KG, Bad Berleburg, Germany) such that the outer surfaces with the cuticle were exposed in the 7 mm orifices. Diffusion cells were filled with deionised water through a hole in the base. This hole and the gap between the bottom and the top of the diffusion cells were subsequently sealed using clear transparent tape (Tesa Film®; Tesa-Werke Offenburg GmbH, Offenburg, Germany). The cells were turned upside down and left overnight to equilibrate. The next morning, the diffusion cells were weighed and placed in a PE box above dry silica gel. The cells were repeatedly weighed on a digital analytical balance (Pioneer TM, OHAUS Europe GmbH, Nänikon, Switzerland) every 2 h for 8 h. The rate of water loss was calculated as described above. The permeance (P, m s^{-1}) of the ES to water vapour loss was

calculated from P = F/(A · ΔC). In this equation, A (m^2) is the area of the orifice of the diffusion cell. Water vapour concentration (C$_i$) inside the fruit/diffusion cell was essentially saturated (19.44 g m^{-3} at 22 °C; [44]), while C$_0$ above dry silica gel was practically zero [45]. The experiment was conducted with 12 replications.

4.5. Data Analyses and Presentation

Data are presented as means and standard errors, except for individual observations. Where error bars are not visible, they are smaller than the data symbols. Data were analysed using analysis of variance, correlation, and regression analyses. Means were compared using Tukey's studentised test ($p \leq 0.05$, package multcomp 1.3-1, procedure glht, R version 3.6.3; R Foundation for Statistical Computing, Vienna, Austria). Regression analyses were carried out using R (version 3.6.3; R Foundation for Statistical Computing) and SigmaPlot (version 12.5; Systat Software, San Jose, CA, USA). SigmaPlot (version 12.5; Systat Software). Significance of coefficients of determination (r^2) at $p \leq 0.05$, 0.01 and 0.001 are indicated by *, ** and ***, respectively.

References

1. Evert, R.F. *Esau's Plant Anatomy: Meristems, Cells, and Tissues of the Plant Body: Their Structure, Function, and Development*, 3rd ed.; John Wiley & Sons, Inc.: Hoboken, NJ, USA, 2006; pp. 427–445, doi:10.1002/0470047380.ch15.

2. Gamble, J.; Jaeger, S.R.; Harker, F.R. Preferences in pear appearance and response to novelty among Australian and New Zealand consumers. *Postharvest Biol. Technol.* **2006**, *41*, 38–47, doi:10.1016/j.postharvbio.2006.01.019.

3. Khanal, B.P.; Ikigu, G.M.; Knoche, M. Russeting partially restores apple skin permeability to water vapour. *Planta* **2019**, *249*, 849–860, doi:10.1007/s00425-018-3044-1.

4. Faust, M.; Shear, C.B. Russeting of apples, an interpretive review. *HortScience* **1972**, *7*, 233–235.

5. Faust, M.; Shear, C.B. Fine structure of the fruit surface of three apple cultivars. *J. Amer. Soc. Hort. Sci.* **1972**, *97*, 351–355.

6. Knoche, M.; Grimm, E. Surface moisture induces microcracks in the cuticle of 'Golden Delicious' apple. *HortScience* **2008**, *43*, 1929–1931, doi:10.21273/HORTSCI.43.6.1929.

7. Tukey, L.D. Observations on the russeting of apples growing in plastic bags. *Proc. Amer. Soc. Hort. Sci.* **1969**, *74*, 30–39.

8. Goffinet, M.C.; Pearson, R.C. Anatomy of russeting induced in concord grape berries by the fungicide chlorothalonil. *Am. J. Enol. Vitic.* **1991**, *42*, 281–289.

9. Jones, K.M.; Bound, S.A.; Oakford, M.J.; Wilson, D. A strategy for reducing russet in Red Fuji apples while maintaining control of black spot (*Venturia inaequalis*). *Aust. J. Exp. Agr.* **1994**, *34*, 127–130, doi:10.1071/Ea9940127.

10. McCoy, C.W. Damage and control of eriophyoid mites in crops: Stylar feeding injury and control of eriophyoid mites in citrus. In *Eriophyoid Mites: Their Biology, Natural Enemies and Control*; Lindquist, E.E., Sabelis, M.W., Bruin, J., Eds.; Elsevier: Amsterdam, The Netherlands, 1996; Volume 6, pp. 481–490.

11. Gildemacher, P.; Heijne, B.; Silvestri, M.; Houbraken, J.; Hoekstra, E.; Theelen, B.; Boekhout, T. Interactions between yeasts, fungicides and apple fruit russeting. *FEMS Yeast Res* **2006**, *6*, 1149–1156, doi:10.1111/j.1567-1364.2006.00109.x.

12. Lindow, S.E.; Desurmont, C.; Elkins, R.; McGourty, G.; Clark, E.; Brandl, M.T. Occurrence of indole-3-acetic acid-producing bacteria on pear trees and their association with fruit russet. *Phytopathology* **1998**, *88*, 1149–1157, doi:10.1094/Phyto.1998.88.11.1149.

13. Bell, H.P. The origin of russeting in the Golden Russet apple. *Can. J. Res.* **1937**, *15c*, 560–566, doi:10.1139/cjr37c-042.

14. Meyer, A. A study of the skin structure of Golden Delicious apples. *Proc. Amer. Soc. Hort. Sci.* **1944**, *45*, 105–110.

15. Skene, D.S. The development of russet, rough russet and cracks on the fruit of the apple Coxs Orange Pippin during the course of the season. *J. Hortic. Sci.* **1982**, *57*, 165–174, doi:10.1080/00221589.1982.11515037.

16. Simons, R.K.; Chu, M.C. Periderm morphology of mature Golden Delicious apple with special reference to russeting. *Sci. Hort.* **1978**, *8*, 333–340, doi:10.1016/0304-4238(78)90055-9.

17. Shi, C.H.; Qi, B.X.; Wang, X.Q.; Shen, L.Y.; Luo, J.; Zhang, Y.X. Proteomic analysis of the key mechanism of exocarp russet pigmentation of semi-russet pear under rainwater condition. *Scientia Hort.* **2019**, *254*, 178–186, doi:10.1016/j.scienta.2019.04.086.

18. Arpaia, M.L.; Kahn, T.L.; Elotmani, M.; Coggins, C.W.; Demason, D.A.; Oconnell, N.V.; Pehrson, J.E. Preharvest rindstain of 'Valencia' orange: Histochemical and developmental characterization. *Sci. Hort.* **1991**, *46*, 261–274, doi:10.1016/0304-4238(91)90049-5.

19. Cohen, H.; Dong, Y.H.; Szymanski, J.; Lashbrooke, J.; Meir, S.; Almekias-Siegl, E.; Zeisler-Diehl, V.V.; Schreiber, L.; Aharoni, A. A multilevel study of melon fruit reticulation provides insight into skin ligno-suberization hallmarks. *Plant Physiol.* **2019**, *179*, 1486–1501, doi:10.1104/pp.18.01158.

20. Schreiber, L.; Franke, R.; Hartmann, K. Wax and suberin development of native and wound periderm of potato (*Solanum tuberosum* L.) and its relation to peridermal transpiration. *Planta* **2005**, *220*, 520–530, doi:10.1007/s00425-004-1364-9.

21. Scharwies, J.D.; Grimm, E.; Knoche, M. Russeting and relative growth rate are positively related in 'Conference' and 'Condo' pear. *HortScience* **2014**, *49*, 746–749, doi:10.21273/HORTSCI.49.6.746.

22. Wertheim, S.J. Fruit russeting in apple as affected by various gibberellins. *J. Hortic. Sci.* **1982**, *57*, 283–288, doi:10.1080/00221589.1982.11515054.

23. Knoche, M.; Khanal, B.P.; Stopar, M. Russeting and microcracking of 'Golden Delicious' apple fruit concomitantly decline due to gibberellin a(4+7) application. *J. Amer. Soc. Hort. Sci.* **2011**, *136*, 159–164, doi:10.21273/JASHS.136.3.159.

24. Creasy, L.L. The correlation of weather parameters with russet of Golden Delicious apples under orchard conditions. *J. Amer. Soc. Hort. Sci.* **1980**, *105*, 735–738.

25. Verner, L. Histology of apple fruit tissue in relation to cracking. *J. Agric. Res.* **1938**, *57*, 813–824.

26. Bally, I.S.E. Changes in the cuticular surface during the development of mango (*Mangifera indica* L.) cv. Kensington Pride. *Sci. Hort.* **1999**, *79*, 13–22, doi:10.1016/S0304-4238(98)00159-9.

27. Tamjinda, B.; Siriphanich, J.; Nobuchi, T. Anatomy of lenticels and the occurrence of their discoloration in mangoes (*Mangifera indica* cv. Namdokmai). *Kasetsart J.* **1992**, *26*, 57–64.

28. Ruess, F.; Stoesser, R. Über die dreidimensionale Rekonstruktion des Interzellularsystems von Apfelfrüchten. *Angew. Bot.* **1993**, *67*, 113–119.

29. Khanal, B.P.; Si, Y.R.; Knoche, M. Lenticels and apple fruit transpiration. *Postharvest Biol. Technol.* **2020**, *167*, doi:10.1016/j.postharvbio.2020.111221.

30. Curry, E.A.; Torres, C.; Neubauer, L. Preharvest lipophilic coatings reduce lenticel breakdown disorder in 'Gala' apples. *HortTechnology* **2008**, *18*, 690–696, doi:10.21273/Horttech.18.4.690.

31. Brown, K.; Considine, J. Physical aspects of growth: Stress distribution around lenticels. *Plant Physiol.* **1982**, *69*, 585–590, doi:10.1104/pp.69.3.585.

32. Knoche, M.; Peschel, S. Deposition and strain of the cuticle of developing European plum fruit. *J. Amer. Soc. Hort. Sci.* **2007**, *132*, 597–602, doi:10.21273/JASHS.132.5.597.

33. Brüggenwirth, M.; Knoche, M. Cell wall swelling, fracture mode, and the mechanical properties of cherry fruit skins are closely related. *Planta* **2017**, *245*, 765–777, doi:10.1007/s00425-016-2639-7.

34. Knoche, M.; Peschel, S. Water on the surface aggravates microscopic cracking of the sweet cherry fruit cuticle. *J. Amer. Soc. Hort. Sci.* **2006**, *131*, 192–200, doi:10.21273/JASHS.131.2.192.

35. Becker, T.; Knoche, M. Water induces microcracks in the grape berry cuticle. *Vitis* **2012**, *51*, 141–142, doi:10.5073/vitis.2012.51.141-142.

36. Khanal, B.P.; Knoche, M. Mechanical properties of cuticles and their primary determinants. *J. Expt. Bot.* **2017**, *68*, 5351–5367, doi:10.1093/jxb/erx265.

37. Khanal, B.P.; Grimm, E.; Knoche, M. Russeting in apple and pear: A plastic periderm replaces a stiff cuticle. *AoB Plants* **2013**, *5*, pls048, doi:10.1093/aobpla/pls048.

38. Knoche, M.; Khanal, B.P.; Brüggenwirth, M.; Thapa, S. Patterns of microcracking in apple fruit skin reflect those of the cuticular ridges and of the epidermal cell walls. *Planta* **2018**, *248*, 293–306, doi:10.1007/s00425-018-2904-z.

39. Karnovsky, M.J. A formaldehyde-glutaraldehyde fixative of high osmolality for use in electron microscopy. *J. Cell Biol.* **1965**, *27*, 137A–138A.

40. Hoenemann, C.; Richardt, S.; Kruger, K.; Zimmer, A.D.; Hohe, A.; Rensing, S.A. Large impact of the apoplast on somatic embryogenesis in Cyclamen persicum offers possibilities for improved developmental control in vitro. *BMC Plant Biol.* **2010**, *10*, doi:10.1186/1471-2229-10-77.

41. Pope, W.T. Mango culture in Hawaii. *Hawaii Agric. Exp. Stn.* **1929**, *Bulletin No. 58*, 1-27, doi:10.5962/bhl.title.118825.

42. Léchaudel, M.; Génard, M.; Lescourret, F.; Urban, L.; Jannoyer, M. Modeling effects of weather and source-sink relationships on mango fruit growth. *Tree Physiol.* **2005**, *25*, 583–597, doi:10.1093/treephys/25.5.583.

43. Wexler, A. Constant humidity solutions. In *Handbook of Chemistry and Physics*, 76th ed.; Lide, D.R., Ed.; CRC Press: Boca Raton, FL, USA, 1995; pp. 15–23.

44. Nobel, P.S. *Physicochemical and Environmental Plant Physiology*, 2nd ed.; Academic Press: San Diego, CA, USA, 1999.

45. Geyer, U.; Schönherr, J. In vitro test for effects of surfactants and formulations on permeability of plant cuticles. In *Pesticide Formulations: Innovations and Developments*; Cross, B., Scher, H.B., Eds.; American Chemical Society: Washington, DC, USA, 1988; Volume 371, pp. 22–33.
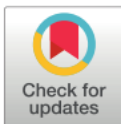
3.3 Low cuticle deposition rate in 'Apple' mango increases elastic strain, weakens the cuticle and increases russet

Authors:

Thomas O. Athoo (**TOA**), Bishnu P. Khanal (**BK**), and Moritz Knoche (**MK**)

Author affiliation:

Institute of Horticultural Production Systems, Fruit Science Section, Leibniz University Hannover, Herrenhäuser Straße 2, 30419 Hannover, Germany

Author Contributions:

Conceptualization, T.O.A. and M.K.; Funding acquisition, M.K.; Investigation, T.O.A.; Methodology, T.O.A., B.P.K. and M.K.; Supervision, M.K., B.P.K.; Visualization, T.O.A. and B.P.K.; Validation, T.O.A. and B.P.K; Writing-original draft, T.O.A., B.P.K. and M.K.; Writing-review & editing, T.O.A., B.P.K. and M.K.; Project administration, M.K.

PLOS ONE

Low cuticle deposition rate in 'Apple' mango increases elastic strain, weakens the cuticle and increases russet

Thomas O. Athoo[ORCID][°], Bishnu P. Khanal[ORCID][°], Moritz Knoche[ORCID]*[°]

Institute for Horticultural Production Systems, Leibniz-University Hannover, Hannover, Germany

[°] These authors contributed equally to this work.
* moritz.knoche@obst.uni-hannover.de

Abstract

Russeting compromises appearance and downgrades the market value of many fruitcrops, including of the mango cv. 'Apple'. The objective was to identify the mechanistic basis of 'Apple' mango's high susceptibility to russeting. We focused on fruit growth, cuticle deposition, stress/strain relaxation analysis and the mechanical properties of the cuticle. The non-susceptible mango cv. 'Tommy Atkins' served for comparison. Compared with 'Tommy Atkins', fruit of 'Apple' had a lower mass, a smaller surface area and a lower growth rate. There were little differences between the epidermal and hypodermal cells of 'Apple' and 'Tommy Atkins' including cell size, cell orientation and cell number. Lenticel density decreased during development, being lower in 'Apple' than in 'Tommy Atkins'. The mean lenticel area increased during development but was consistently greater in 'Apple' than in 'Tommy Atkins'. The deposition rate of the cuticular membrane was initially rapid but later slowed till it matched the area expansion rate, thereafter mass per unit area was effectively constant. The cuticle of 'Apple' is thinner than that of 'Tommy Atkins'. Cumulative strain increased sigmoidally with fruit growth. Strains released stepwise on excision and isolation ($\varepsilon_{exc+iso}$), and on wax extraction (ε_{extr}) were higher in 'Apple' than in 'Tommy Atkins'. Membrane stiffness increased during development being consistently lower in 'Apple' than in 'Tommy Atkins'. Membrane fracture force (F_{max}) was low and constant in developing 'Apple' but increased in 'Tommy Atkin'. Membrane strain at fracture (ε_{max}) decreased linearly during development but was lower in 'Apple' than in 'Tommy Atkins'. Frequency of membrane failure associated with lenticels increased during development and was consistently higher in 'Apple' than in 'Tommy Atkins'. The lower rate of cuticular deposition, the higher strain releases on excision, isolation and wax extraction and the weaker cuticle account for the high russet susceptibility of 'Apple' mango.

Introduction

Russeting of the skin compromises the appearance of many fruitcrop species, including of mango. Although the problem is mostly cosmetic, russeted fruits are usually excluded from

52

high-end and export markets because of their unattractive, blotchy, dull-brown, appearance. Microscopic cracks (microcracks) in the cuticle are the first microscopic signs of russeting. Microcracks impair the barrier function of the cuticle. The consequences are: (1) an increased incidence of fruit rots [1] and (2) an unrestricted water movement into [2] and out of the fruit [3, 4]. Unrestricted water ingress can lead to bursting of epidermal cells and, eventually, to skin macrocracks that propagate deep into the flesh. Unrestricted water egress leads to increased postharvest water (weight) loss and, eventually, to skin shrivel. In a healthy growing fruit, the cuticle's impaired barrier function, initiates the differentiation of a periderm which partially or wholly restores the barrier functions of the fruit skin. The first stage in the development of a periderm is for the cells of the hypodermis to become meristematic (a phellogen), these dividing cells then form stacks of waterproof (suberized) cork cells (the phellem). It is the suberized cell walls of the phellem that are responsible for the rough, dull-brown appearance of a russeted fruit.

The development of russeting is triggered by environmental factors including surface moisture and high humidity [4–6]. Large differences in susceptibility to russeting occur between species and, within species, between cultivars. Among Kenyan mango cultivars, cv. 'Apple' is highly susceptible to russeting, whereas cv. 'Tommy Atkins' is not. Due to its unattractive russeted appearance, the marketing of 'Apple' mango can be difficult.

Stress/strain relaxation analysis of the fruit skin is a tool that provides useful insight into the causal relationships underlying the formation of microcracks [7]. In this analysis, stress is removed stepwise, while the resulting strain releases are monitored [8]. The total area strain (ε_{total}) represents the increase in surface area during fruit growth. This is partitioned into various component strains by stepwise removal of the stresses and monitoring the resulting strain releases. The component stresses leading to ε_{total} include the strain released on excision of an epidermal segment (ε_{exc}), the strain released on (enzymatic) isolation of the cuticle (ε_{iso}) and that released on extraction of the cuticular wax (ε_{extr}). The remaining or residual strain (ε_{resid}) may be calculated as the difference between the ε_{total} minus the sum of ε_{exc}, ε_{iso}, and ε_{extr}. The residual strain ε_{resid} is irreversible, and it remains associated with the extracted cuticular membrane. In general, the buildup of elastic strain is considered not to be critical, provided the overall thinning of the cutin matrix is prevented by the continuous deposition of new cutin beneath it, and of wax within it, as its area expands.

The objective of this work was to understand the basis for the high susceptibility of 'Apple' mangoes to russeting. A better understanding is helpful in developing suitable countermeasures to reduce or prevent russeting in this cultivar. We focus on fruit growth, skin anatomy, cuticle deposition, stress/strain relaxation analysis and the mechanical properties of the cuticle. The russeting non-susceptible mango cultivar 'Tommy Atkins' served for comparison.

Materials and methods

Plant materials

'Apple' and 'Tommy Atkins' mangoes (*Mangifera indica* L.) were grafted on local, unclassified rootstocks. Fruit were harvested from a commercial orchard located in Mwala, Kenya (1°19'S, 37°26'E). The orchard was managed conventionally using local integrated crop management programs. Permission to sample fruit was given by the owner of the orchard Mr. and Mrs. Musyoka.

Fruit growth

The time course of fruit growth was established first. Fruits were sampled every 1–3 weeks from 41 to 159 days after full bloom (DAFB). Fruits were weighed (Sartorius Pro 32/34F micro

53

scales, Sartorious AG, Göttingen, Germany) and their length, and two orthogonal diameters were measured using calipers (CD-30PK; Mitutoyo, Kawasaki/Kanagawa, Japan). Fruit surface area was calculated assuming spherical shape. A sigmoid regression model was fitted through a plot of surface area vs. time. From this model, the rate of surface area growth ($cm^2 d^{-1}$) was calculated from the first derivative.

The relationships between fruit diameter, fruit surface area and fruit mass were established. Briefly, three fruit per cultivar were sampled every 2 to 3 weeks and weighed (Sartorius Pro 32/34F). Calibrated digital photographs were taken from two orthogonal aspects (Lumix DMC-G80; Panasonic Corporation, Osaka, Japan). The three orthogonal fruit diameters were quantified using image analysis (ImageJ 1.53P; National Health Institute, Bethesda, MD, USA). Fruit were then peeled, the peels flattened between two glass plates and digital photographs taken (Lumix DMC-G80; Panasonic Corporation). Peel area was quantified using image analysis (ImageJ 1.53P).

To obtain information on the spatial distribution of the skin area increase over the whole fruit surface, a set of fruit was tagged. A square pattern of four dots of a non-phytotoxic white silicon rubber (RTV 744; Dow Corning, Midland, MI, USA) was printed in five different regions on the fruit surface. The regions were: stem end, cheek, apex, back and nak (see Fig 1). The dot pattern was photographed at regular intervals (Lumix DMC-G80; Panasonic) and the area 'enclosed' by the dots quantified (ImageJ 1.53P). When necessary, dots were reapplied. We calculated the relative area growth rate ($cm^2 d^{-1}$) from a sigmoid curve fitted through a plot of 'enclosed' surface area vs. time for each region.

Anatomy

Tissue blocks were excised from the fruit skin and the outer flesh, and incubated in Karnovsky fixative. These were stored in a cold room until use [9]. For processing, blocks were removed
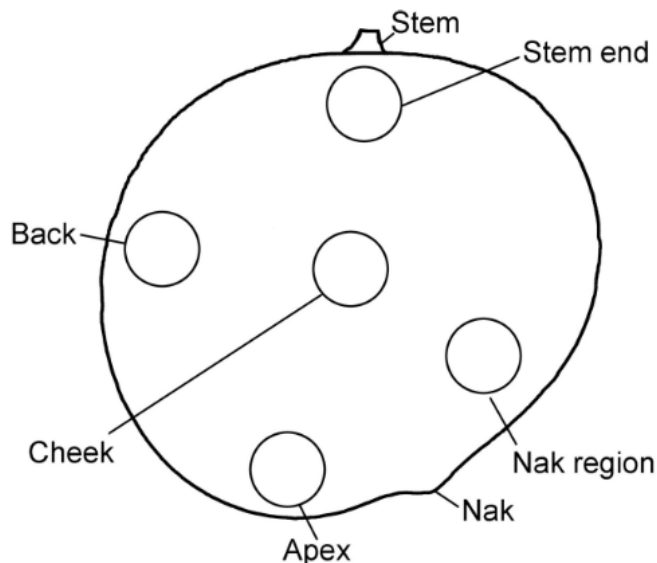

Fig 1. Sketch of mango fruit showing the different regions of the fruit surface sampled. These regions include stem end, cheek, apex, back and nak.

https://doi.org/10.1371/journal.pone.0258521.g001

54

from Karnovsky solution and thoroughly rinsed with deionized water. Thin cross-sections of skin tissue were made in tangential periclinal direction in the cheek region of the fruit. The sections were stained for 5–8 min using 0.1% w/v calcofluor white (fluorescence brightener 28; Sigma-Aldrich Chemie, Munich, Germany), mounted on a microscope slide and transferred to the stage of a fluorescence microscope (BX-60; Olympus Europa Holding GmbH, Hamburg, Germany). Sections were examined under ultraviolet (UV) light (filter U-MWU 330–385 nm excitation, $\geq$420 nm emission; Olympus Europa) and calibrated images taken at ×20 magnification using a digital camera (DP73, Olympus Europa). The number of cells and cell dimensions (periclinal and anticlinal diameters) of the epidermal and three hypodermal cell layers were measured. Preliminary investigations established that epidermal and hypodermal cells are isodiametric in the tangential plane of the fruit as indexed by the absence of significant differences in their periclinal cell dimensions. There was no clear layering of hypodermal cells in either cultivar. We therefore measured the dimensions of all cells in each image (image size 349 × 262 µm) at 30, 50 and 70 µm depths from the surface of the cuticle. The periclinal area of a cell was calculated as the square of the cell's periclinal diameter, the cell's anticlinal aspect ratio as cell anticlinal diameter divided by the cell periclinal diameter. The number of cells per unit fruit surface area was counted.

Lenticel density and area determination

The epidermal segments (ES) were excised from the stem end, cheek, apex, back and nak regions using a biopsy punch (8 mm diameter). The ES were photographed (Lumix DMC-G80; Panasonic) and the number of lenticels per disc counted (ImageJ 1.53P). Lenticel density was established by dividing the number of lenticels per ES by the area of the ES. The number of replicates was 30.

The areas of individual lenticels were quantified using enzymatically isolated cuticles. Lenticels were viewed under bright incident light using a binocular microscope (Leica MZ10F; Leica Microsystems, Wetzlar, Germany). Calibrated digital photographs were taken (Olympus DP 71; Olympus Europa). The areas of three to four lenticels per CM were measured using image analysis (cellSens version 1.7.1.; Olympus Europa). The number of replicates was 60 lenticels from 10 fruits.

Cuticle deposition

Cuticles were isolated enzymatically. Briefly, ES were excised from the cheek region using a biopsy punch (8 or 10 mm diameter; Kai Europe, Solingen, Germany) at regular time intervals. The ES were incubated in an isolation medium containing pectinase (90 ml l^{-1}; Panzym Super E flüssig, Novozymes A/S, Krogshoejvej, Bagsvaerd, Denmark), cellulase (5 ml l^{-1}; Cellubrix L; Novozymes A/S) [10]. The pH was adjusted to 4.0 using NaOH. NaN$_3$ was added at a final concentration of 30 mM to suppress microbial growth. The solution was refreshed regularly until the cuticular membrane (CM) separated from adhering cellular debris. The CM were cleaned using a camel-hair brush, then rinsed at least 5-times using deionized water.

For mass determination, CMs were dried at 40˚C (Memmert 100–800; Memmert, Schwabach, Germany) and then weighed (CPA2P; Sartorius). Wax was extracted in a Soxhlet apparatus using chloroform: methanol (1:1 v/v CHCl$_3$/MeOH) for a minimum of 2 h. The dewaxed cuticular membranes (DCMs) were dried overnight at 40˚C (Memmert 100–800) and weighed. The CM, DCM and wax masses per unit area were calculated. The number of replicates was 10–20.

55

Quantifying the areas of ES, CM and DCM

The ES were photographed (Lumix DMC-G80; Panasonic) and their areas quantified by image analysis (ImageJ 1.53P). Following enzymatic isolation, the fully-hydrated CMs were again photographed using a binocular microscope (Wild M10; Leica Microsysteme; camera DP71, Olympus Europa). Before dewaxing, a square pattern of holes was punched into the center of each CM disc and the hole pattern photographed. This was necessary because the DCMs curled up following extraction and it became impossible to flatten them. Two orthogonal diameters were measured on each ES or CM disc. For the DCM discs the areas enclosed by the hole patterns were calculated.

Calculating apparent and cumulative strains

The developmental time course of change in apparent (ε', %) and cumulative (ε, mm^{2}mm^{-2}) strain of the skin was calculated as the strain released upon excision, and upon isolation, and upon wax extraction [7]. The apparent strains released after excision and isolation of the CM ($\varepsilon'_{exc+iso}$) and that released after dewaxing (ε'_{extr}) were calculated using Eq 1 and Eq 2 respectively:

$$\varepsilon'_{exc+iso} = \frac{A^i - A^i_{CM}}{A^i_{DCM}} \times 100 \qquad (1)$$

and

$$\varepsilon'_{extr} = \frac{A^i_{CM} - A^i_{DCM}}{A^i_{DCM}} \times 100 \qquad (2)$$

In these equations, A^i represents the area of the skin disc before excision; A^i_{CM} is the area of the isolated CM disc and A^i_{DCM} is the area of an entire DCM disc. The latter was calculated from the square pattern of holes in the DCM. The sum of both these strains represents the total apparent strain (ε'_{total}). As pointed out earlier, the area of the extracted CM disc at the particular time of sampling (t = i) serves as the basis of the calculation of apparent strains [7]. Any irreversible strain(s) that occur during growth of the carpel to the fruitlet at the time of sampling and that remain associated with the extracted CM discs are not accounted for.

These pitfalls are avoided when calculating the absolute cumulative strain (ε, mm^{2}mm^{-2}) of developing fruit [7]. Here the increase in fruit surface area with time is accounted for. In this analysis, the total cumulative strain (ε_{total}) is partitioned into several component strains. The total cumulative strain (ε_{total}) at time t = i was estimated as the change in surface area (ΔA^i) relative to the initial surface area (A_0) at time t = 0 (Eq 3). As discussed earlier [7], it is impractical to define the starting surface area and time *ab initio* (i.e., the differentiation of the carpel within a bud). We therefore defined the surface area at the time of initiation A_0 somewhat arbitrarily as about 1 cm^2 and calculated the total cumulative strain from Eq 3 [7].

$$\varepsilon_{total} = \frac{A^i_{total} - A_0}{A_0} \qquad (3)$$

In this equation, A^i_{total} represents the fruit surface area at a particular sampling time (t = i).

The cumulative strains released after excision and CM isolation ($\varepsilon_{exc+iso}$) and after dewaxing (ε_{extr}) were calculated as the differences in areas of the ES disc before excision (A^i), and of the isolated CM (A_{CM}), and of the extracted DCM (A_{DCM}) (Eqs 4 and 5). Thus, A^i equals the cross-sectional area of the biopsy punch corrected for fruit curvature. The A_{CM} and A_{DCM} were determined at each sampling time and then calculated as the A_{CM} and A_{DCM} on a whole-

56

fruit basis at a particular time (t = i). This calculation assumes the amount of strain release is uniform across the entire fruit surface.

$$\varepsilon_{\text{exc+iso}} = \frac{A^i_{\text{total}} - A_{\text{CM}}}{A_0} \tag{4}$$

$$\varepsilon_{\text{extr}} = \frac{A_{\text{CM}} - A_{\text{DCM}}}{A_0} \tag{5}$$

The strain that remains after dewaxing ($\varepsilon_{\text{resid}}$) is fixed mostly by the cutin matrix and is calculated from Eq 6 as follows:

$$\varepsilon_{\text{resid}} = \frac{A_{\text{DCM}} - A_0}{A_0} \tag{6}$$

As explained earlier [7], the total cumulative strain ($\varepsilon_{\text{total}}$) represents the sum of these individual component strains because all were calculated relative to the same base (A_0) (Eq 7):

$$\varepsilon_{\text{total}} = \varepsilon_{\text{exc+iso}} + \varepsilon_{\text{extr}} + \varepsilon_{\text{resid}}. \tag{7}$$

Of the three component strains, $\varepsilon_{\text{extr}}$ and $\varepsilon_{\text{resid}}$ represent the plastic strain ($\varepsilon_{\text{plastic}}$), whereas the $\varepsilon_{\text{exc+iso}}$ is the elastic strain.

Uniaxial tensile tests

Strips (5 mm wide) were excised from the CM isolated between 55 and 159 DAFB using parallel-mounted razor blades. Strips were mounted in a cardboard frame made from masking tape to prevent unintentional strain during handling. Strips were hydrated overnight by incubation in deionized water. Thereafter, strips were mounted in a universal material testing machine (clamping distance l_0 = 10 mm) (Z 0.5; Zwick/Roell, Ulm, Germany) equipped with a 10 N force transducer (KAP-TC; Zwick/Roell). Frames were cut open and the test initiated at a strain rate of 0.25 mm min^{-1}.

Stiffness (S) was calculated as the maximum slope of the force (F, N) vs. strain ($\varepsilon_{\text{tensile}}$, %) diagram. Uniaxial strain was calculated as the ratio of the applied strain (Δl) divided by the length of the relaxed sample, i.e., the clamping distance l_0 (mm) and multiplied by 100. The maximum force (F_{max}) and maximum strain (ε_{max}, %) represent the force and strain recorded at failure. Following testing, the fracture site was inspected on each specimen to identify whether or not the fracture was associated with a lenticel.

Data analysis and presentation

Data are presented as means and standard errors (SE). Where not visible, the SEs are smaller than the data symbols. Data were analyzed using analysis of variance with R statistical software (R version 4.0.3; R Foundation for Statistical Computing, Vienna, Austria) and SAS (SAS Institute, Cary, NC, USA). Means were separated using Turkey's studentized range test (α = 0.05). Regression analyses were conducted in R (R version 4.0.3) and Sigma Plot (version 12.5; Systat Software, San Jose, CA, USA). Significances of regression equations at the 5, 1 and 0.1% levels are indicated by *, ** and ***, respectively.

Results

Fruit mass and surface area increased with time in a sigmoid pattern in both cultivars (Fig 2A and 2B). Fruits of 'Apple' had lower masses, lower surface areas and lower growth rates than
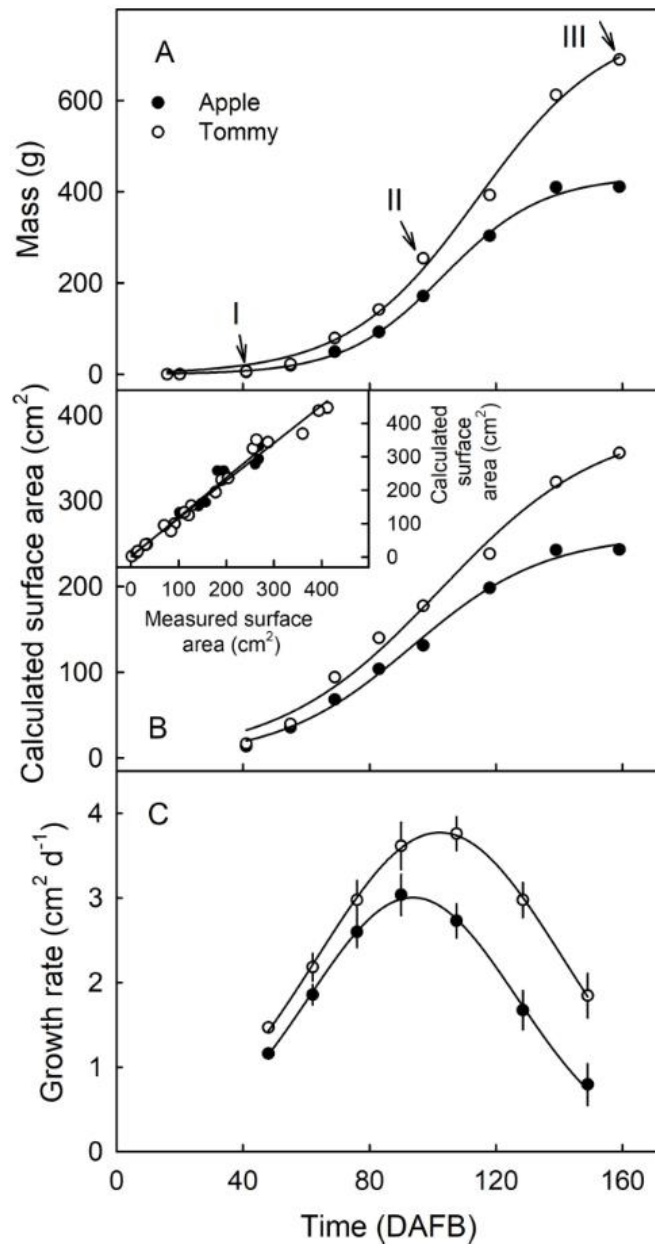
57

Fig 2. Time course of change in mass (A), calculated surface area (B) and growth rate (C) of 'Apple' and 'Tommy Atkins' mango. Inset in B: Plot of measured and calculated surface area of the fruit peel. The area was calculated assuming a spheroid shape. The x-axis scale is in days after full bloom (DAFB). Arrows indicate the sampling dates for histological examination. Data represent means ± SE. The number of individual fruit replicates was 10–20.

58

fruits of 'Tommy Atkins' (Fig 2A). In 'Apple', the area growth rate was at maximum of 3.03 cm^2 d^{-1} at 94 DAFB. On the other hand, 'Tommy Atkins' had a maximum growth rate of 3.85 cm^2 d^{-1} at about 103 DAFB (Fig 2C). There was a strong linear, positive correlation (r^2 = 0.98***) between fruit surface area measured on excised peels and that calculated from fruit dimensions (Fig 2B, inset).

The growths in the different regions of the fruit surface measured using the dot pattern also increased with time in a sigmoid pattern (Fig 3A and 3B). There were no significant differences in cumulative increases in surface area or in growth rates between these regions in either cultivar, during early fruit development (Fig 3).

Periclinal diameters of epidermal and hypodermal cells increased with development, whereas the anticlinal diameter of epidermal cells decreased in both cultivars. The anticlinal diameters of hypodermal cells in 'Apple' remained unchanged, but increased in 'Tommy Atkins' (Fig 4A and 4B). Epidermal cells were smaller than hypodermal cells. There was little difference in the dimensions of epidermal cells between 'Apple' and 'Tommy Atkins', but hypodermal cells had larger periclinal diameters in 'Tommy Atkins' than in 'Apple' (Fig 4A and 4B). Epidermal cells had markedly smaller periclinal areas than the hypodermal cells. There was little difference between the two cultivars. Periclinal areas of hypodermal cells increased in a sigmoid pattern with time. They were smaller in 'Apple' than in 'Tommy Atkins' (Fig 4C and 4D). Epidermal cells changed their anticlinal aspect ratios from 'portrait' to 'square' in both 'Apple' and 'Tommy Atkins'. Compared to the epidermal cells, the change in
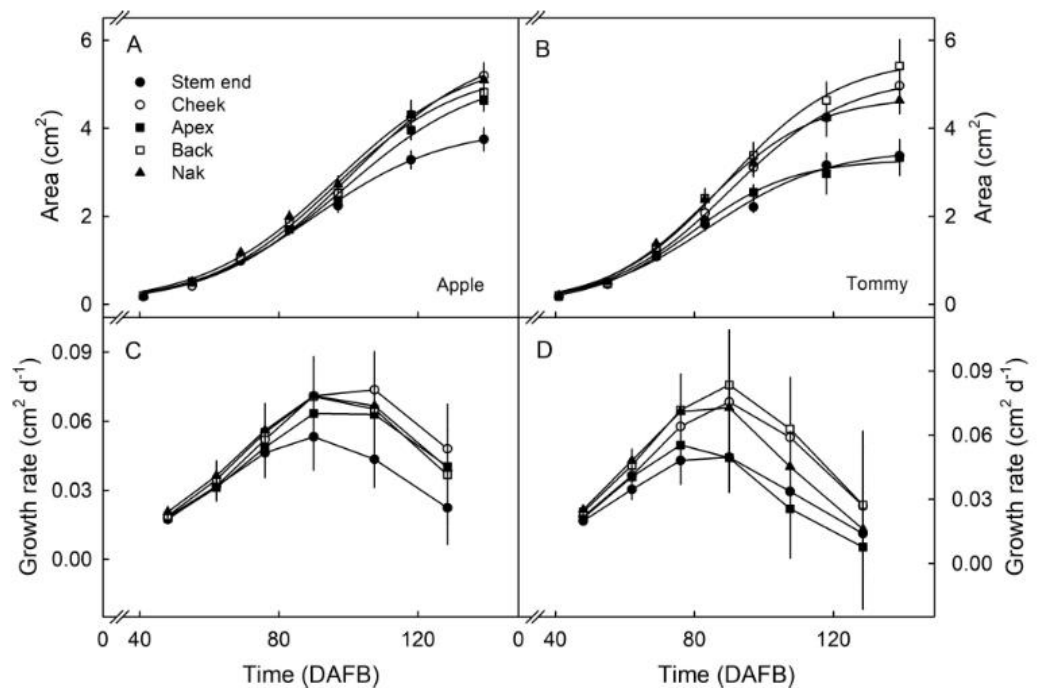
Fig 3. Time course of change in area (A,B) and growth rate (C,D) of selected regions of the fruit surface of 'Apple' (A,C) and 'Tommy Atkins' (B,D) mango. A square pattern of dots of white silicon rubber was printed in the stem end, the cheek, the apex, the back or the nak region of the fruit surface at 41 days after full bloom (DAFB) and the expansion of the dot pattern monitored. For location of the regions on the fruit surface see Fig 1. Data represent means ± SE. The number of replicates was 16–30.
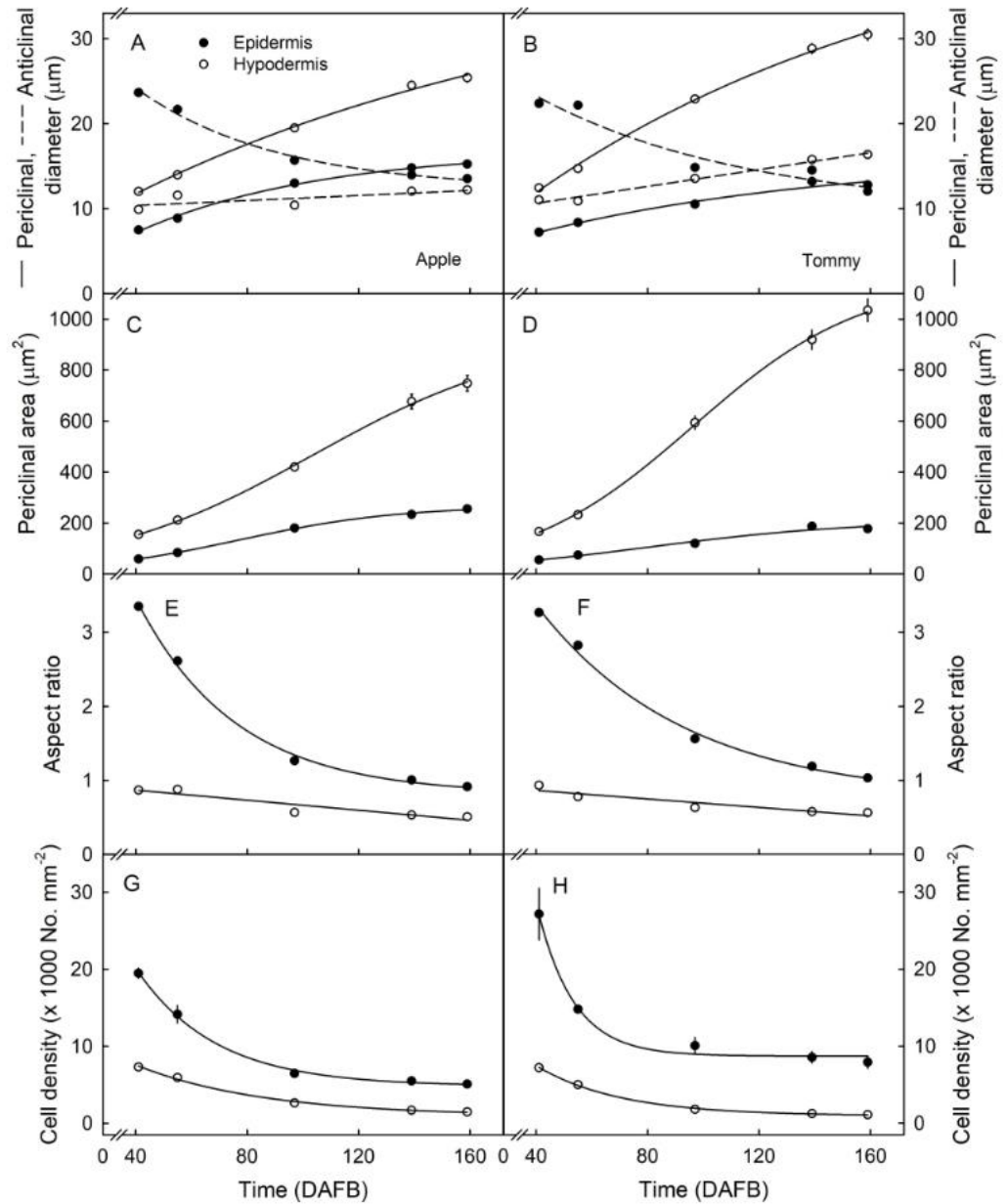
Fig 4. Developmental time course of change in anticlinal and periclinal diameters (A,B), periclinal area per cell (C,D), anticlinal aspect ratio (E,F) and number of epidermal and hypodermal cells per unit fruit surface area (G,H) of 'Apple' (A,C,E,G) and 'Tommy Atkins' (B,D,F,H) mango. The anticlinal aspect ratio was calculated as the anticlinal diameter divided by the periclinal diameter. The periclinal surface area of a cell was calculated as the square of cell periclinal diameter. The x-axis scale is in days after full bloom (DAFB). Data represent means ± SE. The number of individual fruit replicates was 10.

https://doi.org/10.1371/journal.pone.0258521.g004

60

Table 1. Lenticel density established from epidermal section of 'Apple' and 'Tommy Atkins' mango fruit skin.

Cultivar	Time (DAFB)	Lenticel density (No. mm^{-2})					
		Apex	Cheek	Stem End	Back	Nak	Mean $_{Cultivar}$
Apple	78	0.45 ± 0.02 c [a]	0.18 ± 0.01 a	0.26 ± 0.02 b	0.25 ± 0.02 b	0.14 ± 0.01 a	0.26 ± 0.01
	107	0.31 ± 0.02 d	0.08 ± 0.01 a	0.24 ± 0.01 c	0.16 ± 0.01 b	0.09 ± 0.01 a	0.18 ± 0.01
	152	0.28 ± 0.01 d	0.04 ± 0.00 a	0.19 ± 0.01 c	0.10 ± 0.01 b	0.09 ± 0.01 b	0.14 ± 0.01
Tommy Atkins	78	1.05 ± 0.06 c	0.38 ± 0.02 a	0.37 ± 0.03 a	0.62 ± 0.05 b	0.64 ± 0.05 b	0.62 ± 0.03
	107	0.73 ± 0.04 c	0.24 ± 0.02 a	0.23 ± 0.01 a	0.35 ± 0.02 b	0.30 ± 0.02 ab	0.37 ± 0.02
	152	0.40 ± 0.03 b	0.15 ± 0.01 a	0.21 ± 0.02 a	0.18 ± 0.01 a	0.18 ± 0.01 a	0.23 ± 0.01
Mean $_{Region}$ 'Apple'		0.35 ± 0.01	0.10 ± 0.01	0.23 ± 0.01	0.18 ± 0.01	0.11 ± 0.01	0.19 ± 0.01
Mean $_{Region}$ 'Tommy Atkins'		0.73 ± 0.02	0.26 ± 0.02	0.27 ± 0.02	0.38 ± 0.02	0.38 ± 0.02	0.40 ± 0.01
Mean $_{Region}$		0.54 ± 0.01	0.18 ± 0.01	0.25 ± 0.01	0.28 ± 0.01	0.24 ± 0.01	

The ES were excised from the apex, cheek, stem end, back and nak regions of the same fruits at 78, 107 or 152 days after full bloom (DAFB). Data presented as means ± SE. The number of replicates was 30.

[a] Main effect of cultivar, time (DAFB) and fruit region and their interaction significant in a three factorial ANOVA. Means therefore compared across the regions at each time (DAFB) and for each cultivar. Mean separation within rows by Tukey's studentized range test, $P < 0.05$.

https://doi.org/10.1371/journal.pone.0258521.t001

anticlinal aspect ratio of the hypodermal cells was much smaller. The hypodermal cells were nearly isodiametric in the anticlinal plane during early development, but elongated to 'landscape' towards maturity (Fig 4E and 4F). There was no significant difference in cell number per unit surface area between 'Apple' and 'Tommy Atkins' (Fig 4G and 4H).

Lenticel density decreased with time during development and was generally lower in 'Apple' than in 'Tommy Atkins' (Table 1). In both cultivars, the apex had the highest lenticel density while the cheek had the lowest (Table 1). The area per lenticel increased linearly during development (Fig 5). Fruits of 'Apple' mango consistently had larger lenticels than 'Tommy Atkins'.
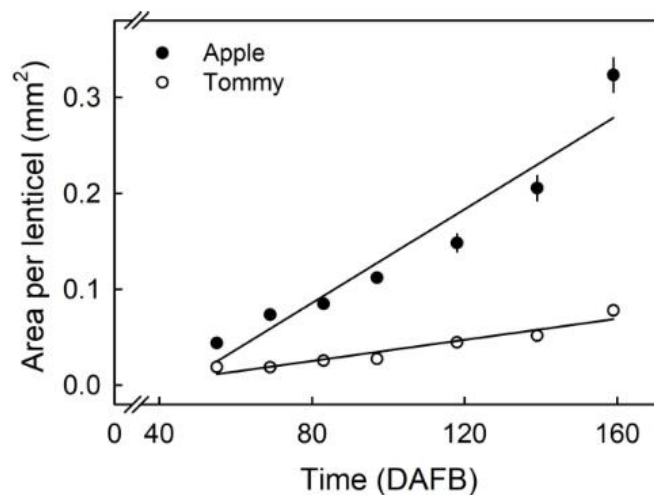

Fig 5. Developmental time course of change in area of lenticels in the cheek region of 'Apple' and 'Tommy Atkins' mango. The x-axis scale is in days after full bloom (DAFB). Data represent means ± SE. The number of replicates was 60 lenticels.
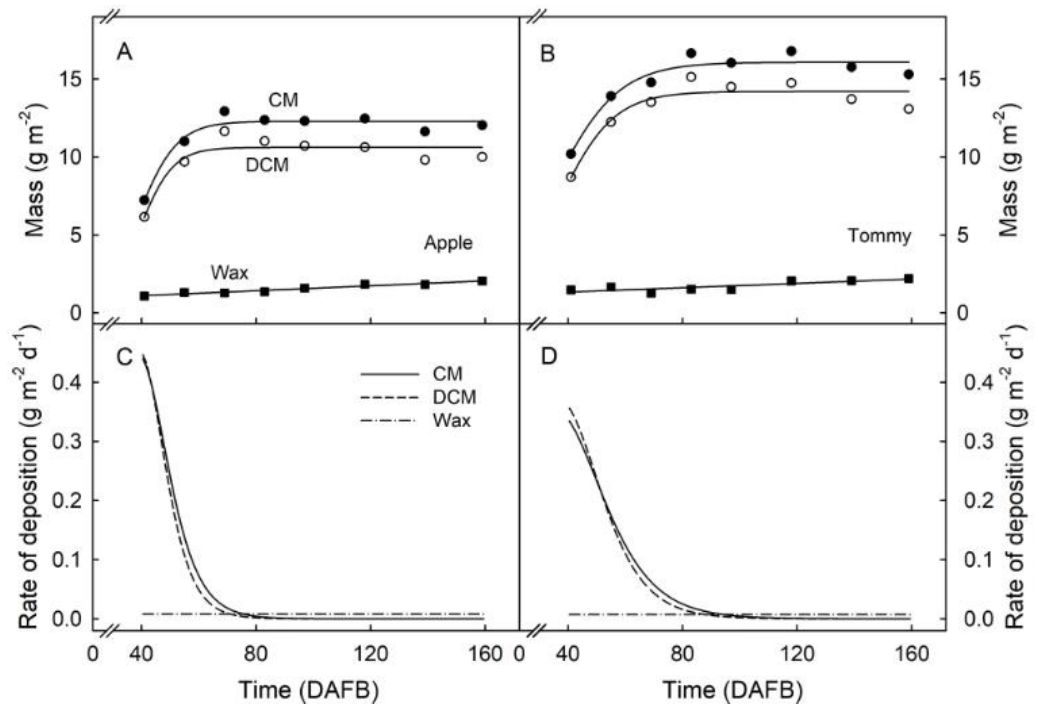
https://doi.org/10.1371/journal.pone.0258521.g005

61

Fig 6. Developmental time course of change in mass of cuticular membrane (CM), dewaxed CM (DCM) and wax of 'Apple' (A) and 'Tommy Atkins' (B) mango. Rates of deposition of CM, DCM, and wax of 'Apple' (C) and 'Tommy Atkins' (D) mango. The rates of deposition were calculated as the first derivative of a regression equation fitted through a plot of CM, DCM or wax mass vs. time. The x-axis scale is in days after full bloom (DAFB). Data in Fig 6A and 6B represent means ± SE. The number of replicates was 33–35.

The deposition of CM and DCM was rapid during early development as indexed by a marked increase in mass per unit area. From about 69 DAFB ('Apple') and 83 DAFB ('Tommy Atkins') onwards, the mass of the CM and DCM per unit area remained constant indicating that the rate of deposition kept pace with surface area expansion (Fig 6A and 6B). The mass of wax per unit area increased slightly during development in both cultivars indicating that the wax deposition rate slightly exceeded that required to compensate for area expansion (Fig 6). In both cultivars, the rates of CM and DCM deposition decreased rapidly during early development but remained constant thereafter (Fig 6C and 6D).

In both cultivars, the apparent strains released on excision and isolation ($\varepsilon'_{exc+iso}$) and those released on wax extraction (ε'_{extr}) increased as fruit surface area increased, particularly from 69 DAFB onwards when the fruit surface area began to increase rapidly. Up to 69 DAFB, ε'_{extr} tended to be larger than $\varepsilon'_{exc+iso}$ in both cultivars (Fig 7). However, during later development, $\varepsilon'_{exc+iso}$ generally exceeded ε'_{extr} (Fig 7). At maturity, the sum of the two ($\varepsilon'_{exc+iso+extr}$) was significantly greater in 'Apple' (28.9 ± 1.1%) than in 'Tommy Atkins' (24.9 ± 1.1%) (Fig 7).

Cumulative strain increased with fruit growth in a sigmoid pattern. In 'Apple' and 'Tommy Atkins', ε_{resid} accounted for most of the total cumulative strain (ε_{total}) (Fig 8). The contributions to ε_{total} of strain due to excision and isolation ($\varepsilon_{exc+iso}$), to wax extraction (ε_{extr}) and their sum ($\varepsilon_{exc+iso+extr}$) were significantly lower than the ε_{resid} (Fig 8).

Plotting $\varepsilon_{exc+iso}$, ε_{extr}, ε_{resid} and $\varepsilon_{plastic}$ vs. ε_{total} revealed biphasic relationships for $\varepsilon_{exc+iso}$ and ε_{extr} vs. ε_{total}, but linear relationships for ε_{resid} and $\varepsilon_{plastic}$ vs. ε_{total} (Fig 9). Initially, $\varepsilon_{exc+iso}$
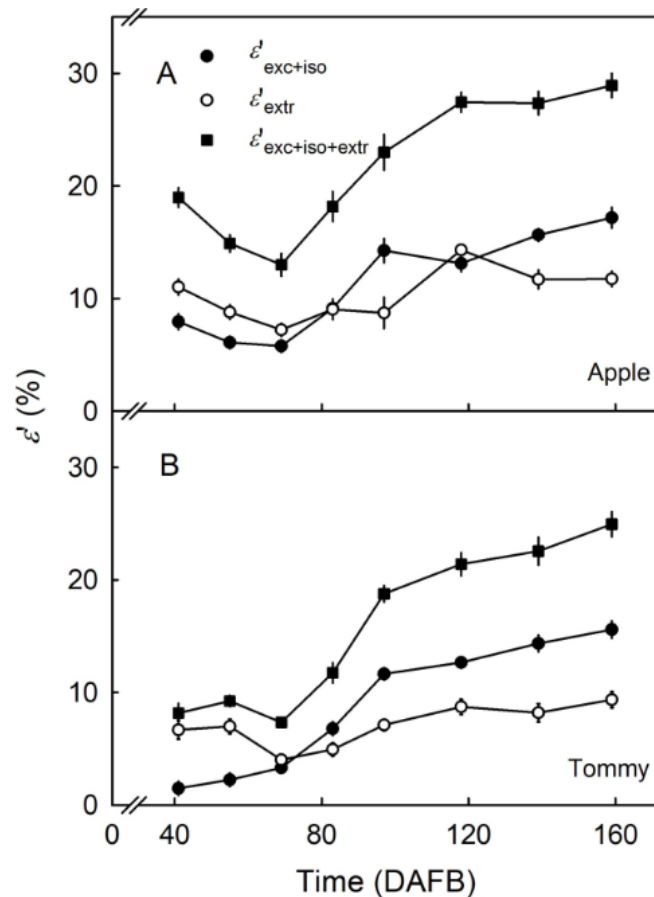
Fig 7. Time course of change in the apparent strain (ε', %) in the cuticular membrane (CM) of 'Apple' (A) and 'Tommy Atkins' (B) mango. These strains were quantified as the releases after excision and isolation of the CM ($\varepsilon'_{exc+iso}$), after wax extraction (ε'_{extr}), and their sum ($\varepsilon'_{exc+iso+extr}$). The x-axis scale is in days after full bloom (DAFB). Data represent means ± SE. The number of replicates was 10–20.

and ε_{extr} increased slowly with ε_{total}. Beyond a breakpoint at ε_{total} about 70, the slope increased and $\varepsilon_{exc+iso}$ and ε_{extr} increased more rapidly. The increases were higher in 'Apple' than in 'Tommy Atkins' (Fig 9A and 9B). In contrast, ε_{resid} increased linearly with ε_{total} and accounted for most of ε_{total} in both cultivars (Fig 9C and 9D).

Stiffness (S) of the CMs increased during development but was consistently lower in 'Apple' than in 'Tommy Atkins' (Fig 10A). There was no significant change in the fracture force (F_{max}) in 'Apple' during development, but F_{max} in 'Tommy Atkins' increased up to about 83 DAFB (Fig 10B). The value of F_{max} was significantly lower in 'Apple' than in 'Tommy Atkins' (Fig 10B). The strain at fracture (ε_{max}) decreased linearly with development. The value of ε_{max} was lower in 'Apple' than in 'Tommy Atkins' (Fig 10C). The frequency of failure associated with lenticels increased during development and was consistently higher in 'Apple' than in 'Tommy Atkins' (Fig 10D).

63
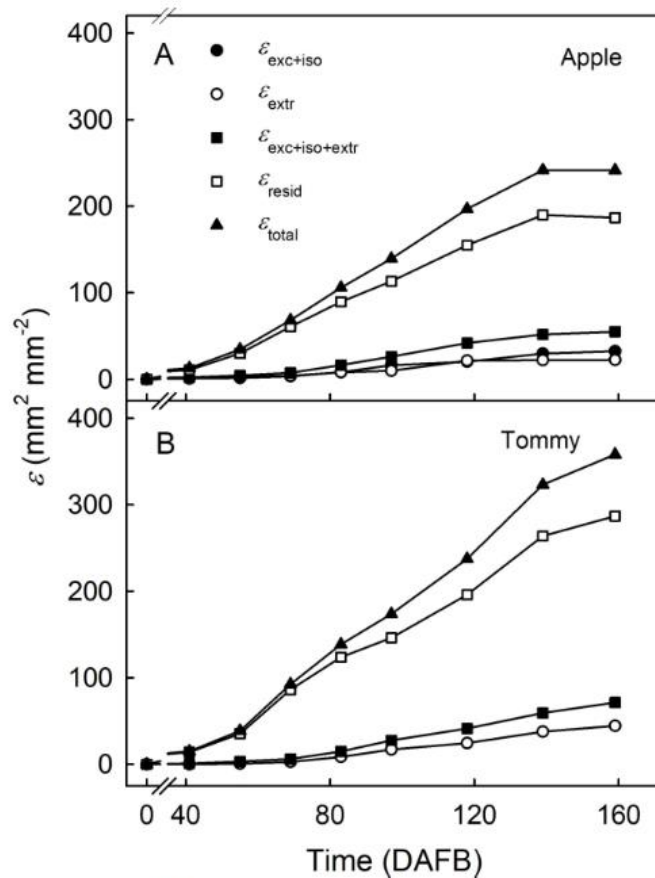
Fig 8. Developmental time course of change in total cumulative strain (ε_{total}), strain released upon excision and isolation of the cuticular membrane (CM) ($\varepsilon_{exc+iso}$), that released after the extraction of wax (ε_{extr}), the sum of the two strains (due to wax and tissue) ($\varepsilon_{exc+iso+extr}$), and the remaining strain (ε_{resid}) of the skin of developing 'Apple' (A) and 'Tommy Atkins' (B) mango. The total cumulative strain of the CM (ε_{total}) was estimated from the increase in surface area with time. The x-axis scale is in days after full bloom (DAFB). Data represent means ± SE. The number of replicates was 10–20.

https://doi.org/10.1371/journal.pone.0258521.g008

Discussion

This discussion focusses on (1) the relationship between fruit growth, cuticle deposition, and stress/strain relaxation and (2) the mechanical characteristics of the cuticle and their relationships to russet susceptibility.

Stress/Strain relaxation behavior of the cuticle reflects fruit growth and cuticle deposition

The stress/strain relaxation analysis reveals several differences between 'Apple' and 'Tommy Atkins'. First, total cumulative strain was greater in 'Tommy Atkins' due to its larger fruit and, hence, greater fruit surface area (Figs 2 and 8). Second, the relationships between $\varepsilon_{exc+iso}$ and ε_{total} (Fig 9A) and between ε_{extr} and ε_{total} were biphasic in both cultivars (Fig 9B). During early

64
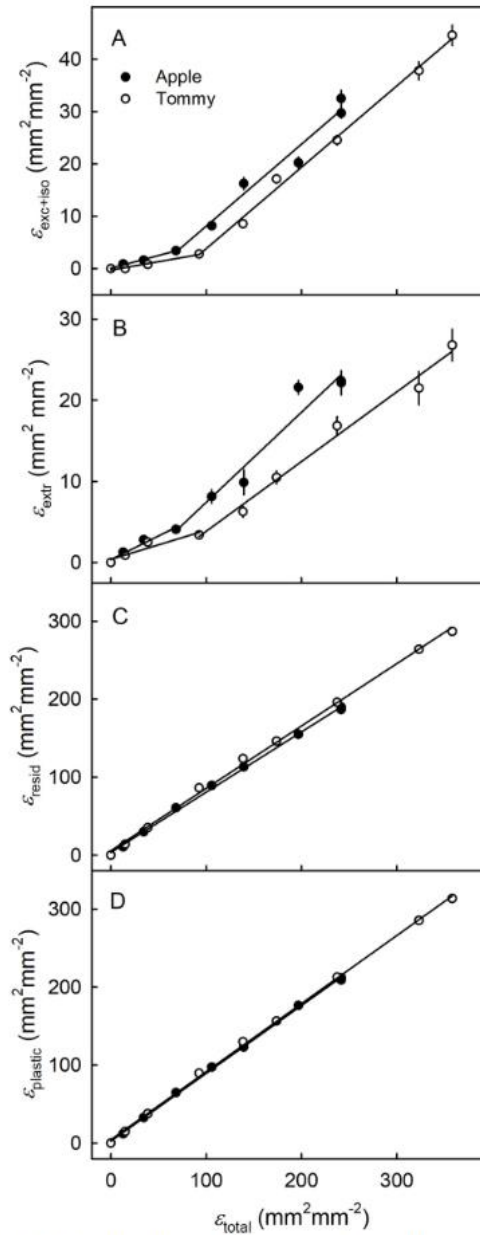
Fig 9. Cumulative strains released after excision and isolation ($\varepsilon_{exc+iso}$) of the cuticular membrane (CM) (A), after wax extraction from the CM (ε_{extr}) (B), the strain that remains in the dewaxed CM (ε_{resid}) (C) and the sum of ε_{extr} and ε_{resid} ($\varepsilon_{plastic}$) (D) plotted against the total cumulative strain (ε_{total}) of the surface of developing 'Apple' and 'Tommy Atkins' mango. The ε_{total} was estimated from the increase in surface area with time relative to the surface area at bloom. The ε_{resid} was estimated as the difference between the total strain (ε_{total}) and the strain due to the wax and tissue ($\varepsilon_{exc+iso+extr}$). Data represent means ± SE. The number of replicates was 10–20.

https://doi.org/10.1371/journal.pone.0258521.g009

65

development, there was little change in $\varepsilon_{\text{exc+iso}}$ and $\varepsilon_{\text{extr}}$ as $\varepsilon_{\text{total}}$ increased. The increase in $\varepsilon_{\text{total}}$ was primarily accounted for by an irreversible increase in $\varepsilon_{\text{resid}}$ (Fig 9C). Mechanically, the increase in $\varepsilon_{\text{resid}}$ resulted principally from a deposition of cutin. In *Malus* apple, the addition of cutin to the inner side (cell-wall side) of the cuticle on the expanding fruit surface resulted in the fixation of elastic strain and, thus, the development of a radial strain gradient within the cuticle [11]. The incorporation of wax into the cutin network also causes a small degree of 'fixation' of elastic strain (reversible) and, hence, also contributes to the plastic strain (irreversible) [12]. Our results indicate the relationships earlier identified in *Malus* apple, also occur in 'Apple' and 'Tommy Atkins' mangoes. Here, the ongoing deposition of CM fixes the reversible elastic strains by converting them into irreversible plastic strains in both 'Apple' and 'Tommy Atkins'. Accordingly, when the rate of CM deposition decreased, approaching an asymptote at 59 DAFB ('Apple'; Fig 6C) and 68 DAFB ('Tommy Atkins'; Fig 6D), during the second phase, $\varepsilon_{\text{exc+iso}}$ and $\varepsilon_{\text{extr}}$ both increased at higher rates as $\varepsilon_{\text{total}}$ also increased (Fig 9). While, from a practical point of view, $\varepsilon_{\text{exc+iso}}$ is truly elastic and reversible, $\varepsilon_{\text{extr}}$ is a plastic strain in the cuticle on an expanding surface. However, mechanically, this strain is also reversible, since the strained cutin polymer relaxes when the wax that blocks the relaxation *in vivo* is extracted *in vitro*. It is particularly interesting that the breakpoint in the above relationships occurs earlier in 'Apple', as indexed by the lower $\varepsilon_{\text{total}}$, than in 'Tommy Atkins' (Fig 9). This observation is also consistent with the earlier breakpoint in CM deposition in 'Apple' as compared to 'Tommy Atkins'. Furthermore, for any given value of $\varepsilon_{\text{total}}$, $\varepsilon_{\text{exc+iso}}$ and $\varepsilon_{\text{extr}}$ were consistently higher in 'Apple' than in 'Tommy Atkins' (Fig 9). This is in line with the lower rate of cutin deposition in 'Apple' than in 'Tommy Atkins' (Fig 6A and 6B). These arguments demonstrate that growth and cuticle deposition are the primary determinants of cuticle stress and strain. Both processes account for the differences between 'Apple' and 'Tommy Atkins' identified in the stress/strain relaxation analysis.

The cuticle of 'Apple' is mechanically weaker than that of 'Tommy Atkins'

Uniaxial tensile tests revealed that the CM of 'Apple' is mechanically weaker than that of 'Tommy Atkins' (Fig 10). Stiffness, F_{max} and ε_{max} in 'Apple' CMs are all significantly lower than in 'Tommy Atkins' CMs. This implies that 'Apple' CMs fracture at lower force and lower strain than 'Tommy Atkins'. The lower cutin mass (Fig 6A and 6B), the larger lenticels (Fig 5), and the greater strain release on excision of the ES and on isolation of the CM (Figs 7 and 9A) and on extraction of the CMs of 'Apple' (Figs 7 and 9B) may explain their relative weakness, compared with the CMs of 'Tommy Atkins' [13]. In addition, the presence of lenticels may also affect the mechanical strength of the CM. Microcracks in the CM are almost always initiated at a lenticel and these are more frequent in 'Apple' than 'Tommy Atkins' (Fig 5, Table 1). Also, as fruit surface area increases, lenticel area also increases, while the number of lenticels per unit area decreases (the total number of lenticels per fruit being constant). The increase in lenticel area occurs at a markedly higher rate in 'Apple' than in 'Tommy Atkins' (Fig 5). At maturity, lenticel area was about three-times greater in 'Apple' than in 'Tommy Atkins'. The contribution of lenticels to the mechanical strength of mango skin is unknown. However, in the skins of grapes, the lenticels represent points of stress concentration and, hence, of weakness [14]. Furthermore, in *Malus* apple the cuticle-periderm boundary is the weak link, often causing skin strips to facture in this region when subjected to uniaxial tensile tests [15]. The larger lenticels of 'Apple' mango also imply a larger cuticle-periderm boundary and hence, a weaker skin. We observed cracking across or around lenticels in 70% and 59% of the CM strips of 'Apple' and 'Tommy Atkins', respectively (data not presented). This is consistent with the above hypothesis. Mechanically, the increase in area per lenticel in 'Apple' mango may also be
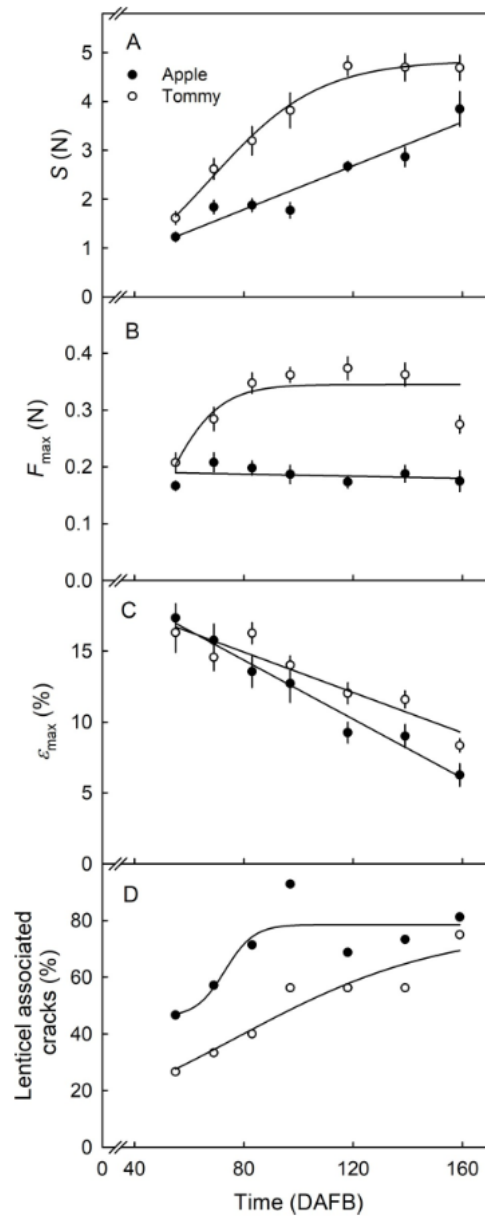
66

Fig 10. Developmental time course of change in stiffness (S) (A), maximum force (F_{max}) (B) and strain at maximum force (ε_{max}) (C) of the cuticular membrane (CM) of developing 'Apple' and 'Tommy Atkins' mango. (D) Frequency of occasions where failure was associated with lenticels. The x-axis scale is in days after full bloom (DAFB). Data in Fig 10A-10C represent means ± SE. The number of replicates was 13–16.

https://doi.org/10.1371/journal.pone.0258521.g010

67

interpreted as a mechanically weak periderm of the lenticel, that fails continuously during fruit expansion, thereby triggering a continuous formation of periderm.

The size, orientations and number of epidermal and hypodermal cells were generally similar in 'Apple' and 'Tommy Atkins' mangoes (Fig 4). In *Malus* apples, the more russet-resistant cultivars are characterized by having smaller and more compactly arranged epidermal and hypodermal cells [16]. Furthermore, the russet-resistant apple cultivars had smaller cells that were less variable in size than those of the more russet-susceptible cultivars [17]. However, there were no comparable and consistent differences between 'Apple' and 'Tommy Atkins' mangoes.

Lower rates of CM deposition and larger lenticels therefore predispose the 'Apple' mango skin to fracture when subjected to strain induced by normal growth, thereby accounting for its higher susceptibility to russeting. The cuticular fractures impair the barrier properties of the skin and trigger the formation of a periderm. This sequence of events is consistent also with the initiation of russeting at lenticels and the exacerbating effects of surface moisture on russeting in 'Apple' mango [3]. 'Apple' mango is not unique in this respect. Similar relationships have been identified in *Malus* apple [18–20]. Unlike susceptible 'Apple' mango, russeting in *Malus* apple is not initiated in the lenticels.

The trigger(s) that initiates the dedifferentiation in the hypodermis, the differentiation of a phellogen and the cell division in the phellogen to produce the phellem is not known. Potential candidates are a change in the O_2 or CO_2 concentrations in the internal atmosphere of the fruit or a local decrease (more negative) in water potential in the region surrounding the microcracks due to increase transpiration [20].

Conclusion

Our findings indicate that the susceptibility to russeting of 'Apple' compared to 'Tommy Atkins' is due to the following sequence of events. Compared to the non-susceptible 'Tommy Atkins', 'Apple' mango has a lower rate of CM deposition which results in higher elastic strain. The high elastic strain serves to initiate cuticular microcracking, which is exacerbated by surface wetness. In this sequence of events, the different elasticity of the lenticels causes local stress concentrations in 'Apple' mango, but not in 'Tommy Atkins' mango. Microcracking weakens the cuticle, that also now has impaired barrier properties as indexed by increased transpiration [3]. The impaired barrier properties are likely to be the trigger for periderm formation that causes the discoloration known as russeting on the surface of russet-susceptible 'Apple' mangoes. Future studies should investigate whether excluding surface moisture by bagging or strengthening the fruit skin by the application of gibberellins are effective in controlling russeting in 'Apple' mango.

Supporting information

S1 File. This is the excel file containing the data presented in Figs 1–10 and Table 1. Where regression lines were fitted, parameter estimates of regression equations and coefficients of determination are provided.
(XLSX)

Acknowledgments

68

orchards and Sandy Lang for helpful discussion and useful comments on an earlier version of this manuscript.

Author Contributions

Conceptualization: Moritz Knoche.

Data curation: Thomas O. Athoo, Bishnu P. Khanal.

Formal analysis: Thomas O. Athoo, Bishnu P. Khanal, Moritz Knoche.

Funding acquisition: Moritz Knoche.

Investigation: Thomas O. Athoo.

Methodology: Thomas O. Athoo, Bishnu P. Khanal, Moritz Knoche.

Project administration: Moritz Knoche.

Supervision: Bishnu P. Khanal, Moritz Knoche.

Validation: Thomas O. Athoo, Bishnu P. Khanal.

Visualization: Thomas O. Athoo, Bishnu P. Khanal.

Writing – original draft: Thomas O. Athoo, Moritz Knoche.

Writing – review & editing: Thomas O. Athoo, Bishnu P. Khanal, Moritz Knoche.

References

1. Borve J, Sekse L, Stensvand A. Cuticular fractures promote postharvest fruit rot in sweet cherries. Plant Dis. 2000; 84:1180–1184. https://doi.org/10.1094/PDIS.2000.84.11.1180 PMID: 30832164

2. Knoche M, Peschel S. Water on the surface aggravates microscopic cracking of the sweet cherry fruit cuticle. J Amer Soc Hort Sci. 2006; 131:192–200. https://doi.org/10.21273/jashs.131.2.192

3. Athoo TO, Winkler A, Knoche M. Russeting in 'Apple' mango: Triggers and mechanisms. Plants 2020; 9:898. https://doi.org/10.3390/plants9070898 PMID: 32708628

4. Khanal BP, Imoro Y, Chen YH, Straube J, Knoche M. Surface moisture increases microcracking and water vapour permeance of apple fruit skin. Plant Biol. 2021; 23:74–82. https://doi.org/10.1111/plb.13178 PMID: 32881348

5. Creasy LL. The correlation of weather parameters with russet of 'Golden Delicious' apples under orchard conditions. J Amer Soc Hort Sci. 1980; 105:735–738.

6. Winkler A, Grimm E, Knoche M, Lindstaedt J, Köpcke D. Late-season surface water induces skin spot in apple. HortScience. 2014; 49:1324–1327. https://doi.org/10.21273/HORTSCI.49.10.1324

7. Lai X, Khanal BP, Knoche M. Mismatch between cuticle deposition and area expansion in fruit skins allows potentially catastrophic buildup of elastic strain. Planta. 2016; 244:1145–1156. https://doi.org/10.1007/s00425-016-2572-9 PMID: 27469168

8. Knoche M, Lang A. Ongoing growth challenges fruit skin integrity. Crit Rev Plant Sci. 2017; 36:190–215. https://doi.org/10.1080/07352689.2017.1369333

9. Karnovsky MJ. A formaldehyde-glutaraldehyde fixative of high osmolality for use in electron microscopy. J cell Biol. 1965; 27:137A–138A.

10. Orgell WH. The isolation of plant cuticle with pectic enzymes. Plant Physiol. 1955; 30:78–80. https://doi.org/10.1104/pp.30.1.78 PMID: 16654733

11. Khanal BP, Knoche M, Bußler S, Schlüter O. Evidence for a radial strain gradient in apple fruit cuticles. Planta. 2014; 240:891–897. https://doi.org/10.1007/s00425-014-2132-0 PMID: 25139276

12. Khanal BP, Grimm E, Finger S, Blume A, Knoche M. Intracuticular wax fixes and restricts strain in leaf and fruit cuticles. New Phytol. 2013; 200:134–143. https://doi.org/10.1111/nph.12355 PMID: 23750808

13. Khanal BP, Knoche M. Mechanical properties of cuticles and their primary determinants. J Exp Bot. 2017; 68:5351–5367. https://doi.org/10.1093/jxb/erx265 PMID: 28992090

14. Brown K, Considine J. Physical aspects of fruit growth—Stress distribution around lenticels. Plant Physiol. 1982; 69: 585–590. https://doi.org/10.1104/pp.69.3.585 PMID: 16662254

69

15. Khanal BP, Grimm E, Knoche M. Russeting in apple and pear: A plastic periderm replaces a stiff cuticle. AoB Plants. 2013; 5:pls048. https://doi.org/10.1093/aobpla/pls048 PMID: 23350024

16. Curry E. Increase in epidermal planar cell density accompanies decreased russeting of 'Golden Delicious' apples treated with gibberellin A_{4+7}. HortScience. 2012; 47:232–237. https://doi.org/10.21273/hortsci.47.2.232

17. Khanal BP, Le TL, Si Y, Knoche M. Russet susceptibility in apple is associated with skin cells that are larger, more variable in size, and of reduced fracture strain. Plants. 2020; 9:1118. https://doi.org/10.3390/plants9091118

18. Faust M, Shear CB. Fine structure of the fruit surface of three apple cultivars. J Amer Soc Hort Sci. 1972; 97:351–355.

19. Faust M, Shear CB. Russeting of apples, an interpretive review. HortScience. 1972; 7:233–235.

20. Chen YH, Straube J, Khanal BP, Knoche M, Debener T. Russeting in apple is initiated after exposure to moisture ends—I. Histological evidence. Plants. 2020; 9:1293. https://doi.org/10.3390/plants9101293 PMID: 33008020

70

3.4 Surface moisture induces microcracks and increases water vapor permeance of fruit skins of mango cv. Apple

Authors:

Thomas O. Athoo (**TOA**) [1], Andreas Winkler (**AW**) [1], Willis O. Owino (**WOO**) [2] and Moritz Knoche (**MK**) [1]

Author affiliation:

[1]   Institute of Horticultural Production Systems, Fruit Science Section, Leibniz University Hannover, Herrenhäuser Straße 2, 30419 Hannover, Germany

[2]   School of Food and Nutritional Sciences (SOFNUS), Jomo Kenyatta University of Agriculture and Technology, P.O. Box 62 000, Nairobi 00200, Kenya

Type of authorship	First author
Type of article	Research article
Journal:	Horticulturae
Impact factor	2.923 (2022)
Date of publication	18 June 2022
DOI	10.3390/horticulturae8060545

Article

Surface Moisture Induces Microcracks and Increases Water Vapor Permeance of Fruit Skins of Mango cv. Apple

Thomas O. Athoo [1] [iD]**, Andreas Winkler** [1] [iD]**, Willis O. Owino** [2] [iD] **and Moritz Knoche** [1,*] [iD]

1   Institute of Horticultural Production Systems, Leibniz University Hannover, Herrenhäuser Straße 2, 30419 Hannover, Germany; t.athoo@obst.uni-hannover.de (T.O.A.); andreas.winkler@obst.uni-hannover.de (A.W.)
2   School of Food and Nutritional Sciences (SOFNUS), Jomo Kenyatta University of Agriculture and Technology, P.O. Box 62 000, Nairobi 00200, Kenya; willis@agr.jkuat.ac.ke
*   Correspondence: moritz.knoche@obst.uni-hannover.de; Tel.: +49-511-762-9020

Abstract: Exposure to surface moisture triggers cuticular microcracking of the fruit skin. In mango fruit cv. apple, microcracking compromises postharvest performance by increasing moisture loss and infections with pathogens. This study reports the effects of exposing the fruit's skin to surface moisture on the incidence of microcracking and on water vapor permeance. Microcracking was quantified microscopically following infiltration with a fluorescent tracer. Water mass loss was determined gravimetrically. Moisture exposure increased cuticular microcracking and permeance. During moisture exposure, permeance increased over the first 4 d, remained constant up to approximately 8 d, then decreased for longer exposure times. Fruit development followed a sigmoid growth pattern. The growth rate peaked approximately 103 days after full bloom. This coincided with the peak in moisture-induced microcracking. There were no increases in water vapor permeance or in microcracking in control fruit that remained dry. When experimental moisture exposure was terminated, microcracking and water vapor permeance decreased. This suggests a repair process restoring the barrier properties of the fruit skin. Histological analyses reveal a periderm forms in the hypodermis beneath a microcrack. Our study demonstrates that surface moisture induces microcracking in mango cv. apple that increases the skin's water vapor permeance and induces russeting.

Keywords: russeting; cuticle; microcracks; permeance; skin; periderm; wax

1. Introduction

Mango cv. apple (*Mangifera indica* L.) is an important commercial fruit crop in Kenya but is prone to russeting. The russeted skins of cv. apple mangoes are typically brown, rough and cracked, rendering them less attractive and thus worth less at point of sale, despite their still excellent flavor [1]. Apart from mango, russeting also occurs in a wide range of other fruit crop species including in *Malus* apples (*Malus* × *domestica* Borkh.) [2–4], pears (*Pyrus communis* L.) [5,6], prunes (*Prunus* × *domestica* L.) [7], citrus (*Citrus reticulata* Blanco × (*C. paradisi* Macf. × *C. reticulate*) [8,9], loquats (*Eriobotrya japonica* (Thunb.) Lindl.) [10], tomatoes (*Solanum lycopersicum* L.) [11] and melons (*Cucumis melo* L.) [12,13]. In anatomical terms, russet represents the formation of a 'secondary skin' in the hypodermis, just below the epidermis. This secondary skin—a periderm—comprises phellem, phellogen and phelloderm [14].

A large number of factors can induce russeting in fruit. These include excessive rates of growth strain [15,16], exposure to surface moisture or even simply to high humidity [17–20], extreme temperatures [10,21,22], excessive sunlight (duration × intensity) [23], mechanical abrasion [7,12], some agrochemicals [16,24,25] and some pests and diseases [8,26,27].

Russeting has been studied extensively in *Malus* apple. The majority of these studies have concluded that microcracks in the cuticle are the first visible signs of insipient rus-

seting [28,29]. Microcracks are minute fissures in the cuticle that are invisible to the naked eye. They are limited to the cuticle and are sufficiently shallow that they rarely penetrate to the outer cellulosic cell walls of the epidermis [30]. Nevertheless, these microcracks do significantly impair the barrier functions of the cuticle. In this way they facilitate invasion by pathogens [31,32] and greatly increase rates of evaporative water loss [17,33].

In our initial studies on mango cv. apple, marked differences in the incidence of russet were observed between different growing sites across Kenya [1]. Correlation analyses revealed that the number of rainy days, temperatures (average, minimum and maximum) and the number of cold nights were particularly conducive to russeting [1]. There was essentially no russeting on fruit cultivated under warm, dry conditions. However, significant russeting occurred in cooler and wetter climates [1]. The most likely explanation for these observations is that moisture induces microcracking of the cuticle of mango cv. apple with the microcracking being followed by the formation of a periderm.

The objective of this study was to establish the role of surface moisture in triggering microcracking in the fruit skins of mango cv. apple. As mango is susceptible to another skin disorder associated with increased rates of water loss, 'shrivel', we also quantified changes in the water vapor permeance of the fruit skin following exposure to surface moisture.

2. Materials and Methods

2.1. Plant Materials

Mango fruits (*Mangifera indica* L.), cv. apple, grafted on an unclassified rootstock, were obtained from a commercial orchard in Mwala, Kenya (1°19′ S, 37°26′ E). Fruit was grown according to standard local practice.

2.2. Moisture Treatment

Developing fruits free of visual defects and selected for uniformity of size and color were tagged. The fruit selected were thus representative for the population of fruit on the tree. Moisture was applied locally to the surface of the fruit. Briefly, conical polyethylene (PE) tubes (8 mm inside diameter) were cut from the tips of microcentrifuge tubes (Sarstedt, Nümbrecht, Germany) and glued to the cheek of the fruit using a non-phytotoxic, fast-curing silicone rubber (Dowsil™ SE 9186 clear sealant; Dow Toray Co., Tokyo, Japan) (Figure S1A) [17]. For the moisture treatment, a tube was filled with distilled water through a hole cut at the tip. The hole was then sealed with silicone rubber. All such tubes were inspected every 2 to 3 days (d) and, if necessary, they were re-sealed to prevent leakage of water. The moisture treatment was eventually terminated by carefully removing the tube. An untreated area of skin on the opposite cheek of the same fruit served as control. In some cases, the control area was enclosed by an identical PE tube but with no water added (Figure S1B).

2.3. Transpiration Assays

Transpiration through the fruit skin was investigated using excised epidermal segments (ES) mounted in stainless steel diffusion cells (7 mm diameter) [34,35]. These ES discs were excised from a moisture-exposed or a control skin area using a biopsy punch (12 mm diameter; Kai Europe, Solingen, Germany). The cut (inner) surface of the ES was blotted dry and immediately mounted in the diffusion cell using high-vacuum grease (Korasilon-Paste; Kurt Obermeier, Bad Berleburg, Germany). Distilled water was injected through the orifice in the base of the cell using a disposable syringe. Water loss from the diffusion cell was restricted to the exposed top (outer) surface of the ES by sealing the orifice in the base and the gap between the lid and the bottom part of the diffusion cell using clear transparent tape (Tesa Film®; Tesa-Werke Offenburg, Offenburg, Germany). The cells were turned upside down and held overnight to stabilize. The next morning, the cell was placed on a metal grid above dry silica gel inside a PE box such that the exposed (outer) ES faced the silica gel and the whole assembly was allowed to equilibrate for at least one hour. Water loss was then quantified gravimetrically by repeated weighing of the cell

on an analytical balance (AUW220D; Shimadzu Corporation, Kyoto, Japan) every 2 h over a 6–8 h period. The rate of water loss (F, g h^{-1}) was estimated from the slope of a linear regression through a plot of mass against time. The permeance (P, m s^{-1}) of the ES was derived from Equation (1).

$$P = \frac{F}{A \times \Delta C} \tag{1}$$

In this equation, A is the area of the ES exposed in the diffusion cell (3.8×10^{-5} m^2) and ΔC the difference in water vapor concentration between the water vapor saturated atmosphere inside the diffusion cell (23.07 g m^{-3} at 25 °C [36]) and the dry atmosphere above the silica gel [34].

2.4. Microcracking

Microcracking was studied using the fluorescent tracer acridine orange [30]. The cheek of the mango including the moisture-exposed or the untreated control area of skin was dipped in 0.1% (w/v) aqueous acridine orange (Carl Roth, Karlsruhe, Germany) for 10 min. Following rinsing with distilled water (5–6 s) and blotting using soft tissue paper, the fruit surface was viewed under a stereo microscope (MZ10F; Leica Microsystems, Wetzlar, Germany) under incident fluorescent light (GFP LP filter, 480–440 nm excitation, $\geq$510 nm emission wavelength). Calibrated images of the moisture-exposed or control skin areas were prepared (Camera DFC7000T; Leica Microsystems). Four images per fruit, per treatment were taken from a total of 8 to 10 fruit. The area infiltrated by the dye as indexed by the area exhibiting yellow-green fluorescence was measured by image analysis (ImageJ 1.53F51; National Health Institute, Bethesda, MD, USA). All images were processed using the same settings and color thresholds.

2.5. Experiments

The time course of microcracking was established using detached fruit. The portion of the fruit surface that was earlier inspected for microcracks was immersed in distilled water for 0, 6, 24 or 48 h to induce microcracking. Fruit used as controls remained dry. Thereafter, microcracking was quantified as described above.

The time course of microcracking was determined on fruit that remained attached to the tree. At 53 days after full bloom (DAFB), a small area of the fruit surface was exposed to moisture for 0, 4, 8, 12 or 16 days. The untreated opposite side of the same fruit served as the control. Microcracking and water vapor permeance were quantified after moisture removal.

The developmental time course of change in fruit mass, fruit surface area, moisture-induced microcracking and permeance to water vapor was investigated. Fruits were harvested at different stages of development in the mornings and processed on the same day. Fruit mass (TX420L; Shimadzu), height and the two orthogonal diameters in the equatorial plane were measured (digital caliper CD-20PKX; Mitutoyo, Kawasaki/Kanagawa, Japan). Fruit surface area was calculated from the measured dimensions assuming a spherical shape. A sigmoid regression curve was fitted through a plot of fruit surface area against time. The surface growth rate was calculated from the first derivative of the regression model. The effects of moisture exposure on microcracking and on water vapor permeance were studied following 8 d of exposure to moisture starting at 33 DAFB. Microcracking and water vapor permeance were quantified as described above. The opposite side of the same fruit was left untreated and served as control.

The time course of change in microcracking and water vapor permeance after termination of moisture exposure was investigated. The fruit surface was exposed to moisture for 8 d at 72 DAFB. Fruit were harvested at 0, 7, 15 or 30 days after moisture exposure had been terminated (DAT). Microcracking and skin permeance were quantified as described above. The opposite side of the same fruit was left untreated and served as control.

To distinguish any effects of mounting a PE tube on the fruit surface from those of moisture exposure, an experiment was established that compared the following treatments:

'untreated' control (no tube, no moisture), 'open tube' (tube, no moisture) and 'moisture treatment' (tube, moisture). For the 'open tube' treatment a cylindrical tube that had the same diameter as the one used for moisture exposure was used. The tube was short to limit any build-up of moisture or high humidity inside the tube. The tubes in the latter two treatments were removed from the surface after 16 days and the treated areas of skin marked using a permanent marker. At maturity, the surface was photographed. Tissue blocks were excised from the treated areas and fixed in Karnovsky solution for histological analysis [37]. Using image analysis (Image J), the russeted area was calculated as a percentage of the tube footprint area exposed to moisture. For the controls without a tube, the average area of the tube footprint was used as an estimate of the exposed area.

2.6. Histology

Tissue blocks previously fixed in Karnovsky solution [37] were rinsed with deionized water. Small sections (5 mm × 2 mm × 2 mm) of these blocks were cut by hand using a razor blade and kept overnight in 70% ethanol at 4 °C. The blocks were then vacuum infiltrated in a series of alcohol solutions of increasing concentration (70, 80, 90, and 96% v/v ethanol and then 100% isopropanol). The blocks were then treated with xylene substitute (AppliClear; PanReac Applichem, Münster, Germany) and thereafter with a 1:1 xylene-substitute: paraffin mixture before embedding in melted paraffin. Embedded blocks were cooled above ice and stored at 4 °C until use. Cross-sections of 10 μm thickness were cut using a microtome (Hyrax M55; Carl Zeiss, Jena, Germany), mounted on a microscope slide over a water bath at 40 °C and oven-dried overnight at 40 °C. Prior to staining, the sections were washed in xylene substitute before rehydrating in a series of decreasing ethanol concentration (96, 80, 70, 60% v/v ethanol and deionized water). Staining was done for a minimum of 1 h using 0.005% (w/v) fluorol yellow 088 dye (Santa Cruz Biotechnology, Dallas, TX, USA) made up by dissolving in a hot mixture of polyethylene glycol (PEG) 4000 (50% w/v; SERVA Electrophoresis; Heidelberg, Germany) and 45% v/v glycerol and 5% deionized water. Following rinsing with deionized water, the microscope slides were placed on the stage of a fluorescence microscope (BX-60; Olympus Europa, Hamburg, Germany), examined under incident bright and fluorescent light (U-MWU filter, 330–385 nm excitation, $\geq$420 nm emission wavelength; Olympus) and photographed (DP73; Olympus).

2.7. Data Analyses

Data symbols in figures represent the means $\pm$ standard errors. Analyses of variance and correlation analyses were conducted using the statistical software package SAS (Version 9.1.3; SAS Institute, Cary, NC, USA).

3. Results

Moisture exposure increased microcracking of the cuticle as indexed by the increase in area infiltrated with acridine orange compared to that of the untreated control. The fluorescing area was initially low but then increased rapidly, reaching an asymptote within 48 h of moisture exposure. There were no changes in the fluorescing areas of the untreated controls (Figure 1).

Quantitatively similar data were obtained for longer exposures to moisture. The percentage infiltrated area was significantly larger following moisture exposure for 8 to 16 d compared to the unexposed controls. There were no significant changes in infiltrated area in the controls (Figure 2A). The amount of water transpired increased linearly with time and was significantly higher in the moisture-exposed areas than in the untreated control areas (Figure 2B). The permeance of the fruit skin to water vapor increased until 4 d of moisture exposure, then remained approximately constant up to 8 d. For longer exposure times skin permeance decreased (Figure 2C). Skin permeance was significantly higher for the water-exposed areas than for the control areas at all times. There were no significant changes in skin permeance in the untreated controls.
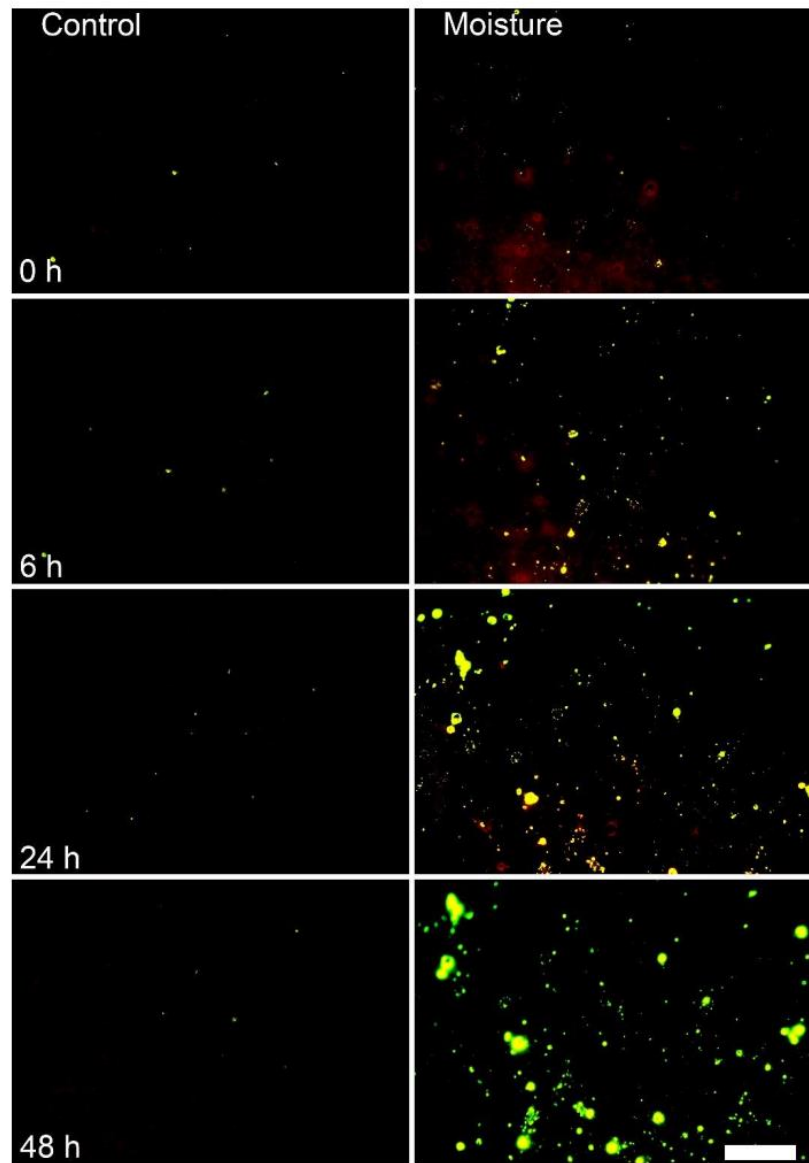
Figure 1. Effect of moisture exposure of the surface of fruit of mango cv. apple on microcracking of the cuticle. The fruit surface was exposed to surface moisture for 0, 6, 24 or 48 h. An untreated surface remained dry and served as the 'control'. Microcracking was visualized by infiltration with aqueous acridine orange. N = 10. Scale bar 1 mm.
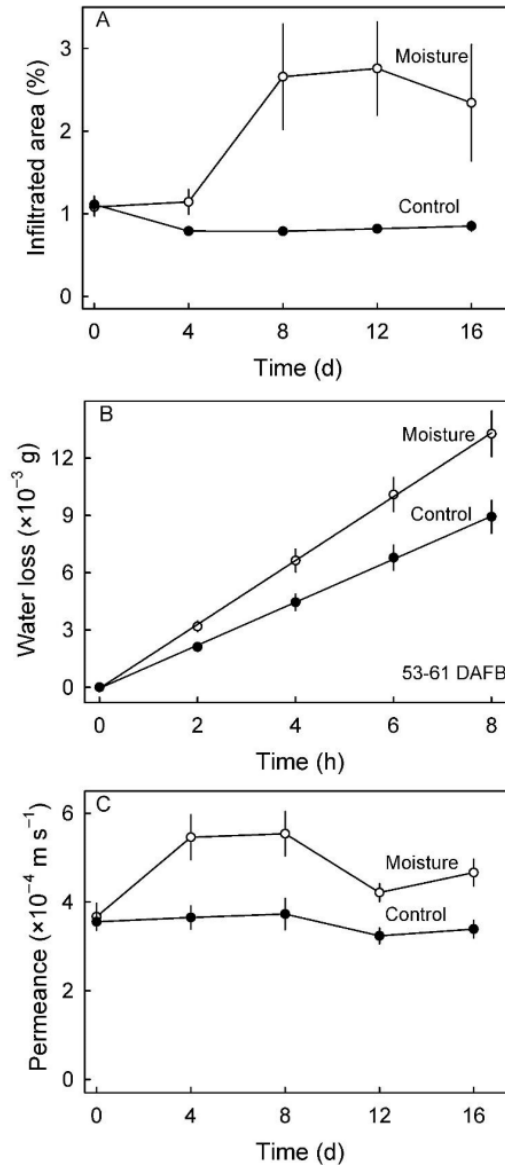
Figure 2. (**A**) Time course of change in moisture-induced cuticular microcracking of fruit of mango cv. apple. (**B**) Time course of water loss through moisture-exposed fruit skins. Skins not exposed to moisture served as controls. The fruits were exposed to moisture for 8 d beginning at 53 days after full bloom (DAFB). (**C**) Time course of change in the water vapor permeance of the fruit skin during moisture exposure. Fruit was exposed to moisture for 4, 8, 12 and 16 d. Microcracking was indexed by quantifying the area infiltrated with aqueous acridine orange. Fruit surfaces that remained dry served as controls. N = 40 (microcracks) and 13–15 (permeance). Data represent the means ± SE.

The increase in mass and surface area of developing fruit of mango cv. apple followed a sigmoid pattern (Figure 3A). The growth rate in surface area peaked at approximately 103 DAFB (Figure 3A, inset). The peak in growth rate at 103 DAFB coincided with a peak in microcracking, as indexed by the areas infiltrated with the fluorescent tracer (Figure 3B). There was only a slight increase in infiltrated surface area in the untreated

control fruit during fruit development (Figure 3B). The change in permeance to water vapor essentially paralleled the change in tracer infiltrated area (Figure 3C). Permeance was higher in moisture-treated ES compared to control ES, irrespective of developmental stage (Figure 3C). There was a significant and positive linear correlation between the permeance of the fruit skin to water vapor and the percentage of surface area infiltrated with acridine orange (Figure 3D).
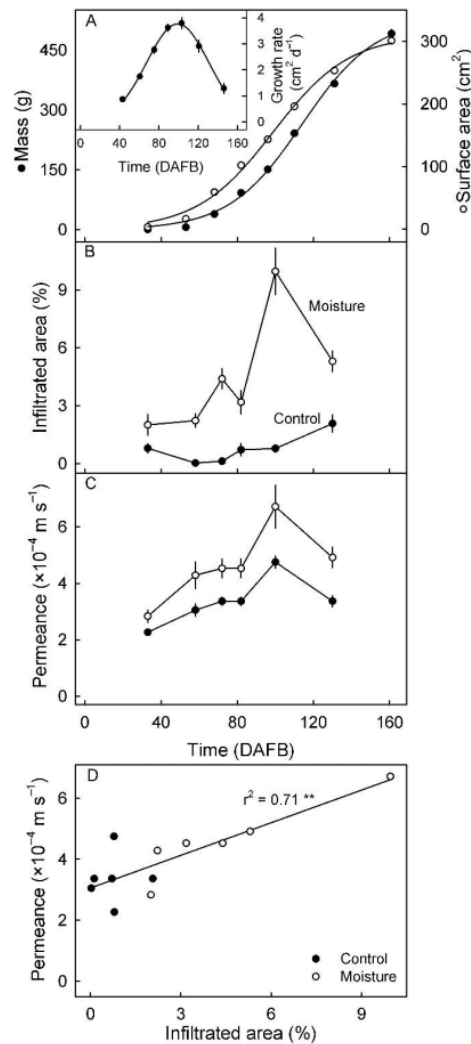
Figure 3. Developmental time course of change in fruit mass and surface area of mango cv. apple (**A**), microcracking following moisture exposure (**B**) and permeance to water vapor (**C**) following 8 days exposure to surface moisture. (**D**) Relationship between permeance to water vapor and microcracking (**D**). Untreated surfaces served as controls. Microcracking was indexed by quantifying the area infiltrated with acridine orange. X-axis scale in A, B and C is days after full bloom (DAFB). N = 20 (mass and surface area), 40 (microcracking) and 13–15 (permeance). Data represent the means $\pm$ SE. Significance of coefficients of determination (r^2) at $p \leq 0.01$ is indicated by **.

The time course of change in infiltrated area and in skin permeance after moisture exposure was terminated revealed a decrease in both infiltrated area and in permeance.

The area infiltrated and the permeance were both higher in moisture-exposed areas than in unexposed control areas (Figure 4).
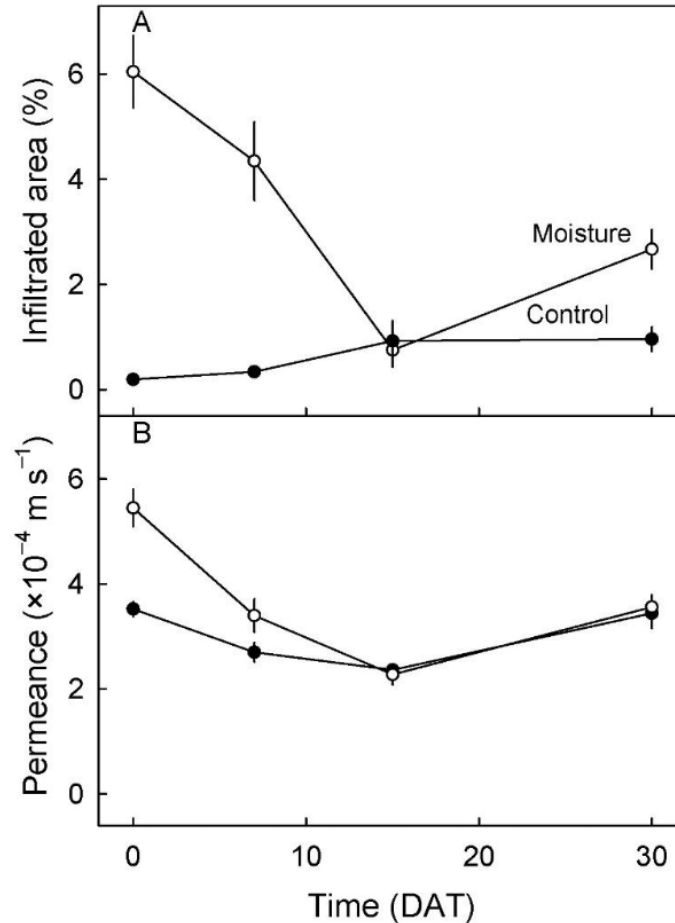
Figure 4. Time course of changes in microcracking (**A**) and permeance to water vapor (**B**) of fruit skin of mango cv. apple after 8 days exposure to moisture. X-axis scale in days after treatment (DAT). At 72 days after full bloom, the cheek of the developing fruit was exposed to moisture for 8 d. Thereafter, the time course of change in microcracking and permeance after moisture termination was followed. Unexposed fruit surfaces served as controls. N = 40 (microcracking) and 12 (permeance). Data represent the means ± SE.

Histological analyses revealed that the brownish appearance of the skin was due to the formation of a periderm in the hypodermis of the moisture-exposed areas of skin (Figure 5I,J). There was no evident periderm in the unexposed skin areas (Figure 5A–F). Moisture-exposed skin areas developed a rough, brownish appearance (Figure 5G).

The areas affected by periderm were consistently and significantly larger in moisture-exposed areas of skin than in unexposed (control) areas and were unaffected by merely attaching a tube to the skin surface (i.e., with no added water) (Table 1).
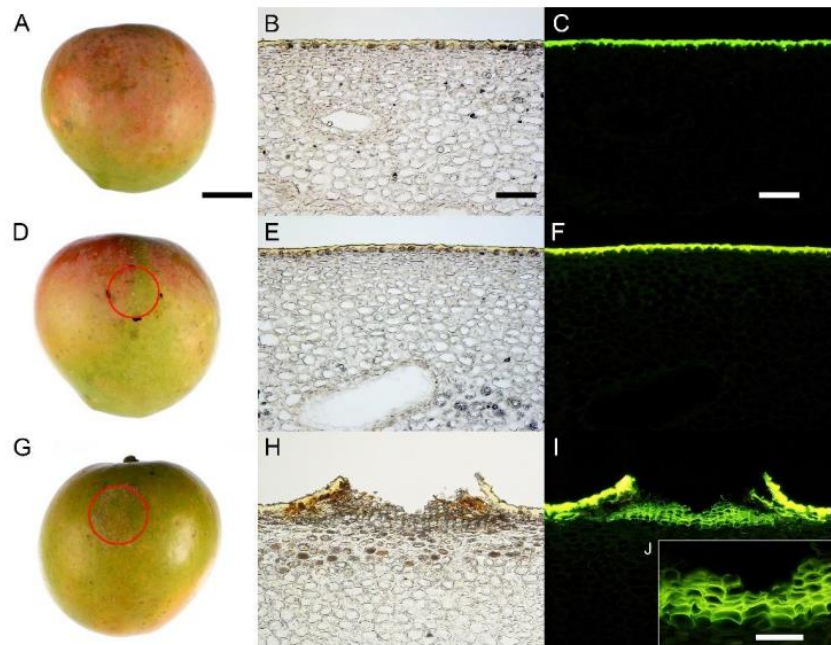
Figure 5. Images of mature fruits of mango cv. apple (**A,D,G**) and histological micrographs of moisture-treated and control fruit skin taken under bright (**B,E,H**) and incident fluorescent light (**C,F,I**) as affected by a surface moisture treatment (see text for details). Control fruit (no tube attached, not exposed to moisture) (**A,B,C**), open tube (tube attached but not exposed to moisture) (**D,E,F**) and moisture-treated fruits (tube attached and exposed to moisture) (**G,H,I**) and enlarged micrograph of moisture-treated skin (**J**). Fruit was exposed to surface moisture by attaching a tube filled with distilled water to the fruit surface for 16 days at 53 days after full bloom (DAFB). Untreated fruit and fruit with an open tube attached that remained dry served as controls. At the end of the treatment period, tubes were removed and fruits were left to grow to maturity. The red circle identifies the area previously enclosed by the plastic tube. N = 18–20 (whole fruits) and 3 (histology). The scale bars are 20 mm (**A,D,G**), 100 μm (**B,C,E,F,H,I**) and 50 μm (**J**).

Table 1. Effect of exposure to surface moisture on the russeting of fruit of mango cv. apple. Fruit was exposed to surface moisture by attaching a short plastic tube filled with distilled water to the fruit surface for 16 d at 53 days after full bloom. Untreated fruit (control) and fruit with an open tube attached (open tube, no water) served as controls. Tubes were removed after 16 d and the fruits left to grow to maturity. Russeting was estimated by expressing the area russeted as a percentage of the area of the footprint of the tube. N = 18–20.

Treatment	Area Russeted (%)
Untreated fruit	1.3 ± 0.2 a
Open tube, no moisture	1.3 ± 0.2 a
Closed tube, moisture	20.2 ± 3.9 b

Mean separation by Tukey Studentized range test, $p \leq 0.05$. Means followed by the same letter are not significantly different. Data represent the means ± SE.

4. Discussion

In our discussion, we focus on (1) the effect of surface moisture on microcracking and russeting in the fruit of mango cv. apple and (2) the increase in skin permeance to water vapor in association with this microcracking.

4.1. Surface Moisture Induces Microcracking and Russeting in Mango cv. Apple

We observed increases in microcracking and russeting following exposure of the fruit surface to moisture. This observation is consistent with reports for many fruit crop species [16,17,19,38]. It is also consistent with reports where surface moisture is absent due to the fruit growing in a dry climate [1,39–41] or in a protected environment [42] or in a bag [43,44] installed to prevent russeting. The level of microcracking in mango cv. apple was, however, low compared with the levels in many other fruit crop species. Nevertheless, levels of microcracking were sufficient to trigger localized russeting in the moisture-exposed areas of the skin. The process of russeting in mango cv. apple is therefore generally similar to that described for *Malus* apples [17,19,38].

Just why surface moisture induces microcracking is not clear. Several factors are likely involved. First, the rheological properties of a cuticle are affected by hydration. For hydrated cuticle, the strain at fracture increases but stiffness and fracture force both decrease [45–47]. The net effect of these rheological changes is a weaker cuticle.

Second, exposure to moisture may cause swelling of cell walls in the fruit skin. This reduces cell-to-cell adhesion [48]. It is the epidermal and hypodermal cell layers, not the cuticle, that represent the main structural component of a fruit skin [46,49]. Hence, cell wall swelling renders a hydrated skin mechanically weaker. The appearance of cuticular microcracking is the first sign that the skin is about to fail [49].

Third, reduced rates of cutin and wax deposition have recently been reported in moisture-exposed skins [19,38]. This reduction has been attributed to a down-regulation of the genes involved in cutin and wax synthesis and deposition. Because wax acts as a filler that 'fixes' elastic strain in an expanding cutin matrix [50,51], decreased wax deposition makes cuticle failure more likely, i.e., more elastic strain builds up during expansion growth because it remains un-fixed. The opposite is also true, namely that the deposition of cutin in the cuticle's inner surface (abutting the cell wall) fixes the elastic strain thereby decreasing the likelihood of failure [52].

Fourth, growth causes the stretching (strain) that predisposes the cuticle to failure (microcracking). In pear, growth strain has been shown to trigger russeting [5] and this russeting is also preceded by microcracking [16,28,29]. Growth strain also seems to be involved in microcracking in mango cv. apple, with peak surface growth rate, coinciding with peak microcracking. A positive correlation between the severity of cuticular microcracking and fruit size has also been demonstrated in peach—particularly during the rapid growth phase [53]. In pear, the occurrence and severity of microcracking depend on the relative growth rate. The strongly tapered pear fruits showing more severe microcracking in the cheek region (larger diameter) than in the neck region (smaller diameter) [5,54]. Finally, the occurrence of microcracks immediately above the anticlinal walls of the epidermal cells of the fruit skin in *Malus* apple has been attributed to the high stress concentrations in this region [55].

Taken together, all these arguments demonstrate that mango cv. apple responds to the presence of moisture on the skin surface in a manner very similar to that already determined for *Malus* apple but at a somewhat reduced level. It is interesting that, after termination of moisture exposure, the infiltration of microcracks by acridine orange gradually decreased to control levels. The most plausible interpretation of this observation is that microcracks successfully 'healed'. We suggest that this is likely the result of the deposition of new wax material in these microcracks [17,19]. The filling of microcracks restored the barrier properties of the cuticle. The mechanical properties of a microcracked cuticle are likely to remain unaffected by the filling. Direct visual evidence for wax filling of microcracks has been published for *Malus* apples [56,57]. In addition, in *Malus* apple, a periderm may be formed following microcracking. This apparently was also the case in mango cv. apple at maturity. Like in *Malus* apple, a surface with periderm (russet) has a higher permeance to water vapor in mango cv. apple than a non-russeted surface (no periderm) [1].

In *Malus* apple, the complex growth processes involved in the formation of this new cellular tissue layer are possibly triggered by an increase in the partial pressure of O_2 just

inside the skin [58,59]. The periderm thus formed partially restores the barrier properties of the microcracked skin, so hindering penetration by the fluorescent dye [15] and reducing the skin's permeance to water vapor [17]. *Malus* apple and mango cv. apple are similar in this respect.

4.2. Microcracking Increased Skin Permeance to Water Vapor

Microcracks compromise the barrier functions of the cuticle. Throughout development, mango cv. apple fruit skins exposed to moisture had increased permeance compared to control fruit. This observation is also consistent with earlier findings for *Malus* apple [17,54]. A microcrack represents an enhanced pathway for water diffusion that is in parallel with those through nearby stomata, lenticels and through the undamaged cuticle itself. It was not possible to quantify the relative contributions of these parallel pathways to total skin permeance in mango cv. apple for two reasons: (1) the water vapor permeance of the fruit skin was highly variable both from fruit to fruit and also from area to area on the surface of a fruit and (2) the limited range in variability of stomatal and lenticellular density (numbers per unit area).

5. Conclusions

The fruit of mango cv. apple responds to exposure to surface moisture by microcracking and russeting in much the same way as has already been established for the fruit of *Malus* apple. However, compared with *Malus* apple, both microcracking and dye infiltration are reduced. Based on the behavioral similarity of the responses of these two fruits to surface moisture, it is considered likely that measures that hinder the deposition of surface moisture on the fruit surface will be effective in reducing the incidence of microcracking and, hence, russeting. These measures include the bagging of fruit using special bags that are sufficiently permeable to water vapor as to prevent the build-up of a high humidity within, while also preventing direct contact with liquid water from outside (rain, dew, mist, condensation). Similarly, the application of gibberellins which has been shown effective in reducing russeting in *Malus* apples [41,60]. Given the importance of mango cv. apple to the Kenyan market, both these two potential avenues for russet mitigation merit further study.

References

1. Athoo, T.O.; Winkler, A.; Knoche, M. Russeting in 'Apple' mango: Triggers and mechanisms. *Plants* **2020**, *9*, 898. [CrossRef] [PubMed]
2. Tukey, L.D. Observations on the russeting of apples growing in plastic bags. *Proc. Amer. Soc, Hort. Sci.* **1969**, *74*, 30–39.
3. Skene, D.S. The development of russet, rough russet and cracks on the fruit of the apple Cox's Orange Pippin during the course of the season. *J. Hortic. Sci.* **1982**, *57*, 165–174. [CrossRef]
4. Bell, H.P. the origin of russeting in the Golden Russet apple. *Can. J. Res.* **1937**, *15c*, 560–566. [CrossRef]
5. Scharwies, J.D.; Grimm, E.; Knoche, M. Russeting and relative growth rate are positively related in "Conference" and "Condo" pear. *HortScience* **2014**, *49*, 746–749. [CrossRef]
6. Macnee, N.C.; Rebstock, R.; Hallett, I.C.; Schaffer, R.J.; Bulley, S.M. A review of current knowledge about the formation of native peridermal exocarp in fruit. *Funct. Plant Biol.* **2020**, *47*, 1019–1031. [CrossRef] [PubMed]
7. Michailides, T.J. Russeting and russet scab of prune, an environmentally induced fruit disorder: Symptomatology, induction, and control. *Plant Dis.* **1991**, *75*, 1114. [CrossRef]
8. McCoy, C.W. Stylar feeding injury and control of eriophyoid mites in citrus. In *World Crop Pests*; Lindquist, E.E., Sabelis, M.W., Bruin, J., Eds.; Elsevier B.V.: Amsterdam, The Netherlands, 1996.
9. Achor, D.S.; Albrigo, L.G.; McCoy, C.W. Developmental anatomy of lesions on 'Sunburst' mandarin leaves initiated by citrus rust mite feeding. *J. Am. Soc. Hortic. Sci.* **1991**, *116*, 663–668. [CrossRef]
10. Avidan, B.; Klein, I. Physiological disorders in loquat (*Eriobotrya japonica* Lindl.). I. Russeting. *Adv. Hortic. Sci.* **1998**, *12*, 190–195.
11. Bakker, J.C. Russeting (cuticle cracking) in glasshouse tomatoes in relation to fruit growth. *J. Hortic. Sci.* **1988**, *63*, 459–463. [CrossRef]
12. Gerchikov, N.; Keren-Keiserman, A.; Perl-Treves, R.; Ginzberg, I. Wounding of melon fruits as a model system to study rind netting. *Sci. Hortic.* **2008**, *117*, 115–122. [CrossRef]
13. Cohen, H.; Dong, Y.; Szymanski, J.; Lashbrooke, J.; Meir, S.; Almekias-Siegl, E.; Zeisler-Diehl, V.V.; Schreiber, L.; Aharoni, A. A multilevel study of melon fruit reticulation provides insight into skin ligno-suberization hallmarks. *Plant Physiol.* **2019**, *179*, 1486–1501. [CrossRef]
14. Evert, R.F. *Esau's Plant Anatomy*, 3rd ed.; Evert, R.F., Ed.; John Wiley & Sons, Inc.: Hoboken, NJ, USA, 2006; ISBN 9780470047385.
15. Knoche, M.; Lang, A. Ongoing growth challenges fruit skin integrity. *CRC. Crit. Rev. Plant Sci.* **2017**, *36*, 190–215. [CrossRef]
16. Winkler, A.; Athoo, T.; Knoche, M. Russeting of fruits: Etiology and management. *Horticulturae* **2022**, *8*, 231. [CrossRef]
17. Khanal, B.P.; Imoro, Y.; Chen, Y.H.; Straube, J.; Knoche, M. Surface moisture increases microcracking and water vapour permeance of apple fruit skin. *Plant Biol.* **2020**, *23*, 74–82. [CrossRef]
18. Sugar, D.; Villardel, P.; Asin, L. Relationship of weather factors to russet incidence in "comice" and "bosc" pear fruit. *Acta Hortic.* **2015**, *1094*, 533–538. [CrossRef]
19. Chen, Y.H.; Straube, J.; Khanal, B.P.; Knoche, M.; Debener, T. Russeting in apple is initiated after exposure to moisture ends—i. Histological evidence. *Plants* **2020**, *9*, 1293. [CrossRef] [PubMed]
20. Asín, L.; Torres, E.; Vilardell, P. Orchard cooling with overtree microsprinkler irrigation to increase fruit russet on 'Conference' pear. *Acta Hortic.* **2011**, *909*, 557–564. [CrossRef]
21. Simons, R.K.; Chu, M.C. Periderm morphology of mature "Golden Delicious" apple with special reference to russeting. *Sci. Hortic.* **1978**, *8*, 333–340. [CrossRef]
22. Joshi, M.; Schmilovitch, Z.; Ginzberg, I. Pomegranate fruit growth and skin characteristics in hot and dry climate. *Front. Plant Sci.* **2021**, *12*, 725479. [CrossRef]
23. Noè, N.; Eccher, T. 'Golden Delicious' apple fruit shape and russeting are affected by light conditions. *Sci. Hortic.* **1996**, *65*, 209–213. [CrossRef]
24. Brown, G.S.; Kitchener, A.E.; Barnes, S. Calcium hydroxide sprays for the control of black spot on apples—Treatment effects on fruit quality. *Acta Hortic.* **1998**, *513*, 47–52. [CrossRef]
25. Palmer, J.W.; Davies, S.B.; Shaw, P.W.; Wünsche, J.N. Growth and fruit quality of 'Braeburn' apple (*Malus domestica*) trees as influenced by fungicide programmes suitable for organic production. *New Zeal. J. Crop Hortic. Sci.* **2003**, *31*, 169–177. [CrossRef]
26. Johnson, R.B.; King, J.R.; Mcbride, J.J. Zineb controls citrus rust mites. *Proc. Florida State Hortic. Soc.* **1957**, *70*, 38–47.
27. Lindow, S.E.; Desurmont, C.; Elkins, R.; McGourty, G.; Clark, E.; Brandl, M.T. Occurrence of indole-3-acetic acid-producing bacteria on pear trees and their association with fruit russet. *Phytopathology* **1998**, *88*, 1149–1157. [CrossRef]
28. Faust, M.; Shear, C.B. Russeting of apples, an interpretive review. *HortScience* **1972**, *7*, 233–235.
29. Faust, M.; Shear, C.B. Fine structure of the fruit surface of three apple cultivars. *J. Am. Soc. Hortic. Sci.* **1972**, *97*, 351–355.
30. Peschel, S.; Knoche, M. Characterization of microcracks in the cuticle of developing sweet cherry fruit. *J. Am. Soc. Hortic. Sci.* **2005**, *130*, 487–495. [CrossRef]
31. Borve, J.; Sekse, L.; Stensvand, A. Cuticular fractures promote postharvest fruit rot in sweet cherries. *Plant Dis.* **2000**, *84*, 1180–1184. [CrossRef]
32. Nguyen-the, C. Structure of epidermis wall, cuticle and cuticular microcracks in nectarine fruit. *Agronomie* **1991**, *11*, 909–920. [CrossRef]
33. Knoche, M.; Grimm, E.; Winkler, A.; Alkio, M.; Lorenz, J. Characterizing neck shrivel in European plum. *J. Am. Soc. Hortic. Sci.* **2019**, *144*, 38–44. [CrossRef]

34. Geyer, U.; Schönherr, J. In vitro test for effects of surfactants and formulations on permeability of plant cuticles. In *Pesticide Formulations: Innovations and Developments*; Cross, B., Scher, H.B., Eds.; American Chemical Society: Washington, DC, USA, 1988; pp. 22–33.

35. Knoche, M.; Peschel, S.; Hinz, M.; Bukovac, M.J. Studies on water transport through the sweet cherry fruit surface: Characterizing conductance of the cuticular membrane using pericarp segments. *Planta* **2000**, *212*, 127–135. [CrossRef] [PubMed]

36. Nobel, P.S. *Physicochemical and Environmental Plant Physiology*, 5th ed.; Academic Press: San Diego, CA, USA, 2020; ISBN 978-0-12-819146-0.

37. Karnovsky, M.J. A formaldehyde-glutaraldehyde fixative of high osmolality for use in electron microscopy. *J. Cell Biol.* **1965**, *27*, 137A–138A.

38. Straube, J.; Chen, Y.-H.; Khanal, B.P.; Shumbusho, A.; Zeisler-Diehl, V.; Suresh, K.; Schreiber, L.; Knoche, M.; Debener, T. Russeting in apple is initiated after exposure to moisture ends: Molecular and biochemical evidence. *Plants* **2020**, *10*, 65. [CrossRef] [PubMed]

39. Sugar, D.; Basile, S.R. Russet induction in "Beurr'e Bosc" and "Taylor's Gold" pears. *Acta Hortic.* **2008**, *800*, 257–261. [CrossRef]

40. Creasy, L.L. The correlation of weather parameters with russet of "Golden Delicious" apples under orchard conditions. *J. Am. Soc. Hortic. Sci.* **1980**, *105*, 735–738.

41. Knoche, M.; Khanal, B.P.; Stopar, M. Russeting and microcracking of "Golden Delicious" apple fruit concomitantly decline due to gibberellin a4+7 application. *J. Am. Soc. Hortic. Sci.* **2011**, *136*, 159–164. [CrossRef]

42. Shi, C.; Qi, B.; Wang, X.; Shen, L.; Luo, J.; Zhang, Y. Proteomic analysis of the key mechanism of exocarp russet pigmentation of semi-russet pear under rainwater condition. *Sci. Hortic.* **2019**, *254*, 178–186. [CrossRef]

43. Yuan, G.; Bian, S.; Han, X.; He, S.; Liu, K.; Zhang, C.; Cong, P. An integrated transcriptome and proteome analysis reveals new insights into russeting of bagging and non-bagging "Golden Delicious" apple. *Int. J. Mol. Sci.* **2019**, *20*, 4462. [CrossRef]

44. Mathooko, F.M.; Kahangi, E.M.; Runkua, J.M.; Onyango, C.A.; Owino, W.O. Preharvest mango (*Mangifera indica* L. 'Apple') fruit bagging controls lenticel discolouration and improves postharvest quality. *Acta Hortic.* **2011**, *906*, 55–62. [CrossRef]

45. Edelmann, H.G.; Neinhuis, C.; Bargel, H. Influence of hydration and temperature on the rheological properties of plant cuticles and their impact on plant organ integrity. *J. Plant Growth Regul.* **2005**, *24*, 116–126. [CrossRef]

46. Khanal, B.P.; Knoche, M. Mechanical properties of cuticles and their primary determinants. *J. Exp. Bot.* **2017**, *68*, 5351–5367. [CrossRef] [PubMed]

47. Knoche, M.; Peschel, S. Water on the surface aggravates microscopic cracking of the sweet cherry fruit cuticle. *J. Am. Soc. Hortic. Sci.* **2006**, *131*, 192–200. [CrossRef]

48. Brüggenwirth, M.; Knoche, M. Cell wall swelling, fracture mode, and the mechanical properties of cherry fruit skins are closely related. *Planta* **2017**, *245*, 765–777. [CrossRef] [PubMed]

49. Khanal, B.P.; Knoche, M. Mechanical properties of apple skin are determined by epidermis and hypodermis. *J. Am. Soc. Hortic. Sci.* **2014**, *139*, 139–147. [CrossRef]

50. Khanal, B.P.; Grimm, E.; Knoche, M. Russeting in apple and pear: A plastic periderm replaces a stiff cuticle. *AoB Plants* **2013**, *5*, 1–12. [CrossRef]

51. Petracek, P.D.; Bukovac, M.J. Rheological properties of enzymatically isolated tomato fruit cuticle. *Plant Physiol.* **1995**, *109*, 675–679. [CrossRef]

52. Khanal, B.P.; Knoche, M.; Bußler, S.; Schlüter, O. Evidence for a radial strain gradient in apple fruit cuticles. *Planta* **2014**, *240*, 891–897. [CrossRef]

53. Gibert, C.; Chadœuf, J.; Vercambre, G.; Génard, M.; Lescourret, F. Cuticular cracking on nectarine fruit surface: Spatial distribution and development in relation to irrigation and thinning. *J. Am. Soc. Hortic. Sci.* **2007**, *132*, 583–591. [CrossRef]

54. Knoche, M.; Grimm, E. Surface moisture induces microcracks in the cuticle of "Golden Delicious" apple. *HortScience* **2008**, *43*, 1929–1931. [CrossRef]

55. Knoche, M.; Khanal, B.P.; Brüggenwirth, M.; Thapa, S. Patterns of microcracking in apple fruit skin reflect those of the cuticular ridges and of the epidermal cell walls. *Planta* **2018**, *248*, 293–306. [CrossRef] [PubMed]

56. Curry, E.; Arey, B. Apple cuticle: The perfect interface. *Scanning Microsc.* **2010**, *7729*, 77291P. [CrossRef]

57. Curry, E.A. Growth-induced microcracking and repair mechanisms of fruit cuticles. In Proceedings of the SEM Annual Conference, Albuquerque, NM, USA, 1–4 June 2009.

58. Lipton, W.J. Some effects of low-oxygen atmospheres on potato tubers. *Am. Potato J.* **1967**, *44*, 292–299. [CrossRef]

59. Wei, X.; Mao, L.; Han, X.; Lu, W.; Xie, D.; Ren, X.; Zhao, Y. High oxygen facilitates wound induction of suberin polyphenolics in kiwifruit. *J. Sci. Food Agric.* **2018**, *98*, 2223–2230. [CrossRef] [PubMed]

60. Wertheim, S.J. Fruit russeting in apple as affected by various gibberellins. *J. Hortic. Sci.* **1982**, *57*, 283–288. [CrossRef]

84

3.5 *Lenticels are sites of initiation of microcracking and russeting in 'Apple' mango*

Authors:

Thomas O. Athoo (**TOA**)[1], Andreas Winkler (**AW**)[1], Willis O. Owino (**WOO**)[2] and Moritz Knoche (**MK**)[1]

Author affiliation:

1. Institute of Horticultural Production Systems, Fruit Science Section, Leibniz University Hannover, Herrenhäuser Straße 2, 30419 Hannover, Germany
2. School of Food and Nutritional Sciences (SOFNUS), Jomo Kenyatta University of Agriculture and Technology, P.O. Box 62 000, Nairobi 00200, Kenya

Author Contributions:

Conceptualization, M.K. and T.O.A.; funding acquisition, M.K. and W.O.O.; investigation, T.O.A. and A.W.; methodology, T.O.A., A.W., W.O.O. and M.K.; supervision, M.K. and

W.O.O.; visualization, T.O.A. and A.W.; writing—original draft, T.O.A. and M.K.; writing -review and editing, T.O.A., A.W., W.O.O. and M.K.

PLOS ONE

Lenticels are sites of initiation of microcracking and russeting in 'Apple' mango

Thomas O. Athoo[1], Andreas Winkler[1], Willis O. Owino[2], Moritz Knoche[1]*

1 Institute for Horticultural Production Systems, Leibniz-University Hannover, Hannover, Germany, 2 School of Food and Nutritional Sciences (SOFNUS), Jomo Kenyatta University of Agriculture and Technology, Nairobi, Kenya

☺ These authors contributed equally to this work.
* moritz.knoche@obst.uni-hannover.de
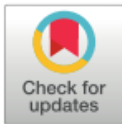
Abstract

The mango cultivar 'Apple' is an important fruitcrop in Kenya, but it is highly susceptible to russeting. The objective was to establish whether lenticels predispose cv. 'Apple' mango to russeting. Fruit mass and surface area increased in a sigmoidal pattern with time. The frequency of lenticels per unit surface area decreased during development. The number of lenticels per fruit was constant. Lenticels were most frequent in the apex region and least common in the cheek and nak (ventral) regions. The cheek region also had lenticels with the largest core areas, whereas the lenticel core areas in the apex region were significantly smaller. Microscopy revealed stomata became covered over with wax deposits at 33 days after full bloom (DAFB). By 78 DAFB, periderm had formed beneath the pore. At 110 and 161 DAFB, cracks had developed and the periderm had extended tangentially and radially. The presence of lenticels increased the strain released upon excision of an epidermal segment, further strain releases occurred subsequently upon isolation of the cuticle and on extraction of the cuticular waxes. The number of lenticels per unit surface area was negatively correlated with the fruit surface area ($r^2 = 0.62$ **), but not affected by fruit size. Mango cv. 'Apple' had fewer, larger lenticels and more russet, compared with 'Ngowe', 'Kitovu' or 'Tommy Atkins' mango. In cv. 'Apple', the lowest lenticel frequency, the largest lenticels and the most russeting occurred at a growing site at the highest altitude, with the highest rainfall and the lowest temperature. Moisture exposure of the fruit surface resulted in enlarged lenticels and more microcracking of the cuticle. Our results establish that russeting in 'Apple' mango is initiated at lenticels and is exacerbated if lenticels are exposed to moisture.

Introduction

Surfaces of young fruit are often stomatous. Stomata regulate gas exchange by changes in their conductance mediated through the opening and closing of the stomatal pore, usually in response to environmental stimuli [1]. In many fruit crops, stomata on the fruit surface later develop into lenticels [1, 2]. In contrast to a stomate, the conductance of a lenticel is not

regulated. Anatomically, lenticels represent a periderm comprising a phellogen that produces stacks of cork cells, the phellem [2]. The phellem that fills the core of these lenticels comprises a volume of loosely packed cells [2, 3], thereby facilitating gas exchange [1, 2]. When the epidermis and cuticle are sloughed off later on during fruit development, the phellem forms the new surface. Lenticels then turn reddish/brown as a result of the suberization of their cell walls.

Lenticels increase the fruit skin's permeance to postharvest water loss [4, 5]. Furthermore, in some fruit crops the lenticels represent sites of preferential infection with pathogens [6] but there is only limited evidence for this last observation in mango [7].

In mango (*Mangifera indica* L.), two important physiological disorders are associated with lenticels—lenticel discoloration and russeting. Lenticel discoloration occurs postharvest and involves the deposition of darkly pigmented phenolics in a distinct zone around the lenticel [8–10]. In contrast, russet develops preharvest and usually covers larger portions of the fruit surface [11]. There is some indication that mechanical stress can be involved in both lenticel discoloration and in russeting [12–14].

The mango cv. 'Apple' is grown widely in Kenya [15]. However, it is highly susceptible to russeting. The skin of a russeted fruit is dull brown and rough [11]. Russeted fruit shrivel faster postharvest [11]. An earlier study suggests russeting in cv. 'Apple' mango is initiated at lenticels [11]. Furthermore, that russeting is triggered by surface wetness [11, 16]. Unfortunately, little is known about the development of lenticels in mango in general [14], nor for russeting in cv. 'Apple' mango in particular. It is not known if or how lenticel development is affected by exposure to surface moisture.

The objective of this study was to identify if and how lenticels predispose cv. 'Apple' mango fruit to russeting. The effects of exposure of the fruit to surface moisture on later russeting development were also investigated.

Materials and methods

Plant materials

Fruits of the mango cvs. 'Apple', 'Kitovu', 'Ngowe' and 'Tommy Atkins' were obtained from a range of commercial orchards in Kenya. From Kakuzi (Murang County, altitude 1327 m) (1˚04'S, 37˚19'E), Kibwezi (Makueni County, 687 m) (2˚20'S, 38˚07'E) and Mwala (Machakos County, 1244 m) (1˚19'S, 37˚26'E). All fruit were grown using integrated pest management programs. Fruit were sampled randomly from trees preselected for uniformity in flowering and tree size and shape. Border trees were avoided. The fruit selected for sampling was free of visible defects and representative in size and color for the population of fruit on the tree. Fruit was processed within 48 hours of sampling.

Methods

Microscopic inspection of the fruit surface. Stomata and lenticels were inspected microscopically. Unless specified otherwise, epidermal segments (ES) were excised from the cheek region of the fruit using a razor blade. The ES were examined under a stereo microscope (MZ10F; Leica Microsystems, Wetzlar, Germany) and photographed (Camera DFC7000T; Leica Microsystems). The magnifications were such that the rectangular windows on the fruit skin selected for measurement ranged from 1.7×1.3 mm to 13.9×10.5 mm. The lenticel frequency (number of lenticels per unit area), the core area and the pore area (opening) per lenticel were quantified by image analysis (ImageJ 1.53P; National Health Institute, Bethesda, MD, USA). See supplementary S1 Fig for an illustration of the core and pore areas of a lenticel.

87

Stomata were investigated before and after the removal of the epicuticular wax. The epicuticular wax was removed by dipping the fruit in a 1:1 (v:v) chloroform: methanol mixture ($CHCl_3$:CH_3OH) for 15 min. The ES were viewed using a digital microscope (VHX-7100; Keyence corporation, Osaka, Japan). The magnification was 1500× (objective VHX-E500, Keyence).

Microscopic inspection of cross-sections. Pieces of the skin and adhering flesh were excised using a razor blade and fixed in a formaldehyde-glutaraldehyde solution [17]. Following rinsing, tissue blocks comprising a portion of the skin and adhering flesh (approx. 5 x 2 x 2 mm) were cut by hand. The blocks were placed inside plastic cassettes (PrintMate biopsy Cassetes; Thermo Fisher Scientific, Kalamazoo, MI, USA), immersed in 70% ethanol and stored overnight at 4°C. The blocks were vacuum infiltrated at 10.8 kPa absolute pressure for 30 min each with aqueous ethanol (70, 80, 90 and 96% v:v) and twice with absolute isopropanol. The blocks were further vacuum infiltrated twice for 40 min with xylene substitute (AppliClear; PanReac Applichem, Muenster, Germany), then once for 40 min in a 1:1 v:v paraffin/xylene substitute mixture. Subsequently, the blocks were vacuum infiltrated in melted paraffin, held at 65°C for 12–14 h (Memmert 100–800; Memmert, Schwabach, Germany) and then embedded in melted paraffin. The embedded blocks were stored at 4°C until use.

Thin sections (10 μm) of embedded tissue were cut with a microtome (Hyrax M55; Carl Zeiss, Jena, Germany) and heat-fixed to a microscope slide at 40°C (Memmert 100–800; Memmert). The paraffin was removed by immersing slides in xylene substitute, twice for 10 min each. The tissue was rehydrated in a descending series of aqueous ethanol (96, 80, 70 and 60% v:v) for 10 min each and rinsed twice with deionized water for 5 min each.

The sections were stained for a minimum of 60 min with 0.005% (w:v) fluorol yellow 088 dye (Santa Cruz Biotechnology, Dallas, TX, USA) dissolved in a 1:1 (v:v) melted polyethylene glycol 4000 (SERVA Electrophoresis; Heidelberg, Germany) and 90% glycerol. The stain was washed-off with deionized water. Sections were examined by fluorescence microscopy (BX-60; Olympus Europa, Hamburg, Germany) and photographed (DP73; Olympus) under incident bright and fluorescent light (U-MWU filter, 330–385 nm excitation, ≥420 nm emission wavelength; Olympus). The number of single fruit replicates was 5.

Developmental time course. The developmental time courses of change in fruit mass, surface area, frequency of lenticels per unit area and the areas of lenticel cores and pores were established. The cv. 'Apple' mango fruits were randomly harvested from pre-selected trees (based on tree shape and flowering density) in an orchard at Mwala. Fruit mass was quantified using a balance (TX420L; Shimadzu Corporation, Kyoto, Japan). Fruit length and two orthogonal diameters (in the equatorial region) were determined using a digital caliper (CD-20PKX; Mitutoyo, Kawasaki/Kanagawa, Japan). Surface area was calculated from the above three fruit dimensions assuming sphericity. Earlier studies established that the surface area thus calculated was always within 98% of the surface area measured on excised peels [18]. A sigmoidal regression model was fitted through a plot of fruit surface area vs. time (days after full bloom; DAFB). The surface area growth rate (cm^2 d^{-1}) was calculated from the first derivative of the regression model. The number of replicates at any sampling date was 20.

Lenticels were inspected microscopically in surface view and also in cross-sections throughout fruit development. Lenticel frequency and the areas of lenticel cores and pores were quantified as above.

Lenticel width and depth were also determined microscopically using the above procedures. The relationships among the lenticel characteristics were analyzed by correlation analysis. The number of replicates was 50.

Lenticels in different regions of the fruit surface. The frequency of lenticels per unit surface area and the lenticel core area were quantified in the 'stem end', 'cheek', 'apex',

'nak'(ventral) and 'back' (dorsal) regions of 'Apple' mango fruit as described by [19, 20]. Fruit were sampled from Mwala. See S2 Fig for the illustration of the different regions of the fruit surface. The 'nak' region contains the stylar scar and is also referred to as the 'beak'.

Effect of fruit size on lenticel characteristics.   The effects of size of 'Apple' mango fruit (site Mwala) on lenticel frequency per unit area, lenticel core area and the number of lenticels per fruit were established at maturity using fruit selected for a maximum range in size. The fruit were peeled, and the peels flattened between two glass plates. The flattened peels were photographed with a digital camera (Lumix DMC-G80; Panasonic Corporation, Osaka, Japan) fitted with a macro lens (Olympus M. Zuiko Digital 60 mm; Olympus Corporation, Tokyo, Japan). A ruler was included in each image for calibration. Peel area and lenticel frequency were quantified by image analysis (ImageJ 1.53P; National Health Institute). The number of lenticels on a whole-fruit basis was calculated as the product, lenticel frequency per unit area × fruit surface area. The number of single fruit replicates was 40.

Cultivar effects.   Visual field observations indicated that russet susceptibility and lenticel morphology markedly differed between mango cultivars. We therefore sampled mature fruits of cvs. 'Apple' (171 DAFB), 'Tommy Atkins' (168 DAFB), 'Ngowe' (171 DAFB) and 'Kitovu' mango (204 DAFB) from a commercial orchard located in Mwala. All cultivars were subjected to the same crop husbandry and sampled at commercial maturity at the same site. Lenticel frequency and lenticel core area of the different cultivars were quantified. Fruits were rated for russet severity and photographed. Severity of russeting was quantified using a scoring scheme [11]. Russet was scored from 0 to 4 on a per fruit basis. Score 0: 0% of the fruit surface area russeted; score 1: 1–10% russeted area; score 2: 11–25% russeted area; score 3: 26–50% russeted area; and score 4: 51–100% russeted area. The number of single fruit replicates was 200 for russet severity and 40 for lenticel frequency and core area per lenticel.

'Apple' mango from different growing sites.   To assess the variability of lenticel characteristics on fruit grown at different sites, the effect of orchard was investigated. Mature 'Apple' mango fruits were sampled from orchards located at different altitudes, i.e., Kakuzi (altitude 1327 m), Mwala (1244 m) and Kibwezi (687 m). Fruits were rated for russet severity. Lenticel frequency and core area per lenticel were quantified. Severity of russeting was quantified using a scoring scheme [11]. Russet was scored from 0 to 4 on a per-fruit basis as described above. Daily values of rainfall, relative humidity (RH) and temperature throughout the growing season were obtained from the website of the NASA Langley Research Center (LaRC) POWER Project (NASA Langley Research Center, Hampton, VA, USA).

Effects of moisture exposure.   The effects of surface moisture on lenticels were investigated in developing 'Apple' mango at the Mwala site at 33, 58, 72, 100 and 130 DAFB. The fruit surface was exposed to moisture by mounting a polyethylene Eppendorf (PE) tube to the cheek of the fruit using a non-phytotoxic silicone rubber (Dowsil™ SE 9186 clear sealant; Dow Toray Co., Tokyo, Japan) [21]. Distilled water (1 ml) was injected into the PE tube through a hole cut in the tip using a disposable syringe. The hole was then sealed with silicone rubber. The tubes were re-inspected every 2–3 days, re-filled with distilled water when necessary and re-sealed to the fruit to prevent leakage. The untreated opposite cheek of the same fruit served as control. After 8 days, the tubes were removed, fruits harvested and treated areas of skin marked using a permanent marker.

Development of microcracks at lenticels was investigated microscopically. Microcracking was indexed by quantifying the area infiltrated by the fluorescent tracer acridine orange [22]. The fruit surface was dipped in a solution of aqueous acridine orange (0.1% w/v) for 10 min. This time was sufficient for acridine orange to penetrate through any openings in the cuticle. There was no penetration through an intact cuticle. Thereafter, the surface was rinsed with distilled water and blotted dry with a soft paper towel. Lenticels were examined using a stereo

89

microscope (MZ10F; Leica Microsystems) under incident bright light and incident fluorescent light (GFP LP filter, 480–440 nm excitation, ≥510 nm emission wavelength). Calibrated images of lenticels were taken using a digital camera (Camera DFC7000T; Leica Microsystems). The area infiltrated by acridine orange was quantified by image analysis (Image J). The number of single fruit replicates was 10.

Effect of lenticels on strain relaxation of the fruit skin. The effect of lenticels on the strains released following excision of an ES and subsequent isolation of the cuticular membrane (CM) and extraction of wax from the CM was investigated in mature 'Apple' mango fruit from Mwala [23]. The ES, both with and without lenticels, were excised from the fruit surface using a biopsy punch (8 mm diameter; Kai Europe, Solingen, Germany) and transferred to a formaldehyde-glutaraldehyde fixative solution [17]. Cuticles were isolated enzymatically by incubating the ES in 50 mM citric acid buffer containing pectinase (90 ml l^{-1}; Panzym Super E flüssig; Novozymes A/S, Krogshoejvej, Bagsvaerd, Denmark), cellulase (5 ml l^{-1}; Cellubrix L; Novozymes A/S) [24, 25] and 30 mM sodium azide. The pH of the solution was adjusted to 4.0 using NaOH. The solution was refreshed periodically until the cuticle separated from adhering tissue. The cuticle was rinsed (at least 5 times) with deionized water. Adhering cellular debris was removed using a soft camel-hair brush.

A square pattern of four holes was punched in the center of the cuticle using a custom-made punch. The hole pattern was needed to allow measurement of strain relaxation of an isolated and dewaxed CM even when the rim of the CM disc curled up. This was typically the case following wax extraction. The hydrated CM was spread on a glass slide and photographed under a dissecting microscope (Wild M10; Leica Microsystems; camera DP71, Olympus). The area of the CM disc (A_{CM}) and the area demarcated by the four holes were quantified using image analysis (Software Cell^P, Olympus Soft Imaging Solution, Muenster, Germany).

To determine strain relaxation upon wax extraction, the dry CM disc was extracted in a soxhlet apparatus using (1:1 v:v) CHCl$_3$/CH$_3$OH for a minimum of 2 h. Following wax extraction, the dewaxed CM (DCM) was dried to remove any solvent residues, then rehydrated overnight using deionized water, spread on a glass slide and photographed (Wild M10; Leica Microsysteme; camera DP71, Olympus). The area demarcated by the hole pattern was re-quantified using image analysis (Software Cell^P, Olympus). The area of the entire DCM (A_{DCM}) disc was then calculated from the area of the square-hole pattern.

The release of apparent strains due to excision of the ES and isolation of the CM ($\varepsilon'_{exc+iso}$), due to wax extraction (ε'_{extr}) and the sum of the two strains (ε'_{tot}) were calculated using the following equations:

$$\varepsilon'_{exc+iso} = \frac{A^i - A^i_{CM}}{A^i_{DCM}} \times 100 \tag{1}$$

$$\varepsilon'_{extr} = \frac{A^i_{CM} - A^i_{DCM}}{A^i_{DCM}} \times 100 \tag{2}$$

$$\varepsilon'_{tot} = \varepsilon^i_{exc+iso} + \varepsilon^i_{extr} \tag{3}$$

In these equations, A^i represents the area of the ES prior to excision. This area is equivalent to the cross-sectional area of the circular biopsy punch. The A^i_{CM}, represents the area of the CM disc after enzymatic isolation and the A^i_{DCM} the area of the DCM (after wax extraction). Using these procedures, the strain relaxations of fruit-skin samples, with and without lenticels, were compared. The number of replicates was 40.

90

Strain relaxation of a lenticel was also quantified. For this, ES were selected having a maximum range of lenticel frequency and were excised. These were enzymatically isolated and wax extracted as described above. The core area per individual lenticel was measured before and after wax extraction. Lenticel strain ($\varepsilon'_{lenticel}$) was quantified on lenticels within the area demarcated by the four holes using Eq 4.

$$\varepsilon'_{lenticel} = \frac{A'_{IL} - A'_{DL}}{A'_{DL}} \times 100 \qquad (4)$$

In this equation, A'_{IL} represents the core area per lenticel after isolation and A'_{DL} the core area after wax extraction.

Data analysis

Unless otherwise stated, data are presented as means ± standard errors. Analyses of variance, regression analyses and correlation analyses were conducted using the statistical software package R (version 4.0.3; R Foundation for Statistical Computing, Vienna, Austria).

Results

Fruit mass and surface area increased sigmoidally with time (Fig 1A and 1B). The surface-area growth rate reached a maximum of 3.7 cm^2 d^{-1} at about 100 DAFB, and declined thereafter (Fig 1C).

The frequency of lenticels per unit surface area decreased during development, whereas the lenticel core area and pore area increased (Fig 2A–2C). The number of lenticels per fruit remained essentially constant (Fig 2A, inset).

Lenticel core area and pore area were significantly and positively correlated ($r^2 = 0.79$ ***). In contrast, core depth had only a weak relationship with core area ($r^2 = 0.22$ **) (Fig 3A and 3B).

The distribution of lenticels over the fruit surface was not uniform (Table 1). Lenticels were most frequent in the distal region and least in the cheek and the nak regions. The cheek region also had lenticels with the largest core areas, whereas the core areas of those in the apex region were significantly smaller (Table 1).

Microscopy at 33 and 78 DAFB revealed stomata on the surface that appeared as whitish spots with no visible pore (Fig 4A). Heavy wax deposits covered the guard cells and stomatal pores completely at 33 DAFB (Fig 4D). The stomatal apparatus became clearly visible only after removal of epicuticular waxes (Fig 4E). Staining with fluorol yellow revealed a cuticle above the epidermal cells. At the guard cells, the cuticle extended into the stomatal antechamber (Fig 4B and 4C). By 78 DAFB, stomata appeared as large openings, the rim of the cuticle surrounding the pore was still intact. Cross-sections revealed the onset of periderm formation several cell layers below the pore (Fig 4F–4H). At 110 DAFB, cracks in the cuticle had begun to form that tore the rim of the pore. By 161 DAFB, the pore rim was torn, and severe cracks developed in the cuticle. The periderm extended laterally, the number of phellem layers increased and eventually filled the entire core volume of the lenticel (Fig 4I–4N).

Compared to a lenticel-free ES, the presence of lenticels increased the strain released by between 1.5- and 1.8-times when an ES was excised and the subsequent isolation of the cuticle ($\varepsilon'_{exc+iso}$) and the extraction of cuticular wax (ε'_{extr}). The sum of these strains, i.e., the total strain, was 1.7 times larger for cuticles with lenticels as compared to those without lenticels (Table 2).

There was no relationship between the strain released from a lenticel and that from the corresponding isolated cuticular membrane (Fig 5A). However, the area of the lenticel core following wax extraction was closely related to the area of the lenticel core in the isolated cuticle
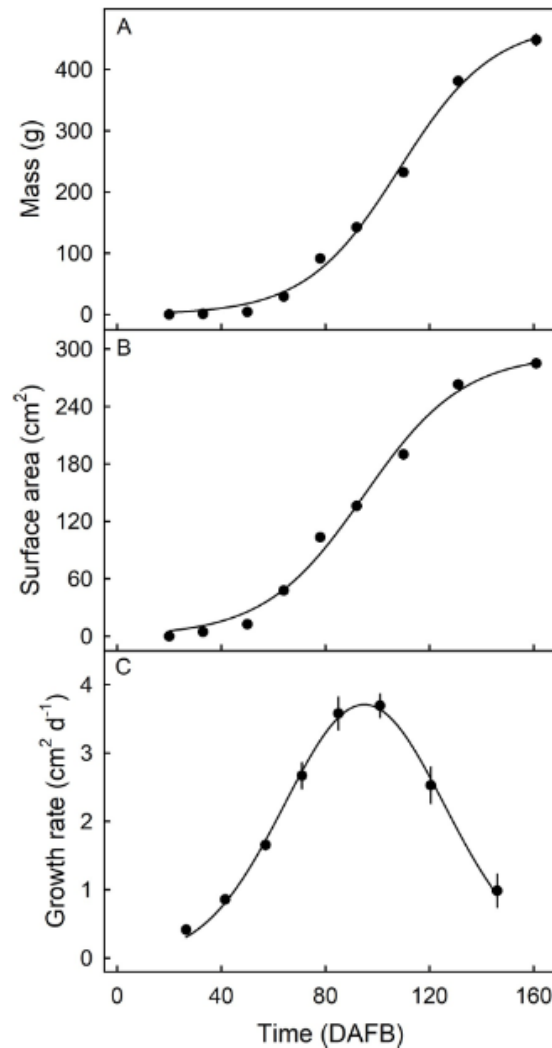
91

Fig 1. Developmental time course of change in fruit mass (A), surface area (B) and surface area growth rate (C) of 'Apple' mango fruits grown in the same orchard. Fruit surface area was calculated from measurements of fruit length and of two orthogonal diameters in the equatorial region, and assuming sphericity. This calculation was previously validated using the following linear model: *Surface area* = 1.18×*peel area*+0.93, $r^2 = 0.98^{***}$ [18]. X-axis time scale in days after full bloom (DAFB). Data represent means ± standard errors. N = 20.

https://doi.org/10.1371/journal.pone.0291129.g001

disc (Fig 5B). The strain released from a lenticel upon isolation and upon wax extraction was highly variable and not related to the core area in the isolated cuticle disc (Fig 5C).

The number of lenticels per unit area of fruit surface was negatively related with the surface area of the fruit ($r^2 = 0.62$ **) (Fig 6A). On a whole-fruit basis, there was no significant difference in the numbers of lenticels between small and large fruit (Fig 6B). The core area per lenticel and the fruit surface area were weakly and positively related ($r^2 = 0.22^{**}$) (Fig 6C).
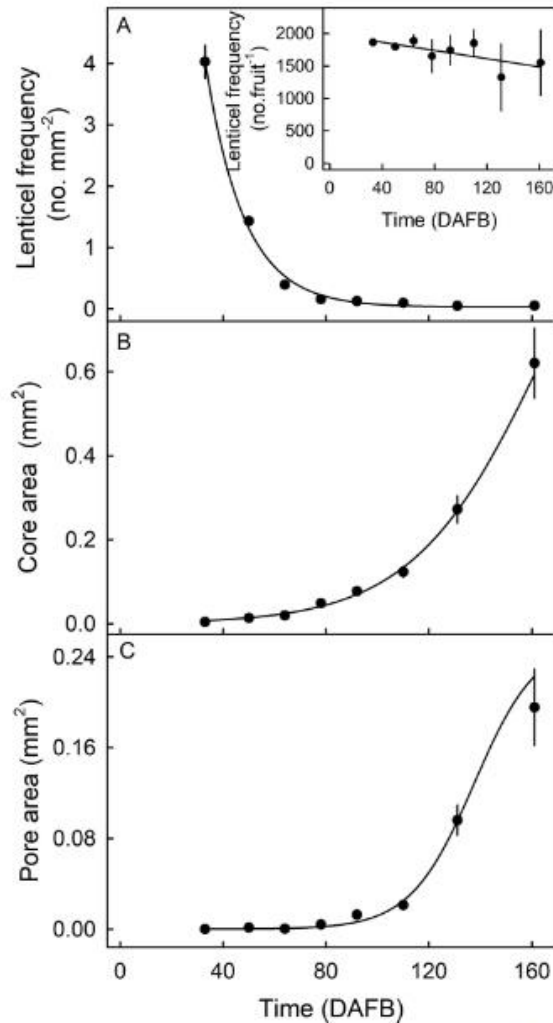
Fig 2. Developmental time course of changes in lenticel frequency (number per unit area and number per fruit) (A and A inset), core area per lenticel (B) and pore area per lenticel (C) in 'Apple' mango. The fruits were grown in the same orchard. The number of lenticels on a whole fruit was calculated as lenticel frequency per unit area × the fruit surface area. X-axis time scale in days after full bloom (DAFB). Data represent means ± standard errors. N = 30.

Compared to 'Ngowe', 'Kitovu' and 'Tommy Atkins' mangos, 'Apple' had the lowest frequency of lenticels and the largest core area per lenticel. Furthermore, russeting was most severe in 'Apple' (Table 3, Fig 7).

Considerable differences in lenticel frequency and core area per lenticel were observed between different growing sites of 'Apple' mango. Russeting was most severe in Kakuzi, intermediate in Mwala and almost absent in Kibwezi. Fruit from Kakuzi exhibited the largest lenticels and the lowest lenticel frequency. On the other hand, fruit from Kibwezi had the smallest lenticels and the highest lenticel frequency. It is interesting that fruit from the three sites also
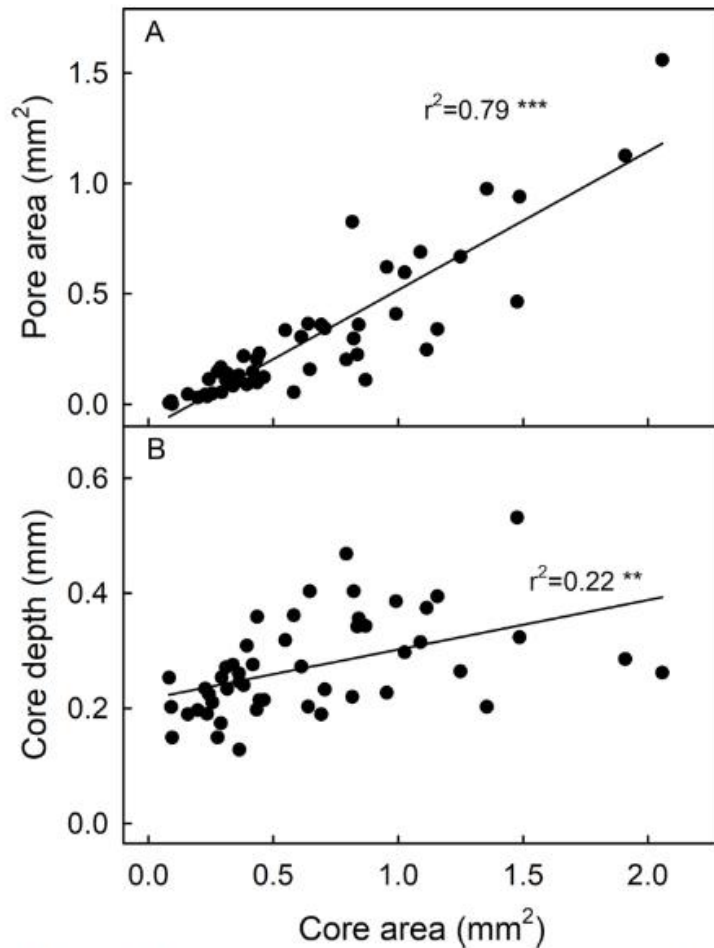
93

Fig 3. Correlation between lenticel pore area and lenticel core area (A) and lenticel core depth and lenticel core area (B) on mature 'Apple' mango. The fruits were grown in the same orchard. Lenticel morphology and cross-section were examined microscopically. N = 50.

differed in (1) russeting and (2) growing conditions, as indexed by altitude, rainfall and temperature which differed markedly between the three sites. Summarizing, the russeted Kakuzi fruit grew at high altitude and were exposed to high rainfall and low temperatures. In contrast, the non-russeted Kibwezi fruit grew at lower altitude and was exposed to lower rainfall and higher temperatures. Intermediate-russeting was observed on fruit from Mwala which is at intermediate altitude, and experiences intermediate rainfall and temperature (Table 4).

On the same fruit, lenticels exposed to moisture fluoresced more than unexposed lenticels (Fig 8). The fluorescing area around lenticels and their core and pore area were small during early development, then increased towards a maximum around 100 DAFB (Figs 8 and 9). The core area, the pore area and the infiltrated area per lenticel in moisture-exposed fruit were consistently larger throughout development than in unexposed control fruit (Fig 9).

94

Table 1. Peak growth rate, lenticel frequency and area per lenticel in different regions of mature 'Apple 'mango (See S2 Fig for nomenclature). The fruit were grown in the same orchard. Data is represented as means ± standard errors. N = 40.

Region	Peek growth rate (cm² d⁻¹)	Lenticels	
		Frequency (No. mm⁻²)	Core area (mm²)
Stem end	0.05 ± 0.01[a]	0.07 ± 0.00 b[b]	0.18 ± 0.02 b
Cheek	0.07 ± 0.02	0.03 ± 0.00 a	0.46 ± 0.05 c
Apex	0.06 ± 0.02	0.09 ± 0.03 c	0.04 ± 0.00 a
Back	0.07 ± 0.02	0.06 ± 0.00 b	0.16 ± 0.02 b
Nak	0.07 ± 0.02	0.04 ± 0.00 a	0.16 ± 0.02 b

[a]Peek growth rate data is taken from [18].

[b]Mean separation within columns by Tukey studentized range test, $P \leq 0.05$.

https://doi.org/10.1371/journal.pone.0291129.t001

Discussion

This discussion focusses on the following three findings;

i. growth strains enlarge lenticels and lead to their eventual rupture,

ii. moisture on the fruit surface increases russet formation by increasing lenticel cracking and

iii. lenticels are sites of russet initiation in 'Apple' mango.

Growth strain enlarges lenticels leading to their rupture

Lenticels on 'Apple' mango increase in both core and pore area during development and this leads to their eventual rupture. The driver for lenticel enlargement and lenticel rupture is the progressive increase in growth strain in the fruit skin [26]. This hypothesis is supported by the following arguments.

First, there was a positive correlation between fruit surface area and lenticel core area (Fig 4). Although the number of lenticels per unit area decreased during development, the number of lenticels per fruit basis did not change–this indicates new lenticels did not appear during fruit development, instead, as the fruit expanded, a constant number of lenticels was distributed over an increasing surface area. The increases in core and pore areas are consistent with this observation. The increase in pore area of a lenticel was simply related to the expansion of the core area. By about 110 DAFB, the limits of extensibility of the lenticels were exceeded and the lenticels started to rupture (Fig 3). 'Apple' mango is not unique in this behavior [14, 27, 28].

Second, the lenticel core area differed between regions on a fruit and these differences were simply related to the rates of fruit surface-area expansion in these regions [18]. We observed larger core areas and a lower frequencies of lenticels in the cheek region, where the rates of increase in surface area are largest [18]. In contrast, the apex region of the fruit, where the rates of surface area growth are low, lenticel frequency was high and the lenticel core area was small [18]. These findings are consistent with earlier reports for *Malus* apple (*Malus* × *domestica* Borkh.) [4]. In *Malus* apple, lenticel core area decreases and lenticel frequency increases from the pedicel end of the fruit to the calyx end [4], whereas the surface growth rate decreases [29].

Third, the time of lenticel rupture and of crack extension into the adjacent cuticle and epidermis, coincides with the time of maximum surface area expansion rate. This suggests a cause (surface growth strain) and effect (cracking of lenticels and surrounding cuticle) relationship. Apparently, the increase in core area of the lenticels was not sufficient to accommodate the
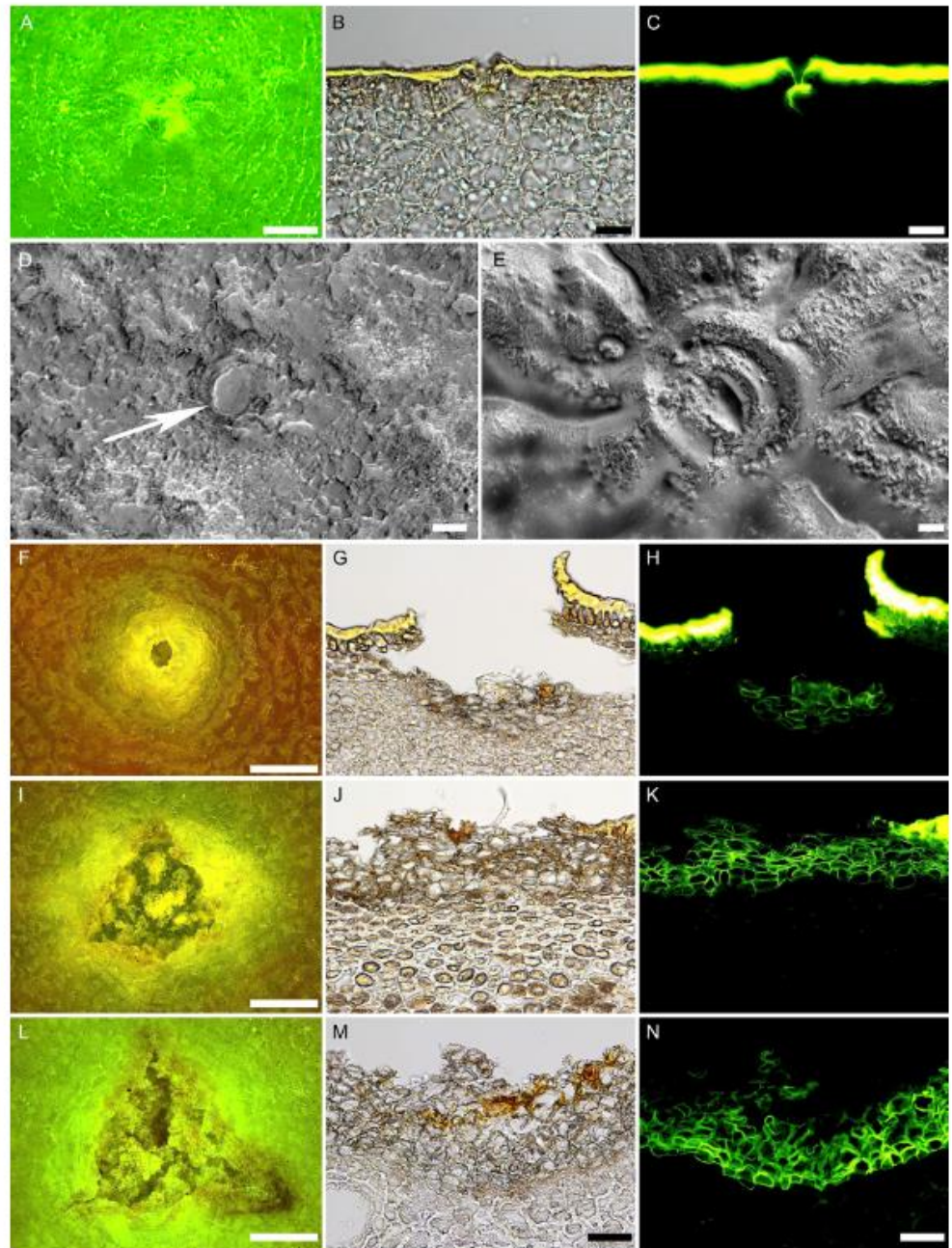
95

Fig 4. Surface (left) and cross-sectional views (middle and right) of stomata and lenticels in developing 'Apple' mango fruits from the same orchard. Fruits were sampled at 33 (A-E), 78 (F-H), 110 (I-K) and 161 (L-N) days after full bloom (DAFB). Surface view was examined under a binocular microscope and a digital microscope. Cross-sections were examined microscopically under incident (middle) and fluorescence (right) light. White arrow indicates stomal pores plugged with wax. Scale bars are 250 (A), 20 (B,C), 10 (D,E), 500 (F, I, L) and 50 μm (G,H,J,K,M,N). N = 10 (surface views) and 5 (cross-sections).

https://doi.org/10.1371/journal.pone.0291129.g004

96

Table 2. Effect of the presence of lenticels on apparent strains (%) in 'Apple' mango skins from the same orchard. Apparent strain was partitioned into strains due to excision and isolation ($\varepsilon'_{exc+iso}$) and wax extraction (ε'_{extr}). The latter two strains were summed up to make the total strain (ε'_{tot}). Data is represented as means ± standard errors. N = 30.

Treatment	$\varepsilon'_{exc+iso}$	ε'_{extr}	ε'_{tot}
With lenticels	12.6 ± 0.6 b[a]	28.1 ± 1.0 b	40.7 ± 1.0 b
Without lenticels	8.5 ± 0.6 a	15.8 ± 0.7 a	24.4 ± 0.9 a

[a]Mean separation within columns by Tukey studentized range test, P≤ 0.05

increase in fruit surface area that accompanies the growth of the underlying tissues [8]; this results in the cracking of the cuticle, immediately adjacent to the lenticel. It also consistent with the higher strain relaxation of skin segments containing lenticels, compared to skin segments with no lenticels.

Fourth, lenticels developed from stomata. At 33 DAFB, we observed stomata but no lenticels. By 78 DAFB, the stomata were gaping and an upward bending of the cuticle surrounding the stomatal pore indicated severe tangential strain. By 110 DAFB, lenticels were fully developed, as indexed by the presence of a fully developed periderm. Similarly, in 'Kensington Pride' and 'Namdokmai' mango cultivars, stomata ruptured and developed into lenticels [13, 30]. In 'Namdokmai' mango, lenticels were fully developed one month after full bloom [13]. Lenticels also develop from ruptured stomata in *Malus* apples [27].

These arguments demonstrate that in 'Apple' mango growth strain is causal in the development of lenticels and their cracking. Interestingly, we observed no cracking of lenticels in 'Tommy Atkins' or 'Ngowe'. Both 'Tommy Atkins' and 'Ngowe' typically have larger fruit, so implying even higher skin strain than in the smaller 'Apple' mango–yet there was no sign of cracking [18]. This observation demonstrates that lenticel morphology also depends on cultivar [9, 10, 31].

Surface moisture induces lenticel cracking

Growth strain is not the only factor involved in lenticel development in 'Apple' mango. Our study provides direct evidence that surface moisture plays a critical role in lenticel development, expansion and cracking.

First, the core and pore areas of lenticels exposed to moisture were as much as 2-fold larger than those of control lenticels unexposed to water.

Second, the area infiltrated by acridine orange was larger for moisture exposed lenticels then for un-exposed lenticels, on the same fruit. Even for lenticels having the same core and pore areas, lenticels exposed to moisture had significantly larger areas of fluorescence around them, than unexposed lenticels. The increase in fluorescing area is explained by increased microcracking around and through the lenticels. Microcracks serve as pathways through the cuticle for rapid dye uptake.

Third, the effects of moisture on lenticel core area and pore area also account for the differences in lenticels between mangos grown at different sites. Fruits grown at lower altitudes (Kibwezi) developed smaller lenticel cores than those at higher altitudes (Kakuzi). Kibwezi has a hot, dry climate with low rainfall, while Kakuzi is cooler, more humid and with higher rainfall. Consequently, fruits grown at Kakuzi had larger lenticels and were more russeted than fruits grown in Kibwezi. These orchard observations are consistent with the effects of moisture exposure on lenticel development and russeting reported in this and in our previous study [11].
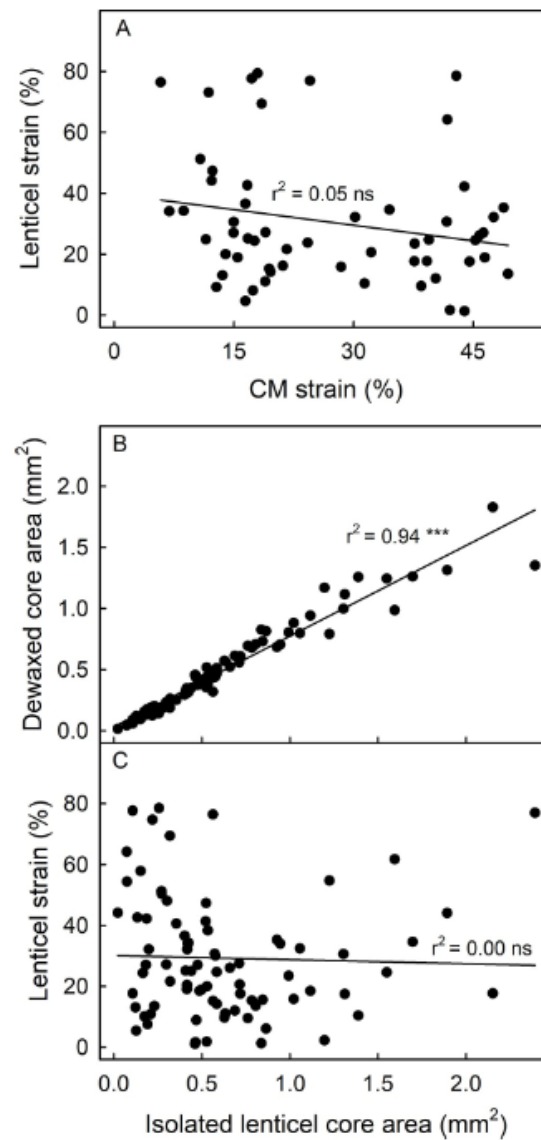
Fig 5. Correlation between the strain released from a lenticel and that released from an excised and isolated cuticular membrane (CM) (A), between the dewaxed core area of a lenticel and the core area in the isolated CM disc (B), and between the strain released from a lenticel and the core area in the isolated CM disc (C). Lenticel core areas in isolated cuticles and in dewaxed cuticles were analyzed by image analysis. N = 40 (lenticels) and 24 (cuticles). The slope of the regression line in B is 0.74 ± 0.02.

A likely explanation for increased rupture of lenticels and microcracking of the cuticle around lenticels is the effect of hydration on the mechanical properties of the cuticle. It is well established that hydrated cuticles fracture at lower forces than dry cuticles [32–34]. In
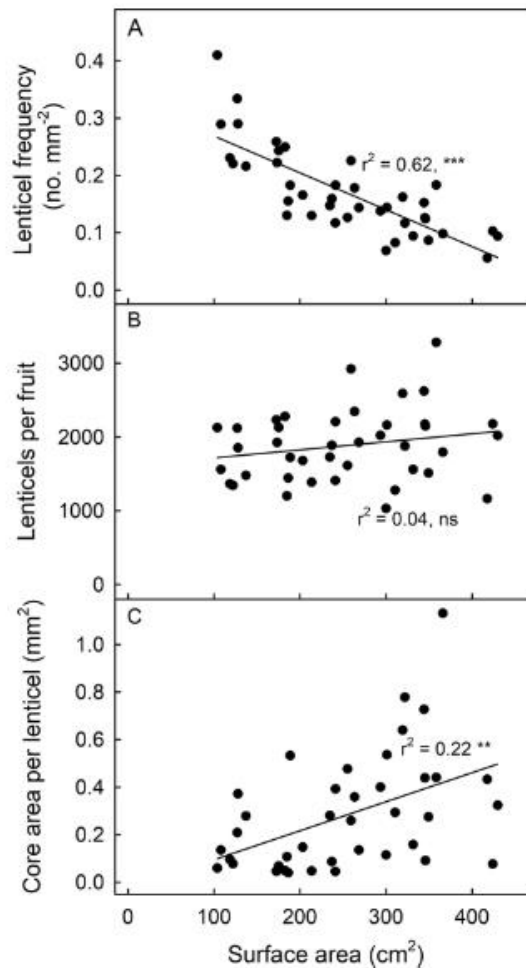
98

Fig 6. Effect of fruit surface area on frequency of lenticels per unit area (A), total lenticels per fruit (B) and the core area per lenticel (C) of mature 'Apple' mango fruit grown under same conditions. The fruit surface area was measured by peeling the fruit, flattening the peel between two glass plates, photography and finally by image analysis. N = 40. For regression equations see the S1 File.

https://doi.org/10.1371/journal.pone.0291129.g006

addition, lenticels function as stress concentrators. They represent islands of differing extensibility that would serve to focus growth stresses at these locations on the fruit surface [35, 36]. The lenticels in 'Apple' mango, would appear to be weak spots, since star-like cuticular microcracks radiate from the gaping lenticels. This was also reported in our earlier study [11]. Our earlier study, found that when cuticles were subjected to uniaxial tensile tests, cuticular failure occurred most frequently across or around the lenticels [18]. In *Malus* apple, a periderm similarly forms under ruptured stomata or in response to microcracking, due to surface moisture [21, 37–39].

99

Table 3. Severity of russet, frequency and areas of lenticels in different mango cultivars. All cultivars were sampled from the same orchard. Severity of russet was quantified using a rating scale from 0 to 4: score 0: 0% of the fruit surface area russeted; score 1: 1–10% russeted area; score 2: 11–25% russeted area; score 3: 26–50% russeted area; and score 4: 51–100% russeted area. Lenticel properties were quantified on the cheek of the fruit. Data is represented as means ± standard errors. N = 200 (russet severity) and 40 (lenticel frequency and area per lenticel).

Cultivar	Russeting (Score)	Lenticels	
		Frequency (No. mm^{-2})	Core area (mm^2)
Apple	1.15 ± 0.05 b[a]	0.05 ± 0.00 a	0.50 ± 0.04 c
Ngowe	0.03 ± 0.01 a	0.19 ± 0.01 c	0.16 ± 0.01 b
Kitovu	0.00 ± 0.00 a	0.15 ± 0.01 b	0.03 ± 0.00 a
Tommy Atkins	0.01 ± 0.01 a	0.33 ± 0.02 d	0.05 ± 0.01 a

[a]Mean separation within columns by Tukey studentized range test, $P \leq 0.05$.

https://doi.org/10.1371/journal.pone.0291129.t003

Cracking of lenticels triggers russeting in 'Apple' mango

In 'Apple' mango, almost all cuticular microcracking develops around lenticels. Russeting in 'Apple' mango begins at lenticels and then gradually spreads over the fruit surface [11]. In botanical terms, russeting represents the formation of a periderm, comprising a cork cambium or phellogen that divides to produce stacks of cork cells, the so called phellem cells [2, 40]. A periderm forms as a typical wound response [26]. Russeting in 'Apple' mango would seem to be similar to that in *Malus* apple [40]. In both cases, a periderm forms in response to a wound, i.e., a cracked lenticel in 'Apple' mango [11] or a microcrack in the cuticle of *Malus* apple [41]. As in *Malus* apple, the periderm forms in the hypodermal cell layers just below the stomata, as indexed by the staining of the suberized cell walls of the phellem [21, 38]. As development progresses, the thickness of the phellem and hence the depth of the lenticels increases [4]. When the fruit's primary surface (the epidermis and the remains of the cuticle) is sloughed off, the phellem and hence the brown lenticels are clearly visible at the surface. This understanding applies to both 'Apple' mango and to *Malus* apple [4, 11, 16, 38]. The above arguments indicate that the initiation and development of russeting in 'Apple' mango follows an essentially identical path to that found in *Malus* apple.

Conclusion

The results demonstrate that russeting in 'Apple' mango is initiated at lenticels. Moisture exposure of developing fruit results in a weakening of lenticels and hence the formation of strain cracking at the lenticels. The wounds and associated increases in water loss, are healed and a degree of waterproofness regained, by the formation of a subtending periderm. The lenticels of 'Apple' mango are much larger than those of the other mango cultivars examined. In addition to this genotypic effect, exposure of developing 'Apple' mango fruits to moisture results in cracking and further increases in lenticel size. It is not clear why moisture should have this effect. The relative weakness of these small areas of periderm probably results from one or several of the following: (1) the large intercellular air-spaces within the periderm of a lenticel and/or (2) the infiltration of lenticels by surface moisture and the subsequent hydration of the periderm cell walls. Coupled with this, the periderm cell walls may have low wax content or their suberization may be incomplete. All these factors will likely reduce cell:cell adhesion within the periderm.

From a horticultural point of view, it is reasonable to conclude that any reduction of exposure of the skins of 'Apple' mangos to moisture is likely to reduce both lenticel cracking and hence russeting. Obvious strategies to achieve this will include focusing the production of 'Apple' mango on sites that enjoy drier climates. Alternative strategies to reduce surface
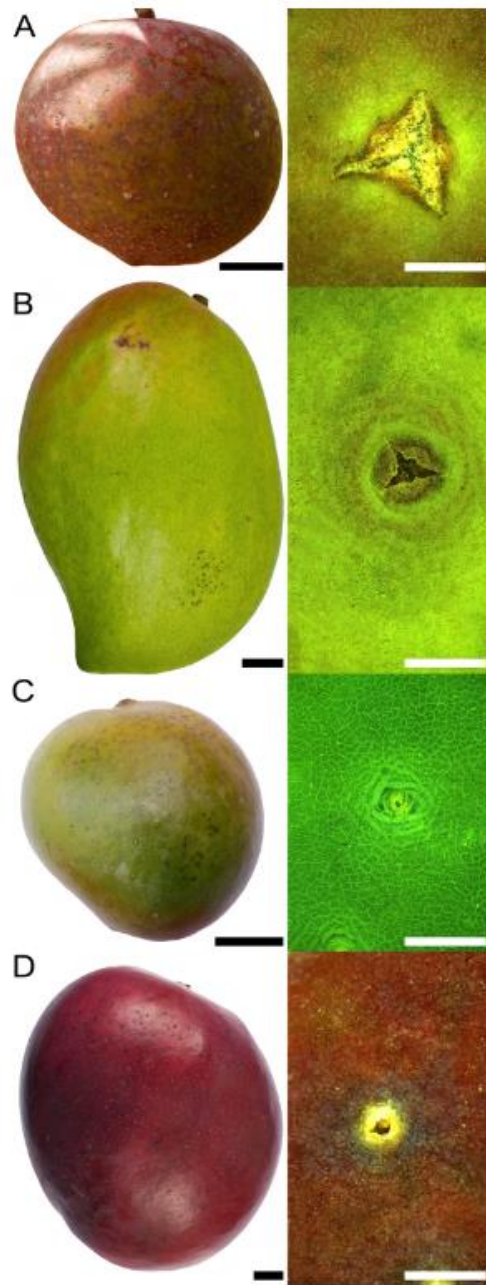
100

Fig 7. Macroscopic view of mature 'Apple' (A), 'Ngowe' (B), 'Kitovu' (C) and 'Tommy Atkins' (D) fruit and microscopic view of lenticels. All fruit were grown at the same site in the same season. Scale bars are 2 cm for macrographs (A-D) and 1 mm for micrographs.

https://doi.org/10.1371/journal.pone.0291129.g007

101

Table 4. Effect of orchard location on russeting and lenticel frequency and lenticel area in cv. 'Apple' mango. The sites were selected based on their differences in altitude—meters above sea level (m.a.s.l.). The climatic variables include: cumulative rainfall, relative humidity (RH), minimum and maximum temperatures. Severity of russet was quantified on a 0 to 4 scoring scheme: Score 0: 0% of the fruit surface area russeted; score 1: 1–10% russeted area; score 2: 11–25% russeted area; score 3: 26–50% russeted area; and score 4: 51–100% russeted area. Data is presented as means ± standard errors. N = 200 (Russeting score) and 40 (lenticel frequency and lenticel area).

Orchard Location	Altitude (m.a.s.l.)	Cumulative rainfall (mm)	RH (%)	Temperature (°C)		Russeting (score)	Lenticels	
				Min.	Max.		Frequency (No. mm^{-2})	Core area (mm^2)
Kibwezi	687	125.7	64.0 ± 0.5	17.1 ± 0.1	30.9 ± 0.2	0.03 ± 0.01 a	0.14 ± 0.01 b	0.03 ± 0.00 a
Mwala	1244	396.0	68.6 ± 0.8	15.4 ± 0.1	28.2 ± 0.2	1.15 ± 0.05 b	0.05 ± 0.00 a	0.50 ± 0.04 b
Kakuzi	1327	459.5	67.4 ± 0.8	16.5 ± 0.1	29.0 ± 0.2	1.72 ± 0.10 c	0.04 ± 0.00 a	1.08 ± 0.08 c

Mean separation by Tukey studentized range test, P≤ 0.05. Means within a column followed by the same letter are not significantly different.

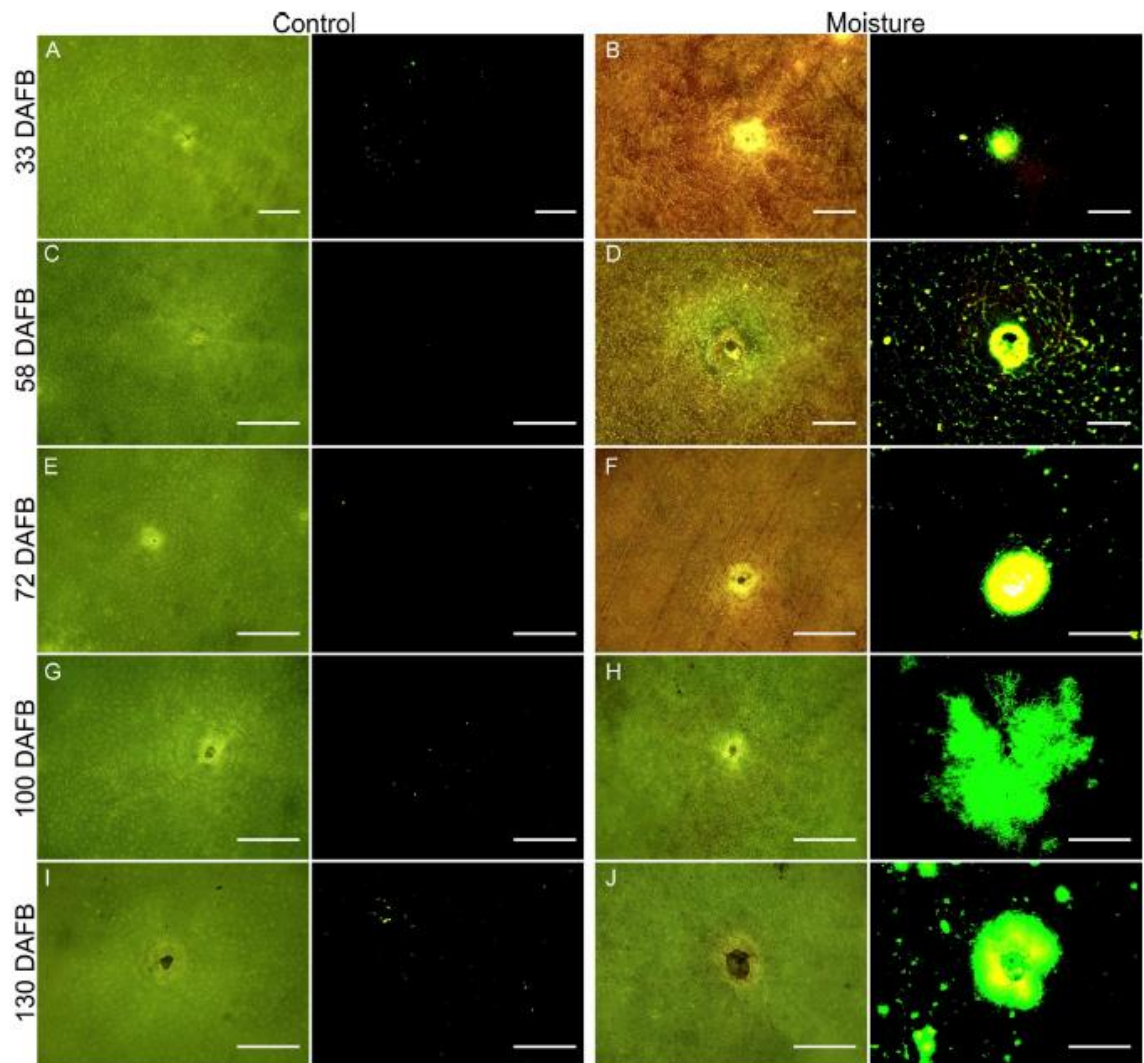https://doi.org/10.1371/journal.pone.0291129.t004

Fig 8. Micrographs of lenticels of developing 'Apple' mango sampled 33 (A-B), 58 (C-D), 72 (E-F), 100 (G-H) and 130 (I-J) days after full bloom (DAFB). The fruit surfaces were either left untreated (A, C, E, G, I) or exposed to surface moisture (B, D, F, H, J). Moisture was presented to a small region on the cheek of a fruit for 8 days by attaching an Eppendorf tube containing water. The surface was later viewed under bright or fluorescence light. N = 10. Scale bar is 500 μm.
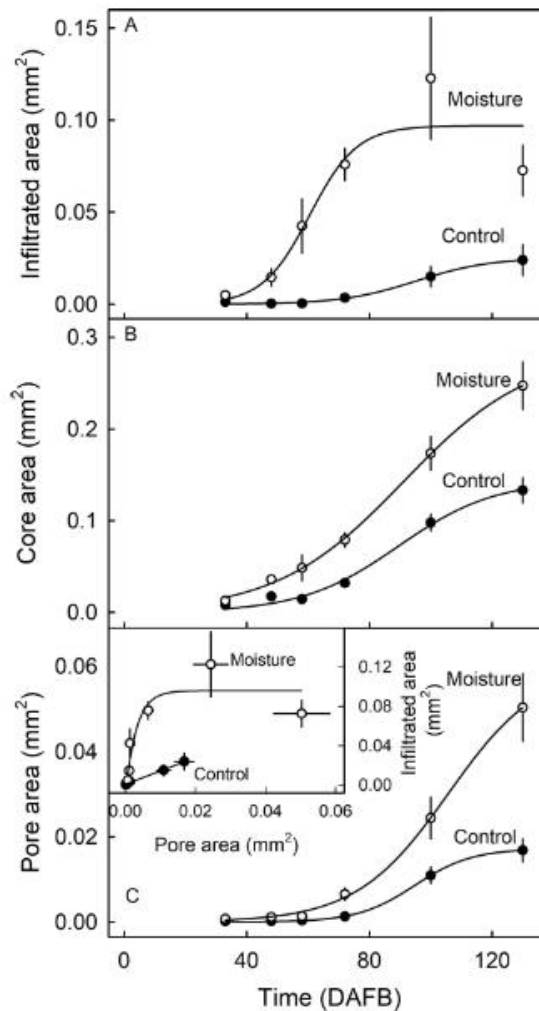
https://doi.org/10.1371/journal.pone.0291129.g008

102

Fig 9. Effect of moisture exposure of the fruit surface of developing 'Apple' mango on (A) the area surrounding a lenticel that is infiltrated by the fluorescent tracer acridine orange, (B) the lenticel's core area and (C) the lenticel's pore area. Inset in C: Infiltrated area as affected by the pore area of the lenticel. Unexposed fruit served as controls. X-axis scale is in days after full bloom (DAFB). The number of replicates ranged from 19 to 46.

https://doi.org/10.1371/journal.pone.0291129.g009

moisture should include bagging the developing fruits on the tree [42], and another strategy would be to cultivate the 'Apple' mangos trees under a rain shelter, on a dwarfing rootstock. These avenues for mitigation of russeting in 'Apple' mango all merit study.

Supporting information

S1 Fig. Fruit skin illustrating the lenticular core (red cycle) and pore (blue circle). We refer to the lenticel pore as the opening and the lenticel core as the area of loosely packed complementary cells including those subtending the pore.
(TIF)

103

S2 Fig. Sketch of mango fruit illustrating the different regions of the fruit surface (Stem end, cheek, apex, back and nak) where skin segments were sampled.
(TIF)

S1 File. This is the excel file containing the data in Figs 1–3, 5, 6 and 9 and Tables 1–4.
(XLSX)

Acknowledgments

Author Contributions

Conceptualization: Moritz Knoche.

Data curation: Thomas O. Athoo, Andreas Winkler.

Formal analysis: Thomas O. Athoo, Andreas Winkler.

Funding acquisition: Moritz Knoche.

Investigation: Thomas O. Athoo, Andreas Winkler.

Methodology: Thomas O. Athoo, Andreas Winkler, Moritz Knoche.

Project administration: Willis O. Owino.

Resources: Willis O. Owino, Moritz Knoche.

Supervision: Andreas Winkler, Willis O. Owino, Moritz Knoche.

Visualization: Thomas O. Athoo, Andreas Winkler.

Writing – original draft: Thomas O. Athoo, Andreas Winkler, Moritz Knoche.

Writing – review & editing: Thomas O. Athoo, Willis O. Owino, Moritz Knoche.

References

1. Crang R, Lyons-Sobaski S, Wise R. Plant anatomy: A concept-based approach to the structure of seed plants. Springer. Cham: Springer International Publishing; 2018. https://doi.org/10.1007/978-3-319-77315-5

2. Evert RF. Esau's plant anatomy. 3rd ed. Evert RF, editor. Hoboken, NJ, USA: John Wiley & Sons, Inc.; 2006. https://doi.org/10.1002/0470047380

3. Everett KR, Hallett IC, Rees-George J, Chynoweth RW, Pak HA. Avocado lenticel damage: The cause and the effect on fruit quality. Postharvest Biol Technol. 2008; 48: 383–390. https://doi.org/10.1016/j.postharvbio.2007.09.008

4. Khanal BP, Yiru S, Knoche M. Lenticels and apple fruit transpiration. Postharvest Biol Technol. 2020; 167: 111221. https://doi.org/10.1016/j.postharvbio.2020.111221

5. Lufu R, Ambaw A, Opara UL. Functional characterisation of lenticels, micro-cracks, wax patterns, peel tissue fractions and water loss of pomegranate fruit (cv. Wonderful) during storage. Postharvest Biol Technol. 2021; 178: 111539. https://doi.org/10.1016/j.postharvbio.2021.111539

6. Guan Y, Chang R, Liu G, Wang Y, Wu T, Han Z, et al. Role of lenticels and microcracks on susceptibility of apple fruit to *Botryosphaeria dothidea*. Eur J Plant Pathol. 2015; 143: 317–330. https://doi.org/10.1007/s10658-015-0682-z

104

7. Pruvost O, Luisetti J. Effect of time of inoculation with *Xanthomonas campestris pv. mangiferaeindicae* on mango fruits susceptibility epiphytic survival of *X. c. pv. mangiferaeindicae* on mango fruits in relation to disease development. J Phytopathol. 1991; 133: 139–151. https://doi.org/10.1111/j.1439-0434.1991.tb00147.x

8. Bezuidenhout JLJ, Robbertse PJ, Kaiser C. Anatomical investigation of lenticel development and subsequent discolouration of 'Tommy Atkins' and 'Keitt' mango (*Mangifera indica L.*) fruit. J Hortic Sci Biotechnol. 2005; 80: 18–22. https://doi.org/10.1080/14620316.2005.11511884

9. Du Plooy W, Combrinck S, Botha B, van der Merwe C, Regnier T. Development of discolouration in mango lenticels. Acta Hortic. 2009; 820: 665–672. https://doi.org/10.17660/ActaHortic.2009.820.82

10. Du Plooy W, Merwe C van der, Korsten L. Differences in the surface structures of three mango cultivars and the effect of kaolin on these structures. South African Mango Grow Assoc Res J. 2004; 24: 29–36.

11. Athoo TO, Winkler A, Knoche M. Russeting in 'Apple' mango: Triggers and mechanisms. Plants. 2020; 9: 898. https://doi.org/10.3390/plants9070898 PMID: 32708628

12. Rymbai H, Srivastav M, Sharma RR, Singh SK. Lenticels on mango fruit: Origin, development, discoloration and prevention of their discoloration. Sci Hortic (Amsterdam). 2012; 135: 164–170. https://doi.org/10.1016/j.scienta.2011.11.018

13. Tamjinda B, Siriphanich J, Nobuchi T. Anatomy of lenticels and the occurrence of their discolouration in mangoes (*Mangifera indica* cv. Namdokmai). Agriculture and Natural Resources. 1992. pp. 57–64.

14. Sinha S. Studies in the diseases of *Mangifera Indica* Linn. V. The structure and development of lenticels in the mango Fruits. J Indian Bot Soc. 1945; 24: 118–127.

15. AFA Horticultural Crops. 2019–2020 validated horticulture report. In: Agriculture and Food Authority (AFA) [Internet]. Nairobi; 2020 [cited 10 Sep 2022] pp. 1–61. Available: http://horticulture.agricultureauthority.go.ke/index.php/statistics/reports

16. Athoo TO, Winkler A, Owino WO, Knoche M. Surface moisture induces microcracks and increases water vapor permeance of fruit skins of mango cv. Apple. Horticulturae. 2022; 8: 545. https://doi.org/10.3390/horticulturae8060545

17. Karnovsky MJ. A formaldehyde-glutaraldehyde fixative of high osmolality for use in electron microscopy. J Cell Biol. 1965; 27: 137A–138A.

18. Athoo TO, Khanal BP, Knoche M. Low cuticle deposition rate in 'Apple' mango increases elastic strain, weakens the cuticle and increases russet. PLoS One. 2021; 16: 1–19. https://doi.org/10.1371/journal.pone.0258521 PMID: 34644345

19. Paull RE, Duarte O. Tropical Fruits. 2nd ed. Atherton J, editor. CAB International. Oxfordshire: CAB International; 2011.

20. Griesbach J. Mango growing in Kenya. Nyamu AM, Simons T, editors. Nairobi: World Agroforestry Centre (ICRAF); 2003.

21. Khanal BP, Imoro Y, Chen YH, Straube J, Knoche M. Surface moisture increases microcracking and water vapour permeance of apple fruit skin. Plant Biol. 2020; 1–9. https://doi.org/10.1111/plb.13178 PMID: 32881348

22. Peschel S, Knoche M. Characterization of microcracks in the cuticle of developing sweet cherry fruit. J Am Soc Hortic Sci. 2005; 130: 487–495. https://doi.org/10.21273/JASHS.130.4.487

23. Lai X, Khanal BP, Knoche M. Mismatch between cuticle deposition and area expansion in fruit skins allows potentially catastrophic buildup of elastic strain. Planta. 2016; 244: 1145–1156. https://doi.org/10.1007/s00425-016-2572-9 PMID: 27469168

24. Orgell WH. The isolation of plant cuticle with pectic enzymes. Plant Physiol. 1955; 30: 78–80. https://doi.org/10.1104/pp.30.1.78 PMID: 16654733

25. Yamada Y, Wittwer SH, Bukovac MJ. Penetration of ions through isolated cuticles. Plant Physiol. 1964; 39: 28–32. https://doi.org/10.1104/pp.39.1.28 PMID: 16655874

26. Knoche M, Lang A. Ongoing growth challenges fruit skin integrity. CRC Crit Rev Plant Sci. 2017; 36: 190–215. https://doi.org/10.1080/07352689.2017.1369333

27. Ruess F, Stösser R. Über "Öffnungen" in der Schale von Apfelfrüchten und ihren Verschluss. Erwerbsobstbau. 1993; 35: 148–152.

28. Lai PH, Gwanpua SG, Bailey DG, Heyes JA, East AR. Skin topography changes during kiwifruit development. Acta Hortic. 2018; 1218: 427–434. https://doi.org/10.17660/ActaHortic.2018.1218.59

29. Skene DS. The distribution of growth and cell division in the fruit of Cox's Orange Pippin. Ann Bot. 1966; 30: 493–512. https://doi.org/10.1093/oxfordjournals.aob.a084092

30. Bally IS. Changes in the cuticular surface during the development of mango (*Mangifera indica* L.) cv. Kensington Pride. Sci Hortic (Amsterdam). 1999; 79: 13–22. https://doi.org/10.1016/S0304-4238(98)00159-9

105

31. Durić G, Mićić N, Pasalić B. Lenticels as pomological characteristic of apple and pear fruits. Acta Hortic. 2015; 1099: 771–775. https://doi.org/10.17660/ActaHortic.2015.1099.97

32. Knoche M, Peschel S. Water on the surface aggravates microscopic cracking of the sweet cherry fruit cuticle. J Am Soc Hortic Sci. 2006; 131: 192–200. https://doi.org/10.21273/jashs.131.2.192

33. Khanal BP, Knoche M. Mechanical properties of cuticles and their primary determinants. J Exp Bot. 2017; 68: 5351–5367. https://doi.org/10.1093/jxb/erx265 PMID: 28992090

34. Edelmann HG, Neinhuis C, Bargel H. Influence of hydration and temperature on the rheological properties of plant cuticles and their impact on plant organ integrity. J Plant Growth Regul. 2005; 24: 116–126. https://doi.org/10.1007/s00344-004-0015-5

35. Brown K, Considine J. Physical aspects of fruit growth. Plant Physiol. 1982; 69: 585–590. https://doi.org/10.1104/pp.69.3.585 PMID: 16662254

36. Considine JA. Physical aspects of fruit growth: Cuticular fracture and fracture patterns in relation to fruit structure in *Vitis Vinifera*. J Hortic Sci. 1982; 57: 79–91. https://doi.org/10.1080/00221589.1982.11515027

37. Chen YH, Straube J, Khanal BP, Knoche M, Debener T. Russeting in apple is initiated after exposure to moisture ends—i. Histological evidence. Plants. 2020; 9: 1–18. https://doi.org/10.3390/plants9101293 PMID: 33008020

38. Chen Y, Straube J, Khanal BP, Zeisler-Diehl V, Suresh K, Schreiber L, et al. Apple fruit periderms (russeting) induced by wounding or by moisture have the same histologies, chemistries and gene expressions. PLoS One. 2022; 17: e0274733. https://doi.org/10.1371/journal.pone.0274733 PMID: 36174078

39. Straube J, Chen Y-sH, Khanal BP, Shumbusho A, Zeisler-Diehl V, Suresh K, et al. Russeting in apple is initiated after exposure to moisture ends: Molecular and biochemical evidence. Plants. 2020; 10: 65. https://doi.org/10.3390/plants10010065 PMID: 33396789

40. Winkler A, Athoo T, Knoche M. Russeting of fruits: Etiology and management. Horticulturae. 2022; 8: 231. https://doi.org/10.3390/horticulturae8030231

41. Meyer A. A study of the skin structure of Golden Delicious apples. Am Soc Hortic Sci. 1944; 45: 105–110.

42. Mathooko FM, Kahangi EM, Runkua JM, Onyango CA, Owino WO. Preharvest mango (*Mangifera indica* L. 'Apple') fruit bagging controls lenticel discolouration and improves postharvest quality. Acta Hortic. 2011; 906: 55–62. https://doi.org/10.17660/ActaHortic.2011.906.7

106

3.6 Bagging prevents russeting and decreases postharvest mass loss of mango fruit cv. 'Apple'

In preparation for "Postharvest Biology and Technology Journal"

Authors:

Thomas O. Athoo (**TOA**)[1], Denis Yegon (**DY**)[2], Willis O. Owino (**WOO**)[2] and Moritz Knoche (**MK**)[1]

Author affiliation:

1 Institute of Horticultural Production Systems, Fruit Science Section, Leibniz University Hannover, Herrenhäuser Straße 2, 30419 Hannover, Germany

2 School of Food and Nutritional Sciences (SOFNUS), Jomo Kenyatta University of Agriculture and Technology, P.O. Box 62 000, Nairobi 00200, Kenya

Author Contributions:

Conceptualization, M.K. and T.O.A.; funding acquisition, M.K. and W.O.O.; investigation, T.O.A. and D.Y.; methodology, T.O.A., D.Y., W.O.O. and M.K.; formal analysis, T.O.A., D.Y.; supervision, M.K. and W.O.O.; visualization, T.O.A.; writing—original draft, T.O.A., D.Y. and M.K.; writing -review and editing, T.O.A., D.Y., W.O.O. and M.K.

Bagging prevents russeting and decreases postharvest water loss of mango fruit cv. 'Apple'

Thomas O. Athoo[1], Denis Yegon[2], Willis O. Owino[2], and Moritz Knoche*[1]

[1] Institute for Horticultural Production Systems, Leibniz-University Hannover, Herrenhäuser Straße 2, 30419 Hannover, Germany

[2] School of Food and Nutritional Sciences (SOFNUS), Jomo Kenyatta University of Agriculture and Technology, P.O. Box 62 000 – 00200 Nairobi, Kenya.

*Corresponding author

E-mail: moritz.knoche@obst.uni-hannover.de (MK)

Highlights

- Bagging increased fruit size and decreased cuticle thickness
- Bagging did not change background color, soluble solids or total acidity
- Bagging decreased anthocyanin content and blush area of the fruit surface
- Bagging reduced cuticular microcracking, russeting and postharvest water loss

1   **Abstract**

2

3   In Kenya, the mango (*Mangifera indica* L) cultivar 'Apple' is commercially

4   important but it often suffers excessive russeting, which both compromises its

5   appearance and impairs its postharvest performance. Together, these effects

6   seriously reduce its market potential. Exposure to surface moisture is implicated in

7   russeting of cv. 'Apple' mango.

8   The objective was to establish the effect of bagging on russeting. Developing fruit

9   were bagged at the onset of the exponential growth phase, using brown paper bags

10   (Blue star®). Un-bagged fruit served as controls. The brown paper bags were

11   selected because of their high permeance to water vapor.

12   At harvest maturity, bagged fruit were larger, less russeted and had smaller lenticels

13   than un-bagged control fruit. Staining with aqueous acridine orange in conjunction

14   with fluorescence microscopy revealed numerous microcracks and larger lenticels

15   on un-bagged control fruit but these were not evident on bagged fruit.

16   Postharvest mass loss (principally water loss) of bagged fruit was lower than of un-

17   bagged control fruit. In the un-bagged control fruit, the skin's water permeance

18   increased as the russeted surface area increased ($r2 = 0.88$ **). Fruit skins were less

19   permeable to water vapor than the brown paper bags. The brown paper bags

20   contributed not more than 4.2 to 9.1% of the total in-series diffusion resistance of

21   skin + bag.

22   The masses of isolated cuticular membranes, and of dewaxed cuticular membranes,

23   and of wax per unit surface area were higher for un-bagged control fruit than for

24   bagged fruit.

25   Bagged fruit were also greener and showed less blush. There was little difference

26   in skin carotenoid content between bagged and un-bagged control fruit, but skin

27   anthocyanin content was lower in bagged fruit. The rates of respiration and ethylene

28   evolution of bagged fruit were lower than those of un-bagged control fruit. There

29   were no differences between bagged and un-bagged control fruit in their
30   organoleptic and nutritional properties including titratable acidity, total soluble
31   sugars, sucrose, glucose, fructose, vitamin C and calcium content.

32   In conclusion, bagging decreased russeting and increased postharvest performance
33   of fruit of mango cv. 'Apple'.

34

35   *Keywords:*

36   Bagging, quality, russeting, lenticel, cuticle, skin permeance

1. Introduction

The mango cultivar 'Apple' is important in Kenya, where it is grown widely because of its excellent taste and textural properties. However, 'Apple' mango suffers from russeting. As a consequence, its appearance and postharvest performance are compromised. Russeted fruit is excluded from export to high-end markets, so russeting severely limits the market potential of this cultivar.

Russeting in 'Apple' mango occurs particularly in fruit from highland regions that are subject to extended periods of surface wetness (Athoo et al., 2020). To induce russeting for experimental purposes, deliberate exposure to surface wetness works well, especially during periods of most rapid growth (Athoo et al., 2022).

In botanical terms, 'russeting' refers to formation of a periderm and this is often triggered by rupture of the cuticle which in turn can be caused either by mechanical wounding or by microscopic cracking ('microcracking') (Faust and Shear, 1972; Winkler et al., 2022). As a consequence, a phellogen forms that divides and, to the outside, produces stacks of cork cells, the so called phellem (Evert, 2006). The cell walls of the phellem are impregnated with lignin and suberin (Legay et al., 2015) making them more waterproof and, so, partially restoring the barrier function previously exercised by the cuticle. The suberin is responsible for the brownish appearance of a russeted fruit surface and the irregular arrangement of the phellem cells for its dullness. Russeting is not unique to mango cv. 'Apple' but also occurs in a wide range of other fruit species including apple (*Malus domestica* Borkh.), pear (*Pyrus communis* L.), plum (*Prunus domestica* L.) and others (Faust and Shear, 1972; Skene, 1982; Michailides, 1991; Cohen et al., 2019; Shi et al., 2019; Winkler et al., 2022).

It is now well established that moisture on the fruit surface triggers microcracking of the strained cuticle in mango cv. 'Apple' (Athoo et al., 2022) and also in apples (Knoche and Grimm, 2008; Khanal et al., 2020), sweet cherries (Knoche and Peschel, 2006), and grapes (Becker and Knoche, 2012). The fruit cuticle is strained as a result of ongoing expansion growth. This stretches it as the underlying epidermal cells divide and extend (Knoche and Lang, 2017; Si et al., 2021). It has been shown that exposure to surface moisture alters the

66 rheological properties of the cuticle in such a way as to increase the likelihood of failure

67 (Edelmann et al., 2005; Khanal and Knoche, 2014, 2017). In 'Apple' mango, russeting is

68 initiated close to lenticels (Athoo et al., 2020). These structures are stiffer than the general

69 fruit surface and so serve to focus the growth stresses on the lenticel and its immediate

70 vicinity (Brown and Considine, 1982; Considine, 1982). This fits with the observation that

71 the lenticels in an area of moisture-exposed fruit skin are markedly larger than those in a

72 similar but un-exposed area (Athoo et al., 2023).

73 At present, there are no agronomic strategies for russeting prevention or mitigation in

74 mango cv. 'Apple'. Due to the known role of surface moisture in exacerbating russeting, it

75 is hypothesized that bagging of fruit at the beginning of the period of most rapid surface

76 expansion growth will shorten the duration of surface wetness or even prevent it entirely.

77 This being the case, cuticular microcracking will be reduced or prevented and thus

78 russeting. Comparable effects have been reported for pear (Amarante et al., 2002; Lin et

79 al., 2008) and *Malus* apples (Tukey, 1969; Moon et al., 2016; Yuan et al., 2019). Bagging

80 reduced lenticel discoloration in mango cv. 'Apple' (Mathooko et al., 2011).

81 The objective of this study is to determine the effect of bagging developing fruit of mango

82 cv. 'Apple' on russeting and postharvest performance.

83

2.   Materials and methods

2.1. Plant Materials

Fruit of mango (*Mangifera indica* L.) cv 'Apple' grafted on seedling rootstocks was
obtained from commercial orchards located in Kaiti (1°45'S, 37°28'E) and Kambirwa
(0°44'S, 37°12'E), Kenya. Unless otherwise specified, fruit were harvested at commercial
maturity based on raised shoulders and fullness of the cheeks and freedom from visual
defects. Fruit were examined within 48 h of harvest.

2.2. Experiments

2.2.1   Selecting the bags

We investigated the water vapor permeance and light absorption characteristics of a brown
paper bag (Blue star; King Plastic Industries, Nairobi, Kenya), a waxed white paper bag
(Majimaji; King Plastic Industries) and a single layered white paper bag with clamping
wire (G-26; Kobayashi Bag Manufacturing Company, Lida, Japan). We will refer to these
as 'brown paper bag', 'waxy white paper bag' and 'white paper bag', respectively (See
supplementary Fig. S1 for illustration).

To determine the permeance of the bags to water vapor, paper discs (15 mm in diameter)
were punched from the bags and mounted in custom made stainless steel diffusion cells
(Geyer and Schönherr, 1988; Knoche et al., 2000) using high-vacuum grease. The gap
between the lid and the bottom of the diffusion cell was sealed using clear transparent
adhesive tape (Tesa Film®; Tesa-Werke Offenburg, Offenburg, Germany). Deionized
water was injected into the cells through an orifice in the lower part using a disposable
syringe and the orifice subsequently tape sealed. The cells were turned upside down and
left overnight to equilibrate under ambient conditions. The cells were then placed upside
down in a sealed polyethylene (PE) box containing dry silica gel, such that the exposed
bag surface in the diffusion cell faced the silica gel. The diffusion cells were weighed at 2-
h intervals for up to 8 h. The rate of water loss (F, g h^{-1}) was calculated from the slope of
a linear regression fitted through a plot of diffusion cell mass (g) against time (h). The

112 average r^2 was usually better than 0.99. The permeance (P, m s^{-1}) of the bag was then
113 calculated using equation 1 (Nobel, 2020).

114 $$P = \frac{F}{A \times \Delta C}$$ (Equation 1)

115 In this equation, A is the exposed area of the diffusion cell (3.85 x 10^{-5} m^2) and ΔC the
116 difference in water vapor concentration between the water vapor saturated atmosphere
117 inside the diffusion cell (20.59 g m^{-3} at 23 °C) and the dry environment inside the PE box
118 (approximately 0 g m^{-3} at 23 °C) (Nobel, 2020). The resistance (R; s m^{-1}) was calculated
119 as the inverse of permeance. The number of replicates was 20 per bag.

120 The light absorbance of the bags was determined by photometry. A piece of the bag was
121 mounted on the surface of a semi-micro UV cuvette (Brand 759150; Brand GmbH + CO
122 KG, Wertheim, Germany). Absorbance was recorded in 2 nm steps between 220 and 850
123 nm using a spectrophotometer (Specord 210; Analytik Jena GmbH, Jena, Germany). An
124 empty cuvette without a bag sample served as control.

125 The photosynthetic active radiation (PAR) absorbed by the bags was measured in full
126 sunlight using a LI-250 light meter fitted with a quantum sensor (LI-COR Biosciences
127 GmbH, Bad Homburg, Germany). The sensor was either left uncovered to face the sun
128 (control) or covered by a single layer of the bagging material. The PAR absorbance of the
129 bags was expressed as a percent fraction of the PAR reading by the uncovered light sensor.
130 The number of replicates was three.

131 Based on its water vapor permeance and the product availability (see below), the brown
132 paper bag was selected for subsequent experimentation.

133 Fruit were bagged at 59 days after full bloom (DAFB) at Kambirwa and at 60 DAFB at
134 Kaiti. This timing corresponded to the onset of the exponential growth phase at the two
135 sites. The open end of the bag was tied to the peduncle using a fine wire. A small hole (1
136 cm^2) was cut at the bottom of the bag to drain away any free water that may have entered
137 the bag along the peduncle. The bags were left attached to the fruit until maturity; un-
138 bagged fruit served as controls.

139

2.2.2   Developmental time course in fruit growth and cuticle deposition

141   The developmental time course of change in fruit mass, surface area and cuticle deposition

142   was established. Fruit mass was determined by weighing (TX420L; Shimadzu Corporation,

143   Kyoto, Japan). Fruit length and the two orthogonal diameters recorded at the equatorial

144   plane were measured using a digital caliper (CD-20PKX; Mitutoyo, Kawasaki/Kanagawa,

145   Japan). Fruit surface area was calculated from the measured dimensions assuming a

146   spherical shape. An earlier study established that the calculated and measured surface areas

147   using excised peels are closely related: $Calculated\ area\ (spheroid) = 0.93 +$

148   $1.18\ (\pm0.04) \times measured\ peel\ area, r^2 = 0.98\ **$ (Athoo et al., 2021). A sigmoid

149   regression curve was fitted through a plot of fruit surface area against time. The growth

150   rate ($cm^2\ d^{-1}$) was calculated as the first derivative of the model. The number of individual

151   fruit replicates was 30.

152   To quantify cuticle deposition, skin segments (ES) were excised from the cheek using a

153   biopsy punch (8 mm diameter; Kai Europe, Solingen, Germany). The ES were incubated

154   in 50 mM citric acid buffer solution containing cellulase (5 mL L^{-1}; Cellubrix L;

155   Novozymes A/S), pectinase (90 mL L^{-1}; Panzym Super E flüssig; Novozymes A/S,

156   Krogshoejvej, Bagsvaerd, Denmark) and 30 mM sodium azide to prevent bacterial growth

157   (Orgell, 1955). The pH was adjusted to pH 4.0 using NaOH. The solution was refreshed

158   periodically until the cuticle separated from the adhering tissues. The isolated cuticles were

159   cleaned using a soft, camel hair brush. Following thorough rinsing with deionized water,

160   the cuticular membranes (CM) were dried overnight at 40 $^{\circ}$C and then weighed (CPA2P;

161   Sartorius AG, Göttingen, Germany). The CM were Soxhlet extracted for 2 h to remove

162   cuticular wax using a chloroform:methanol mix (1:1 v:v CHCl$_3$:MeOH). The dewaxed CM

163   (DCM) were dried overnight at 40 °C and then re-weighed (CPA2P; Sartorius). The masses

164   per unit area of the CM, DCM and wax were calculated. The number of CMs processed at

165   each sampling time was 20.

166

167   *2.2.3   Fresh mass and russeting*

168 Mature fruit were harvested at 117 DAFB at Kaiti and at 126 DAFB at Kambirwa. Fresh

169 mass was recorded (TX420L, Shimadzu). Russeting was quantified using a discontinuous

170 five-step rating scheme (Athoo et al., 2020). The ratings were: score 0 = 0% of the fruit

171 surface area russeted, score 1 = 1–10% of the surface area russeted, score 2 = 11–25% of

172 the area russeted, score 3 = 26–50% of the area russeted and score 4 = >51% of the area

173 russeted. An earlier study had established that these rating scores were closely correlated

174 to russeted surface area as measured by digital photography and image analysis.

175 $Russeted\ area\ (rating\ score) = \sqrt{(0.23(\pm0.01) \times measured\ area\ (\%)}, r^2 =$

176 $0.96^{***})$ (Athoo et al., 2020). The number of individual fruit replicates was 135 for Kaiti

177 and 193 for Kambirwa.

178

179 *2.2.4   Lenticel size*

180 The effect of bagging on lenticel size was determined at maturity. Briefly, ES were excised

181 from the fruit cheek using a biopsy punch (8 mm diameter; Kai Europe, Solingen,

182 Germany). The ES were viewed under a stereo microscope (MZ10F; Leica Microsystems,

183 Wetzlar, Germany) and photographed (Camera DFC7000T; Leica Microsystems). The

184 core area and the pore area of each lenticel were quantified by image analysis (ImageJ

185 1.53P; National Health Institute, Bethesda, MD, USA). Here, we refer to the entire

186 subepidermal lenticel as the 'core' and the open, cracked area of the lenticel as the 'pore'.

187 The number of individual fruit replicates was 25.

188

189 *2.2.5   Microcracking of the cuticle*

190 To study the effect of bagging on formation of microscopic cuticular cracks (microcracks),

191 bagged and un-bagged control fruit were dipped in 0.1% aqueous acridine orange solution

192 for 10 min (Peschel and Knoche, 2005). Aqueous acridine orange penetrates the epidermal

193 layer through a microcrack in the cuticle surface but not through the intact cuticle.

194 Following rinsing with distilled water, the fruit surface was inspected for microcracks

195 under a stereo microscope (MZ10F; Leica Microsystems) in brightfield and fluorescing

196   light (GFP LP filter, 480–440 nm excitation, ≥510 nm emission wavelength). Calibrated

197   images were taken with a digital camera (Camera DFC7000T; Leica Microsystems). The

198   number of individual fruit replicates was five.

199

200   *2.2.6   Postharvest water loss*

201   The effect of bagging on postharvest water loss was investigated. Bagged and un-bagged

202   control fruit were rated individually for russeting. Fruit mass, and orthogonal dimensions

203   were determined and the fruit surface area calculated.

204   The time course of transpiration was established on a whole-fruit basis. Transpiration was

205   restricted to the skin by sealing the stem end using a fast-curing silicone rubber (Dow

206   Corning SE 9186; Dow Corning Corp, Midland, MI, USA). After a minimum curing period

207   of 20 min, fruit were placed in a polyethylene (PE) box containing a saturated solution of

208   NaCl (relative humidity 75%) (Wexler, 1995). Under these conditions the difference in

209   water vapor concentration across the fruit skin was 4.67 g m^{-2} (Wexler, 1995). Fruit were

210   weighed individually every 24 h for up to 96 h. The rate of water loss, the permeance and

211   the resistance were calculated as described above. The number of individual fruit

212   replications was 20.

213   From the permeance estimates of the bag, of the russeted and the un-russeted fruit skins,

214   the relative contributions of the bag to total resistance (bag + skin) were calculated using a

215   'resistors-in-series' model according to the following equations (Nobel, 2020):

216                  $R = \dfrac{1}{P}$ and   (Equation 2)

217                  $R_{tot} = R_{bag} + R_{skin}$ (Equation 3)

218   In this equation resistance (R; s m^{-1}) equals the inverse of the permeance (P; m s^{-1}) and

219   total resistance of bag plus skin (R $_{tot}$) equals the some of the resistance of the bag (R $_{bag}$)

220   plus that of the skin (R $_{skin}$) in analogy to resistors arranged in series in an electrical circuit

221   (Nobel, 2020).

222

223 *2.2.7   Peel color*

224   Peel color was quantified in the CIE LAB 1976 (L*, a*, b*) color space using a

225   spectrophotometer (CM-23D, 8 mm orifice; Konica Minolta, Osaka, Japan; software:

226   SpectraMagic™ NX Professional/Lite v 3.3). A total of four fruit were measured, making

227   four measurements per fruit. Hue angles were calculated from the a* and b* values

228   according to McGuire (1992).

229

230   *2.2.8   Carotenoids and anthocyanins*

231   Whole fruit were peeled and the peel stored at -18 °C until use. Following thawing,

232   adhering flesh was removed from the peel by gentle scraping, to leave just the epidermis

233   and hypodermis. The peel was then chopped into small fragments. To quantify carotenoids,

234   a sample of 3 g of peel was ground in 10 mL acetone in a mortar. The resulting acetone

235   extract was then transferred to a 50 mL volumetric flask. The peel was extracted several

236   times until the extracts were colorless. The extracts were combined and brought up to 50

237   mL volume using acetone. Petroleum ether (30 mL) was added to a separation funnel

238   followed by the acetone extract. Distilled water was then added to remove the acetone. The

239   procedure was repeated three times, the extracts were combined and brought up to 50 mL

240   volume by adding petroleum ether. Absorbance of the extract was determined at 450 nm

241   using a UV-Vis spectrophotometer (UV-1800 spectrophotometer, Shimadzu) (Heinonen,

242   1990; Rodriguez-Amaya and Kimura, 2004). Carotenoid content was calculated from

243   equation 4 (Rodriguez-Amaya and Kimura, 2004).

244   $$Carotenoids = \frac{A \times V \times 10^4}{AC \times Sample\ weight} x\ 100 \qquad \text{(Equation 4)}$$

245   In this equation A is the absorbance of the extract read at 450 nm, V (ml) the volume of

246   the extract and *AC*, the absorbance coefficient of β-carotene in petroleum ether (Rodriguez-

247   Amaya and Kimura, 2004). Results are given on a fresh weight basis. The number of

248   individual fruit replicates was three.

249   Anthocyanins were determined using the pH differential method (Lee et al., 2005). Briefly,

250   3 g of peel was ground in a mortar, then extracted in 10 mL of methanol for 72 h on a

251 shaker, in the dark. The extract was divided into two aliquots. The first was buffered in 25

252 mM KCl buffer at pH 1.0. The second was buffered in 400 mM Na-acetate buffer at pH

253 4.5. The pH was adjusted to 1.0 or 4.5 using HCl. Solutions were filtered (filter paper grade

254 1; cut-off pore size 11 µm) to remove any particulate matter (turbidity). Absorbance of the

255 filtrate was measured at 520 and 700 nm within 20-50 min of preparation of the extracts

256 using a spectrophotometer (UV-1800; Shimadzu). The anthocyanin pigment concentration

257 was calculated as cyanidin-3-glucoside equivalents using equation 5 (Lee et al., 2005).

258 $$Anthocyanin \ = \ \frac{A \times MW \times DF \times 10^3}{\varepsilon \times l}$$ (Equation 5)

259 and

260 $$A = \left(A_{520}^{ph1} - A_{700}^{ph1}\right) - \left(A_{520}^{ph4.5} - A_{700}^{ph4.5}\right)$$

261 In this equation A is the differential absorbance of the buffered extracts at pH 1.0 and 520

262 nm (A_{520}^{pH1}), pH 1.0 and 700 nm (A_{700}^{pH1}), at pH 4.5 and 520 nm ($A_{520}^{pH4.5}$) and at pH 4.5 and

263 700 nm ($A_{700}^{pH4.5}$) , MW the molar mass of cyanide-3-glucoside (449.2 g mol^{-1}), DF is the

264 dilution factor, ε the molar extinction co-efficient (26900 L mol^{-1} cm^{-1}) of cyanidin-3-

265 glucoside and l is the path length of the beam through the extract (cm) (Lee et al., 2005).

266 Results are given on a fresh weight basis. The number of individual fruit replicates was

267 three.

268

269 *2.2.9 Respiration and ethylene synthesis*

270 Rates of respiration and ethylene synthesis were determined during shelf life at ≈25 °C for

271 up to 15 d after harvest (DAH) with three to six individual fruit replicates.

272 The rate of respiration was estimated as the rate of CO_2 production per unit fruit mass. Fruit

273 were individually incubated in gastight plastic jars (volume 2 L) for 1-1.5 h at ambient

274 temperature (23-25 °C). A gas sample (1 mL) was drawn from the headspace using a

275 gastight syringe and injected into a gas chromatograph. The CO_2 concentration was

276 determined using a GC (GC-8A; Shimadzu) equipped with a Porapack Q column and a

277 thermal conductivity detector. The injector temperature was 150 °C, the column and

278   detector temperatures 120 °C. Helium was used as a carrier gas at a flow rate of 20 mL

279   min^{-1}. The rate of CO_2 production was calculated from the increase in CO_2 concentration

280   in the incubation jar during the incubation interval.

281   Ethylene was quantified on a GC (GC-9A; Shimadzu) equipped with an activated alumina

282   column (Sepax HP- Amino, 5 µL; Sepax™ Technologies Inc, Newark, DE, USA) and a

283   flame ionization detector. The injector temperature was set at 220 °C, the column

284   temperature at 150 °C, and the detector temperature at 240 °C. The carrier gas was N_2 at a

285   flow rate of 50 mL min^{-1}. Hydrogen and synthetic air were used as the burning gas for the

286   detector at flow rates of 50 mL min^{-1} for H_2 and 5 mL min^{-1} for synthetic air. The rate of

287   ethylene evolution was calculated from the increase in ethylene concentration during the

288   incubation interval. Calibration curves were established to calculate CO_2 and ethylene

289   concentrations from the respective peak areas.

290

291   *2.2.10 Firmness*

292   Fruit firmness was measured during shelf life, before and after peeling, using a rheometer

293   (probe diameter 5 mm) (Compac-100; Sun scientific, Tokyo, Japan). The distance of travel

294   was set at 20 mm and the travel speed adjusted to 600 mm min^{-1}. The number of individual

295   fruit replicates ranged from 12 to 16.

296

297   *2.2.11 Total acidity and total soluble solids*

298   Pulp samples were prepared from fruit flesh using a blender. Briefly, 5 g of pulp was added

299   to 50 mL of distilled water. The indicator phenolphthalein (40-60 µl) was added to a 10

300   mL aliquot of the solution and titrated against 0.1 N NaOH until color change. From the

301   volume of base consumed, total acidity (TA) was calculated as the amount (g) of citric acid

302   equivalent per 100 g of fruit according to ISO 750:1998 (factor for citric acid 0.064; (ISO,

303   1998)). Total soluble solids (TSS) of the pulp were determined using a digital refractometer

304   (PAL-S; Atago, Tokyo, Japan). The number of individual fruit replicates was three.

305

306 *2.2.12 Sucrose, glucose and fructose*

307 The sucrose, glucose and fructose contents of the pulp of bagged and un-bagged control

308 fruit was quantified during shelf life using the method described by Li (1996). About 2 g

309 of pulp was boiled in 20 mL of ethanol for 1 h inside a reflux condenser (SF-6, Sanshin

310 Industrial Co, Kobe, Japan). Upon cooling, the extract was filtered, and the solvent

311 evaporated from the filtrate in a rotary evaporator (DGU-20A 5R, Shimadzu). The residue

312 was taken up in 5 mL of acetonitrile and water (1:1 v/v). An aliquot (1 mL) of supernatant

313 was micro-filtered (Nylon syringe filter, pore size 0.45 µm; Membrane Solutions LLC,

314 Auburn, WA, USA) into a vial. Sucrose, glucose and fructose were analyzed by high-

315 performance liquid chromatography (HPLC) (LC-20AD; Shimadzu) fitted with a

316 refractive index (RI) detector (model 10A, Shimadzu). The HPLC was run using the

317 following settings: oven temperature 30°C, injection volume 20 µL, mobile phase

318 acetonitrile:water (75:25) at 0.5-1.0 mL min^{-1}. Calibration lines were established using

319 standards. Total sugars were calculated as the sum of glucose, fructose and sucrose. Results

320 are given on a fresh weight basis. The number of individual fruit replicates was three.

321

322 *2.2.13 Vitamin C*

323 The change in ascorbic acid content during shelf life was analyzed by HPLC using the

324 procedure of Vikram et al. (2005). About 2.5 g of pulp was weighed and dissolved in 0.8%

325 metaphosphoric acid. The solution was then centrifuged for 10 min at 11739 g and 40 °C.

326 The supernatant was filtered through a 0.45 µm filter (Nylon syringe filter; Membrane

327 Solutions LLC). A 20 µL sample of the filtrate was injected into an HPLC (Model 20A;

328 Shimadzu) equipped with a UV- Vis detector (SPD 20A; Shimadzu). Absorbance was read

329 at 266 nm. The settings of the HPLC were: oven temperature 30 °C and flow rate of 1.2

330 mL min^{-1}. Metaphosphoric acid (0.8%) was also used as a solvent. This acid was vacuum-

331 filtered (Rocker-Chemker 300; Rocker Scientific, New Taipei, Taiwan) and degassed using

332 an ultrasonic cleaner (GT sonic 3; GT International (HK) Group, Shenzhen, China).

333 A calibration curve was prepared using ascorbic acid standards in a concentration range

334 from 20 to 100 mg mL^{-1}. Results are given on a fresh weight basis. The number of

335 individual fruit replicates was three.

336

337 *2.2.14 Calcium*

338 Flesh calcium content was analyzed by spectrophotometry following dry ashing (Isaac and

339 Johnson, 1975; Osborne and Voogt, 1978). Briefly, 5 g of pulp was placed into a pre-

340 weighed crucible. The sample was ashed in a muffle furnace (Advantec KL-420; Electric

341 Muffle furnace, Toyo Seisakusho Kaisha, Chiba, Japan). The temperature of the furnace

342 was increased to 550 °C, held constant for 1 h and decreased thereafter. The ash was taken

343 up in 20 mL of 0.5N HNO$_3$, then heated to 80-90 °C on a hotplate for 5 min and brought

344 up to 100 mL volume using 0.5N HNO$_3$. The solution was filtered (filter paper grade 1;

345 cut-off pore size 11 µm). Lanthanum chloride (0.5 mL at 0.12 M) and distilled water (9

346 mL) were added to 0.5 mL of sample to make the test solution. Absorbance of the solution

347 was read using an atomic absorption spectrophotometer (Model AA-7000 with ASC-7000

348 Auto sampler; Shimadzu). A calibration curve was prepared prior to analysis. The number

349 of individual fruit replicates was three.

350

351 *2.3. Data analysis, statistics and terminology*

352 Data are presented as means ± se. Where not visible, the standard error bars were smaller

353 than the data symbols. Data were analyzed using analysis of variance with R statistical

354 software (R version 4.0.3; R Foundation for Statistical Computing, Vienna, Austria).

355 Means were separated using Turkey's studentized range test (α = 0.05). Regression

356 analyses were conducted in R and Sigma Plot (version 12.5; Systat Software, San Jose,

357 CA, USA). We refer to microcracking of the cuticle that is associated with lenticels as

358 'lenticel cracking'.

359

360 **3. Results**

361   Cumulative water vapor loss through the different bagging materials increased linearly

362   with time indicating a constant permeance to water vapor (Supplementary Fig. S2). The

363   resistance to water vapor movement was highest for the waxy white paper bag and

364   markedly lower for both the white paper bag and the brown paper bag (Table 1).

365   The waxy white paper bag and the white paper bag absorbed less PAR compared with the

366   brown paper bag (supplementary Table S1, supplementary Fig. S3). Most of the absorption

367   occurred in the range of short wavelengths. There was less absorption at wave lengths

368   above 400 nm with little difference between the different bags (supplementary Fig. S3).

369   Based on these data and local availability, the brown paper bags were selected for the

370   bagging experiment.

371

372   Fruit mass and surface area increased sigmoidally with time. Surface area growth rate

373   reached at maximum of 4.2 cm^2 d^{-1} at 94 DAFB (Figure 1A). The mass of CM, DCM and

374   wax per unit surface area all increased during development. The CM, DCM and wax mass

375   were significantly higher for the un-bagged control fruit than for the bagged fruit (Figure

376   1B-D).

377

378   At maturity, the mass of the bagged fruit exceeded that of the un-bagged control fruit (Table

379   2). Fruit grown in Kaiti, was consistently larger than that from Kambirwa (Table 2).

380

381   Bagged fruit were less russeted and had markedly smaller lenticels than those of un-bagged

382   control fruit (Figure 2, Tables 3,4). There were no significant differences in russeting or in

383   lenticel size between fruit from Kaiti or Kambirwa (Tables 3,4).

384

385   Fluorescence microscopy revealed numerous dye infiltrated microcracks and lenticels on

386   the surface of un-bagged control fruit, but there were no microcracks or infiltrated lenticels

387   on the surface of bagged fruit (Figure 2).

388   Simulated postharvest mass loss from bagged and un-bagged control fruit increased

389   linearly with time (Figure 3 A,B). Mass loss (mostly water loss) and skin permeance were

390   about 1.8-fold higher in un-bagged control fruit, compared with bagged fruit (Figure 3B).

391   For control fruit, permeance was positively and linearly related to the area of russeted

392   surface ($r^2 = 0.88**$) (Figure 3C). Compared to the bag material, fruit skins were markedly

393   less permeable and thus had a much higher resistance to water vapor loss than either the

394   brown paper bag or the white paper bag (Table 1). Consequently, the brown paper bag and

395   the white paper bag contributed to at most only 4.2 and 4.5%, respectively, to the maximum

396   total resistance. This result contrasted with that with the waxy white bag, which contributed

397   up to 94.4% to the maximum total resistance (Table 1). Thus, the relative humidity inside

398   the bags would have been markedly higher in the waxy white bags as compared with either

399   the brown paper bag or the white paper bag.

400

401   Bagged fruit were greener and had less blush on the surface than un-bagged control fruit,

402   as indexed by a lower hue angle (Figure 4). The hue angle decreased during ripening,

403   indicating de-greening. This change was in part due to an increase in total carotenoids as

404   the fruit ripened (Figure 4B,C). There was no significant difference in carotene content

405   between bagged and un-bagged control fruit. Anthocyanin content increased with ripening

406   and was consistently higher for un-bagged control fruit compared with bagged fruit (Figure

407   4D).

408   The rates of respiration, as indexed by CO_2 release, increased with ripening, peaked at

409   about 10 days after harvest (DAH) and then declined. The respiration rate of un-bagged

410   control fruit exceeded that of bagged fruit by up to 1.4-fold. A similar pattern was observed

411   for ethylene synthesis, which increased with time, reached a peak at about 4 and 8 DAH in

412   the un-bagged control and the bagged fruit, respectively, and decreased thereafter. The

413   peak in ethylene synthesis was about two-fold higher in the un-bagged control than in the

414   bagged fruit (Figure 5).

415

416   Titratable acidity (TA) decreased, whereas total soluble sugars (TSS) increased with shelf

417   life. There was no difference between un-bagged control and bagged fruit (Figure 6). There

418   were also no differences in firmness, sucrose, glucose, fructose, vitamin C or calcium

419   contents between bagged and un-bagged control fruit (Supplementary Figs. S4-6 and

420   supplementary Table S2).

4. Discussion

Bagging improved pre- and postharvest performances of 'Apple' mango by i) reducing lenticel cracking and russeting, and ii) by decreasing postharvest water loss.

4.1 Bagged fruit had less lenticel cracking and was less russeted than un-bagged control fruit.

Bagging reduced lenticel cracking as indexed by lenticels with smaller core and pore areas. In 'Apple' mango, lenticels are sites where russet is initiated (Athoo et al., 2020). From a materials science point of view, lenticels represent stiffer areas in a larger area of less-stiff (more extensible) cuticle. Lenticels therefore tend to concentrate stresses (Brown and Considine, 1982; Considine, 1982) and this increases susceptibility to cracking (Athoo et al., 2021, 2023). In mango cv. 'Apple', the lenticels would seem to be far more susceptible to microcracking than those in other mango cultivars (Athoo et al., 2021, 2023). Our finding that lenticels serve as initiation points for microcracking is consistent with reports for other fruitcrop species including for pear (Amarante et al., 2002; Lin et al., 2008) and pomegranate (Sarkomi et al., 2019). Our bagged 'Apple' mango fruit also suffered less microcracking around the lenticels and also less microcracking on the intervening fruit surface, so the fruit were almost russet-free.

The reduction in lenticel cracking and the decrease in russeting in the bagged fruit would seem to be the result of reduced surface wetness as surface wetness has previously been shown to trigger microcracking and russeting in 'Apple' mango (Athoo et al., 2022) and *Malus* apple (Tukey, 1969; Knoche and Grimm, 2008; Chen et al., 2020; Khanal et al., 2020). Exposure to surface moisture alters the rheological properties of the strained cuticle and this increases the likelihood of failure (Khanal and Knoche, 2017). It is interesting that the CM, DCM and wax mass were all significantly lower in the bagged fruit, compared with the un-bagged controls. The bags probably acted as a transpiration barrier due to the resistance of the bag itself arranged in series to the cuticle plus the boundary layer resistance of the still air inside the bag. Both factors reduce transpiration. Lower

450   transpiration inside the bags may have suppressed CM deposition (Skoss, 1955; Hao et al.,

451   2011). Suppressed CM deposition has been reported in shaded compared to sun-exposed

452   mango (Léchaudel et al., 2013) or grape berries (Rosenquist and Morrison, 1989). Our

453   findings are consistent with effects of bagging on CM deposition in pear and persimmon

454   (Amarante et al., 2002; Katagiri et al., 2003).

455

456   *4.2 Bagging improved postharvest performance in 'Apple' mango.*

457   Bagging improved postharvest performance. First, bagged fruit maintained a more intact

458   cuticle barrier that is effective in restricting transpiration and in pathogen defense. In fact,

459   bagging has been reported to reduce the incidence of anthracnose and stem end rot in 'Nam

460   Dok Mai #4' and 'Keitt' mango (Hofman et al., 1997; Chonhenchob et al., 2011). Similar

461   findings have been reported for pear, pummelo, papaya etc. (Kitagawa et al., 1992;

462   Issarakraisila, 2018; Gao et al., 2022). Second, bagged fruit had lower postharvest water

463   loss than un-bagged control fruit. Non-russeted fruit surfaces have a lower permeance than

464   russeted surfaces in 'Apple' mango (Athoo et al., 2020) and *Malus* apple (Khanal et al.,

465   2019). Third, bagging increased peel quality in 'Apple' mango and many other fruitcrops

466   e.g., pear (Amarante et al., 2002). Fruit appearance was improved by reduced russeting.

467   The ground color was not affected by bagging, as indicated by the hue angle of the peel.

468   There was no change in carotenoid content, this is in line with earlier studies in other mango

469   cultivars (Hofman et al., 1997; Ding and Syakirah, 2010). That bagging decreased the red

470   blush and reduced anthocyanin content compared with un-bagged control fruit, is not

471   unique to 'Apple' mango, but has also been reported for bagged *Malus* apple (Chen et al.,

472   2012), peach (Jia et al., 2005), and pomegranate (Sarkomi et al., 2019). See Ali et al. (2021)

473   for a detailed review. Reduced anthocyanin content is common in shaded compared to sun-

474   exposed fruit (Bible and Singha, 1993; Karanjalker et al., 2018). This is due to the reduced

475   exposure to UV light in bagged fruit – UV is required for anthocyanin synthesis (Ubi et al.,

476   2006; Karanjalker et al., 2018). We show that brown paper bags absorb light in the UV

477   wavelength range.

478   We detected no adverse effects of bagging on fruit quality. Organic acids, sugars, vitamin

479   C and Ca were largely unaffected. The lack of an effect of bagging on Ca content is

480   consistent with earlier studies in 'Kensington Pride', 'Sensation' and 'Keitt' mango

481   (Hofman et al., 1997; Joyce et al., 1997; Hofman et al., 1999).

482

483 **5. Conclusion**

484 The results presented here indicate that preharvest bagging is a commercially attractive

485 procedure able to reduce russeting in 'Apple' mango. In addition, bagged fruit were larger

486 and suffered lower postharvest weight loss than un-bagged control fruit. Except for a

487 reduced blush, there were no adverse effects of bagging on fruit quality or nutritional value.

488 Thus, pre-harvest bagging offers an opportunity for small-scale farmers to produce high

489 quality 'Apple' mangos suitable for discerning export markets.

490

491

CRediT author statement

Thomas O. Athoo: Conceptualization, Methodology, Supervision, Investigation, Validation, Formal analysis, Data curation, Writing -original draft, Writing - review & editing. **Denis Yegon**: Investigation, Formal analysis. **Willis O. Owino**: Supervision, Writing - review & editing. **Moritz Knoche**: Conceptualization, Funding acquisition, Methodology, Supervision, Project administration, Writing - original draft, Writing - review & editing.

Declaration of competing interest

The authors report no competing financial or personal interests that could have inappropriately influenced this work.

Funding

Data availability statement

The data that support the findings of this study will be made available upon request.

Acknowledgements

Bibliography

Ali, M.M., Anwar, R., Yousef, A.F., Li, B., Luvisi, A., De Bellis, L., Aprile, A., Chen, F., 2021. Influence of bagging on the development and quality of fruits. Plants 10, 358. https://doi.org/10.3390/plants10020358

Amarante, C., Banks, N.H., Max, S., 2002. Preharvest bagging improves packout and fruit quality of pears (Pyrus communis). New Zeal. J. Crop Hortic. Sci. 30, 93–98. https://doi.org/10.1080/01140671.2002.9514203

Athoo, T.O., Winkler, A., Knoche, M., 2020. Russeting in 'Apple' mango: Triggers and mechanisms. Plants 9, 898. https://doi.org/10.3390/plants9070898

Athoo, T.O., Khanal, B.P., Knoche, M., 2021. Low cuticle deposition rate in 'Apple' mango increases elastic strain, weakens the cuticle and increases russet. PLoS One 16, 1–19. https://doi.org/10.1371/journal.pone.0258521

Athoo, T.O., Winkler, A, Owino, W.O., Knoche, M., 2022. Surface moisture induces microcracks and increases water vapor permeance of fruit skins of mango cv. Apple. Horticulturae 8, 545. https://doi.org/10.3390/horticulturae8060545

Athoo, T.; Winkler, A.; Owino, W.O.; Knoche, M., 2023. Lenticels are sites of initiation of microcracking and russeting in 'Apple' mango. PlosOne 18, e0291129. https://doi.org/10.1371/journal.pone.0291129

Hofman, P.J, Joyce, D.C., Beasley, D.R., 1999. Effect of preharvest bagging and of embryo abortion on calcium levels in 'Kensington Pride' mango fruit. Austr. J. Exp. Agric. 39, 345-349. https://doi.org/10.1071/EA98060

Becker, T., Knoche, M., 2012. Water induces microcracks in the grape berry cuticle. Vitis - J. Grapevine Res. 51, 141–142. https://doi.org/10.15488/3851

Bible, B.B., Singha, S., 1993. Canopy position influences CIELAB coordinates of peach color. HortScience 28, 992–993. https://doi.org/10.21273/HORTSCI.28.10.992

Brown, K., Considine, J., 1982. Physical aspects of fruit growth: Stress distribution around lenticels. Plant Physiol. 69, 585–590. https://doi.org/10.1104/pp.69.3.585

541 Chen, C.S., Zhang, D., Wang, Y.Q., Li, P.M., Ma, F.W., 2012. Effects of fruit bagging on
542   the contents of phenolic compounds in the peel and flesh of 'Golden Delicious', 'Red
543   Delicious', and 'Royal Gala' apples. Sci. Hortic. 142, 68–73.
544   https://doi.org/10.1016/J.SCIENTA.2012.05.001

545 Chen, Y.H., Straube, J., Khanal, B.P., Knoche, M., Debener, T., 2020. Russeting in apple
546   is initiated after exposure to moisture ends—i. Histological evidence. Plants 9, 1–18.
547   https://doi.org/10.3390/plants9101293

548 Chonhenchob, V., Kamhangwong, D., Kruenate, J., Khongrat, K., Tangchantra, N.,
549   Wichai, U., Singh, S.P., 2011. Preharvest bagging with wavelength-selective materials
550   enhances development and quality of mango (*Mangifera indica* L.) cv. Nam Dok Mai
551   #4. J. Sci. Food Agric. 91, 664–671. https://doi.org/10.1002/jsfa.4231

552 Cohen, H., Dong, Y., Szymanski, J., Lashbrooke, J., Meir, S., Almekias-Siegl, E., Zeisler-
553   Diehl, V.V., Schreiber, L., Aharoni, A., 2019. A multilevel study of melon fruit
554   reticulation provides insight into skin ligno-suberization hallmarks. Plant Physiol. 179,
555   1486–1501. https://doi.org/10.1104/pp.18.01158

556 Considine, J.A., 1982. Physical aspects of fruit growth: Cuticular fracture and fracture
557   patterns in relation to fruit structure in *Vitis Vinifera*. J. Hortic. Sci. 57, 79–91.
558   https://doi.org/10.1080/00221589.1982.11515027

559 Ding, P., Syakirah, M.N., 2010. Influence of fruit bagging on postharvest quality of
560   "Harumanis" mango (*Mangifera indica* L.). Acta Hortic. 877, 169–174.
561   https://doi.org/10.17660/ActaHortic.2010.877.15

562 Edelmann, H.G., Neinhuis, C., Bargel, H., 2005. Influence of hydration and temperature
563   on the rheological properties of plant cuticles and their impact on plant organ integrity.
564   J. Plant Growth Regul. 24, 116–126. https://doi.org/10.1007/s00344-004-0015-5

565 Evert, R.F., 2006. Esau's plant anatomy, 3rd ed. John Wiley & Sons, Inc., Hoboken, NJ,
566   USA. https://doi.org/10.1002/0470047380

567 Faust, M.., Shear, C.B., 1972. Russeting of apples, an interpretive review. HortScience 7,
568   233–235. https://doi.org/10.21273/hortsci.7.3.233

569　Gao, C., Zhang, Y., Li, H., Gao, Q., Cheng, Y., Ogunyemi, S.O., Guan, J., 2022. Fruit
570　　　bagging reduces the postharvest decay and alters the diversity of fruit surface fungal
571　　　community in 'Yali' pear. BMC Microbiol. 22, 239. https://doi.org/10.1186/s12866-
572　　　022-02653-4

573　Geyer, U., Schönherr, J., 1988. In vitro test for effects of surfactants and formulations on
574　　　permeability of plant cuticles, in: Cross, B. and Scher, H.B. (Ed.), Pesticide
575　　　Formulations: Innovations and Developments. Washington, DC, USA, pp. 22–33.
576　　　https://doi.org/10.1021/bk-1988-0371.ch003

577　Hao, Y., Zhao, Q., Liu, Q., Li, W., 2011. Effects of the micro-environment inside fruit bags
578　　　on the structure of fruit peel in "Fuji" apple. Shengtai Xuebao/ Acta Ecol. Sin. 31,
579　　　2831–2836.

580　Heinonen, M.I., 1990. Carotenoids and provitamin A activity of carrot (Daucus carota L.)
581　　　cultivars. J. Agric. Food Chem. 38, 609–612. https://doi.org/10.1021/jf00093a005

582　Hofman, P.J., Smith, L.G., Joyce, D.C., Johnson, G.I., Meiburg, G.F., 1997. Bagging of
583　　　mango (*Mangifera indica* cv. 'Keitt') fruit influences fruit quality and mineral
584　　　composition. Postharvest Biol. Technol. 12, 83-91. https://doi.org/10.1016/S0925-
585　　　5214(97)00039-2

586　Isaac, R.A., Johnson, W.C., 1975. Collaborative study of wet and dry ashing techniques
587　　　for the elemental analysis of plant tissue by atomic absorption spectrophotometry. J.
588　　　AOAC Int. 58, 436–440. https://doi.org/10.1093/jaoac/58.3.436

589　ISO, 1998. ISO 750:1998 Fruit and vegetable products — Determination of titratable
590　　　acidity, 2nd ed. International Organization for Standardization (ISO), Geneva,
591　　　Switzerland.

592　Issarakraisila, M., 2018. Effect of types of bagging materials on growth, quality and
593　　　disease-insect damages in pummelo fruit in tropical humid conditions. Acta Hortic.
594　　　1208, 319–323. https://doi.org/10.17660/ActaHortic.2018.1208.43

Jia, H.J., Araki, A., Okamoto, G., 2005. Influence of fruit bagging on aroma volatiles and skin coloration of "Hakuho" peach (*Prunus persica* Batsch). Postharvest Biol. Technol. 35, 61–68. https://doi.org/10.1016/j.postharvbio.2004.06.004

Joyce, D.C., Beasley, D.R., Shorter, A.J., 1997. Effect of preharvest bagging on fruit calcium levels, and storage and ripening characteristics of 'Sensation' mangoes. Austr. J. Exp. Agric. 37, 383. https://doi.org/10.1071/EA96074

Karanjalker, G.R., Ravishankar, K. V., Shivashankara, K.S., Dinesh, M.R., 2018. Influence of bagging on color, anthocyanin and anthocyanin biosynthetic genes in peel of red colored mango cv. 'Lily.' Erwerbs-Obstbau 60, 281–287. https://doi.org/10.1007/s10341-018-0371-0

Katagiri, T., Satoh, Y., Fukuda, T., Kataoka, I., 2003. Improving marketability of "Fuyu" persimmon fruit by bagging culture. Acta Hortic. 601, 213-217. https://doi.org/10.17660/ActaHortic.2003.601.30

Khanal, B.P., Knoche, M., 2014. Mechanical properties of apple skin are determined by epidermis and hypodermis. J. Am. Soc. Hortic. Sci. 139, 139–147. https://doi.org/10.21273/jashs.139.2.139

Khanal, B.P., Knoche, M., 2017. Mechanical properties of cuticles and their primary determinants. J. Exp. Bot. 68, 5351–5367. https://doi.org/10.1093/jxb/erx265

Khanal, B.P., Ikigu, G.M., Knoche, M., 2019. Russeting partially restores apple skin permeability to water vapour. Planta 249, 849–860. https://doi.org/10.1007/s00425-018-3044-1

Khanal, B.P., Imoro, Y., Chen, Y.H., Straube, J., Knoche, M., 2020. Surface moisture increases microcracking and water vapour permeance of apple fruit skin. Plant Biol. 23,74-82. https://doi.org/10.1111/plb.13178

Kitagawa, H., Manabe, K., Esguerra, E.B., 1992. Bagging of fruit on the tree to control disease. Acta Hortic. 321, 871–875. https://doi.org/10.17660/ActaHortic.1992.321.110

Knoche, M., Peschel, S., Hinz, M., Bukovac, M.J., 2000. Studies on water transport through the sweet cherry fruit surface: Characterizing conductance of the cuticular

623   membrane using pericarp segments. Planta 212, 127-135.

624   https://doi.org/10.1007/s004250000404

625 Knoche, M., Grimm, E., 2008. Surface moisture induces microcracks in the cuticle of

626   "Golden Delicious" apple. HortScience 43, 1929–1931.

627   https://doi.org/10.21273/hortsci.43.6.1929

628 Knoche, M., Peschel, S., 2006. Water on the surface aggravates microscopic cracking of

629   the sweet cherry fruit cuticle. J. Am. Soc. Hortic. Sci. 131, 192–200.

630   https://doi.org/10.21273/jashs.131.2.192

631 Knoche, M., Lang, A., 2017. Ongoing growth challenges fruit skin integrity. CRC. Crit.

632   Rev. Plant Sci. 36, 190–215. https://doi.org/10.1080/07352689.2017.1369333

633 Léchaudel, M., Lopez-Lauri, F., Vidal, V., Sallanon, H., Joas, J., 2013. Response of the

634   physiological parameters of mango fruit (transpiration, water relations and antioxidant

635   system) to its light and temperature environment. J. Plant Physiol. 170, 567–576.

636   https://doi.org/10.1016/J.JPLPH.2012.11.009

637 Lee, J., Durst, R.W., Wrolstad, R.E., Barnes, K.W., Eisele, T., Giusti, M. M., Haché, J.,

638   Hofsommer, H., Koswig, S., Krueger, D.A., Kupina, S., Martin, S. K, Martinsen, B. K,

639   Miller, T.C., Paquette, F., Ryabkova, A., Skrede, G., Trenn, U., Wightman, J.D., 2005.

640   Determination of total monomeric anthocyanin pigment content of fruit juices,

641   beverages, natural colorants, and wines by the pH differential method: Collaborative

642   study. J. AOAC Int. 88, 1269–1278. https://doi.org/10.1093/jaoac/88.5.1269

643 Legay, S., Guerriero, G., Deleruelle, A., Lateur, M., Evers, D., André, C.M., Hausman,

644   J.F., 2015. Apple russeting as seen through the RNA-seq lens: strong alterations in the

645   exocarp cell wall. Plant Mol. Biol. 88, 21–40. https://doi.org/10.1007/s11103-015-

646   0303-4

647 Li, B.W., 1996. Determination of sugars, starches, and total dietary fiber in selected high-

648   consumption foods. J. AOAC Int. 79, 718–723. https://doi.org/10.1093/jaoac/79.3.718

649   Lin, J., Chang, Y., Yan, Z., Li, X., 2008. Effects of bagging on the quality of pear fruit
650   and pesticide residues. Acta Hortic. 772, 315–318.
651   https://doi.org/10.17660/actahortic.2008.772.52

652   Mathooko, F.M., Kahangi, E.M., Runkua, J.M., Onyango, C.A., Owino, W.O., 2011.
653   Preharvest mango (Mangifera indica L. 'Apple') fruit bagging controls lenticel
654   discolouration and improves postharvest quality. Acta Hortic. 906, 55–62.
655   https://doi.org/10.17660/ActaHortic.2011.906.7

656   McGuire, R.G., 1992. Reporting of objective color measurements. HortScience 27, 1254–
657   1255. https://doi.org/10.21273/hortsci.27.12.1254

658   Michailides, T.J., 1991. Russeting and russet scab of prune, an environmentally induced
659   fruit disorder: Symptomatology, induction, and control. Plant Dis. 75, 1114-1123.
660   https://doi.org/10.1094/PD-75-1114

661   Moon, Y.J., Nam, K.W., Kang, I.K., Moon, B.W., 2016. Effects of tree-spray of calcium
662   agent, coating agent, GA_{4+7} + BA and paper bagging on russet prevention and quality
663   of 'Gamhong' apple fruits. Hortic. Sci. Technol. 34, 528-536.
664   https://doi.org/10.12972/kjhst.20160054

665   Nobel, P.S., 2020. Physicochemical and environmental plant physiology, 5th ed. Academic
666   Press, San Diego, California. pp. 617-628. https://doi.org/10.1016/c2018-0-04662-9

667   Orgell, W.H., 1955. The isolation of plant cuticle with pectic enzymes. Plant Physiol. 30,
668   78–80. https://doi.org/10.1104/pp.30.1.78

669   Osborne, D.R., Voogt, P., 1978. The analysis of nutrients in foods. Academic Press Inc,
670   London, pp. x-251.

671   Peschel, S., Knoche, M., 2005. Characterization of microcracks in the cuticle of
672   developing sweet cherry fruit. J. Am. Soc. Hortic. Sci. 130, 487–495.
673   https://doi.org/10.21273/JASHS.130.4.487

674   Rodriguez-Amaya, D.B., Kimura, M., 2004. Handbook for carotenoid analysis.
675   International Food Policy Research Institute (IFPRI), Washington, DC. pp. 1-52.

676   Rosenquist, J.K., Morrison, J.C., 1989. Some factors affecting cuticle and wax

677   accumulation on grape berries. Am. J. Enol. Vitic. 40, 241–244.

678   https://doi.org/10.5344/ajev.1989.40.4.241

679   Sarkomi, F.H., Moradinezhad, F., Khayat, M., 2019. Pre-harvest bagging influences

680   sunburn, cracking and quality of pomegranate fruits. J. Hortic. Postharvest Res. 2, 131–

681   142. https://doi.org/10.22077/jhpr.

682   Shi, C., Qi, B., Wang, X., Shen, L., Luo, J., Zhang, Y., 2019. Proteomic analysis of the

683   key mechanism of exocarp russet pigmentation of semi-russet pear under rainwater

684   condition. Sci. Hortic. 254, 178–186. https://doi.org/10.1016/j.scienta.2019.04.086

685   Si, Y., Khanal, B.P., Schlüter, O.K., Knoche, M., 2021. Direct evidence for a radial

686   gradient in age of the apple fruit cuticle. Front. Plant Sci. 12, 1–12.

687   https://doi.org/10.3389/fpls.2021.730837

688   Skene, D.S., 1982. The development of russet, rough russet and cracks on the fruit of the

689   apple 'Cox's Orange Pippin' during the course of the season. J. Hortic. Sci. 57, 165–

690   174. https://doi.org/10.1080/00221589.1982.11515037

691   Skoss, J.D., 1955. Structure and composition of plant cuticle in relation to environmental

692   factors and permeability. Bot. Gaz. 117, 55–72. https://doi.org/10.1086/335891

693   Tukey, L.D., 1969. Observations on the russeting of apples growing in plastic bags. Proc.

694   Amer. Soc. Hortic. Sci. 74, 30–39.

695   Ubi, B.E., Honda, C., Bessho, H., Kondo, S., Wada, M., Kobayashi, S., Moriguchi, T.,

696   2006. Expression analysis of anthocyanin biosynthetic genes in apple skin: Effect of

697   UV-B and temperature. Plant Sci. 170, 571–578.

698   https://doi.org/10.1016/j.plantsci.2005.10.009

699   Vikram, V.B., Ramesh, M.N., Prapulla, S.G., 2005. Thermal degradation kinetics of

700   nutrients in orange juice heated by electromagnetic and conventional methods. J. Food

701   Eng. 69, 31–40. https://doi.org/10.1016/j.jfoodeng.2004.07.013

702   Wexler, A., 1995. Constant humidity solutions, 76th ed, Handbook of chemistry and

703   physics. CRC Press, Boca Raton, FL.

704   Winkler, A., Athoo, T., Knoche, M., 2022. Russeting of fruits: Etiology and management.

705   Horticulturae 8, 231. https://doi.org/10.3390/horticulturae8030231

706   Yuan, G., Bian, S., Han, X., He, S., Liu, K., Zhang, C., Cong, P., 2019. An integrated

707   transcriptome and proteome analysis reveals new insights into russeting of bagging

708   and non-bagging 'Golden Delicious' apple. Int. J. Mol. Sci. 20, 4462.

709   https://doi.org/10.3390/ijms20184462

710

711

712

Table 1

Resistances and relative contributions of bagging material to total resistance to water vapor loss from bagged cv. 'Apple' mango. The bagging materials were brown paper, waxy white paper and white paper bags. Resistance was calculated as the inverse of permeance (m s^{-1}). Permeance was calculated from the rate of cumulative water loss vs time through samples of the bag materials mounted in diffusion cells (see supplementary Fig. S2). The number of replicates was 20.

Bagging material	Resistance bag (s m^{-1})	Total resistance (Skin +bag)		Contribution of bag to total resistance (%)	
		min	max	min	max
Brown paper bag	181	1995	4320	9.1	4.2
Waxy white paper bag	69341	71156	73480	97.5	94.4
White paper bag	197	2011	4336	9.8	4.5

The minimum (1814 s m^{-1}) and maximum resistances (4139 s m^{-1}) of the fruit skin were calculated as the inverse of the permeances of a non russeted fruit (russet score 0 = 0% russeted area) and a russeted fruit skin (russet score 4 = 50-100% russeted area) from the regression line in Fig. 3.

713

714

715

716

717

718

719

720

721

Table 2

Average (means ± se) fruit mass of bagged and un-bagged control 'Apple' mango. The fruit were bagged at 59 day after full bloom (DAFB) in Kambirwa and at 60 DAFB in Kaiti using brown paper bags. Un-bagged fruit served as controls. The number of replicates was 193 in Kambirwa and 135 in Kaiti.

Treatment	Mass (g)		
	Kaiti	Kambirwa	Mean Treatment
Control	371.7 ± 9.0	313.5 ± 7.0	342.6 ± 5.8 a [y]
Bagged	424.4 ± 8.9	348.8 ± 5.8	386.6 ± 5.4 b
Mean Site	398.0 ± 6.5 b [z]	331.2 ± 4.6 a	

Main effect of treatment [y] and orchard site [z] but not interaction significant following two factorial ANOVA at P≤ 0.05. Mean separation by Tukey's Studentized Range test, P≤ 0.05

722

723

Table 3

Average (mean± se) russeting in bagged and un-bagged control 'Apple' mango from Kaiti and Kambirwa production sites. The fruit were bagged at 59 day after full bloom (DAFB) in Kambirwa and at 60 DAFB in Kaiti using brown paper bags. Un-bagged fruit served as controls. Russeting was quantified using a five-score rating scheme. Score 0 = 0% of the fruit surface area russeted, score 1 = 1–10% russeted area, score 2 = 11-25% russeted area, score 3 = 26-50% russeted area and score 4 = 50-100% russeted area. The number of replicates was 193 in Kambirwa and 135 in Kaiti.

Treatment	Russeting (rating)		
	Kaiti	Kambirwa	Mean $_{Site}$
Control	1.8 ± 0.1 b^z	2.3 ± 0.1 b	2.1 ± 0.1
Bagged	0.2 ± 0.0 a	0.2 ± 0.0 a	0.2 ± 0.0
Mean $_{treatment}$	1.0 ± 0.0	1.3 ± 0.1	

^{z}Interaction treatment x site significant by two factorial ANOVA. Therefore, ANOVA run by sites. Means within the rows followed by the same letter are not significantly different. Mean separation by Tukey studentized range test, $P \leq 0.05$

725

726

727

728

Table 4

Pore (opening) and core (underlying cavity) area of lenticels in bagged and un-bagged control mature 'Apple' mango. The fruit were bagged at 59 days after full bloom (DAFB) in Kambirwa and at 60 DAFB in Kaiti using brown paper bags. Un-bagged fruit served as controls. The number of replicates was 193 in Kambirwa and 135 in Kaiti.

Treatment	Lenticel area (mm^2)			
	Kaiti		Kambirwa	
	Pore area	Core area	Pore area	Core area
Control	0.39 ± 05 b[z]	0.95 ± 0.13 b	0.35 ± 05 b	0.95 ± 0.13 b
Bagged	0.01 ± 00 a	0.05 ± 0.01 a	0.00 ± 00 a	0.04 ± 0.01 a

[z] Main effect treatment significant by two factorial ANOVA. Mean separation according to the Tukey Studentized Range test, $p \leq 0.05$.

729

730

Figure Legends

732

733 **Fig. 1.** Developmental time course of change in fruit mass and surface area (A) and surface
734 area growth rate (A, inset), deposition of the cuticular membrane (CM) (B), the dewaxed
735 CM (DCM) (C) and wax of 'Apple' mango. Vertical arrows indicate the time at which the
736 fruit were bagged at Kambirwa using brown paper bags. Un-bagged fruit served as
737 controls. X-axis scale in days after full bloom (DAFB). Data represent means ± se. The
738 number of replicates was 30 in A, and 20 in B, C, and D.

739

740 **Fig. 2.** Representative images of un-bagged ('Control') (A) and bagged ('Bagged') (B)
741 'Apple' mango at maturity. Microscopic view of fruit surface (C-E) and lenticels (G-J) of
742 un-bagged (C,D,G,H) and bagged (E,F,I,J) 'Apple' mango at harvest. Fruit were viewed
743 under incident bright (C,E,G,I) or under incident fluorescent light to visualize microcracks
744 (D,F,H,J). Areas of the fruit surface were incubated in 0.1 % aqueous acridine orange prior
745 to microscopy. Scale bar is 1 cm (A,B) and 1 mm (C-E). The number of replicates was
746 five.

747

748 **Fig. 3.** Time course of fruit mass loss (A) and change in permeance (B) of mature 'Apple'
749 mango. The fruit were either bagged ('Bagged') or remained un-bagged ('Control') at
750 Kambirwa at 59 days after full bloom. Data represent means ± se. (C) Relationship between
751 the permeance of the fruit skin to water vapor and the portion of the fruit surface area
752 russeted. Russeting was quantified using a five-point scoring scheme. Score $0 = 0\%$ of the
753 fruit surface area russeted, Score $1 = 1–10\%$ russeted area, score $2 = 11\text{-}25\%$ russeted area,
754 score $3 = 26\text{-}50\%$ russeted area and score $4 = 50\text{-}100\%$ russeted area. Data in C represent
755 individual fruits. The number of individual fruit replicates was 15. The regression equation
756 was: $Permeance\ (\times 10^{-4}\ m^{-1}) = 2.22\ (\pm 0.1) + 0.71\ (\pm 0.1) \times russet\ score,\ r^2 =$
757 0.88 **.

758

759   **Fig. 4.** Hue angle (A), carotenoid (B), and anthocyanin content (C) in the skin of un-bagged

760   ('Control') and bagged ('Bagged') 'Apple' mango. Fruit were bagged using brown paper

761   bags at 60 days after full bloom in Kaiti. X-axis scale in days after harvest (DAH). Data

762   represent means ± se of 12 to 16 (A) and 3 (B,C) fruit.

763

764   **Fig. 5.** Rates of respiration and ethylene release from mature bagged ('Bagged') and un-

765   bagged ('Control') 'Apple' mango. The fruit were bagged using brown paper bags at 60

766   days after full bloom in Kaiti. X-axis scale in days after harvest (DAH). Data represent

767   means ± se of three to six fruit.

768

769   **Fig. 6.** Titratable acidity (TA) (A) and total soluble solids (TSS) (B) of the pulp of mature

770   bagged ('Bagged') and un-bagged ('Control') 'Apple' mango. The fruit were bagged using

771   brown paper bags (Blue star®) at 60 days after full bloom at Kaiti. X-axis scale in days

772   after harvest (DAH). Data represent means ± se of 15 fruit.

773

774

775

776   Fig. 1.

A Control

B Bagged
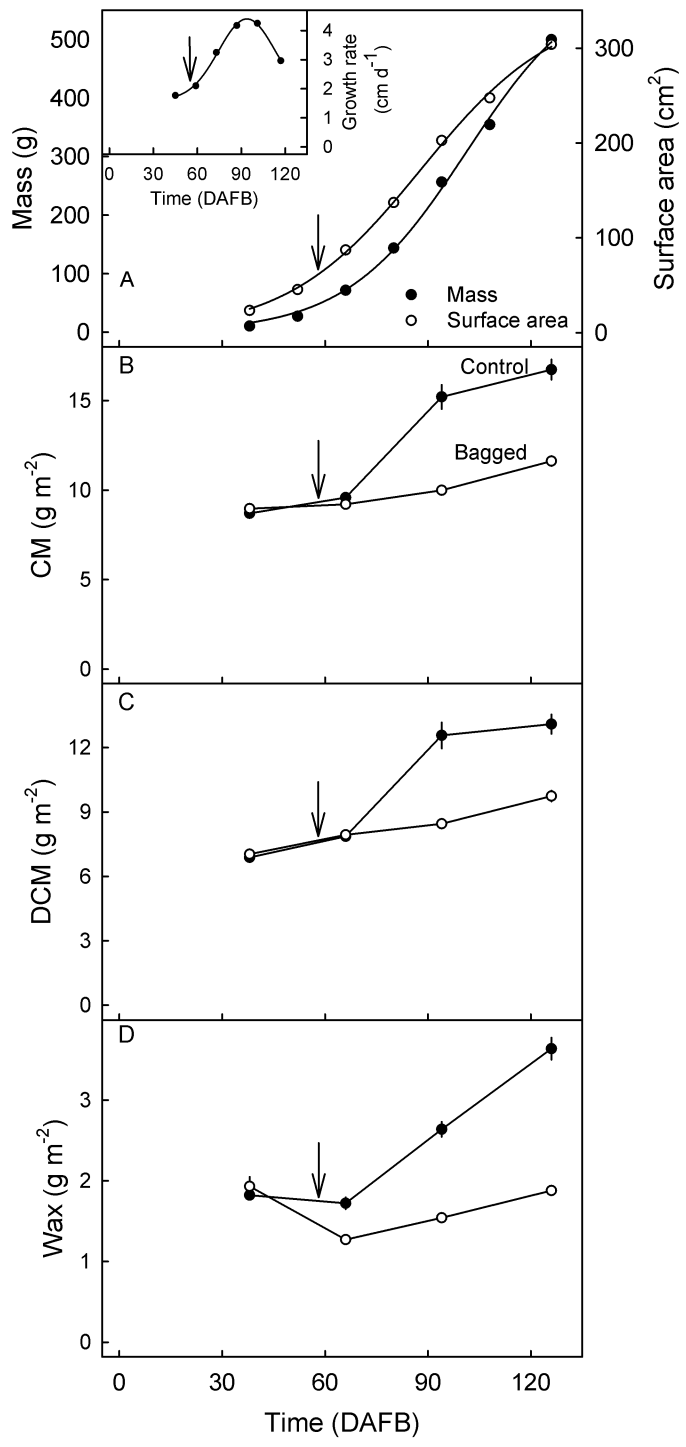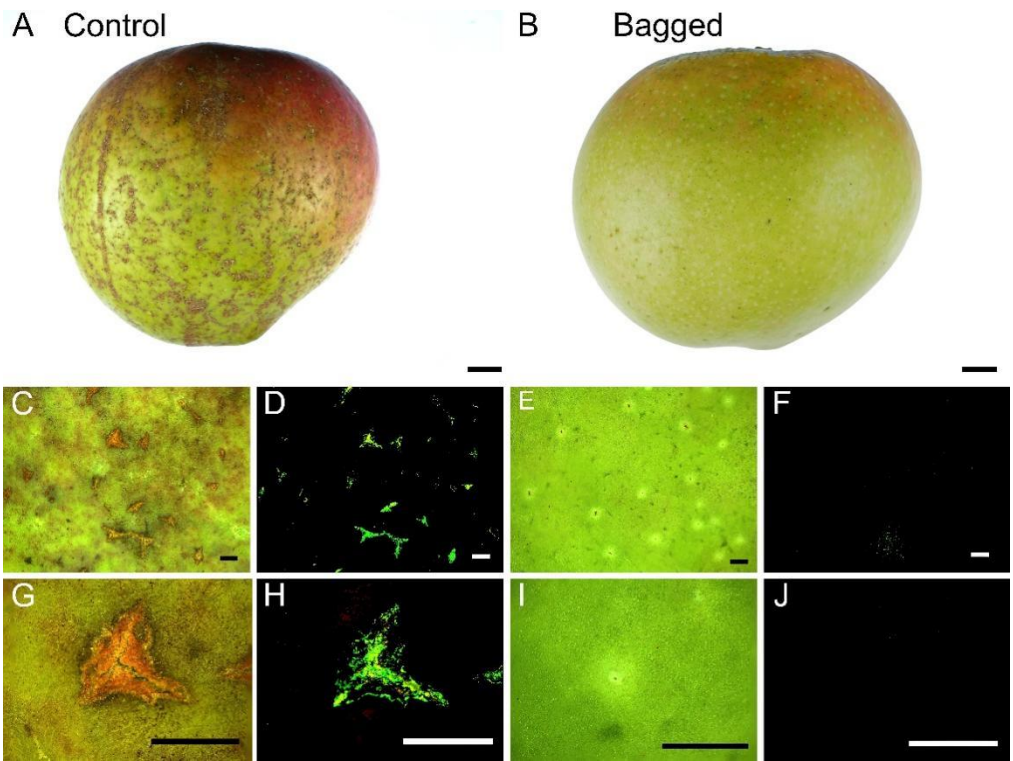
777

778

779   Fig. 2.
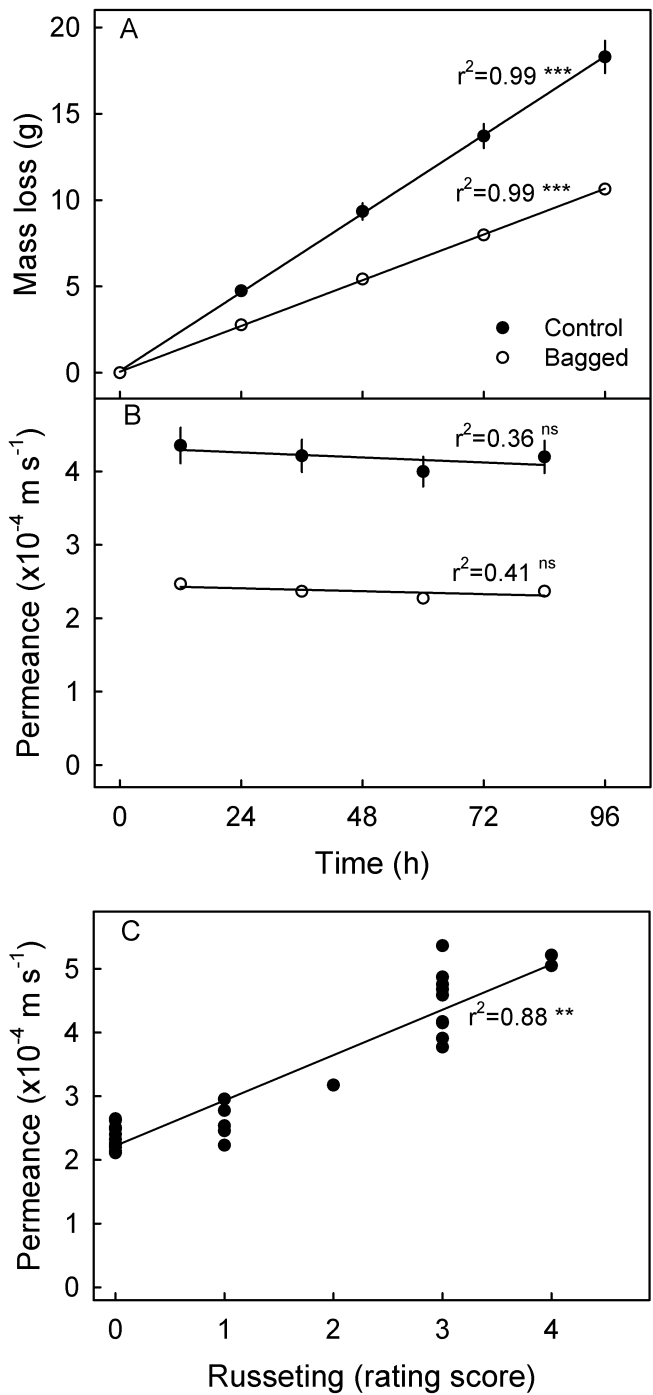
780

781

782   Fig. 3.

783
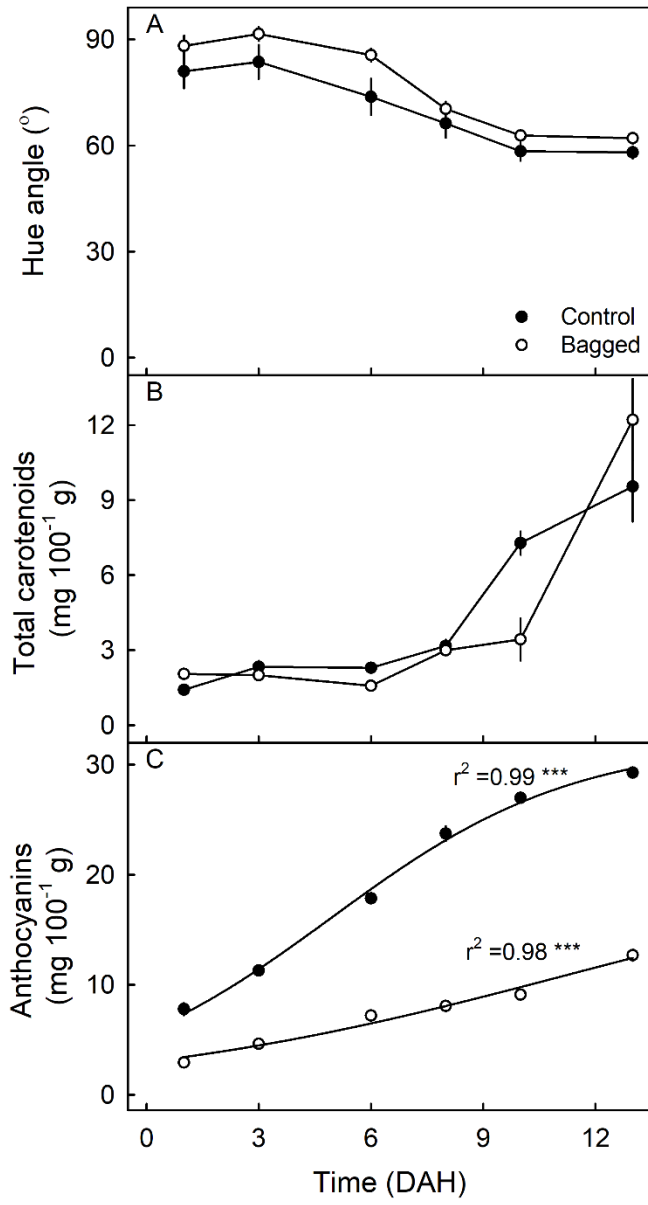
784

785   Fig. 4

786

787

788
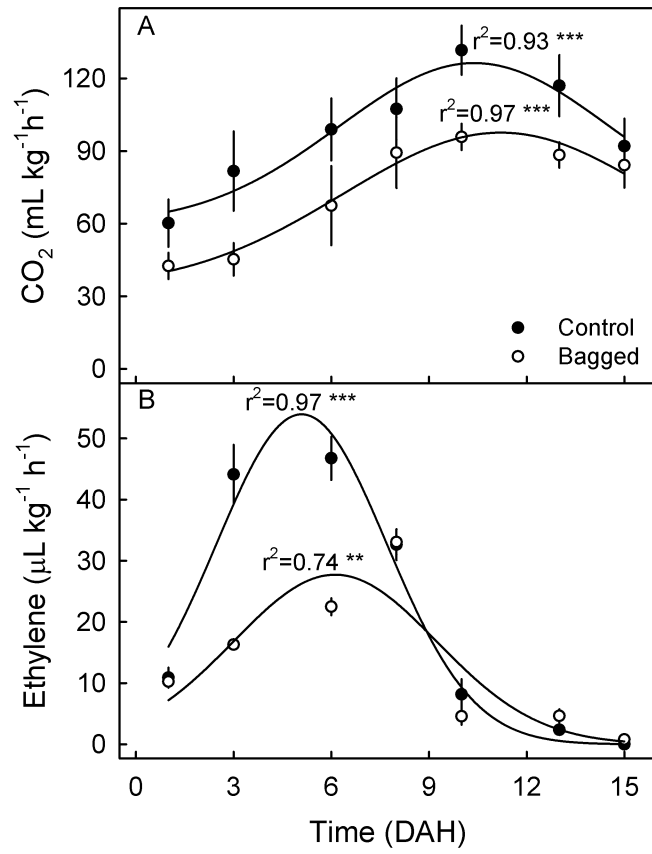
789

790

791   Fig. 5.

792
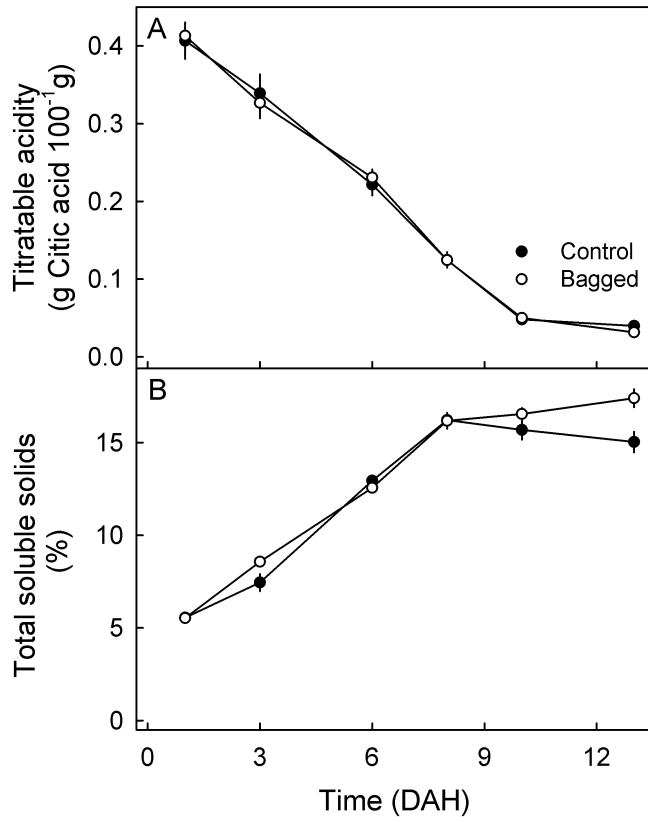
793

794

795   Fig. 6.

796

797

Supplementary material

Supplementary Table S1

Photosynthetically active radiation (PAR) and percentage PAR absorption of the three different bagging materials. Measurements were made on in full sunlight and a bright sky. Control was measurement without any bagging material. The number of replicates was three. Data represent means ± se.

Fruit bag	PAR (μmol s^{-1} m^{-2})	PAR absorbed (%)
None (Control)	2022.7 ± 0.3	0.0
Waxy white paper	1325.7 ± 11.2	34.5
Brown paper	595.7 ± 1.8	70.6
White paper	1416.0 ± 17.6	30.0

Supplementary Table S2

Effect of bagging on the calcium content of the pulp of 'Apple' mango. The fruit were bagged using brown paper bags at 60 days after full bloom at Kaiti. Un-bagged fruit served as controls. Data is represented as means ± se. The number of replicates was nine (three technical reps per fruit and three fruit)

Treatment	Calcium (mg 100 g^{-1})
Un-bagged (control)	25.6 ± 0.5 a
Bagged	25.8 ± 0.7 a

There were no significant differences between treatments at $p \leq 0.05$.

803

804

805

806

807

Supplementary Fig. S1. Photographs of the different bags used in the study. The bags
tested were; white paper bag (Left), Brown paper bags (Middle) and the waxy white paper
bag (Right).

808
809
810

811

812
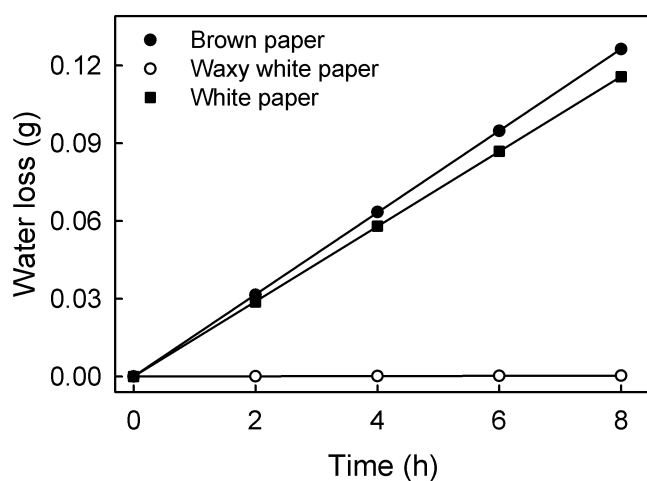
Supplementary Fig. S2. Cumulative water loss through samples of different bagging
materials with time. The patches were mounted inside custom made diffusion cells and

813
814

815   incubated above dry silica inside a polyethylene box. The bags were made of brown paper,

816   waxy white paper and white paper. The number of replicates was 20.

817
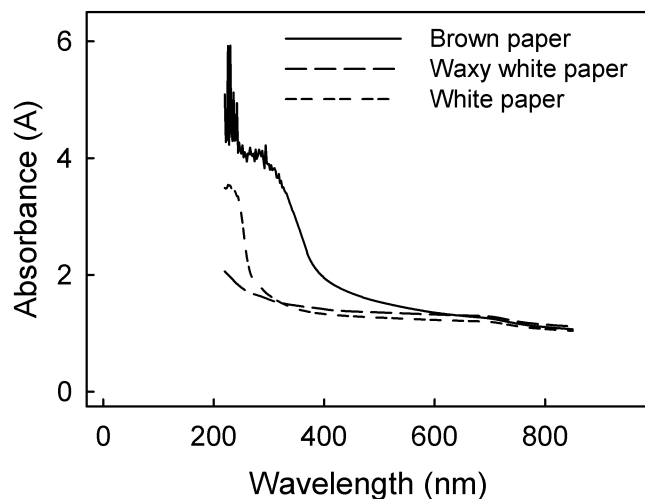
818

819   **Supplementary Fig. S3.** Light absorbed by different bag materials at wavelengths between

820   220-850 nm was measured using a photometer. A single layer of bag material was mounted

821   on a cuvette for the absorbance measurement, an empty cuvette was measured for

822   reference. The bags were made of brown paper or waxy white paper or white paper. The

823   number of individual replicates was three.

824

825

826
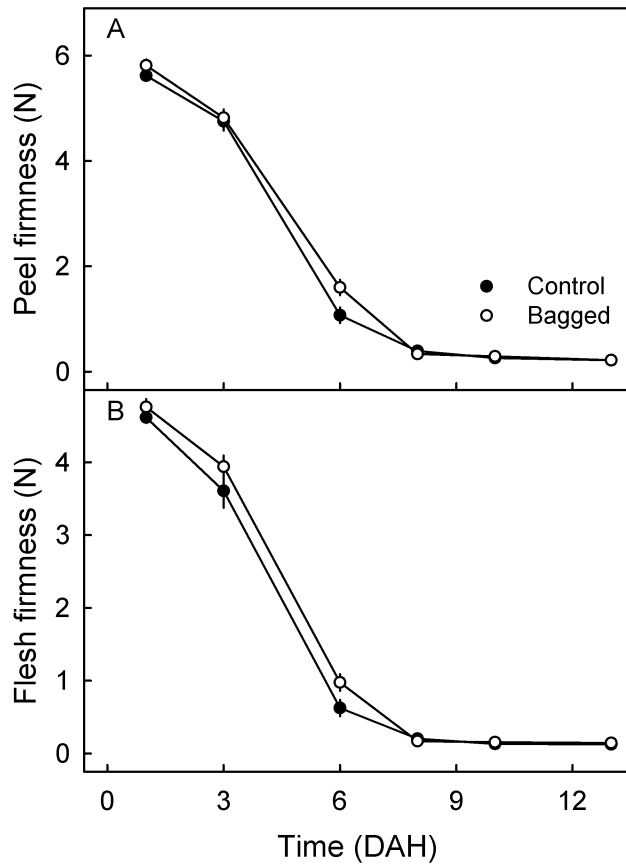
Supplementary Fig. S4. Effect of bagging developing 'Apple' mango fruit on the change in firmness of the pulp, during a two-week shelf life. The fruit had been surrounded by a brown paper bag at 60 days after full bloom at the Kaiti production site. Un-bagged fruit served as controls. The X-axis scale is in days after harvest (DAH). Data are presented as means ± se. The number of individual fruit replicates was 12-16.

832
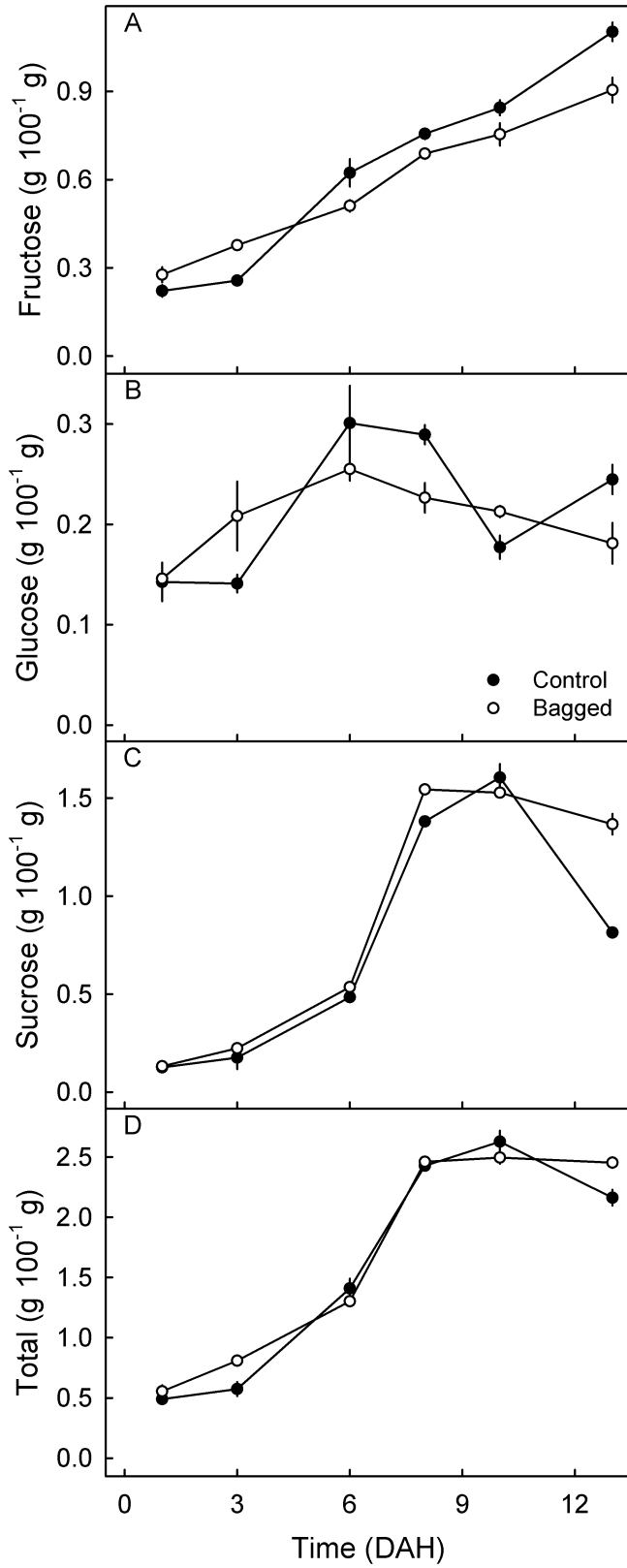
834 **Supplementary Fig. S5**. Effect of bagging developing 'Apple' mango fruit on the change

835 in pulp fructose (A), glucose (B), sucrose (C) and total sugars (D) during a two-week shelf

836 life. The fruit had been surrounded by a brown paper bag at 60 days after full bloom at the

837 Kaiti production site. Un-bagged fruit served as controls. X-axis scale is in days after

838 harvest (DAH). Data are represented as means ± se. The number of individual fruit

839 replicates was three.

840

841
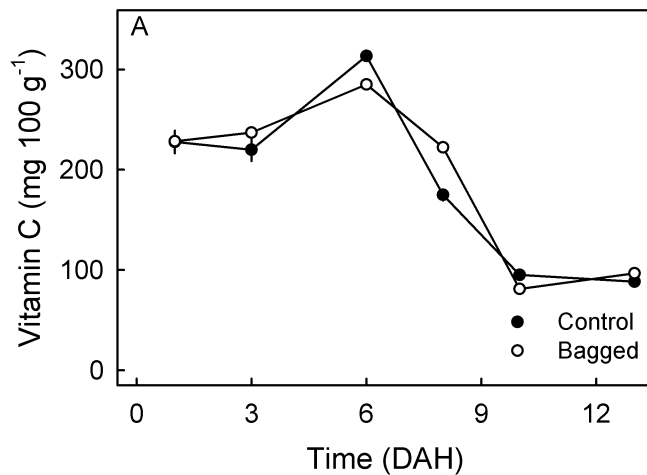
842

843 **Supplementary Fig. S6.** Effect of bagging developing 'Apple' mango fruit on the change

844 in vitamin C content during a two-week shelf life. The fruit had been surrounded by a

845 brown paper bag at 60 days after full bloom at the Kaiti production site. Un-bagged fruit

846 served as controls. X-axis scale is in days after harvest (DAH). Data are represented as

847 means ± se. The number of individual fruit replicates was three.

848

4. General Discussion

The main objectives of this research were to study the mechanistic basis for mango fruit russeting and develop strategies to manage the disorder. The main finding of this thesis shows similar mechanistic basis and prevention strategies between russet disorder of 'Apple' mango and many surface disorders in other fruits such as apples, pear, prune, citrus etc.

Specifically, this study found out that:

1) Fruit russeting generally involves formation of a periderm in response to microcracking of the CM (chapter 3.1)
2) Russeting in 'Apple' mango involves cracking of the fruit surface, formation of periderm beneath the cracks, and that growing conditions conducive for surface wetness exacerbate russeting (see chapter 3.2).
3) Low cuticle deposition and higher growth strains predispose 'Apple' mango to microcracking and subsequently to russeting (see chapter 3.3).
4) Moisture on the fruit surface aggravates microcracking and russet development in 'Apple' mango fruit (see chapter 3.4).
5) Lenticels are sites of initiation of microcracking and of russeting in 'Apple' mango (see chapter 3.5)
6) Preharvest bagging prevents surface wetness thereby improves peel appearance and postharvest performance of 'Apple' mango (see chapter 3.6)

Readers are referred to the respective chapters for a detailed discussion of these specific findings. This section discusses briefly how these results potentially explain mechanistic basis of other fruit surface disorders in many fruits, the consequences of openings on the fruit surface and suggest countermeasures against some of these disorders. These are therefore discussed under the following points:

1. Comparison between russet development of 'Apple' mango and development of other surface disorders in many fruit crops.
2. Consequences of openings on the fruit surface
3. Countermeasures to prevent surface disorders

4.1 Comparison between russet development in 'Apple' mango and development of other fruit surface disorders

Russet formation in 'Apple' mango bears a number of similarities with many surface disorders in other fruit crop species. We found out that growth stress (strain) and surface wetness is essential in its development. Also, russeting of 'Apple' mango uniquely occurred at the lenticels. Similarly, growth stress, surface wetness and openings on the fruit surface triggers the development of many surface disorders in a variety of fruit crops. These openings on fruit surface include stomates, lenticels, trichome scar, wound, micro- and macro-cracks, suture (the carpel juncture in prune fruits), stem and calyx cavities.

Russeting disorder of 'Apple' mango fruit developed in the same manner to that described in *Malus* apple, pear, grapes or prune. Cuticular cracking marked its ontogeny. In our studies, surface expansion and prolonged surface wetness triggered microcrack formation on the cuticle (Athoo et al., 2022, 2021, 2020). These mechanistic basis are similar to those found in *Malus* apple (Chen et al., 2022; Faust and Shear, 1972a, 1972b; Knoche and Grimm, 2008). Just like in *Malus* apple, 'Apple' mango fruit skin was particularly susceptible to water-induced microcracking during the phase of greatest increment in tangential growth (Athoo et al., 2022; Faust and Shear, 1972a; Khanal et al., 2020a). Moisture may have hydrated the cuticle (Edelmann et al., 2005) making it mechanically weaker (Khanal and Knoche, 2017; Matas et al., 2005). Contrary to what is known in other fruit crops, russeting in 'Apple' mango began specifically at the lenticels. 'Apple' mango lenticels enlarged more with growth and when the skin was artificially moistened (Athoo et al., 2023). We suspect higher concentration of stress around the lenticels (Brown and Considine, 1982). Heightened stress coupled by higher moisture uptake at the lenticels therefore caused lenticels to swell and crack (Athoo et al., 2023). Further stress buildup extends these cracks to the epidermis or hypodermis (Meyer, 1944). A signal, potentially caused by elevated O_2 (Lipton, 1967; Wei et al., 2018), is detected in the hypodermis (Legay et al., 2016). The cork cambium (phellogen) divides to initiate phellem and phelloderm below the crack (Bell, 1937; Faust and Shear, 1972a). It is the suberized cells walls of the phellem that gives the brown appearance of a russeted skin (Macnee et al., 2020). Russeting only manifest when these events occur during the earlier phases of fruit development. Late season cuticular failure results into many other surface disorders (O'Hare et al., 1999; Winkler et al., 2014).

Splitting (macrocracking, split-pit, calyx or stem end cracking) of many fruits follow similar mechanism to russeting in 'Apple' mango. Moisture on the surface, rapid fruit expansion or irrigation following periods of water stress are essential (Byers et al., 2019; Claypool et al., 1972; Emmons and Scott, 1997; Joshi et al., 2021; Li and Chen, 2017; Li et al., 2019; Opara et al., 2000). Moisture uptake through the microcracks, wounds, lenticels, trichome scar, calyx-end or stem-end reduce cell : cell adhesion (Schumann et al., 2019). The skin gives way and the fruit splits (Schumann et al., 2019).

'Etch', lenticel discoloration, lenticel breakdown *and* ***skin spot*** *disorders* of fruits manifest at harvest or immediately after fruit removal from cold storage (Bezuidenhout et al., 2005; Curry et al., 2008; O'Hare et al., 1999; Rymbai et al., 2012; Winkler et al., 2014). Pre- and postharvest exposure of fruit to moisture or other surfactants is similarly cited. Similar to russeting of 'Apple' mango, microcracks consequently develop on the CM or on the lenticels. Phenolic compounds accumulate on the outer boundaries of the cell walls below the cracks (Du Plooy et al., 2006), resulting in browning of protoplasts (Grimm et al., 2012; O'Hare et al., 1999). Unlike russeting of 'Apple' mango, periderm formation was avoided.

Pericarp browning of litchi, ***shrivel disorder*** of plums and **maturity bronzing** in banana also follow similar mechanistic basis to russeting of 'Apple' mango. Factors that influenced growth such as moisture triggered these disorders. Microcracks developed on the cuticle following growth stress (Underhill and Critchley, 1992; Underhill and Simons, 1993). Just like in 'Apple' mango, most of the microcracks in shriveled plum cultivars associated with stomata (Knoche and Peschel, 2007). These cracks may extend deeper into the fruit mesocarp (Underhill and Simons, 1993). Under desiccating conditions, localized shrivel occur (Knoche et al., 2019). Susceptible plum cultivars developed shrivel symptoms towards the pedicel end region (Knoche et al., 2019). Interestingly, this region had more microcracks compared to non-shriveled calyx end (Knoche et al., 2015). In litchi, pericarp browning occur when the anthocyanin-containing mesocarp is exposed to desiccating conditions (Holcroft and Mitcham, 1996; Underhill and Critchley, 1992; Underhill and Simons, 1993). The mesocarp disintegrates and anthocyanins leak out (Holcroft and Mitcham, 1996). In banana, solid red-brown necrotic lesions form on the skin (Williams et al., 1990). These lesions are localized to the upper one to two cell layers (Williams et al., 1990).

4.2 Consequences of openings on the fruit surface

Our study revealed reduced skin's barrier function because of openings on the fruit surface. Water loss was enhanced because of cracked lenticels and russeting (chapter 3.6). Histologically, the sub-stomatal or lenticel cavity is filled with a volume of loosely packed cells (Everett et al., 2008; Evert, 2006). Additionally, the hydrophobic cuticle is either intermittent or absent (Ruess and Stösser, 1993). The stem cavity, trichome and stylar scars also act as puddles permitting water to remain attached to the surface for longer time (puddle and pending droplet). This accelerates water uptake or loss. The higher permeance to water loss observed in 'Apple' mango, was consistent with increased cuticular cracking (Athoo et al., 2022). Similar finding for increased permeance to water vapor uptake/loss as a result of microcracks was found in strawberries (Hurtado and Knoche, 2021), *Malus* apple (Maguire et al., 1999) and sweet cherries (Peschel and Knoche, 2005). Cracked fruit cuticles of *Malus* apple were 12 times more permeable to water vapor loss than intact ones (Maguire et al., 1999). In Banana, stomata accounted for about 44% of total fruit transpiration (Khanal et al., 2022). Also, permeance correlated positively with lenticel density and area per lenticel in pomegranate and *Malus* apples (Khanal et al., 2020b; Lufu et al., 2021). Periderm formation restores water barrier functions but only in part. In kiwifruit, decline in fruit water loss occurred after degeneration of the hairs on the skin and evolution of periderm (Celano et al., 2009). However, we observed higher permeance to water loss by the periderms compared to intact CM in 'Apple' mango (Athoo et al., 2020). Our observation was also consistent with higher permeance by the periderms in 11 *Malus* apple cultivars (Khanal et al., 2019). Although less effective, periderms make better barriers compared to openings on the fruit surface without periderms.

Secondly, we infer that openings on the surface predispose fruit to pathogenic intrusion. 90% of all fruit decays starts at stem scars (Cappellini, 1977), wounds (Goudarzi et al., 2021), lenticels, microcracks and macrocracks (Guan et al., 2015). In stone fruits, fruit infection increased linearly with increase in cuticular cracks (Borve et al., 2000; Fogle and Faust, 1975). Fruit infection incidence increased with increasing microcracking and increasing inoculum density (Gibert et al., 2009). Incidentally, surface wetness increase cuticular cracking (Athoo et al., 2022) and is necessary for conidial germination (Gibert et al., 2009). On the contrary, pathogenic infections reduce when periderm develop under the wounds (Lulai and Corsini, 1998). Peridermal membrane (PM) presents a compactly arranged cellular structure (Khanal et al., 2013b). The phellem cell

walls are suberized and lignified (Legay et al., 2016), physically resisting fungal hydrolases (Ranathunge et al., 2011). Again, the phenolic and aliphatic compounds in the PM possess some antimicrobial properties (Lulai and Corsini, 1998). Nonetheless, PM penetration by certain pathogens is still possible. These pathogens enters the skin through the intercellular spaces (O'Gara et al., 2015) or the PM:CM border (Hawthorne and Sutherland, 1992). Rots occurred more frequently at the edges of scar tissue than elsewhere on the *Cucurbita maxima* fruit (Hawthorne and Sutherland, 1992). *Monilinia* rot infection occurred after suberization of the nectarine fruit lenticels (Fogle and Faust, 1975). Wound periderm therefore provides a "first aid" response but its protection against certain pathogens is insufficient. Efficiency of periderms on reducing susceptibility of mango fruit to postharvest rots will be worth studying in future.

Thirdly, this study inferred reduced mechanical strength of the fruit skin as consequence of openings on the surface. We argue that, 1) openings on the surface without periderms are structurally weaker due to presence of large intracellular spaces (Li et al., 2013) and intermittent or absent cuticle. 2) These openings accelerate water uptake and subsequent reduction of cellular adhesion (Brüggenwirth and Knoche, 2017; Schumann et al., 2019). 3) These openings cause localized stress concentration (Khanal et al., 2023). Surface openings with periderms like lenticels, also represent weaker spots in a strained skin. This is because of their limited extensibility compared to the adjoining CM (Khanal et al., 2013b). In this study, cuticles with lenticels were more strained compared to lenticel free ones (Athoo et al., 2023). Also, 'Apple' mango CM failed at lower fracture force compared to those of 'Tommy Atkins' (Athoo et al., 2021). We attribute this failure to larger lenticel area in 'Apple' mango. Lenticels often cracked at their tips (Athoo et al., 2020; Lufu et al., 2021).

4.3 Countermeasures to prevent surface disorders

We propose pre-harvest bagging of fruits, fruit production under rain shelter and breeding as strategies to prevent some of these disorders. Fruit bagging is used commercially in Asia to produce blemish-free fruits (Kitagawa et al., 1992). Pre-harvest bagging prevents these disorders by keeping the surface dry. Consequently, microcracking of the fruit surface is prevented. Significant russet reduction occurred when we bagged 'Apple' mango (chapter 3.6). Reduction in

surface disorders with bagging is also reported in 'Apple' and 'Nam Dok Mai#4', mango (Chonhenchob et al., 2011; Mathooko et al., 2011), peach (Zhang et al., 2015), pear (Amarante et al., 2002; Lin et al., 2008), pummelo, persimmon (Katagiri et al., 2003), pomegranate (Sarkomi et al., 2019) and *Malus* apple (Tukey, 1969; Yuan et al., 2019). However, reduced red color and high labor demand may limit its adoption (Hua et al., 2016; Karanjalker et al., 2018). Also, careful selection must be made to avoid bags with low permeability to water vapor. Materials like polyethylene bags yield high water vapor concentrations around the fruit causing subsequent microcracks and russeting (Tukey, 1969), Nonetheless, improved peel appearance, reduced chemical residue, reduced pest and disease incidence (Blasi et al., 2017; Estrada, 2004; Gao et al., 2022; Lin et al., 2008) justify preharvest bagging.

Rain shelters work in similar manner to bagging. They prevent disorders by keeping the surface dry. Unlike bagging, rain shelters water-proofs the entire tree. Currently, significant production of high valued fruits like sweet cherries occur under rain shelters. Production of fruits under rain shelter reduced incidences of russeting (Shi et al., 2019), cracking (Cline et al., 1995) and diseases (Lim et al., 2015). Their use is limited to crops with shorter canopy.

Breeding could provide a long-term solution to reduce russeting. Breeding targeting the fruit biomechanics is suggested. The strength of a fruit skin is affected by cell size, cell number and arrangement of cells (Khanal and Knoche, 2017, 2014), lenticel structure and size (Athoo et al., 2021, 2023), quantity and volume of intracellular spaces (Cybulska et al., 2010), and cell wall structure and composition (Li et al., 2013; Zykwinska et al., 2008). Breeding for less susceptible genotypes should consider: (1) smaller and uniformly sized epidermal and hypodermal cells. These are able to withstand increased growth strains and are less likely to fail (Curry, 2012; Winkler et al., 2022). (2) uniform stress distribution within the cuticle especially around the stomata, lenticels or trichomes. Breeding should therefore target uniform connection between the cuticle and stomatal/lenticel apparatus. (3) Enhanced cuticle and wax deposition to help fix growth strain (Khanal et al., 2013a) thus reduce risk of lenticel cracking.

5. Reference

AFA Horticultural Crops, 2020. 2019 - 2020 validated horticulture report, Agriculture and Food Authority (AFA). Nairobi.

AFA Horticultural Crops, 2018. 2017-2018 Horticulture validated report, Agriculture and Food Authority (AFA). Nairobi.

Amarante, C., Banks, N.H., Max, S., 2002. Preharvest bagging improves packout and fruit quality of pears (*Pyrus communis*). New Zeal. J. Crop Hortic. Sci. 30, 93–98. https://doi.org/10.1080/01140671.2002.9514203

Athoo, T.O., Winkler, A., Knoche, M., 2020. Russeting in 'Apple' mango: Triggers and mechanisms. Plants 9, 898. https://doi.org/10.3390/plants9070898

Athoo, T.O., Khanal, B.P., Knoche, M., 2021. Low cuticle deposition rate in 'Apple' mango increases elastic strain, weakens the cuticle and increases russet. PLoS One 16, 1–19. https://doi.org/10.1371/journal.pone.0258521

Athoo, T.O., Winkler, A., Owino, W.O., Knoche, M., 2022. Surface moisture induces microcracks and increases water vapor permeance of fruit skins of mango cv. Apple. Horticulturae 8, 545. https://doi.org/10.3390/horticulturae8060545

Athoo, T.; Winkler, A.; Owino, W.O.; Knoche, M., 2023. Lenticels are sites of initiation of microcracking and russeting in 'Apple' mango. PlosOne 18, e0291129. https://doi.org/10.1371/journal.pone.0291129

Bakker, J.C., 1988. Russeting (cuticle cracking) in glasshouse tomatoes in relation to fruit growth. J. Hortic. Sci. 63, 459–463. https://doi.org/10.1080/14620316.1988.11515879

Bally, I.S.., 1999. Changes in the cuticular surface during the development of mango (*Mangifera indica* L.) cv. Kensington Pride. Sci. Hortic. 79, 13–22. https://doi.org/10.1016/S0304-4238(98)00159-9

Barbosa-Martínez, C., Ponce de León-García, L., Pelayo-Zaldívar, C., 2009. Morpho-histology of 'Manila' and 'Haden' fruit development. A comparative study with postharvest implications. Acta Hortic. 820, 281–288. https://doi.org/10.17660/ActaHortic.2009.820.31

Bargel, H., Barthlott, W., Koch, K., Schreiber, L., Neinhuis, C., 2004. 10 Plant cuticles: Multifunctional interfaces between plant and environment, in: Hemsley, A.R. and Poole, I. (Eds), The Evolution of Plant Physiology. Elsevier, Amsterderm, Netherlands, pp. 171-194. https://doi.org/10.1016/b978-012339552-8/50011-1

Bell, H.P., 1937. The origin of russeting in the 'Golden Russet' apple. Can. J. Res. 15, 560–566. https://doi.org/10.1139/cjr37c-042

Bezuidenhout, J.L.J., Robbertse, P.J., Kaiser, C., 2005. Anatomical investigation of lenticel development and subsequent discolouration of 'Tommy Atkins' and 'Keitt' mango (*Mangifera indica* L.) fruit. J. Hortic. Sci. Biotechnol. 80, 18–22. https://doi.org/10.1080/14620316.2005.11511884

Blasi, E., Pancino, B., Passeri, N., Franco, S., 2017. Environmental and economic benefits of the preharvest fruit bagging technique: Trade-off evaluation in a Mediterranean area, Acta Hortic. 1160, 313-318. https://doi.org/10.17660/ActaHortic.2017.1160.45

Borve, J., Sekse, L., Stensvand, A., 2000. Cuticular fractures promote postharvest fruit rot in sweet cherries. Plant Dis. 84, 1180–1184. https://doi.org/10.1094/PDIS.2000.84.11.1180

Brown, K., Considine, J., 1982. Physical aspects of fruit growth: Stress distribution around lenticels. Plant Physiol. 69, 585-590. https://doi.org/10.1104/pp.69.3.585

Brüggenwirth, M., Knoche, M., 2017. Cell wall swelling, fracture mode, and the mechanical properties of cherry fruit skins are closely related. Planta 245, 765–777. https://doi.org/10.1007/s00425-016-2639-7

Byers, R.E., Carbaugh, D.H., Presley, C.N., 2019. Stayman' fruit cracking as affected by surfactants, plant growth regulators, and other chemicals. J. Am. Soc. Hortic. Sci. 115, 405–411. https://doi.org/10.21273/jashs.115.3.405

Camacho-Vázquez, C., Ruiz-May, E., Guerrero-Analco, J.A., Elizalde-Contreras, J.M., Enciso-Ortiz, E.J., Rosas-Saito, G., López-Sánchez, L., Kiel-Martínez, A.L., Bonilla-Landa, I., Monribot-Villanueva, J.L., Olivares-Romero, J.L., Gutiérrez-Martínez, P., Tafolla-Arellano, J.C., Tiznado-Hernandez, M.E., Quiroz-Figueroa, F.R., Birke, A., Aluja, M., 2019. Filling gaps in our knowledge on the cuticle of mangoes (*Mangifera indica*) by analyzing six fruit

cultivars: Architecture/structure, postharvest physiology and possible resistance to fruit fly (*Tephritidae*) attack. Postharvest Biol. Technol. 148, 83–96. https://doi.org/10.1016/j.postharvbio.2018.10.006

Cappellini, R.A., 1977. Vulnerability of stem-end scars of blueberry fruits to postharvest decays. Phytopathol. 77, 118-119. https://doi.org/10.1094/Phyto-67-118

Carella, A., Gianguzzi, G., Scalisi, A., Farina, V., Inglese, P., Lo Bianco, R., Baptista, P., Carillo, P., 2021. Fruit growth stage transitions in two mango cultivars grown in a mediterranean environment. Plants. 10, 1332. https://doi.org/10.3390/plants10071332

Celano, G., Minnocci, A., Sebastiani, L., D'Auria, M., Xiloyannis, C., 2009. Changes in the structure of the skin of kiwifruit in relation to water loss. J. Hortic. Sci. Biotechnol. 84, 41–46. https://doi.org/10.1080/14620316.2009.11512477

Cerri, M., Reale, L., 2020. Anatomical traits of the principal fruits: An overview. Sci. Hortic. 270, 109390. https://doi.org/10.1016/j.scienta.2020.109390

Chen, Y., Straube, J., Khanal, B.P., Zeisler-Diehl, V., Suresh, K., Schreiber, L., Debener, T., Knoche, M., 2022. Apple fruit periderms (russeting) induced by wounding or by moisture have the same histologies, chemistries and gene expressions. PLoS One 17, e0274733. https://doi.org/10.1371/journal.pone.0274733

Chonhenchob, V., Kamhangwong, D., Kruenate, J., Khongrat, K., Tangchantra, N., Wichai, U., Singh, S.P., 2011. Preharvest bagging with wavelength-selective materials enhances development and quality of mango (*Mangifera indica* L.) cv. Nam Dok Mai #4. J. Sci. Food Agric. 91, 664–671. https://doi.org/10.1002/jsfa.4231

Claypool, L.L., Uriu, K., Lasker, P.F., 1972. Split-pit of 'Dixon' cling peaches in relation to cultural factors. J. Am. Soc. Hortic. Sci. 97, 181–185. https://doi.org/10.21273/JASHS.97.2.181

Cline, J.A., Meland, M., Sekse, L., Webster, A.D., 1995. Rain cracking of sweet cherries: II. Influence of rain covers and rootstocks on cracking and fruit quality. Acta Agric. Scand. Sect. B — Soil Plant Sci. 45, 224–230. https://doi.org/10.1080/09064719509413108

Cohen, H., Dong, Y., Szymanski, J., Lashbrooke, J., Meir, S., Almekias-Siegl, E., Zeisler-Diehl,

V.V., Schreiber, L., Aharoni, A., 2019. A multilevel study of melon fruit reticulation provides insight into skin ligno-suberization hallmarks. Plant Physiol. 179, 1486–1501. https://doi.org/10.1104/pp.18.01158

Combrink, N.J.J., Agenbag, G.A., Langenhoven, P., Jacobs, G., Marais, E.M., 2001. Anatomical and compositional changes during fruit development of 'Galia' melons. South African J. Plant Soil 18, 7–14. https://doi.org/10.1080/02571862.2001.10634393

Considine, J.A., 1982. Physical aspects of fruit growth: Cuticular fracture and fracture patterns in relation to fruit structure in *Vitis vinifera*. J. Hortic. Sci. 57, 79–91. https://doi.org/10.1080/00221589.1982.11515027

Curry, E., 2012. Increase in epidermal planar cell density accompanies decreased russeting of 'Golden Delicious' apples treated with Gibberellin A_{4+7}. HortScience 47, 232–237. https://doi.org/10.21273/hortsci.47.2.232

Curry, E., Arey, B., 2010. Apple cuticle: the perfect interface. Scanning Microsc. 7729, 349–359. https://doi.org/10.1117/12.853913

Curry, E.A., Torres, C., Neubauer, L., 2008. Preharvest lipophilic coatings reduce lenticel breakdown disorder in 'Gala' apples. Horttechnology 18, 690–696. https://doi.org/10.21273/HORTTECH.18.4.690

Cybulska, J., Konstankiewicz, K., Zdunek, A., Skrzypiec, K., 2010. Nanostructure of natural and model cell wall materials. Int. Agrophysics 24, 107-114.

Davenport, T.L., 2009. The mango: Botany, production and uses, 2nd ed. CABI, Wallingford, UK. pp 98-145. https://doi.org/10.1079/9781845934897.0000

Dietz, T.H., Thimma Raju, K.R., Joshi, S.S., 1989. Studies on loss of weight of mango fruits as influenced by cuticles and lenticels. Acta Hortic. 231, 685-687. https://doi.org/10.17660/ActaHortic.1989.231.31

Drogoudi, P., Pantelidis, G.E., Vekiari, S.A., 2021. Physiological disorders and fruit quality attributes in pomegranate: Effects of meteorological parameters, canopy position and acetylsalicylic acid foliar spray. Front. Plant Sci. 12,645547. https://doi.org/10.3389/fpls.2021.645547

Du Plooy, W., Merwe, C. van der, Korsten, L., 2004. Differences in the surface structures of three mango cultivars and the effect of kaolin on these structures. South African Mango Grow. Assoc. Res. J. 24, 29–36.

Du Plooy, G.W., Van Der Merwe, C.F., Korsten, L., 2006. Lenticel discolouration in mango (*Mangifera indica* L.) fruit – a cytological study of mesophyll cells from affected tissue. J. Hortic. Sci. Biotechnol. 81, 869–873. https://doi.org/10.1080/14620316.2006.11512152

Edelmann, H.G., Neinhuis, C., Bargel, H., 2005. Influence of hydration and temperature on the rheological properties of plant cuticles and their impact on plant organ integrity. J. Plant Growth Regul. 24, 116–126. https://doi.org/10.1007/s00344-004-0015-5

Emmons, C.L.W., Scott, J.W., 1997. Environmental and physiological effects on cuticle cracking in tomato. J. Am. Soc. Hortic. Sci. 122, 797–801. https://doi.org/10.21273/JASHS.122.6.797

Estrada, C.G., 2004. Effect of fruit bagging on sanitation and pigmentation of six mango cultivars. Acta Hortic. 645, 195-199. https://doi.org/10.17660/ActaHortic.2004.645.17

Everett, K.R., Hallett, I.C., Rees-George, J., Chynoweth, R.W., Pak, H.A., 2008. Avocado lenticel damage: The cause and the effect on fruit quality. Postharvest Biol. Technol. 48, 383–390. https://doi.org/10.1016/j.postharvbio.2007.09.008

Evert, R.F., 2006. Esau's plant anatomy, 3rd ed. John Wiley & Sons, Inc., Hoboken, NJ, USA. pp. 427-445. https://doi.org/10.1002/0470047380

Faust, M.., Shear, C.B., 1972a. Russeting of apples, an interpretive review. HortScience 7, 233–235. https://doi.org/10.21273/hortsci.7.3.233

Faust, M.., Shear, C.B., 1972b. Fine structure of the fruit surface of three apple cultivars. J. Am. Soc. Hortic. Sci. 97, 351–355. https://doi.org/10.21273/jashs.97.3.351

Fogle, H.W., Faust, M., 1975. Ultrastructure of nectarine fruit surfaces. J. Am. Soc. Hortic. Sci. 100, 74–77. https://doi.org/10.21273/JASHS.100.1.74

Gao, C., Zhang, Y., Li, H., Gao, Q., Cheng, Y., Ogunyemi, S.O., Guan, J., 2022. Fruit bagging reduces the postharvest decay and alters the diversity of fruit surface fungal community in

'Yali' pear. BMC Microbiol. 22, 239. https://doi.org/10.1186/s12866-022-02653-4

Gazzola, R., Alves, R.E., Filgueiras, H.A.C., 2004. Physical state of epicuticular waxes during development of 'Tommy Atkins' mangoes. Acta Hortic. 645, 595–599. https://doi.org/10.17660/ActaHortic.2004.645.78

Gibert, C., Chadœuf, J., Nicot, P., Vercambre, G., Génard, M., Lescourret, F., 2009. Modelling the effect of cuticular crack surface area and inoculum density on the probability of nectarine fruit infection by *Monilinia laxa*. Plant Pathol. 58, 1021–1031. https://doi.org/10.1111/j.1365-3059.2009.02121.x

Goudarzi, A., Samavi, S., Amiri Mazraie, M., Majidi, Z., 2021. Fungal pathogens associated with pre- and postharvest fruit rots of mango in southern Iran. J. Phytopathol. 169, 545–555. https://doi.org/10.1111/jph.13027

Griesbach, J., 2003. Mango growing in Kenya. World Agroforestry Centre (ICRAF), Nairobi.

Grimm, E., Khanal, B.P., Winkler, A., Knoche, M., Köpcke, D., 2012. Structural and physiological changes associated with the skin spot disorder in apple. Postharvest Biol. Technol. 64, 111–118. https://doi.org/10.1016/j.postharvbio.2011.10.004

Guan, Y., Chang, R., Liu, G., Wang, Y., Wu, T., Han, Z., Zhang, X., 2015. Role of lenticels and microcracks on susceptibility of apple fruit to *Botryosphaeria dothidea*. Eur. J. Plant Pathol. 143, 317–330. https://doi.org/10.1007/s10658-015-0682-z

Hawthorne, B.T., Sutherland, P.W., 1992. Wound repair processes in fruit of the *Cucurbita maxima* hybrid 'Delica' and the role of scar tissue in the development of fungal rots on stored fruit. New Zeal. J. Crop Hortic. Sci. 19, 53–60. https://doi.org/10.1080/01140671.1991.10418106

Holcroft, D.M., Mitcham, E.J., 1996. Postharvest physiology and handling of litchi (*Litchi chinensis* Sonn.). Postharvest Biol. Technol. 9, 265–281. https://doi.org/10.1016/S0925-5214(96)00037-3

Hua, Y., Yang, B., Zhou, X.G., Zhao, J., Li, L., 2016. A novel progressively delivered fruit bagging apparatus. J. Appl. Hortic. 18, 123-127. https://doi.org/10.37855/jah.2016.v18i02.21

Huang, J.S., Snapp, S.S., 2004. The effect of boron, calcium, and surface moisture on shoulder check, a quality defect in fresh-market tomato. J. Am. Soc. Hortic. Sci. 129, 599–607. https://doi.org/10.21273/JASHS.129.4.0599

Hurtado, G., Knoche, M., 2021. Water soaking disorder in strawberries: Triggers, factors, and mechanisms. Front. Plant Sci. 12, 694123. https://doi.org/10.3389/fpls.2021.694123

Jeffree, C.E., 1996. Structure and ontogeny of plant cuticles, in: Kerstiens, G. (Ed.), Plant Cuticles. Bios Scientific Publishers Ltd, Oxford, UK, pp. 33–82.

Johnson, R.B., King, J.R., Mcbride, J.J., 1957. Zineb controls citrus rust mites. Proc. Florida State Hortic. Soc. 70, 38–47. https://doi.org/10.2307/3492220

Joshi, M., Schmilovitch, Z., Ginzberg, I., 2021. Pomegranate fruit growth and skin characteristics in hot and dry climate. Front. Plant Sci. 12,725479 https://doi.org/10.3389/fpls.2021.725479

Karanjalker, G.R., Ravishankar, K. V., Shivashankara, K.S., Dinesh, M.R., 2018. Influence of bagging on color, anthocyanin and anthocyanin biosynthetic genes in peel of red colored mango cv. 'Lily.' Erwerbs-Obstbau 60, 281–287. https://doi.org/10.1007/s10341-018-0371-0

Katagiri, T., Satoh, Y., Fukuda, T., Kataoka, I., 2003. Improving marketability of "Fuyu" persimmon fruit by bagging culture. Acta Hortic. 601, 213-217. https://doi.org/10.17660/ActaHortic.2003.601.30

Kennard, W.C., 1955. Development of the fruit, seed, and embryo of the 'Paheri' mango. Bot. Gaz. 117, 28–32. https://doi.org/10.1086/335886

Khanal, B.P., Grimm, E., Finger, S., Blume, A., Knoche, M., 2013a. Intracuticular wax fixes and restricts strain in leaf and fruit cuticles. New Phytol. 200, 134–143. https://doi.org/10.1111/nph.12355

Khanal, B.P., Grimm, E., Knoche, M., 2013b. Russeting in apple and pear: a plastic periderm replaces a stiff cuticle. AoB Plants. 5, pls048. https://doi.org/10.1093/aobpla/pls048

Khanal, B.P., Knoche, M., 2014. Mechanical properties of apple skin are determined by

epidermis and hypodermis. J. Am. Soc. Hortic. Sci. 139, 139–147. https://doi.org/10.21273/jashs.139.2.139

Khanal, B.P., Knoche, M., 2017. Mechanical properties of cuticles and their primary determinants. J. Exp. Bot. 68, 5351–5367. https://doi.org/10.1093/jxb/erx265

Khanal, B.P., Ikigu, G.M., Knoche, M., 2019. Russeting partially restores apple skin permeability to water vapour. Planta 249, 849–860. https://doi.org/10.1007/s00425-018-3044-1

Khanal, B.P., Imoro, Y., Chen, Y.H., Straube, J., Knoche, M., 2020a. Surface moisture increases microcracking and water vapour permeance of apple fruit skin. Plant Biol. 23,74-82. https://doi.org/10.1111/plb.13178

Khanal, B.P., Yiru, S., Knoche, M., 2020b. Lenticels and apple fruit transpiration. Postharvest Biol. Technol. 167, 111221. https://doi.org/10.1016/j.postharvbio.2020.111221

Khanal, B.P., Sangroula, B., Bhattarai, A., Almeida, G.K., Knoche, M., 2022. Pathways of postharvest water loss from banana fruit. Postharvest Biol. Technol. 191, 111979. https://doi.org/10.1016/j.postharvbio.2022.111979

Khanal, B.P., Pudasaini, K., Sangroula, B., Knoche, M., 2023. Factors determining the mechanical properties of banana fruit skin during induced ripening. Postharvest Biol. Technol. 198, 112252. https://doi.org/10.1016/j.postharvbio.2023.112252

Kitagawa, H., Manabe, K., Esguerra, E.B., 1992. Bagging of fruit on the tree to control disease. Acta Hortic. 321, 871–875. https://doi.org/10.17660/ActaHortic.1992.321.110

Knoche, M., Peschel, S., Hinz, M., Bukovac, M.J., 2000. Studies on water transport through the sweet cherry fruit surface: Characterizing conductance of the cuticular membrane using pericarp segments. Planta. 212, pages 127–135. https://doi.org/10.1007/s004250000404

Knoche, M., Peschel, S., 2007. Deposition and strain of the cuticle of developing european plum fruit. J. Am. Soc. Hortic. Sci. 132, 597–602. https://doi.org/10.21273/JASHS.132.5.597

Knoche, M., Grimm, E., 2008. Surface moisture induces microcracks in the cuticle of 'Golden Delicious' apple. HortScience 43, 1929–1931. https://doi.org/10.21273/hortsci.43.6.1929

Knoche, M., Athoo, T.O., Winkler, A., Brüggenwirth, M., 2015. Postharvest osmotic dehydration of pedicels of sweet cherry fruit. Postharvest Biol. Technol. 108, 86-90. https://doi.org/10.1016/j.postharvbio.2015.05.014

Knoche, M., Grimm, E., Winkler, A., Alkio, M., Lorenz, J., 2019. Characterizing neck shrivel in European plum. J. Am. Soc. Hortic. Sci. 144, 38–44. https://doi.org/10.21273/jashs04561-18

Kunst, L., Samuels, A.L., 2003. Biosynthesis and secretion of plant cuticular wax. Prog. Lipid Res. 42, 51–80. https://doi.org/10.1016/s0163-7827(02)00045-0

Lara, I., Belge, B., Goulao, L.F., 2014. The fruit cuticle as a modulator of postharvest quality. Postharvest Biol. Technol. 87, 103–112. https://doi.org/10.1016/j.postharvbio.2013.08.012

Léchaudel, M., Lopez-Lauri, F., Vidal, V., Sallanon, H., Joas, J., 2013. Response of the physiological parameters of mango fruit (transpiration, water relations and antioxidant system) to its light and temperature environment. J. Plant Physiol. 170, 567–576. https://doi.org/10.1016/j.jplph.2012.11.009

Legay, S., Guerriero, G., André, C., Guignard, C., Cocco, E., Charton, S., Boutry, M., Rowland, O., Hausman, J.F., 2016. MdMyb93 is a regulator of suberin deposition in russeted apple fruit skins. New Phytol. 212, 977–991. https://doi.org/10.1111/nph.14170

Legay, S., Guerriero, G., Deleruelle, A., Lateur, M., Evers, D., André, C.M., Hausman, J.F., 2015. Apple russeting as seen through the RNA-seq lens: strong alterations in the exocarp cell wall. Plant Mol. Biol. 88, 21–40. https://doi.org/10.1007/s11103-015-0303-4

Li, J., Chen, J., 2017. Citrus fruit-cracking: Causes and occurrence. Hortic. Plant J. 3, 255–260. https://doi.org/10.1016/j.hpj.2017.08.002

Li, N., Fu, L., Song, Y., Li, J., Xue, X., Li, S., Li, L., 2019. Water entry in jujube fruit and its relationship with cracking. Acta Physiol. Plant. 41, 162. https://doi.org/10.1007/s11738-019-2954-2

Li, Z., Yang, H., Li, P., Liu, J., Wang, J., Xu, Y., 2013. Fruit biomechanics based on anatomy: A review. Int. Agrophysics 27, 97–106. https://doi.org/10.2478/v10247-012-0073-z

Lim, K.-H., Gu, M., Kim, B.-S., Kim, W.-S., Cho, D.-H., Son, J.-H., Park, S., Choi, K.-J., Jung, S.-K., Choi, H.-S., 2015. Tree growth and fruit production of various organic Asian pear (*Pyrus pyrifolia* Nakai) cultivars grown under a rain-shelter system. J. Hortic. Sci. Biotechnol. 90, 655–663. https://doi.org/10.1080/14620316.2015.11668728

Lin, J., Chang, Y., Yan, Z., Li, X., 2008. Effects of bagging on the quality of pear fruit and pesticide residues. Acta Hortic. 772, 315–318. https://doi.org/10.17660/actahortic.2008.772.52

Lipton, W.J., 1967. Some effects of low-oxygen atmospheres on potato tubers. Am. Potato J. 44, 292–299. https://doi.org/10.1007/BF02862531

Lobo, G.M., Sidhu, J.S., 2017. Handbook of mango fruit:, Production, Postharvest Science, Processing Technology and Nutrition. Wiley, Chichester, UK. pp 37-60. https://doi.org/10.1002/9781119014362

Lufu, R., Ambaw, A., Opara, U.L., 2021. Functional characterisation of lenticels, micro-cracks, wax patterns, peel tissue fractions and water loss of pomegranate fruit (cv. Wonderful) during storage. Postharvest Biol. Technol. 178, 111539. https://doi.org/10.1016/j.postharvbio.2021.111539

Lulai, E.C., Corsini, D.L., 1998. Differential deposition of suberin phenolic and aliphatic domains and their roles in resistance to infection during potato tuber (*Solanum tuberosum* L.) wound-healing. Physiol. Mol. Plant Pathol. 53, 209–222. https://doi.org/10.1006/pmpp.1998.0179

Macnee, N.C., Rebstock, R., Hallett, I.C., Schaffer, R.J., Bulley, S.M., 2020. A review of current knowledge about the formation of native peridermal exocarp in fruit. Funct. Plant Biol. 47, 1019–1031. https://doi.org/10.1071/FP19135

Maguire, K.M., Lang, A., Banks, N.H., Hall, A., Hopcroft, D., Bennett, R., 1999. Relationship between water vapour permeance of apples and micro-cracking of the cuticle. Postharvest Biol. Technol. 17, 89–96. https://doi.org/10.1016/S0925-5214(99)00046-0

Martin, J.T., Juniper, B.., 1970. The cuticles of plants. Edward Arnold (Publishers) Ltd, Edinburg, UK.pp. 1-347.

Matas, A.J., López-Casado, G., Cuartero, J., Heredia, A., 2005. Relative humidity and temperature modify the mechanical properties of isolated tomato fruit cuticles. Am. J. Bot. 92, 462–468. https://doi.org/10.3732/ajb.92.3.462

Mathooko, F.M., Kahangi, E.M., Runkua, J.M., Onyango, C.A., Owino, W.O., 2011. Preharvest mango (*Mangifera indica* L. 'Apple') fruit bagging controls lenticel discolouration and improves postharvest quality. Acta Hortic. 906, 55–62. https://doi.org/10.17660/ActaHortic.2011.906.7

McCoy, C.W., 1996. Stylar feeding injury and control of eriophyoid mites in citrus, in: Lindquist, E.E., Sabelis, M.W., Bruin, J. (Eds.), World Crop Pests. Elsevier B.V., Amsterdam, The Netherlands, pp. 513-526. https://doi.org/10.1016/s1572-4379(96)80032-7

Meyer, A., 1944. A study of the skin structure of 'Golden Delicious' apples. Am. Soc. Hortic. Sci. 45, 105–110.

Michailides, T.J., 1991. Russeting and russet scab of prune, an environmentally induced fruit disorder: Symptomatology, induction, and control. Plant Dis. 75, 1114-1123. https://doi.org/10.1094/PD-75-1114

Mukherjee, S.K., Litz, R.E., 2009. Introduction: Botany and importance., in: Litz, R.E. (Ed.), The mango: Botany, production and uses. CABI, Wallingford, pp. 1–18. https://doi.org/10.1079/9781845934897.0001

Nobel, P.S., 2020. Physicochemical and environmental plant physiology, 5th ed. Academic Press, San Diego, California. pp. 617-628.

O'Gara, E., Howard, K., McComb, J., Colquhoun, I.J., Hardy, G.E.S.J., 2015. Penetration of suberized periderm of a woody host by *Phytophthora cinnamomi*. Plant Pathol. 64, 207–215. https://doi.org/10.1111/ppa.12244

O'Hare, T.J., Bally, I.S.., Dahler, J.M., Saks, Y., Underhill, S.J.., 1999. Characterisation and induction of 'etch' browning in the skin of mango fruit. Postharvest Biol. Technol. 16, 269–277. https://doi.org/10.1016/S0925-5214(99)00030-7

Opara, L.U., Hodson, A.J., Studman, C.J., 2000. Stem-end splitting and internal ring-cracking of 'Gala' apples as influenced by orchard management practices. J. Hortic. Sci. Biotechnol. 75,

465-469. https://doi.org/10.1080/14620316.2000.11511270

Peschel, S., Knoche, M., 2005. Characterization of microcracks in the cuticle of developing sweet cherry fruit. J. Am. Soc. Hortic. Sci. 130, 487–495. https://doi.org/10.21273/JASHS.130.4.487

Ponce de León, G.L., Barbosa, M.C., Guillén, G.E., García, I.V., Sepúlveda, S.J., Hernández, C.G., 2000. Advances in the development of early mango fruit. Acta Hortic. 509, 253-258. https://doi.org/10.17660/ActaHortic.2000.509.26

Riederer, M., 2018. Introduction: Biology of the plant cuticle, in: Riederer, M., Müller, C. (Eds.), Annual Plant Reviews Online. John Wiley & Sons, Ltd, Chichester, UK, pp. 1–10. https://doi.org/10.1002/9781119312994.apr0229

Riederer, M., Schreiber, L., 2001. Protecting against water loss: analysis of the barrier properties of plant cuticles. J. Exp. Bot. 52, 2023–2032. https://doi.org/10.1093/jexbot/52.363.2023

Ranathunge, K., Schreiber, L., Franke, R., 2011. Suberin research in the genomics era-New interest for an old polymer. Plant Sci. 180, 399–413. https://doi.org/10.1016/j.plantsci.2010.11.003

Ruess, F., Stösser, R., 1993. Über "Öffnungen" in der Schale von Apfelfrüchten und ihren Verschluss. Erwerbsobstbau 35, 148–152.

Rymbai, H., Srivastav, M., Sharma, R.R., Singh, S.K., 2012. Lenticels on mango fruit: Origin, development, discoloration and prevention of their discoloration. Sci. Hortic. 135, 164–170. https://doi.org/10.1016/j.scienta.2011.11.018

Sarkomi, F.H., Moradinezhad, F., Khayat, M., 2019. Pre-harvest bagging influences sunburn, cracking and quality of pomegranate fruits. J. Hortic. Postharvest Res. 2, 131–142. https://doi.org/10.22077/jhpr.

Scharwies, J.D., Grimm, E., Knoche, M. 2014. Russeting and relative growth rate are positively related in 'Conference'and 'Condo'pear. HortScience. 49, 746-749. https://doi.org/10.21273/HORTSCI.49.6.746

Schumann, C., Winkler, A., Brüggenwirth, M., Köpcke, K., Knoche, M., 2019. Crack initiation

and propagation in sweet cherry skin: A simple chain reaction causes the crack to 'run.' PLoS One 14, 1–22. https://doi.org/10.1371/journal.pone.0219794

Shi, C., Qi, B., Wang, X., Shen, L., Luo, J., Zhang, Y., 2019. Proteomic analysis of the key mechanism of exocarp russet pigmentation of semi-russet pear under rainwater condition. Sci. Hortic. 254, 178–186. https://doi.org/10.1016/j.scienta.2019.04.086

Skene, D.S., 1982. The development of russet, rough russet and cracks on the fruit of the apple Cox's Orange Pippin during the course of the season. J. Hortic. Sci. 57, 165–174. https://doi.org/10.1080/00221589.1982.11515037

Skoss, J.D., 1955. Structure and composition of plant cuticle in relation to environmental factors and permeability. Bot. Gaz. 117, 55–72. https://doi.org/10.1086/335891

Tafolla-Arellano, J.C., Zheng, Y., Sun, H., Jiao, C., Ruiz-May, E., Hernández-Oñate, M.A., González-León, A., Báez-Sañudo, R., Fei, Z., Domozych, D., Rose, J.K.C., Tiznado-Hernández, M.E., 2017. Transcriptome analysis of mango (*Mangifera indica* l.) fruit epidermal peel to identify putative cuticle-associated genes. Sci. Rep. 7, 1–13. https://doi.org/10.1038/srep46163

Tamjinda, B., Siriphanich, J., Nobuchi, T., 1992. Anatomy of lenticels and the occurrence of their discolouration in mangoes (*Mangifera indic*a cv. Namdokmai). Agric. Nat. Resour. 26, 57-64

Tharanathan, R.N., Yashoda, H.M., Prabha, T.N., 2006. Mango (*Mangifera indica* L.), "The King of Fruits"—An Overview. Food Rev. Int. 22, 95–123. https://doi.org/10.1080/87559120600574493

Trivedi, P., Nguyen, N., Hykkerud, A.L., Häggman, H., Martinussen, I., Jaakola, L., Karppinen, K., 2019. Developmental and environmental regulation of cuticular wax biosynthesis in fleshy fruits. Front. Plant Sci. 10. https://doi.org/10.3389/fpls.2019.00431

Tukey, L.D., 1969. Observations on the russeting of apples growing in plastic bags. Proc. Amer. Soc, Hort. Sci. 74, 30–39.

Underhill, S.J.R., Critchley, C., 1992. The physiology and anatomy of lychee (*Litchi chinensis* Sonn.) pericarp during fruit development. J. Hortic. Sci. 67, 437–444.

https://doi.org/10.1080/00221589.1992.11516269

Underhill, S.J.R., Simons, D.H., 1993. Lychee (*Litchi chinensis* Sonn.) pericarp desiccation and the importance of postharvest micro-cracking. Sci. Hortic. 54, 287–294. https://doi.org/10.1016/0304-4238(93)90107-2

Wagner, G.J., Wang, E., Shepherd, R.W., 2004. New approaches for studying and exploiting an old protuberance, the plant trichome. Ann. Bot. 93, 3–11. https://doi.org/10.1093/aob/mch011

Wang, Y. zhi, Dai, M. song, Cai, D. ying, Zhang, S., Shi, Z. bin, 2016. A review for the molecular research of russet/semi-russet of sand pear exocarp and their genetic characters. Sci. Hortic. 210, 138–142. https://doi.org/10.1016/j.scienta.2016.07.019

Wei, X., Mao, L., Han, X., Lu, W., Xie, D., Ren, X., Zhao, Y., 2018. High oxygen facilitates wound induction of suberin polyphenolics in kiwifruit. J. Sci. Food Agric. 98, 2223–2230. https://doi.org/10.1002/jsfa.8709

Williams, M.H., Vesk, M., Mullins, M.G., 1990. Development of the banana fruit and occurrence of the maturity bronzing disorder. Ann. Bot. 65, 9–19. https://doi.org/10.1093/oxfordjournals.aob.a087913

Winkler, A., Athoo, T., Knoche, M., 2022. Russeting of fruits: Etiology and management. Horticulturae 8, 231. https://doi.org/10.3390/horticulturae8030231

Winkler, A., Grimm, E., Knoche, M., Lindstaedt, J., Köpcke, D., 2014. Late-season surface water induces skin spot in apple. HortScience 49, 1324–1327. https://doi.org/10.21273/HORTSCI.49.10.1324

Yeats, T.H., Rose, J.K.C., 2013. The formation and function of plant cuticles. Plant Physiol. 163, 5–20. https://doi.org/10.1104/pp.113.222737

Yuan, G., Bian, S., Han, X., He, S., Liu, K., Zhang, C., Cong, P., 2019. An integrated transcriptome and proteome analysis reveals new insights into russeting of bagging and non-bagging "Golden Delicious" apple. Int. J. Mol. Sci. 20, 4462. https://doi.org/10.3390/ijms20184462

Zhang, B.B., Guo, J.Y., Ma, R.J., Cai, Z.X., Yan, J., Zhang, C.H., 2015. Relationship between the bagging microenvironment and fruit quality in 'guibao' peach [*Prunus persica* (L.) batsch]. J. Hortic. Sci. Biotechnol. 90, 303–310. https://doi.org/10.1080/14620316.2015.11513187

Zykwinska, A., Thibault, J.-F., Ralet, M.-C., 2008. Competitive binding of pectin and xyloglucan with primary cell wall cellulose. Carbohydr. Polym. 74, 957–961. https://doi.org/10.1016/j.carbpol.2008.05.004

List of Publications

Athoo, T.O., Winkler, A., Owino, W.O., Knoche, M., 2022. Surface moisture induces microcracks and increases water vapor permeance of fruit skins of mango cv. Apple. Horticulturae 8, 545. https://doi.org/10.3390/horticulturae8060545

Winkler, A., Athoo, T., Knoche, M., 2022. Russeting of fruits: Etiology and management. Horticulturae 8, 231. https://doi.org/10.3390/horticulturae8030231

Athoo, T.O., Khanal, B.P., Knoche, M., 2021. Low cuticle deposition rate in 'Apple' mango increases elastic strain, weakens the cuticle and increases russet. PLoS One 16, 1–19. https://doi.org/10.1371/journal.pone.0258521

Athoo, T.O., Winkler, A., Knoche, M., 2020. Russeting in 'Apple' mango: Triggers and mechanisms. Plants 9, 898. https://doi.org/10.3390/plants9070898

Athoo, T.; Winkler, A.; Owino, W.O.; Knoche, M., 2023. Lenticels are sites of initiation of microcracking and russeting in 'Apple' mango. PlosOne 18(9): e0291129. https://doi.org/10.1371/journal.pone.0291129

Knoche, M., Athoo, T.O., Winkler, A., Brüggenwirth, M., 2015. Postharvest osmotic dehydration of pedicels of sweet cherry fruit. Postharvest Biol. Technol. 108, 86–90. https://doi.org/10.1016/j.postharvbio.2015.05.014

Athoo, T.O., Winkler, A., Owino, W.O., Knoche, M., 2015. Pedicel transpiration in sweet cherry fruit: Mechanisms, pathways, and factors. J. Amer. Soc. Hort. Sci.140, 136-143. https://doi.org/10.21273/JASHS.140.2.136

Acknowledgements

Curriculum Vitae

Name	Thomas Ochieng Athoo
Gender	Male
Date of Birth	20th August 1981
Place of Birth	Suba
Nationality	Kenya

Education

2019 - 2023 **PhD Candidate**

Specialization	Fruit science
Institution	Institute of Horticultural Production Systems: Fruit Science Section, Leibniz University Hannover, Germany
Thesis title	Peel russeting in 'Apple' mango (*Mangifera indica* L.): characterization, mechanism and management
Supervisor	Prof. Dr. Moritz Knoche

2012-2014 **Master of Science (M.Sc.) in International Horticulture**

Major	Fruit science
Grade	Summa Cum Laude
Institution	Institute of Horticultural Production Systems: Fruit Science Section, Leibniz University Hannover, Germany
Thesis title	Transpiration from the pedicel surface of sweet cherry fruit: Mechanism, pathways and factors
Supervisor	Prof. Dr. Moritz Knoche

2005-2007 **Bachelor of Science (B.Sc.) in Horticulture**

Grade	1st class Honors
Institution	Egerton University, Kenya

2000-2004 **Diploma in Horticulture**

Grade	Distinction
Institution	Egerton University, Kenya

1995-1998   **Kenya Certificate of Secondary Education**

Grade   B- minus (66 out of 100 points)

Institution   Mirogi Boys Secondary School

Work Experience

Dates	Title	Responsibilities
2008 - 2019	Principal Quality Assurance Officer: **Kenya Bureau of Standards (KEBS)**	• Conducting 3rd party conformity assessments under KEBS product certification schemes. • Auditing quality and food safety management systems on behalf of KEBS Certification body. • Training food safety and quality management systems audits on behalf of the National Quality Institute (NQI) of Kenya. • Providing consultancy services on product and process quality to industry and stakeholders.
2007-2008	Production Supervisor: **Red Lands Roses Ltd**	• Planning and co-coordinating cutflower production in the assigned area • Accounting for the production area's resources: physical, financial and human • Documentation of operations. • Controlling the quality of harvested produce prior to final processing

Awards

1. DAAD Scholarship (2019-2022): To study PhD in Horticulture at Gottfried Wilhelm Leibniz University Hannover

2. DAAD Scholarship (2012-2014): To study Msc degree in Horticulture at Gottfried Wilhelm Leibniz University Hannover

3. Egerton University Alumni Association Award (2007): For the best overall among the 2007graduating class.

Participation in conferences

1   22nd HAK Workshop on sustainable horticultural production in the tropics

Topic	Strain, cuticle deposition and mechanical properties of 'Apple' and 'Tommy Atkins' mango cultivars
Presentation type	Oral
Dates	28th November – 2nd December 2022
Place	Jomo Kenyatta University of Agriculture and Technology, Kenya
Organizer	Horticulture association of Kenya

2   21st HAK Workshop on spatial aspects of biodiversity in horticultural production systems"

Topic	Russeting in 'Apple' Mango: Triggers and Mechanisms
Presentation type	Oral
Dates	29th November – 3rd December 2021
Place	Karatina University, Kenya
Organizer	Horticulture association of Kenya

3   19th HAK Workshop on horticultural production in the tropics

Topic	A review of russeting of fruits: Characterization, causes and management
Presentation type	Oral
Dates	25th - 29th November 2019
Place	Kericho, Kenya
Organizer	Horticulture association of Kenya